Imperial College London

PERFORMANCE BASED DESIGN OF OFFSHORE STRUCTURES SUBJECTED TO BLAST LOADING

A thesis submitted to Imperial College London for the degree of

Doctor of Philosophy

By

Rafee Makbol Mohamed Ali

Department of Civil and Environmental Engineering
Imperial College London
London SW7 2AZ
United Kingdom

October 2007

ABSTRACT

Topside structures of offshore installations have to support heavy process plant dealing with large volumes of oil and gas under high pressure. Many of these platforms have to be operated in very remote areas in a harsh environment with little supporting infrastructure. It is therefore necessary to design these high risk installations to various types of extreme loadings. One of these extreme scenarios is blast loading from a possible hydrocarbon explosion. Although this is a comparatively low frequency accidental event, it has the capability to cause major fatalities to personnel and serious structural damage which could lead to the complete loss of the platform. At present, most topside structures are designed based on working stress design (WSD), or load and resistance factor design (LFRD), which is quite safe but not economical due to the uncertain extent of the levels of protection. For these reasons, a Performance Based Design Methodology is proposed, which emphasizes the structure's predictable behaviour and the protection of personnel and assets. The end result will be an optimum design which satisfies the function of a system without compromising safety.

A performance based design guideline for the assessment of topside structures subjected to blast loading is proposed. The guideline, which reasonably incorporated some statistical findings, simplifies the evaluation of performance levels for the topside structure without quantitative risk assessment (QRA) data. The assessment of topside structures is not complete if the proper behaviour and response is not fully understood. It has been shown in the study that the roles of secondary structural members i.e. deck plates and stringer beams cannot be overlooked. Having substantial deformations on secondary members averts severe damage on primary members. A simplified deck plate analytical model is proposed and the optimum slenderness ratio for deck plate design is recommended. Although accuracy of the proposed analytical method is found slightly offset from the finite element result at extreme overpressure, the model is straightforward and provides a quick method to assess the deck plate capacity. The study has also highlighted the weakness of sniped bottom flanges for stringer beams, a necessary condition to facilitate practical fabrication. This shortcoming is overcome by strengthening with angles, a novel idea which is simple and practical with minimum interference to the existing structural configuration.

Based upon a typical topside framing, the performance level of the topside is evaluated for reference which can be applied to other topsides. The study has investigated a number of mitigation techniques for improving beam to beam connections. The techniques comprise studies based on some conventional approaches, typical fabrication methods and a new proposal with tubular braces. Finally, the effect of equipment on the topside structure is investigated and recommendations are made to minimise unnecessary damage.

ACKNOWLEDGEMENTS

The research involved in this thesis was carried out in the Department of Civil and Environmental Engineering, Imperial College London.

The author wishes to express his gratitude and thanks to the following:

Dr. L.A. Louca, who supervised this work, for his guidance, involvement, expertise and encouragement.

MARA (Majlis Amanah Rakyat), a statutory body under the Government of Malaysia for providing financial assistance to pursue the study at Imperial College.

Dr. S. Yasseri for his patience in answering a wide range of queries and helps in understanding the principle concept of performance based design.

Dr. A. Wadee for a fruitful discussion on plate analysis.

Mr. T. Rasheed of Imperial College ICT team for IT and ABAQUS support especially during the author's laptop was stolen without which the rerun of analyses would have never been completed.

The author's colleagues in the structures section for their valuable discussions in particular Dr. A. S. Fallah, Dr. H. Johnson, Dr. A M.A. Ibrahim, Dr. R.B Cruise and Dr. A. Y. M. Yassin.

The staff members at the Department of Civil and Environment Engineering of Imperial College London who made this place an ideal environment for carrying research work.

Finally, the author's family for their supports in every aspect. Without their affection and encouragement, certainly not much could have been achieved.

Table of Contents

CHAPTER THREE - PERFORMANCE BASED DESIGN FOR BLAST RESISTANT OFFSHORE STRUCTURES

CHAPTER FOUR - A SIMPLIFIED ANALYTICAL MODEL FOR THE DECK PLATE OF OFFSHORE TOPSIDES

List of Tables

List of Tables

List of Tables

List of Figures

List of Figures

List of Figures

List of Figures

List of Figures

List of Figures

List of Figures

List of Figures

List of Figures

List of Figures

List of Figures

Chapter One

Introduction

1.1 Preamble

Offshore installations in the oil and gas industry are high risk structures because of their exposure to hazardous and flammable hydrocarbon materials. The worst-case scenario that is likely to occur on the platform is a hydrocarbon explosion that generates blast loading. A topside structure which forms a portion of the superstructure where most facilities of the process plant are located must be protected against this loading. Traditionally, safety aspects and prevention measures on offshore installations are very stringent, hence the likely occurrence of an explosion is comparatively low. However, the damaging effects caused by explosions can be devastating in terms of loss of life, assets and the environment. This was tragically demonstrated in the North Sea with the loss of the Piper Alpha platform mentioned by Lees (1996).

At present, most design methods on topside structures are based on working stress designs that are safe and suitable for normal pre-commissioning and operating conditions which emphasise minimum obstruction to process flows and the platform shut down time. However, under extreme loads, especially explosion loads in which magnitudes are much higher than ordinary operating loads, the end product using this design methodology will result in elephantine structural members. These final structural sections will not only be unacceptable to the client, but also uneconomical due to an unknown level for the protection of a structural system.

The approach of performance based design was first adopted in the 1960s in the building industry. In the 1980s the world body for standardization, i.e. ISO, enacted the approach to its building codes. In the early 1990s, this was implemented in the UK and New Zealand. Half a decade later the methodology was adopted by other nations: the US, Australia and Japan.

For offshore installations, each platform design is unique because it must be in accordance with the process requirement. With some constraints, as mentioned in chapter three, the development of a performance based approach did not occur at the same pace that was achieved in the building industry. However, with the recent advancements in technology, environmental consciousness and new regulations imposed on operators, they have potentially supported the application of performance based design for offshore structures.

The main aim of performance based design for blast resistant offshore installations emphasizes the predictable response to the topside structure, the protection of assets as well as meeting the pre-requisite conditions.

1.2 Background to the study

This study proposes a guideline using the methodology of performance based design for the assessment of topside structures against blast loading. Explosions produce circular shock front waves which induce overpressure loads over short duration of time. Assuming the propagation of waves are not obstructed, the strength and its impact depend on rise time, maximum peak pressure and duration. As the magnitude of the blast load is usually many times more than the conventional loads on topside structures, any design, without an appropriate risk assessment and a reliable method to quantify the applied loading is not recommended for design.

Implementing the concept of performance based design and the proposed performance level, a typical topside structure has been modelled using a finite element program for evaluating its behaviour and response. The study looked into the performance of structural components in relation to the defined damage level. From the damage status, a summary of the overall performance for the global structural system could be easily justified.

1.3 Offshore installations and offshore hazards

A conventional offshore installation with piled foundations comprises a steel jacket to support topsides that consist of a number of deck levels. While for some installations in deeper water supports are made of concrete, steel template jackets are still the preferred method because the fabrication of steel components can be implemented simultaneously by various fabricators in different places. Furthermore, the assembling of steel components has no restrictions on the site with regard to the depth of the jacket.

Typically, offshore installations are compact process plants and consist of the following parts: the supporting structure (for examples piled platform, concrete or bottom-founded platform and tension leg platform); the wellhead area at which lines of piping that carry fluids, a mixture of crude oils, hydrocarbon gases and water from the reservoir terminate; the production separator in which fluids are separated into oil, gas condensate, gas and water; the compression facility at which gases from separators are compressed, dried, purified and ready for export; and a living quarters (LQ), which is the accommodation for the personnel.

Offshore installations are designed to a unique load combination. Besides process plant aspects and inherent hazard factors by plant activity, the design must account for the criteria during in-service conditions such as environmental conditions and distances to onshore facilities; and also during pre-service conditions, conditions before commissioning work such as fabrication work, load-out of structures onto barges, sea-transportation and installation work.

In the current situation, due to the fact that there are still exist some constraints in the technology for processing hydrocarbon fluids, for safety reasons some unprocessed hydrocarbon gases have to be burnt by flaring or venting into the atmosphere. In addition, corrosion caused by seawater and the high content of carbon dioxide and sulphur in crude oils add to the cost and complexity of maintenance work on offshore installations. Often, these installations have to be operated in hostile environments. As a result, the design of offshore installations must be kept as simple as possible with maximum throughput every time without sacrificing the safety aspects.

Being located offshore, oil and gas installations are exposed to many kinds of hazard compared to onshore structures. Sometimes these hazards start with a minor accident and when they are combined with other potential sources of hazards, eventually leads to a major accident. For example, explosions can damage the pipelines, which are followed by fires that reduce the yield strength of steel sections and subsequently can cause the catastrophic collapse of the platform. Table 1.1 lists main principal hazards on typical offshore installations.

1.4 Hydrocarbon explosions

A hydrocarbon explosion is defined as a process in which combustion of a premixed hydrocarbon gas-air cloud causes a rapid increase of pressure waves that generate blast loading. In an unconfined area, the pressure waves are emitted in all possible directions within the duration of few milliseconds as a pressure impulse. The magnitude of overpressure for the unconfined area is lower than a confined area.

A topside on which most facilities are in-placed consists of structural members, piping, equipment, cables and other appurtenances that can obstruct the free movement of these waves as shown by Figure 1.1. Hence, introducing congestion and confinement significantly increases the magnitude of overpressure loads.

Table 1.1

Typical offshore hazards

Principal offshore hazards	**The effects and prevention works**
• Accidental forces :- i.) Falling objects from ongoing daily activities such as lifting and removing objects by a platform crane. ii.) Boat collisions due to navigation failures of vessels or the warning system on installations.	i.) Minor damages to major damages if the object falls on main lines or control equipment. Protection frames or bumper guides are typically provided for potentially hazardous elements. ii). Major damages if collisions occur at main structural supports. Possible total collapse after the impact. A fender system is typically provided around sub-structure legs.
• Environmental forces and severe weather. Unexpected natural disasters such as typhoon/ hurricanes and iceberg.	New installations must be designed to meet these conditions. Mitigation work and prediction of the return period to determine performance levels on existing installations.
• Earthquakes. Structures are located on active seismic zone.	Structures must be designed to fulfil the strength and ductility requirements
• Fires – hydrocarbon sources.	Loss of strength for steel members when the temperature reaches above 400^{o}C. Develop a compartment or install firewall to separate areas. Application of fire retardant or passive fire protection to the structural frame.
• Explosions – hydrocarbon sources.	Generate overpressure and are sometimes followed by fire. Set demand levels and use ductile steels. Protection of lives and assets by installing blast walls and consider the effect of venting out the pressure and water spraying system.

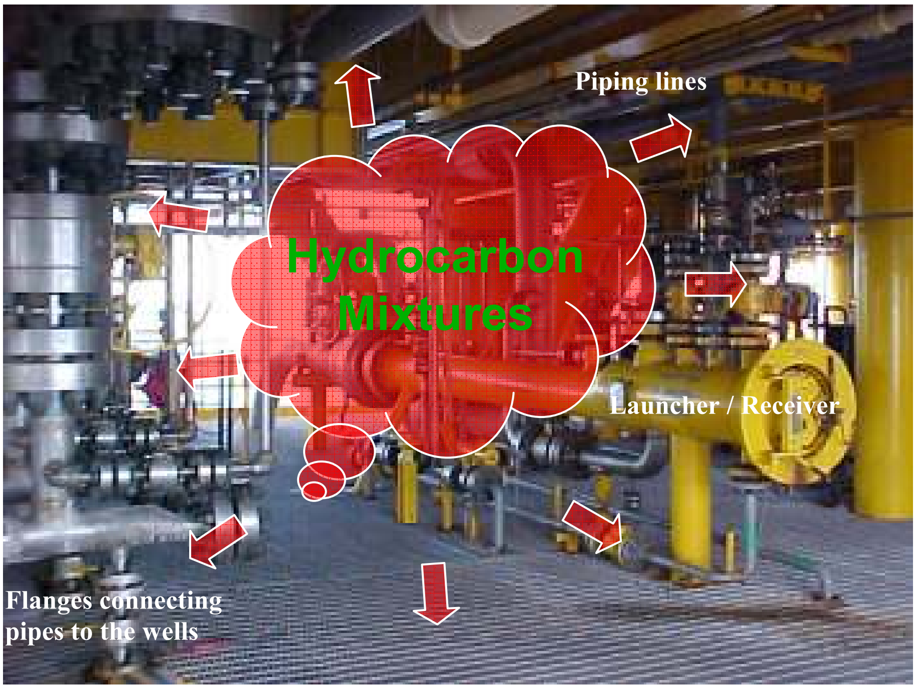

Figure 1.1

Typical inventories on topside structure with a possible cloud release of hydrocarbon mixtures

For large inventories, such as walls or vessels, this pressure impulse will exert blast loading on one side of the object. For small elements such as piping lines or cable trays, the pressure pulse will not cause a large pressure difference, but the effect of wind from blast waves will drag and may pull the elements off supports and cause rupture by bending. Further damage to piping work and process equipment can cause a further release of hydrocarbons and can sometimes lead to major fires and missiles caused by flying objects. Combination of these two effects can also damage the fire compartmentalisation of the topside, which may also threaten the nearby living quarters. The severity of explosions is dependent upon the following factors:

<u>**The influencing factors**</u>	<u>**The effects**</u>
• The geometry of the platform	Open space area allows quick venting, hence lowers the overpressure
• The ignition location	Longer distance from venting, higher flame acceleration can take place, therefore increases the overpressure
• Degree and layout of congestion	Higher degree of confinement causes higher degree of turbulence that induces formation of a vortex, which

	increases the overpressure.
• Fuel type and concentration	Natural gas gives low overpressure; propane and butane give higher overpressure compared with natural gas; however, ethylene is the most reactive hydrocarbon.

In the Piper Alpha incident (1988), where 167 people were killed, a major part of the installation was burnt down. The incident started with a rather small gas explosion in a compressor module that caused a fire which subsequently resulted in the rupture of a riser. It is therefore, a challenge for offshore structural engineers, especially for a new development project that the effects of blast loadings should be taken into serious consideration from the outset of the design stage.

1.5 The objective and scope of the study

The thesis is focused on developing a design guideline for offshore topside structures for resisting blast loading subjected to hydrocarbon explosions by adopting the approach of performance based design. The components of a typically fabricated topside structure with a high likelihood of being exposed to blast load are studied for evaluating the behaviour and improving the performance of structural members. An important by-product of the study is the proposal of a simple and workable mitigation solution. The primary objectives of the study are outlined as follows:

i. To demonstrate that the method of performance based design for offshore topsides is compatible with other conventional design methods and offers a lesser amount of steel required in design without sacrificing the stability and integrity of the whole structural system. Although, in some instances, some secondary members are expected to be damaged, the performance of the structural system is not jeopardized and rehabilitation is feasible.

ii. To propose damage levels and the expected performance level for a typical topside. In the absence of the quantitative risk assessment (QRA) data, the proposed table will facilitate evaluation and offers designers and clients a quick appraisal to assess the designed topside structure. On existing platforms, the result from the damage level will provide a basic framework for future mitigation work.

iii. To optimise the design for a new structure so that by adopting the approach, the design for blast resistance will not be a determining factor that will govern the design of topsides.

iv. To recommend a simplified solution for improving ductility of structural components. The proposed solution can easily be implemented with minimum interruption to the ongoing activities of the platform and the current layout plan.

v. To identify and offer a solution to any anomalies that can degrade the performance of structural members due to commonly practiced fabrication procedures.

The scope of the study, in conjunction with the defined objectives and parallel with a literature survey, encompasses the development of a topside structure model. From the main model, each topside model is refined for meeting the intended plan, outlined as follows:

i) From the literature survey, ABAQUS models are developed to simulate the conditions of the experimental result. All selected cases are quite close or comparable with the condition of the topside structure. This is for the validation of the topside model.

ii) Development of the deck plate analytical model; although the deck plate is considered as a secondary member, this structural component plays an important role during the blast period because its surface area is larger than other structural components and it is characteristic in developing the membrane strain. The study also includes parametric study for determining the optimum size of deck plate. At present, most designers for offshore installations emphasize the strength of the primary members, and minimum attention is given to deck plates. The scope of plate design is usually limited to blast containment rather than integrating the design with proper structural configuration that can improve the global structural performance.

iii) Adopting performance based design methodology for topside structures, the study generalises the performance level for structural components. Knowing the ductility ratio for each structural component, the damage level can be defined as well as the global performance of the whole structural system.

iv) Assessment of the proposed mitigation work and collaboration of strengthening details in the topside structure model.

v) Assessment of inventories subjected to blast loads and its correlation to the structural components.

vi) Development of performance based design guidelines for blast resistant offshore topside structure.

1.6 Layout of the thesis

A brief description of offshore installations is introduced in **Chapter One**. This is followed by the incentive, objective and scope of the present study.

Chapter Two presents a literature survey on the performance based design methodology and the general expectation as a result of adopting the approach in design work. A brief summary of performance levels for seismic load implemented in building design is included for comparison with topside structures.

The current available design codes on blast load are compared and reviewed to ensure key elements in terms of safety and lives protection are not jeopardized, as well as the integrity of the structural system which must at least meet the requirement in terms of functionality, serviceability and reliability.

One of the components to maintain the integrity of a structural system is the connection for load transfer. Many methods have been proposed for the improvement of column to beam connection in building design but relatively very few have looked into the beam to beam connection which is a common feature in offshore installations. Under extreme load, such as blast loading, having improved the connection alone cannot guarantee the optimum performance of the structural system. Secondary structural components, such as deck plates and deck stringer beams, are expected to absorb much more energy and deform reasonably to minimize damage in major structural connections.

The measurement of performance for structural components can be estimated by applying a ductility ratio. For a fully welded connection, ductility can be improved by having a better physical configuration at the connection, but with a poor welding preparation may further expose the connection to brittleness. The existence of brittleness causes premature failure, resulting in early loss of resistance. As the occurrence of a blast is very rare, but the effect is acute on the structure, effective mitigation work for improving the performance should ensure it is maintenance free throughout the design life.

Chapter Three focuses on the application of performance based design for offshore structures. The first section discusses the methodology of the approach accompanied by a design algorithm assessment in which principles of performance based design are emphasized in order to achieve the specific demand level for the attainment of performance objectives. As the approach is based on behaviour rather than prescriptive performance, uncertainties are removed, which attributes to a precise design compared with a traditional design method.

In the context of offshore installations, particularly for topside structures where safety cannot be compromised, this will lead to an economical design as well as meeting the functionality of a system from pre to post explosion regimes.
The second section of Chapter Three demonstrates step by step performance based design guidelines followed by a design example to assess the deck plate resistance against the defined blast load level. A comparison is made between the current approach and the typical working stress design (WSD) method.

Acknowledging the importance of deck plates, **Chapter Four** presents a simplified analytical model for deck plates in topside offshore structures. The proposed method is based on the theory of virtual work and the assumed deformed shape functions in Cartesian coordinates, for which a set of equilibrium equations in terms of energy is developed. The equations are formed as a static case and a dynamic case with unsolved variables defined in generalised coordinates. When these equations are re-arranged, they are equivalent to modal analyses, which can be solved using the Lagrange's equation method. The generalized coordinates in the static case can be solved manually, while in the dynamic case the ordinary differential equations are solved numerically by developing a computer program using MAPLE software.

The proposed method is comparable with finite element analysis results up to a certain threshold at which point the development of membrane strain and plasticity modes becomes dominant. When comparing the result to the reported experimental data, the proposed shape functions for deformations in lateral directions are modified in order to accommodate the observed behaviour. The results compare favourably with test data and finite element analysis as a control case.

Chapter Five presents a study which investigates the behaviour of a typical offshore topside structure subjected to blast loading caused by a hydrocarbon explosion. The pressure load caused by the explosion is idealized as a linearised triangular impulse which is simultaneously applied on two deck levels modelled using the finite element program, ABAQUS Explicit.

Two cases were developed: the original case representing a typical offshore fabricated deck flooring with sniped bottom flanges at connections for stringer beams, and the strengthened case which was a modified form of the original case but with rolled steel angles welded at sniped bottom flanges of the stringer beams and plate girders. Results from the analysis show that load directions and structural configuration play a prominent role in the response of the topside. The strengthening indicates the beneficial redistribution of local yielding at the sniped connections of the beams to mid-spans, which consequently improves the performance level of the structural system.

Haunch details are found to cause local failures on plate girders but the failure mechanism is useful for developing a technique to avert further damage.
Finally, generalised ductility ratios derived from the normalisation of responses at the end-spans and mid-spans of structural components are compared with commonly used design values to justify the damage level and performance when subjected to blast loadings.

Chapter Six presents a study for improving the connections of topside structure, many of which are connections between load carrying beams to supporting beams. The study divides these connections into two main groups; the first comprises beams with equal overall depth while the second is for beams with different depths and requires a built-up haunch section to make up the difference of depth.

The study focuses on commonly fabricated structural connections whereby an IP 600 beam is selected as a load carrying beam as well as for the support beam in the first case, while in the second case the support beam is a plate girder PG 1000 as defined in Chapter Five. A single brace and a pair of diagonal horizontal braces with slotted gusset plates at both ends are proposed. One side of the gusset plate is connected to the middle span while the other far end is connected to the support beam. Although the method contributes minimum stiffness at the connection, it has a significantly improved ductility ratio on the existing structural configuration by sharing the deformation along the tubular brace which results in the reduction of strain at the supports. The proposed bracings are introduced in the present topside model for ensuring the workability of the design and the consistency of responses, as was observed in the simplified beam to beam model.

Chapter Seven describes the study of a topside structure with equipment. Equipment is modelled to the actual scale in the ABAQUS topside model and subjected to a blast load together with structural members. The model has incorporated live loads to represent temporary equipment during drilling and maintenance periods. The most prominent and immediate effects exhibited by equipment on structural members components during blast and post blast regimes are studied. Mitigation work is proposed to protect the equipment and structural components.

Chapter Eight includes a main summary and conclusion of the study carried out in this thesis.

Finally, recommendations for future work with reference to new findings from the present study are discussed in **Chapter Nine**.

1.7 Originality and main contributions

The thesis describes the application of a performance based design methodology for topside structures of offshore installations. The main features and originality of the work can be summarized in the following points:

a. Performance based design level for blast resistance of offshore topsides

A simplified performance based design level of blast resistance for topside structure is proposed. The proposed performance level can be used for benchmarking the local component of structural members and the global structural system. The proposed levels are quantified from the response of structural elements of a typical topside structure together with a combination of statistical, factual and empirical data from various findings. The study has demonstrated the advantage of adopting a performance based approach in blast design that not only can avoid conservatism but also that the expected capacity and resistance of the designed structural component are much more coherent compared to the commonly adopted design methodology (WSD) used in the offshore industry. Hence, a good engineering justification, which is more presentable and acceptable, can be delivered to all level of stakeholders

b. Damage level for structural components

The proposed damage levels for design of structural components are as follows:

Support and primary truss members $2 \leq \mu < 3$

Primary members $3 \leq \mu < 6$

Secondary members $4 \leq \mu < 6$

where μ is defined as a ratio of the maximum displacement or rotation against displacement or rotation at yield.

A lower value should be used when secondary members are used as equipment support. With proper modelling techniques, the plate can be allowed to have a higher damage level of μ greater than 6 but not to exceed damage level μ equals 10 that accounted for membrane strain development. Furthermore, deck plates are easy to replace as long as secondary support beams are still intact.

c. A simplified design method and optimum slender ratio for deck plate

A simplified analytical model of the deck plate which is comparable with finite element analysis (ABAQUS) and experimental result is proposed. The method can be used to estimate the response under both static and dynamic conditions by solving ordinary differential equations (ODE) using the available built-in commands of the MAPLE software. For optimum deck plate design, plate slenderness in the range of 70 to 100 is recommended for design. At this range, the change of response is more predictable. The change of deformation is very steady from elastic to plastic regimes followed by a gradual transformation of membrane strain before leading to rupture.

d. Improved structural details for blast resistance

The method of sniping at the bottom flange of deck stringer beams is a technique for minimizing distortion on the web of support beams as well as cost saving in fabrication. Despite these merits, the method is proven to cause a reduction in terms of structural performance, both locally and globally. A novel method for mitigation with angle L150 x 150 x 8 is proposed under the sniped area. The method is simple, workable and causes minimum obstruction to existing structural members. With a sniped detail, yielding of elements first appears at the bottom web of the support at sniped area while with angles yielding of elements is relocated and the first appearance occurs in the middle span of the beam.

Haunches can be developed into a mechanism to prevent damage at the connections (see Figures 5.3 and 6.5). Yielding of elements usually occurs at the kink or the transition of the slope, therefore a haunch with a gentle slope will yield the farthest from the connection. Extending the bottom flange of the beam from the haunch starting point to the support beam where the sniped bottom flange is made at the end span shows insignificant structural performance compared with the totally removed bottom flange case. Similarly, there is not much difference in terms of performance between the presence of a cope hole that is created for avoiding overlapping of new welds on the existing weld and for achieving full penetration.

The layout and arrangement of structural framing designed for explosions should be arranged for a direct exposure to the overpressure blast load. The blast reaction from the response must be transferred to designated supports in the shortest possible load path which will avert unnecessary damage occurring to other structural members. The introduction of diagonal brace with gusset plates at both ends between primary members assists the load distribution by sharing deformation in terms of axial force.

As the brace is weaker than the primary members it will yield first and deform much more resulting in better performance for the primary beams. The damaged brace can easily be removed by cutting the gusset plate without affecting existing structural members.

e. Equipment supports

Critical equipment on topside structures is recommended to be placed on a separate skid frame for better load distribution, instead of sitting directly on support beams. The skid frame will prevent damage originating from structural members to be passed onto the equipment. The critical condition for the structural supports is identified in the rebound regime during which the displaced equipment moves in opposite directions but towards the supports. This can lead to buckling and shear failure on support webs. Similarly, smaller inventories, such as piping lines and cables, are found to fail because of the impact on structural members during the rebound regime. More supports or hangers are recommended to prevent the damaged parts from flying freely as missiles. Extra loops and bends allow piping and cable trays to elongate and be more flexible, thus reducing stress caused by large relative displacement between support points.

Chapter Two

Literature Review

2.1 The general basis of performance based design

In a simple definition, performance based design is supposed to guarantee a freedom from the design process as long as performance objectives and performance levels are satisfied. Performance objectives consist of various design events or the possibility of design scenarios while performance levels are a requirement that must be achieved should the event occur, Thompson and Bank (2006). Comparing the approach with a traditional design method, performance based design provides goal setting in the early stages of the design process which requires interaction between designers in order to achieve an efficient system. The defined goal also helps the design team to focus their efforts on specific aspects. Without a performance goal there will be no effort to achieve minimum criteria including budget constraints, time schedule, safety and functionality, although designers may work for an efficient design. Thus, the results at the end of the project are usually mediocre.

The application of performance based methodology is not only limited to design work, it can also be broadened to many other fields, such as performance based order for selection of contractors, whereby contractors must prepare solutions by their own ideas, performance based standardization by which quality approximates performance, performance based prescriptive for requesting a minimum specific demands etc. Inokuma (2002) disclosed that despite its merits, the fully fledged performance based design of public works has been attempted only in very rare circumstances. This is because a good design proposal will require a design consultant to perform extra work, however the extra hours spent are usually not being paid for by the client which demotivates the design consultant to carry out the design work in the future.

In the context of a structural design, adopting performance based offers a shift from a dependence on empiricism and experience based conventions towards a more realistic prediction that a structure will experience in its whole design life. The assessment process and performance evaluation are the contribution from all structural components that form the integrity of a system. Hence, designers should be aware that behaviour of structural components is a pre-requisite to the system behaviour. However, if any of the isolated components fails to meet specific acceptance criteria, it is irrational to conclude that the system is unable to perform to the expected level.

Many of the current studies on structures for performance based design focus on earthquake design ((Alimoradi et al. (2003), Floren and Mohammadi (2001), Haldar et al. (2004), SEAOC (1995)) but extensive research has also been performed on wind, wave and fire hazards. In each case, although the scope of work may be different, the basic principals i.e. assessment, management and mitigation of risk, are almost equivalent to each other. Furthermore, because the method emphasizes accurate characterisation and prediction, performance based approach will probably be, and has the potential to be, a prominent feature in the future design for most engineering work.

2.2 Application of performance based design for building under seismic load

The occurrence of two major earthquakes, Northridge in California (1994) and the great Hanshin earthquake in Kobe Japan (1995), had caused major fatalities and the destruction of major infrastructures such hospitals and bridges. As the impacts on the people and economy were so significant in the aftermath of the earthquake, the two incidences stimulated and accelerated the development of performance based design methodology amongst the earthquake engineering groups.

Performance objectives for seismic load are primarily for the protection of building occupants by preventing collapse and falling debris in the event of a large earthquake, SEAOC (1995) while performance levels are generally dependent on the roles of building in a post earthquake emergency, the economic relevance to business, the material and structural types, Haldar et al. (2004).

Depending on the selected performance level, structural and non-structural damage are computed based on the overall performance of a structure. Table 2.1 summarises the recommended performance levels by SEAOC (1995). The definition of the performance levels is listed as follows:

Operational- Facilities continue in operation with negligible damage

Functional- Facilities continue in operation with minor damage and minor disruption to non essential services.

Life safety- Life safety is substantially protected, damage is moderate to extensive.

Near collapse- Life safety is at risk, damage is severe, structural collapse is prevented.

Table 2.1

Performance levels of performance based seismic engineering for buildings

Earthquake design level	Recurrence (years)	Recommended drift (%) [71]	Probability of exceedance
Frequent –Operational	43	0.5	50 percent in 30 years
Occasional –Functional	72	1.5	50 percent in 50 years
Rare – Life Safety	475	2.5	10 percent in 50 years
Very rare –Near Collapse	970	3.8	10 percent in 100 years

As described by Whittaker et al. (2003), adopting performance based design for designing a moment resisting frame against seismic actions, the method was not only found effective in distributing load over the structural system but also capable of arresting the progressive collapse of the structure. This has been demonstrated by the New York WTC buildings on September 11, 2001. The twin towers took about two hours to collapse, globally while the Deutsche Bank building, which was loaded by the falling debris of WTC was still standing, despite sustaining damage to column members.

A typical case for prescriptive design in the analysis of seismic load will be based on the code specified applied lateral load. The uncertainty in design is usually taken into account by adopting the maximum ground motion. In some cases, designers only consider the flexural actions of structural members for load distribution instead of allowing structural members to develop their behaviours at allowable inelastic deformation. As a result, the design of members is conservative with design sizes larger than that actually required.

Under performance based design, design considerations include the levels for displacement, loads and stress, target of damage states, and the maximum number of injuries or fatalities as mentioned by Floren and Mohammadi (2001).

Although both approaches, performance based and prescriptive based, will result in a safe structure, the by-product of performance based design outshines prescriptive design as it eliminates uncertainties and is more cost effective.

2.3 Application of performance based design for offshore structures

The methodology of performance based design for blast loads caused by hydrocarbon explosions on offshore installations includes procedures for the assessment of risk scenarios as mentioned by Williams (1986), Hutcheon and Waldram (1994), Vinnem (2000), Yasseri (2003b), and Fires and Explosions Guidance Part 0 to 2 with respect to a design-specific basis in order to describe the performance level at the initial stage, which then pursues by evaluation of the structure whether the specified performance objectives have been achieved. As most resources to the probable scenarios depend on the quantity of inventories placed on each of the deck levels of the installation, the risk is quantified based on either a deterministic or a probabilistic basis of possible events. The occurrence of events has it own risk, which is then related to specific losses and the structure performance levels.

2.3.1 Design consideration for topside structures

Response and behaviour are the main factors in performance based design. The input parameter of the approach for the assessment should not only consider the safety and integrity of a structure but also how the effects of blast escalations can be eliminated as stated by Walker et al. (2003), Yasseri (2002), and Yasseri and Menhennett (2003). These responsibilities lie with the operator and design engineers who commence by defining design considerations at the initial stage of the design phase. Table 2.2 summarises variables of the design considerations and the underlying engineering parameters in meeting the performance based design for a typical offshore installation subjected to hydrocarbon explosions.

The collection of design considerations will generate the cumulative likely event of occurrences and magnitude for which the structure will be analysed and designed. This will lead to the definition of performance levels that can be transformed to consequences. Each of the consequences is related to a safety level which can easily be understood and appreciated by the stakeholders, notably the client and regulatory body.

Table 2.2

Summary of performance based engineering for offshore installations, Yasseri (2003b), Yasseri and Menhennett (2003), Hamburger and Whittaker (2003)

Design Considerations	Parameters
Sources of blast loading	• Type of explosions deflagration (maximum 8 bar) or detonation (maximum 20 bar) • Location and area degree of congestion and confinement • Intensity of loads category of the overpressures duration of peaks
Engineering demands	Demand to capacity ratios for the following structural components :- • Primary members (members that support structures, equipment supports and part of the truss system), columns, girders and beams - axial load, moment, shear, ductility • Secondary members (members that support appurtenances e.g. walkway, staircase, wall support etc.) – axial load, moment, shear and plastic deformation. • Tertiary members (deck plate and walls)- displacement and development of membrane forces.
Damage measures	• Casualties and loss of lives • Platform shutdown times • Damage and repair costs
Decision variables	Performance objectives :- • Explosion return period (Occasional, rare and remote) • Performance levels (**see Table 2.3**)

2.3.2 Performance level and design requirement

As the operating conditions between offshore structures and onshore buildings differ markedly, the performance based design against blast loads for offshore installations emphasises functionality, minimises loss, repairable conditions, operable and avoiding conservatism. However, there are two major obstacles as noted by Bruce (1995) and Yasseri (2003b); the uncertainties in the study of hazard assessment and the evaluation of the structural performance caused by explosions.

The hazard assessments are the combined studies of the computational fluid dynamics (CFD) and quantitative risk assessment (QRA), which define the concept of return period or the probability of exceedance diagram of explosions. The structural performance is inherent in multi disciplines of engineering design and the complexities of overpressures/blast loads, both of which are the function of strength, stiffness, structural configuration and the dynamic nature of loads.

The performance based design approach optimises the limit state design method and the working stress design method. The working stress design approach is a rational design for meeting the pre-requisite and can be regarded as a performance based standard. The limit state design applies the concept of probability as the verification method while the performance based design provides freedom to verification method. Hence, under the blast load condition, both the working stress method and the limit state method will push up design costs compared with the performance based design approach.

Despite having a similar objective for optimum design by applying performance based design, seismic design is dependent on the location of the seismic zone, and any new additions would not change the hazard level. For offshore installations, the blast loads, on the other hand, are specific to an installation and any new additions are new potential hazards.

Table 2.3

Offshore installations –Performance levels
The category of performance levels is defined by designers/operators subjected to the results of risk and hazard analyses conducted on the installation

The degree of performance levels	Damages descriptions	Shutdown time
•Operational	No damage or minimum and negligible.	24 hours
•Asset protection and life safety ; i.) structural components ii.) non structural components	Damage control and structural stability; i.) Local damage of structural columns and beams but repairable and no collapse, deformations [101,102] are limited to 50 % and 100 % for primary and secondary members, respectively; injuries at the affected area but no threatening injuries in other areas. ii.) Back-up systems, communication and fire fighting are fully functional; adequate escape routes.	A few days and maximum of 4 weeks
•Collapse prevention	Globally, severe structural and non structural damages, deformation[101, 102] are limited to 75 % and 100 % for primary and secondary respectively; incipient to collapse; restricted escape routes; minimum loss of lives.	Not applicable

2.4 The present design codes on blast design

Reference is made to the current design codes for an overview and for comparison between design practices as well as to establish the objective in terms of safety and health levels. Despite the fact that each design code has a unique approach in the design methodology, the goals are basically about safety and life protection. This awareness is crucial for setting the minimum level of performance that fulfils operability under regular working conditions and functionality under blast condition.

2.4.1 API RP 2FB (2006)

Under fire and blast loading events, an offshore platform may collapse, causing loss of lives and pollution of the environment. Preventative measures and hazard analyses by facility engineers will assist structural engineers in design to optimize the performance criteria of the structures against the occurrence of these events. The code has divided the risk assessment process into three levels: the first level, screening, which is the simplest and lowest risk, and also not required beyond the adoption of good practice; the second level, nominal loads, which the facility must meet the performance criteria for the survival of the platform; the third level, event based, which combines the probability of occurring and consequences of the events. This leads to the development of a risk matrix for low and high risks as shown in Figure 2.1

<table>
<tr><td rowspan="5">Probability of Occurrence (depends on facilities, product type, structure type, sources, operation, management)</td><td>High</td><td>MR</td><td>HR</td><td>HR</td></tr>
<tr><td>Medium</td><td>LR</td><td>MR</td><td>HR</td></tr>
<tr><td>Low</td><td>LR</td><td>LR</td><td>MR</td></tr>
<tr><td rowspan="2"></td><td>Low</td><td>Medium</td><td>High</td></tr>
<tr><td colspan="3">Consequence of occurrence
(subjects to life, environmental, operator and public interest)</td></tr>
<tr><td colspan="5">Legends :

HR = High Risk
Consider blast as a load condition i.e. blast overpressure and blast drag loads, implement prevention and mitigation, may require change in layout or structural design.

MR = Medium Risk
Further risk assessment and mitigation measures.

LR = Low Risk
Insignificant risk and need not be considered for structural design purposes.</td></tr>
</table>

Figure 2.1

Blast load/ explosions - The risk matrix

Although the performance level is not explicitly discussed, the code has addressed the issue of performance criteria. Some nominal overpressures are proposed in the commentary but there is no definitive requirement (resistant capacity) for the structural member. However, the assessment for a new design structure may be evaluated by one of the following methods; screening check (conservative design basis), strength level analysis (linear elastic) or ductility level analysis.

2.4.2 N-004 NORSOK Standard (1998) - Structural Steel Design

Under Annex A of the code, responses are classified into three categories which relate to the ratio of duration of explosions (t_d) against the fundamental period of vibration (T_N) given by Table 2.4.

Table 2.4

The domain responses

Domain	Relativity to fundamental period	Equations
Impulsive	$t_d / T_N < 0.3$	$I = \int_0^{td} F(t)dt = \sqrt{2m_{eq}\int_0^{w_{\max}} R(w)dw}$
Dynamic	$0.3 < t_d / T_N < 3$	$\overline{m}\ddot{w} + \overline{k}w = \overline{F}(t)$
Quasi-Static	$3 < t_d / T_N$	$w_{\max} = \frac{1}{F_{\max}}\int_0^{w_{\max}} R(w)dw$ or $F_{\max} = R(w_{\max})$

Solutions of the equations shown in Table 2.4 are solved either iteratively or by numerical integration. For the SDOF analogy, the code adopted Biggs and Baker methodologies. The two approaches are used by the code to determine the resistance curves and transformation factors for plates and beams.

In the Biggs' method, an appropriate displacement shape function is assumed hence the equivalent SDOF is given as below:

$$\left\{\Sigma\, K_{LM}\, M\right\} \ddot{y} \;+\; k\;y = F\;(t) \qquad (2.1)$$

where

$K_{LM}\ M$ = load mass transformation factor x masses (uniform distributed load or point loads)

$F\ (t)$ = the blast load

$k\,y$ = stiffness and response of the system

For a linear system, K_{LM} and k are constant while in a non-linear system (sometimes specified by equivalent bi-linear or tri-linear systems), they are dependent on the response. The response can be obtained from design charts which are developed for different rise times.

In Baker's method, the pressure-impulse diagram (iso-damage curve) is developed using the maximum response in the impulsive and quasi-static domains for a specific condition. The diagram provides a pressure asymptote, impulse asymptote and a curve line joining the two which represents the transition loading conditions.

The code emphasises attention towards the structural analysis while issues of risk assessment are left for the operator to determine. Neither the issue of performance level nor performance criteria is addressed in the code. However, the code provides the domain response which will be useful for the prediction of structure behaviour before plastic deformation.

2.4.3 Army technical manual TM5 - 1300 (1990)

The manual was developed for US military organisations for the purposes of designing facilities against explosions and for the protection of personnel and important valuable equipment.

The document provides design guidelines for concrete and steel structures and it also underlines the qualitative comparison in design using these two materials. In summary, the code concludes that steel sections are considered rather more slender and allow larger deformation compared with concrete sections. In steel design, connection integrity is to be given special attention as well as stress interaction while the reinforced concrete design is an independent system because separate steel reinforcements are to be provided for flexure, shear and torsion.

Deformation criteria presented in the manual are based on a single accidental occurrence on the structure for the whole life time and some checks are referred to AISC plastic design. Although the manual allows higher deformation up to rotation of 12 degrees or ductility ratio 20 to fail with adequate bracings for stability, the deformation for beams and plates is limited to 2 degrees or a ductility ratio of 10, whichever governs as illustrated by Figure 2.2.

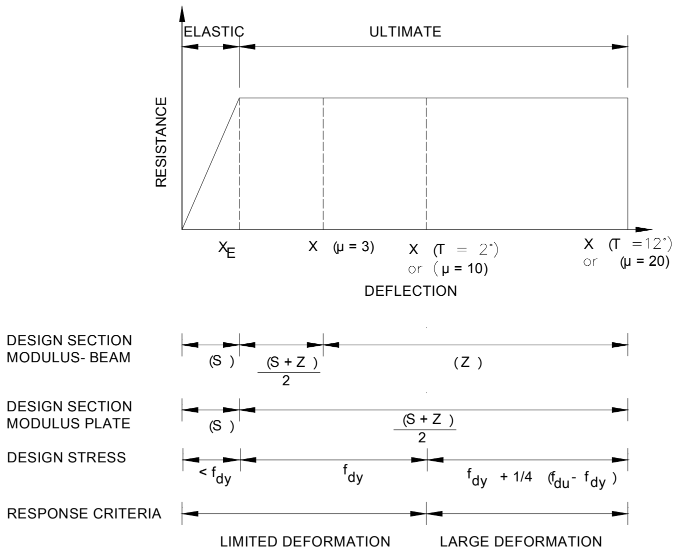

Figure 2.2

The criteria of design limits for plates and beams

The manual also prescribes some simplified formulae for the design plastic moment (M_p) and simplified resistance (R_u) which are given as follows :

$M_p = f_{ds}$ (S + Z)/2 ; (beam with ductility ratio ≤ 3) (2.2)

$M_p = f_{ds}$ Z; (beam and beam-column with ductility ratio > 3) (2.3)

Where

f_{ds} = the dynamic design stress

S = the elastic section modules

Z = the plastic section modulus

R_u= 12M_p /L* two-span continuous (2.4)

R_u = 11.7 M_p/L* exterior span of continuous beam with three or more spans (2.5)

R_u = 16.0 M_p/L* interior span of continuous beam with three or more spans (2.6)

('*' denotes for uniform distributed load and span length (L) difference not to exceed by 20 percent)

As the code is purposely for the design of buildings, it emphasizes a single explosion occurrence, whereas for offshore installations, designers have to consider several levels of explosion occurrences for ensuring that operations can be resumed as quickly as possible, or alternatively the platform has to be abandoned completely for safety reasons. The manual provides deformation criteria that can be transformed into a damage level which is valuable for evaluating topside structural members.

2.4.4 Fire and explosion guidance

The fire and explosion guidance is supported by the United Kingdom Offshore Operators Association (UKOOA) and the United Kingdom Health and Safety Executive (HSE). The guidance document consists of four parts; Part 0 (2003) discusses hazard management; Part 1 (2003) provides guidelines for avoidance and mitigation of explosions, an update of IGN (1992) (interim guidance notes); similarly, Part 2 (2006) provides guidelines for avoidance and mitigation of fires; Part 3 will provide design practices for fire and explosion engineering. At the present time, only the first three documents are available for reference.

Part 0 describes the management scheme for evaluation and assessment of risk on offshore installations. The highest level recommended by the guidance is 10^{-3} per annum beyond which is considered an unacceptable region under ALARP (as low as reasonably practicable). Part 1 provides reasonable information on explosions and includes the issue on the acceptance criteria. Similar to API RP 2FB (2006), the main objective is to provide sufficient or acceptable standards in terms of structural integrity for safe refuge and minimum exposure starting from the conceptual phase to final operation phase. Performance standards are emphasized for the control system and the safety of critical elements (for example pipelines, detection system, topside structures, and escape routes). The assessment of the structure is to be based on two levels; strength level blast and ductility level blast which is equivalent to N-004 Norsok (1998).

Although the guidance has rated risk as a summation of logarithmic frequency rating in terms of annual probability while logarithmic severity rating in terms safety, environment and asset as given by Table 2.5, there is no direct correlation to the nominal overpressure level which can be used to define the acceptance criteria of a structural system. Without this, there is a possibility that the risk study will result in an upper bound load level and impractical values that certainly can not be adopted in the design.

Table 2.5

The frequency and severity ratings

Category	Annual Probability (per year)	Frequency Rating	Category	Severity Rating
Frequent	$> 10^{-1}$	5	Severe	5
Occasional	10^{-1}-10^{-2}	4	Critical	4
Infrequent	10^{-2}-10^{-3}	3	Substantial	3
Unlikely	10^{-3}-10^{-4}	2	Marginal	2
Rare	$< 10^{-4}$	1	Negligible	1
Risk rating = Frequency rating + Severity Rating Tolerable (min) $2 \leftarrow -^{3} -^{4} -^{5} -^{6} -^{7} -^{8} -^{9} \rightarrow 10$ (max) Intolerable				

2.5 Improving the structural connection

In general, a connection at which a minimum of two or more structural components will be joined together requires special attention for effective load transfer and for controlling deformation. Investigations by Krauthammer (1999) show that the detailing of connection is crucial for determining the behaviour of structures subjected to blast loads. The author performed numerical studies on both reinforced concrete and steel connections according to TM5- 1300 design guidelines.

In one of the concrete models shown in Figure 2.3, a haunch was created at the corner between the column and beam joint. The haunch was reinforced with diagonal bars that were laid passing through the section which terminated inside the column and the beam closer to the external surface on the far side. New radial bars were hooked to diagonal bars and were spread radially into the area of column-beam. The radial bars were introduced to prevent concrete cracks parallel to the diagonal bar inside the connection. They were terminated by hooking to the main reinforcement bars of the beam and the column. With diagonal bars in-place, failure were detected outside the connection region at which the diagonal bars terminated, and the connection itself was still intact. On the other hand, in the case without diagonal bars, severe damages were found at the connection and no damage was found either on the column side or the beam side.

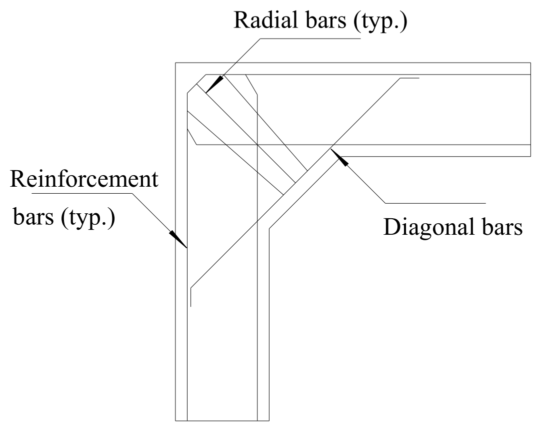

Figure 2.3

Strengthening beam to column in concrete design, Krauthammer (1999)

In the steel connection, deformation is directly linked to rigidity and flexural capacity. In the study, half span beam and half columns were modelled. The blast load was applied on both members (the column and the beam) as isosceles triangular loads. The severe local deformation was due to large rotation and substantial straining with cracks on welding was found at the interface between the flanges of the beam to the column face. Experimental data from the case study was used as a validation case and presented under section 5.8.

In a similar study of steel connection by Sabuwala et al. (2005) under the Northridge moment connection study, the beam W36 x 160 (grade A36) to column W14 x 426 (grade 50) connection was designed to AISC codes and was verified numerically (by the finite element program ABAQUS) against blast load criteria specified by TM5-1300. The existing connection was strengthened by adding 15.8 mm cover plates to the top and bottom flanges as shown by Figure 2.4. Connectivity between column and beam was achieved by continuous welding along the perimeter of the plate; butt welds to the column flange and fillet welds on the beam flange.

The findings from the study are quite interesting for column protection; with cover plates, the plastic hinge was relocated and reformed a distance away from the connection zone. A high stress concentration was observed at the ends of the plates on the beam rather than on the column. The new detail was also found to be efficient in reducing stress concentrations on the groove welds.

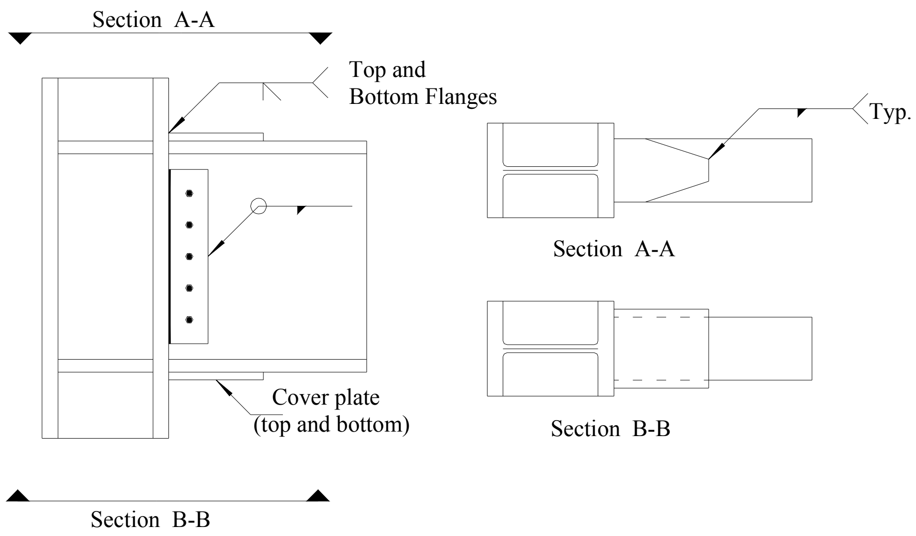

Figure 2.4

Strengthening beam to column with cover plates, Sabuwala et al. (2005)

In a study to improve ductility for a joint, free flange moment connections were developed at the University of Michigan, Choi et al. (2003), Figure 2.5. A portion of the beam web at a column interface was removed and it was replaced with a new gusset plate. There was no connectivity between the new gusset plate to the top and bottom flanges. The gusset plate was then joined with full penetration weld within a range of one sixth to one third of the plate height (effective areas) to the top and bottom of the column-beam interface area. Similarly, the gusset plate on the beam side was welded with a continuous fillet weld. The method relieved some stiffness in beam flanges and subsequently allowed unstrained flanges to deform freely in bending and axially which resulted in smaller concentrations of curvature on the flanges.

The authors showed that the shear in the flange was inversely proportional to the cubic power of the free flange length, which was the length of the web cut back. From their analytical study, a free flange connection would experience less than 10 percent of the total shear at the connection. To validate the study, experiments were conducted with variable cut configurations at webs and changes in thickness for gusset plates. The findings show that the beam with extended cut is effective in reducing web plate bending in the beam compared with a straight cut; a strong gusset plate deforms the beam to a complete plastic hinge which is away from the connection, while a weak gusset plate shows excessive deformation and causes kinking in the column. Hence, a desirable design for the gusset plate should respond with the formation of a complete plastic hinge but will limit the severe local and lateral torsional buckling on the beam.

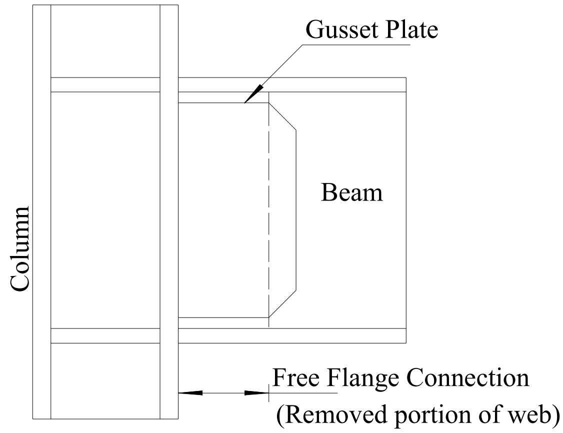

Figure 2.5

The free flange connection, Choi et al. (2003)

A portion of web area at end span is removed and replaced with gusset plate that gives free deformation on the beam.

Although the free flange connection method with gusset plate improves ductility at the beam column joint, the column will experience additional moment due to load eccentricity of the single gusset plate which is not in line with the column centreline. A continuous welding with minimum nominal weld thickness is recommended for connection between the gusset plate and the column to avoid the development of micro-cracks at weld toes caused by repetitive loadings and the development of corrosion caused by entrapped seawater. As offshore structures are subjected to various load scenarios and repair work is very costly, further tests on this type of joint need to be carried out before it is implemented practically on offshore topside structures.

In another development for improving ductility, Chen et al. (2003) investigated the effect on the beam (H588 x 300 x 12 x 20 – A36) to column (H550 x 550 x 30 x 40 – Grade 50) with a single lengthened rib plate welded on the top and bottom beam flanges as shown by Figure 2.6.

The authors divided the rib into three parts: the main reinforced part which connected the column and the beam; the intermediate part or the curved part which was intended for smooth transition between the main part and the extended rib part; the extension of the rib was for reducing the stress concentration at the end connection. This configuration allowed an access hole for a complete joint penetration weld to the column, and a single rib ensured transfer of shear to column web in the same plan. An experiment was conducted with two thicknesses for the rib. The proposed connection was analysed using ANSYS with structural members modelled as brick elements. The model plasticity was defined by Von Mises criterion and the isotropic hardening rule.

Results from the analysis showed that yielding and plastification occurred within the rib extension area, and the highest stress of the modelled connection was observed at the joint between the rib and the column. A similar observation was also noted from the experiment whereby the formation of a plastic hinge can been seen at the extended zone of the rib.

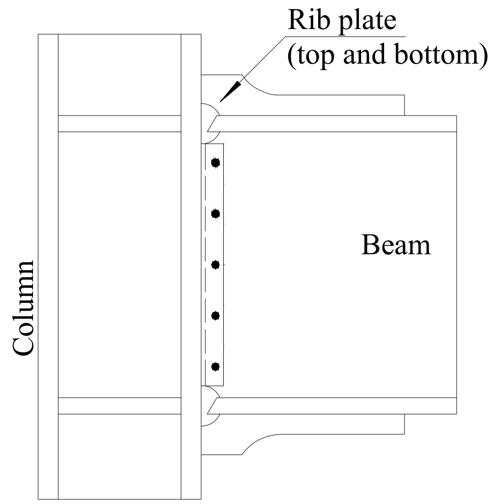

Figure 2.6

Connection strengthened with rib plate, Chen et al. (2003)

Shear tab is welded to column face and bolted to beam web.

Although both experiment and analysis have concluded that the extension of the rib has improved the ductility of the joint, no definite methods are presented in this paper to determine the effective length of the extended rib.

While other researchers improve the connection with additional material, Chen et al. (2001) enhanced the performance of the existing beam-column of the concrete floor slab by removing a portion of bottom flange close to the connection face as given by Figure 2.7. In a typical connection design, contribution of capacity by the floor slab is excluded, which contributes additional over-strength of moment capacity by approximately 16 percent as mentioned in the study. Trimming is done such that the provided moment capacity is about the same capacity to the demand level for seismic design load. This encourages enlargement of the plastic zone as well as improvements on the deformation capacity. Although reasonably successful in reducing the strain, the method still depends on good workmanship and welding quality at the connection.

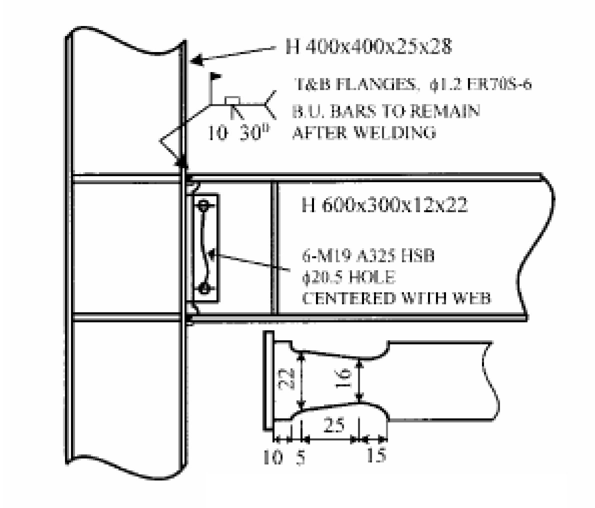

Figure 2.7

Removed bottom flange for ductility enhancement, Chen et al. (2001)

Welding at any joint depends on workmanship, drawing detailing, materials of members to be joined and the exposed conditions during welding. Dubina and Stratan (2002) performed studies on connections of moment resisting frames with various material properties and welding types.

In the conducted experiment, fifty four (54) specimens were tested. The varied parameters were the steel grades (S235 and S355), the strain rates ($\dot{\varepsilon}$ = 0.001, 0.03 and 0.06 s^{-1}), the welding types (fillet weld, single bevel butt weld and double bevel butt weld) and the applied loads (monotonic and cyclic). Based on welding defects and cyclic loading results, the main findings recommend a double bevel butt weld as an ideal weld.

There is no doubt that double bevel butt welds will remarkably minimise defects and provide a better connection compared with the other welding types. However, factors such as cost, time and condition during joint preparation, adequate access to perform the welding and functionality of structural members should also be justified in order not to jeopardize the running of the project in terms of costs and schedule. For a fillet weld, the welding is usually performed on non critical members. When fillet welds are to be applied on load carrying members, they require strict site verification of the final welding size. Single bevel butt welds are typically performed on a joint which has no access on either side or when the member is too thin for edge preparation.

Prior to the Northridge earthquake, a research program at the University of Lehigh was conducted by Moa et al (2001) and Ricles et al. (2002) to investigate the causes of brittleness for welded moment connections. Three main components that were found to have a remarkable influence on the connection behaviour were investigated; the weld access hole geometry, beam web attachment and strengthening method at the panel zone (around the connection area).

The interesting finding, which is relevant to topside design, is the effect of the access hole as given by Figure 2.8. The study involved 9 access hole configurations. These configurations were analysed using ABAQUS finite element program by measuring the development of plastic equivalent strain. The results show that configuration 2 with no access hole has the lowest PEEQ index. The next lowest PEEQ is configuration 6, where the access hole has a gentle slope and a reasonable horizontal distance to the groove area.

The access hole is important for achieving a full penetration weld, especially for a very thick material. Most access holes for primary members on offshore installations are filled up during welding or covered with plates to avoid corrosion, which can easily occur at the weld toe.

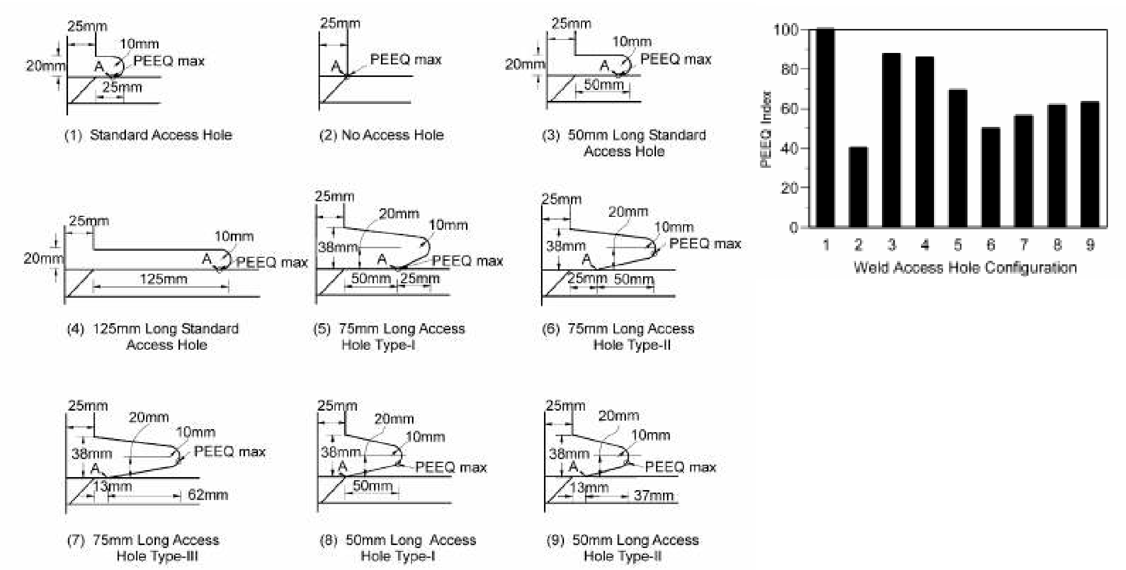

Figure 2.8

The study of access holes (cope hole) for improving connection behaviour, Moa et al. (2001) and Ricles et al. (2002)

For bolted connection designs with end plates, Mofid et al. (2005) proposed an analytical method to estimate ultimate and yielding moments with four pre-tensioned bolts. The method used a virtual work approach in association with the connection dimensions and a yield line mechanism to derive the ultimate moment capacity. The ultimate moment capacity of the connection is determined by selecting the lowest value of consolidated capacities at failures of the connecting parts which were the end plate, column (web and flange), bolts and beam (yielding moment). The theoretical Figures calculated from the method are in good agreement with experiment results by others.

Using a different approach, Da Silva and Coelho (2001) proposed a ductility model for steel connections. The connection was represented by an assembly of springs and rigid links. By identifying the tension, compression and shear zones of the connection the maximum rotation at the connection was predicted using the elastic post-buckling and bi-linear properties of the defined components, which were introduced into the model. The approach was validated against the numerical model (by the authors) and the bolted end plate of the steel beam-column (by others).

Similar to the bolted connection, but with a different material for bolts, Ocel et al. (2004) studied the possibility of using Shape Memory Alloy (SMA) bars which have shape memory effects, pseudoelasticity, high damping performances, and austenitic behaviour at higher temperature given by Figure 2.9.

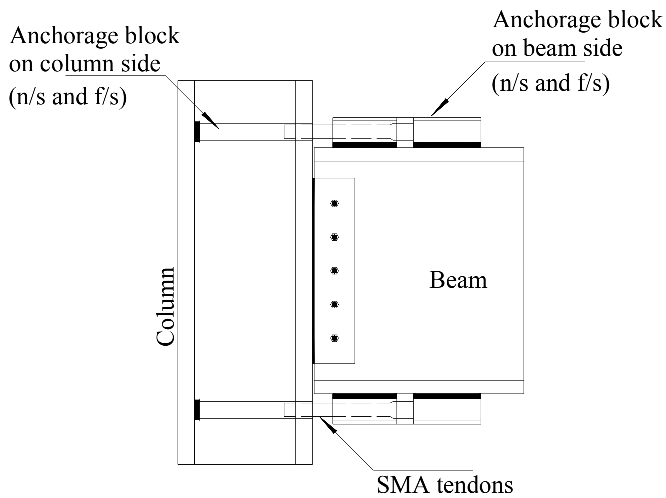

Figure 2.9

SMA tendons for column-beam connection

The tendons are anchored inside sleeves which are welded onto flange faces.

The material properties of SMA bars depend on temperatures and external forces. When external forces are applied to SMA members, the SMA twinned martensite (original shape) will undergo inter-granular dislocations and change to SMA de-twinned martensite. If heat is applied to the alloys the SMA de-twinned will change to austenite, and cooling down through transformation temperature will bring the alloys back to the original twinned martensite. In the experiment, the beam flanges were welded to the anchorage blocks that hold the SMA tendons (two tendons each at top and bottom) to a column while shear force was transferred to the column flange through a shear tab with five holes. The failed SMA tendons were heated using an oxy-acetylene torch to recover their original shape. In the current situation, the application of SMA materials are still at an experiment stage on structures although they are widely used in biomedical applications. The ability of SMA to recover from deformation, either in free or restrained conditions, is an advantage but uncontrolled heating would intentionally generate a large heat affected zone (HAZ) at the connection, which can weaken instead of improving the connection.

The main aim of the design of connections subjected to blast loading is to prevent catastrophic collapse by allowing small deformations or relocating significant deformations away from the connection itself. The connected components, usually the beams with existing loads, are expected to experience some degree of damage within the acceptable reduction in structural integrity, mentioned by Baker et al. (1983) and N-004 Norsok (1998). As the impact of the blast is quite significant, but is a relatively low recurrence event, any method proposed to overcome the shortcomings should have the merits of minimum maintenance, be workable, and cost efficient. It is also worth noting that on most offshore installations, due to the nature of the surrounding environments, maintenance reasons together with a combination of cyclic loading from equipment, bolt connections are unfavourable for the connection of primary members or truss joints.

2.6 Secondary structural members - plates

Thin plates are commonly used on offshore installations as deck flooring and for compartmentalizing process areas. Despite the fact that these plates are classified as secondary structural components (easy to be replaced and large distortion is allowed), their behaviours are notably relevant to the response of supporting beams.

Schleyer and Campbell et al. (1996) and Schleyer et al.(2003) developed simplified analytical techniques to predict the response of the structural components subjected to blast and fire loadings in which an energy method and heat balance approach are employed to estimate the deformation of the clamped plate and temperature rise for thinned wall sections. The assessments of the study were validated by a series of experiments conducted inside a blast pressurized chamber and jet fire test facility respectively.

Corrugated profiled barriers studied by Boh et al. (2004a) concluded that deep sections exhibit brittle behaviour and are sensitive to imperfections, while shallow sections exhibit more ductile behaviour and are non-sensitive to imperfection. The authors suggested that a scheme of a minimum of 3 bays of the profiled barriers or more, which depended on the ratio length/width with fine meshing, would be adequate to capture post peak and ductility responses.

The performance of the profiled barriers was also linked to the material idealization and the boundary conditions. A typical idealization of elastic perfectly plastic material behaviour would underestimate the deflection response after yielding and showed no correlation with the actual stress-strain curve of the material. Improper constraints imposed at the edges were also found to affect the post buckling response and the mobilization of membrane forces.

The study on profiled barriers was further extended by the same authors (Boh et al. (2005)) with a diagonal structural member (passive impact barrier system) placed behind the panel with an offset. A small offset limits the deformation of the panel and may require a heavy section, while a large offset is considered ineffective due to a reduction in contact area. This mitigation technique improves the dissipation of energy to the system, especially on the panel and the brace. As much more energy is dissipated on these two components, it reduces the energy transfer to the supports and consequently, delaying the failure at the supports. Having a brace fixed to a support frame and behind the panel, the capacity was enhanced to more than 50 percent and 80 percent for deep and shallow blast walls respectively.

Similarly, from the experiment results performed by Langdon and Schleyer (2005) on profiled panels, and Langdon et al. (2005) it was showed that as supports became less restrained and more flexible, connections tended to move inwards and increase the central displacement. However, these connections were independent of overpressure directionality for asymmetric profiled panels. A short outstand was found to retain much of the strength in the post buckling regime, while a long outstand collapsed and exhibited no post-buckling regime at all. Optimization of these parameters that related to behaviour performance is key in designing profiled barrier walls that could prevent damage to main supporting structures, allow as much as energy absorption in bending and stretching, and limit the displacement.

The study of flat plates with stiffeners conducted by Yuen et al. (2005) and Langdon et al. (2005) reveal the following; for the unstiffened case, plastic hinges occur along the diagonal from centre to corner, followed by tearing at the middle of the edge supports; for single and double stiffeners, similar responses are observed with a reduction in displacement; for cross stiffeners, they demonstrate higher resistance compared with double stiffeners, thinning is observed at the cross; for double cross-stiffeners, the response is similar to cross stiffeners, less displacement compared with cross stiffeners, and the occurrence of localized tearing. Based on ABAQUS analyses, the results compared favourably with the experiments.

Most studies have considered plates as a separate structural entity. For deck plates, the more realistic approach is to consider existing deformations caused by the interaction with in-place loads and to be combined concurrently with dynamic load effects.

It is quite common on the topside structure for a secondary structural frame system to consist of vertical posts and slightly heavier stringer beams as horizontal members are provided to support the blast panel. Many more studies should be conducted to look into proper connectivity between the panel for ensuring load transfer effectively from the secondary frame system to main framing as well as the possibility of disengagement from the supports that are likely to occur after substantial damage to the panel.

2.7 Ductility for blast design and brittleness of steel connection

A ductile material is a material which allows plastic deformation without losing its strength before fracture occurs, while a brittle material is a material which allows little or no plastic deformation. Low temperature and strain rates are the two main physical factors that have a greater impact on the ductility of a material. Typically, materials become brittle at temperatures below room temperature; the effects of higher strain rates at plastic deformation decrease the toughness, and this is crucial for a blast resistant design because high strain rates are expected as discussed by many authors including Izzuddin and Smith (1997) and Alves (2000).

In a study by Boh et al. (2004b) on the connections of stainless steel corrugated firewalls subjected to hydrocarbon explosions, a modified Cowper-Symonds equation was adopted to allow for strain rate effects. Two failure models were also used to model tearing, a spot-weld model (discrete weld points) and a shear model (rupture strain). By embracing the effects of strain rates in both models, they showed an increased in loading capacity for supporting welds because of stiffening during plastic strain hardening. It was also found that the time of plastic yielding was insensitive to the strain rate while the dissipated energy depended on the failure criteria adopted in the model.

During hydrocarbon explosions on offshore installations, the ductility of joints is the key safety element which relates to structural performance as well as the level of damage. Primary members of the installation must not collapse and provide safe escape after the event; all main connections should not have yield strength much higher than expected which can overload and prevent yielding of adjacent members. Therefore, in blast engineering where safety is the main concern, requirement of ductility for materials and the responses against the accidental loads are critical issues, which can only be achieved through a better understanding of fracture characteristics, both brittle and ductile.

As most joints on offshore platforms are welded connections, preparation work for pre and post welding procedures are necessary for minimizing defects during which brittleness on welds can occur and reduce ductility. Table 2.7 summarises the possible sources of brittleness caused by fabrication work and impurities added during making of steel for improving strength. Mitigation measures to combat brittleness should include both fabrication procedures and quality checks on materials.

Under performance based design prescription, major oil operators such as BP and ExxonMobil have set up some common values of ductility ratios for use in the design work of offshore installations. The following lists the recommended ductility ratios currently being used in design of structural components:

Part of structural members	Ductility ratios
Load bearing panels	1
Beams and non-load bearing	5
Rotation beam-column	2 or 12^{o}

Design consultant Company, Brown & Root recommended the following ductility ratios:

Part of structural members	Ductility ratios
Secondary structures	1.5
Blast wall	2.5

However, Scheler et al. (1991) from Mobil recommended the following:

Part of structural members	Deformation
Steel beam rotation (compact section)	12^o
Plates rotation	12^o

The structural member is considered to fail if the ductility ratio has exceeded 20 as given by TM 5 1300, Figure 2.2. On the other hand, Yasseri (2005) contextualised ductility ratios into five ranked levels of damages as shown by Table 2.6. In his approach, the author has limited ductility ratios into a range of performances. Lower damage is allowed for compensating deformation caused by membrane forces. A higher ductility ratio greater than six is classified as high in economic loss terms whereas a ductility ratio of less than one, which is within the elastic region as classified as negligible loss with no repair work.

Table 2.6

Damage levels, Yasseri (2005)

Ranking of Damage levels	Acceptable Limits
High (Beyond repair and total loss)	$\mu \geq 6$
Substantial (Repairable damage for main load bearing system but major loss for equipment with shutdown.)	$4 \leq \mu \leq 6$
Moderate (Repairable damage and interruption to production; resume production after inspection, repair and replacement)	$2 \leq \mu \leq 4$
Light (Minimum repair and no interruption to production)	$1 \leq \mu \leq 2$
Negligible (No repair is required)	$\mu < 1$

Table 2.7
Reduction in ductility at the connection: effects and improvement techniques

Sources of Brittleness	The effects	The Mitigations
• Heat from welding process	Creation of brittle martensite by the heat from welding process followed by a rapid cooling process.	Preheat the base metal prior to welding and maintain the heat thorough out the welding process.
• Flame Cutting	For examples: making access hole , cutting of plates and surface preparation for connections create brittle martensite.	All cut regions and surfaces must be ground smooth.
• Hydrogen	Trapped hydrogen gas at rapid cooling after welding generates high pressure and potential micro cracks.	Use low hydrogen and oven-dried electrodes prior to welding.
• Weld restraint	Improper welding sequence and weld configuration induce internal stresses due to weld shrinkage	Engage qualified welders and implement control welding procedures. The procedures must be prepared by experienced welding engineers.
• Partial weld penetration	Applied loading exceeds the weld carrying capacity, initiates crack at the root of partial weld.	Remove the uncertainties by avoiding this type of welding.
• Presence of alloys (C, Mn, Si, Cr, Mo, V, Ni, and Cu)	Added alloys for increasing the toughness and strength by the mills	Control quantity of alloys using carbon equivalent content based on provided steels' mill certificates.
• Very thick plates (thickness greater than 65 mm)	Prone to lamellar tearing, welding distortion and shrinkage.	Implement post weld heat treatment, PWHT. The common PWHT is performed after the last pass of welding at 230^oC Funderburk (1998) and to be maintained 1 hour per inch of thickness. This method must be justified with requirement and cost.
• Lamellar tearing	Commonly found in thick plates, originates from mills with presence of non-metallic compounds during rolling and flattening induces micro-cracks that grow and link with each other when stresses are applied in through thickness direction	These plates can not be used as main primary members such as plate girders and lifting padeyes

2.8 Concluding remarks

The design chasm between the performance based approach and the strength design methodology is about a design which is based on the behaviour and response exhibited by members, either as components or as a whole system. Structural members are checked against the conclusive levels that are being determined by involved parties rather than a specified design specification. Nevertheless, existing available references can not be totally ignored and discarded in the design process as they are quite useful for benchmarking purposes. Although the attainment of design goals in performance based design methodology involves rigorous inputs and intensive re-works for deciding the performance levels, the end result is certainly worthwhile for consideration as the design approach has accounted for safety and economic aspects.

It has been acknowledged that an effective load transfer and the protection of structure subjected to blast loads depend on types of joints, materials and workmanship, as highlighted in most literatures. Unfortunately, only a few authors have recognised the importance of maintenance work, probably because they are onshore based where most connections are well protected, easily accessed and not exposed to aggressive environments. As most topside structures are made from steel and located remotely, the main culprit of joint deterioration is caused by environmental and process plant factors i.e. corrosion. All structural joints and primary members must be periodically checked. Prevention is made as early as possible starting with the fabrication period where major joints compulsorily undergo non-destructive testing until the last day of decommissioning by visual inspection. Therefore, an effective and workable design must be kept as simple as possible with minimum maintenance and some opportunities for strengthening in the future.

Under mitigation work, the intention for improving the joint by adding additional plates will have to be given proper consideration and it is highly likely that it may involve substantial work for major connections. This is because of the effect of reactions from the existing equipment loads. The loads should be temporarily transferred to the other supports or removed elsewhere in order to minimise distortion due to the welding process and for ensuring the effectiveness of the newly added plate.

The current design practices emphasise ductility evaluation as a last resort when the strength based check has exceeded the stress unity ratio. The recommended design value is individually based and is primarily for the main members. As the available reserved capacity of these members are uncertain therefore the design of the secondary members will not be optimised. For an ideal case, theoretically, a large deformation on secondary members will minimise damage on main members as more energy will be absorbed. In the forthcoming chapters the present study will demonstrate the major contribution made by secondary members, which has sometimes been overlooked during the design process for improving the global performance of the topside structure.

Chapter Three

Performance Based Design for Blast Resistant Offshore Structures

3.1 Introduction - The aim of performance based design

The methodology of performance based design is not a new approach in civil engineering applications. The concept was first implemented in 1963 for the construction of buildings by Nordiska Komitten for Byggbestammelser (NKB) in Olso and reported by Inokuma (2002). The approach was then converted into a five stage framework called NKB level for use in five countries in Northern Europe. In 1980 and 1984, these criteria were enacted by The International Organization for standardization (ISO) in the building codes (ISO 6420-1980/ BS 6019:1980 and ISO 6421-1984). The implementation by ISO was later followed by other nations, such as the UK in The Building Regulation (1991), the New Zealand Building code (1992), the US in seismic resistance performance of buildings (1995), Australia’s Building Codes Board (1996), and Japan’s Standard Building Law (1998).

Generally, the design steps of the approach for building design given by Figure 3.1 begin by setting the required performance as a paramount goal to be achieved, followed by verifying consequences in which situations or conditions are evaluated and finally solving problems within acceptable limits based upon the actual behaviours of building components during evaluation.

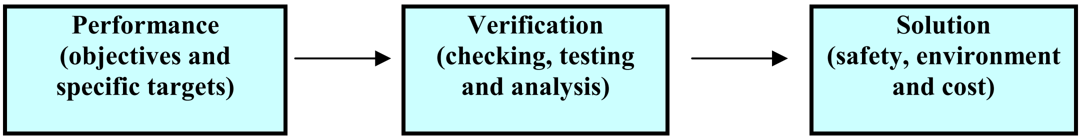

Figure 3.1

The basis of performance based design in building design
(Arrows denote the flow of the process)

In the oil and gas industry for the design of offshore structures, the application of performance based design was not as well received when compared with the building industry. This was due to:

a. The complexity of design conditions (i.e. load out, lifting, sea transport, installation, commissioning) for which structures were to be designed and atypical design processes for each of the platforms that is dependent on reservoir capacity and impurities in hydrocarbon sources.

b. The fast track nature of offshore projects as most design work commences immediately after confirmation of the supply contract between the operator and buyers in which the duration of the project is fixed within a specific time. Any late changes in design are unacceptable as they might affect the ordered materials, delay the fabrication work, increase costs as well as the project overall schedule.

c. The limitation of the hardware and software for evaluating and predicting structural behaviour in the non linear range.

However, with the recent advancements in computing technology, such as the availability of non linear analysis software packages, high speed machines with faster run times and improvements at testing facilities (at large scales) has potentially allowed the application of the approach in the offshore design environment.

For the topside structures under extreme design loads, the terminology and the basis of performance based design are related to the minimum use of the design codes in which the design is to be based on the characteristic behaviour of a single component or a combination of responses by a group of individual components as a global based structural system. From the likely scenarios of blast events, a set of demand levels for a topside structure is assigned. The demand levels consist of multi-stages of design approach for engineers to evaluate the structural performance under a number of explosion scenarios based on previous incidents and a large volume of data generated experimentally and numerically. The more likely scenarios are normally highlighted in a quantitative risk assessment.

The approach of performance based design for topside structures presented in this chapter starts by defining objectives, postulating possible scenarios, identifying consequences, setting engineering demands, and improving and mitigating for these so that a marked reduction in failures can be achieved.

A facility that meets the defined requirements is judged as acceptable in the sense that adequate protection to personnel is provided such that the risk is as practically and reasonably low as possible (ALARP), and which is economically and politically acceptable.

3.2 Performance based design assessment and evaluation

The primary objective of performance based design for blast resistance on offshore installations is to optimise the predictable interaction behaviour of supporting structures in relation to functions of a system in terms of risk containment and avoiding conservatism, Louca and Mohamed Ali (2007). Whether the installations are the new planned platforms (i.e. at the design stage level) or the existing platforms (i.e. a mitigation case with new inventories), a design assessment on individual topsides shall be set out such that the fundamental principles of the methodology shall meet the defined design performance objectives. Designers and operators will be working together in defining the required performance levels of an installation while regulator bodies will look after the interests of the public (i.e. environment and safety). The end product of the design assessment shall be a robust structure in which the safety of critical elements is taken into account, as well as the likely risk as a result of hydrocarbon explosions is minimised.

The flowchart shown in Figure 3.2 is a proposed method for the assessment of offshore installations subject to blast load with respect to performance based design methodology. The chart is applicable for evaluating structural components and a global structural system. Each of the algorithms shown in the chart is discussed in the following sub-sections.
A point worth noting is that although the method of performance based design is supposed to be the minimum use of design codes, some elements of design aspects from the codes are discussed in this paper for ensuring continuity in the structural performance.

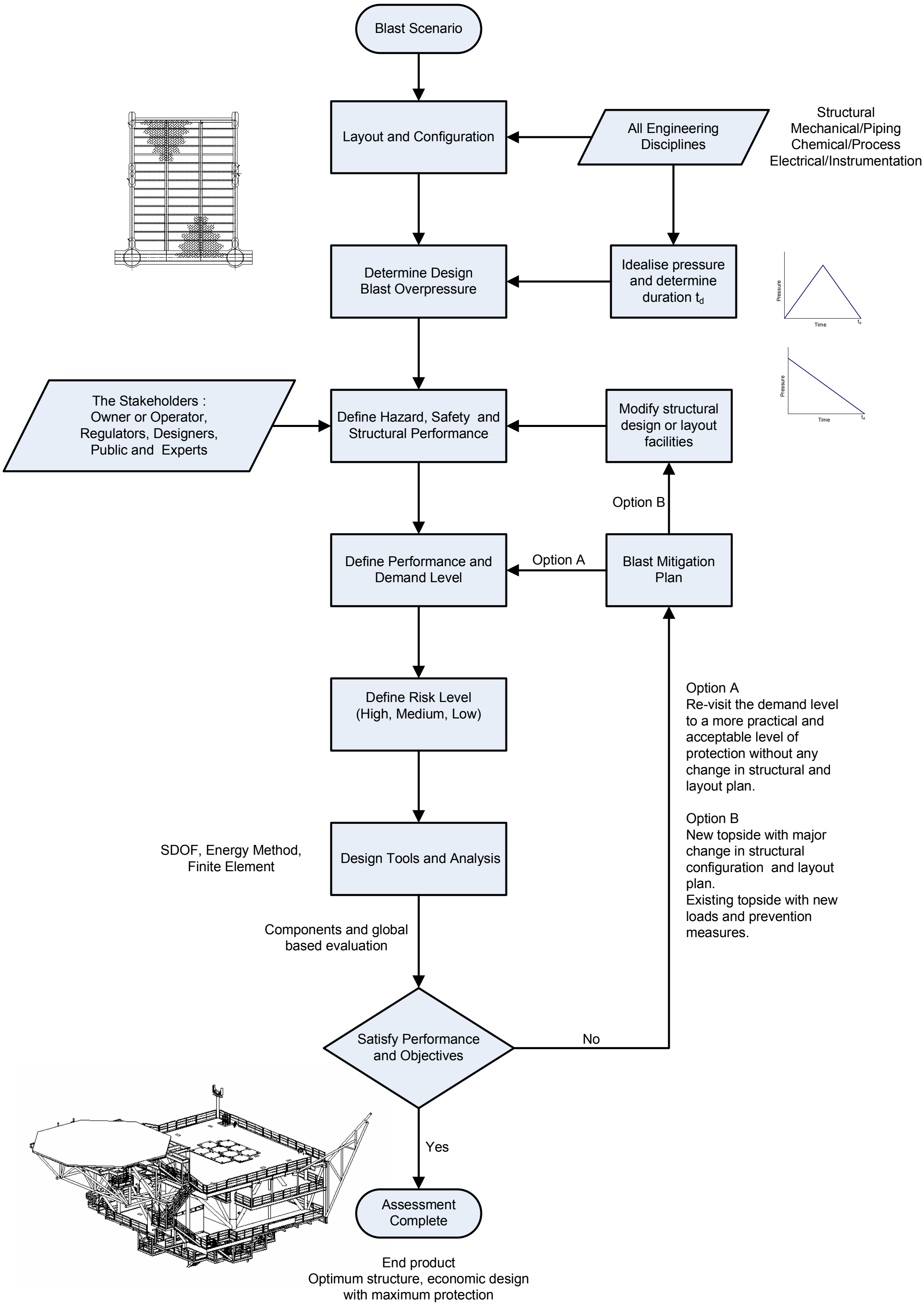

Figure 3.2

The proposed performance based design assessment for blast of topside structures of offshore installations

3.2.1 Blast scenario on offshore topsides

Most explosions on offshore installations are caused by the ignition of air mixed with accidental and release of hydrocarbon sources. The impact creates a sudden and violent release of energy during which the surrounding air is compressed and moves in all directions. Any obstruction along the wave propagation generates overpressure load.

From the safety point of view, these incidences must be kept as low as possible, whilst from the design point of view, all possible scenarios must be accounted for in the design. However, the design should be selective as failure on a single component is not an indication of the structural global failure. These are the two major obstacles in performance based design highlighted by Yasseri (2003b). Thus, defining the blast load level at this stage is crucial in order to define the performance levels and for meeting the engineering demands. Having designed according to the specific levels, the components must also exhibit sufficient capacity for operation and maintenance of the platform.

The combined physical and cultural factors (human behaviour) that can promote the implication of blast load on the platform are as follows (Bruce (1995), Lees (1996), Crawley and Grant (1997), Carter et al. (2003), Fire and Explosion Guidance Part 0, 1 (2003) and 2 (2006), API RP 2 FB (2006)):

a. too many inventories

b. concentration of equipment, piping and valves in certain areas

c. ignition sources, risers and wells

d. production type

e. deck type (openness and ventilation), location and weather

f. design life, re-supply frequency, maintenance and safety management

g. negligence application of safety procedures.

Integrating these factors with blast scenarios results in conditions that involve multiple failures, which should be considered and analysed. This calls for the implementation of Quantitative Risk Assessment (QRA).

In simplified terminology, QRA is a study to estimate and evaluate risks as well as mitigation for use by both internal (designers and clients) and external communities. Although there are some disadvantages (e.g. human errors, software failures and safety cultures) in this approach as described by Apostolakis (2004), the advantages outnumber the drawbacks. In the context of performance based design, in which decision making is risk informed, the usefulness of QRA will lead to the following outcomes:

a) a complete in-depth understanding of the topside structure failure modes.

b) a clear cut relationship rather than a complex interaction between the event of explosions and a system which suits the client's requirements.

c) a common understanding of the problem facilitating communication among the various stakeholders involved in the project.

d) provide proactive solutions as a result of combined input from multi disciplines of engineering and public views.

e) identify the dominant risk of blast on which designers can concentrate, thus no waste of resources or other insignificant risk.

f) identify the aspect of uncertainties (such as human errors and the physical phenomena of the blast) which need further research.

As a rule of thumb in design, when an area on the installation has the potential for being exposed to hydrocarbon sources, it should be classified as a hazardous area. Any equipment with potential leaks is to be considered as a great risk. Combining the effects of leakage and escalation, they can be transformed into categories of damage levels which then can be used to benchmark the performance of a structural system.

3.2.2 Layout and structural configuration

The development of a layout plan and structural configuration are the combined inputs and efforts originating from multi-disciplines which enable safety engineers to distinguish safe areas for protection from hazardous areas. It will be an advantage in design if the main layout plan and structural configuration can be finalised at an early stage of the design work as not only design uncertainties will be removed in QRA study but also will allow design engineers to concentrate on areas with high a probability of explosive occurrences.

The performance of the structural components can be monitored by having references at critical points in the layout, particularly at equipment supports, major connections and middle spans. Structural engineers are also responsible for ensuring that the load path of the blast loads will be transmitted efficiently to supporting structural members. The layout and structural configuration should be peer reviewed by a third party, independent checkers or qualified professionals for ensuring all aspects related to blast loads have been covered and evaluated.

Due to the fact that layout is generally governed by the process plant, pro-active contributions from engineers of other disciplines are crucial to assist structural engineers in developing a scheme which is simple, workable, cost effective and low risk.

3.2.3 Design blast loads

The main output of a blast caused by a hydrocarbon explosion is overpressure load followed by drag loading from blast wind, and possible missile loads from small flying objects as a secondary effect. Fire and Explosion Part 0 (2003) under section 5, discusses the current findings and behaviour of the blast loads. As the three aforementioned features of explosions occur consecutively in a very short period of time, their occurrences must be given attention for avoiding scenarios which could further cause an unprecedented scale of damage.

3.2.3.1 Overpressure load

Hydrocarbon gas explosions are comparatively low frequency accidental events with the capability of serious impacts, either through direct exposure or as a result of an escalation of the initial event. The duration of the explosion, t_d is typically in the range of between 50 ms to 200 ms, which is quite close to the fundamental period for typical topside structures. Typical values of fundamental period of offshore installations lie between 300 ms to 1100 ms. The dominant characteristics of overpressure include; rate of rise, peak pressure and area under the curve, which shall be maintained when idealizing pressure time curve. Due to the large number of parameters involved, the process to determine overpressure load has evolved from deterministic techniques (possible events), followed by phenomenological models (empirical correlation) and computational fluid dynamics (3-D finite volume model).

The aforementioned techniques, which fall under QRA study, provide engineers with the nominal overpressure values or alternatively the overpressure exceedance (probability of any particular level of overpressure being exceeded) for design purposes. Figure 3.3 shows a graph of exceedance – overpressure as an indicative reference for typical hydrocarbon explosions while a compilation of design overpressure is given by Table 3.1 As shown in the Figure, low overpressure values are dominated by a higher frequency of exceedance values and vice versa. The maximum peak pressure (at low frequency of exceedance) of 3.0 bar up to 4.0 bar is recommended for the design of primary supporting trusses, while nominal load for open deck flooring is recommended between 0.5 bar to 1.0 bar (at high frequency of exceedance) .

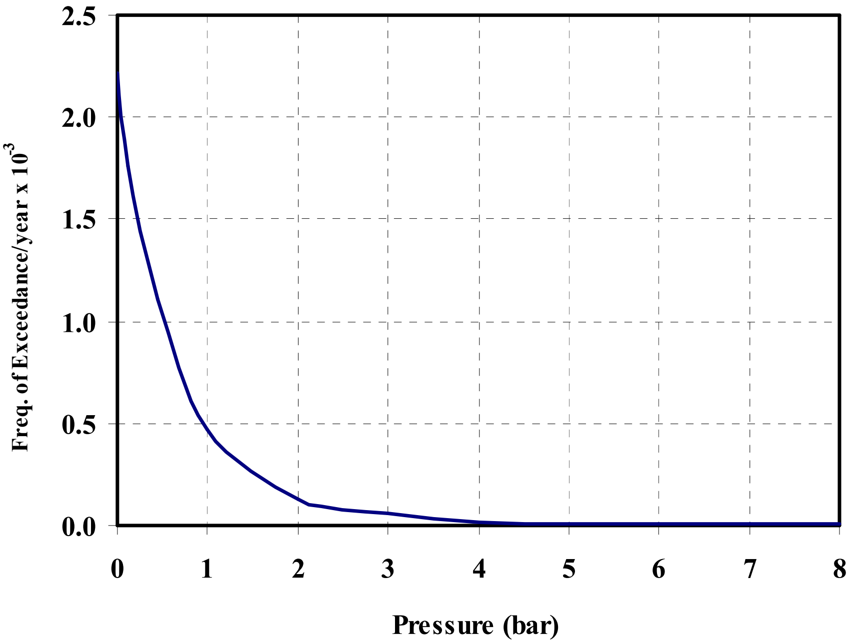

Figure 3.3

The frequency of exceedance – overpressure Corr et al. (1999)

(High overpressure with low occurrence results in a longer year of return period

Corr et al. (1999) proposed the probabilities of 10^{-3}, 10^{-4} and 10^{-5} as high, moderate and low events respectively. High probability events represent a platform that will initially close down but can resume operation within a couple of days, while low probability events are referred to as severe damages and the platform is expected to survive for safe escape of personnel.

For moderate events, some equipment is expected to be operable while secondary structural members will sustain allowable deformation with some minor damages on primary structural members.

Rather than having fixed values, as was mentioned by Corr et al. (1999), Fire and Explosion Guidance Part 0 (2003) provides some general terms of equivalent annual probabilities of occurrences whereby a rare case is defined with probability less than 10^{-4} while a frequent case is defined with probability greater than 10^{-1}. In between these two extreme cases, three more additional cases are introduced, which are occasional (probability from 10^{-1} to 10^{-2}), infrequent (probability from 10^{-2} to 10^{-3}) and unlikely (probability from 10^{-3} to 10^{-4}).

Table 3.1

Nominal blast overpressure

Blast area	Pressure (bar)*
Wellhead deck	2.0 to 2.5
Gas separation facilities	1.5 to 2.0
Gas treatment compression facilities	1.0 to 1.5
Process area, large or congested	0.5
Process area, small and not congested	0.2
Open drill floor	0.2
Totally enclosed compartment	4.0

* IGN (1992), Fire and Explosion Guidance Part 0 and 1 (2003), API RP 2FB (2006)

3.2.3.2 Drag load

Drag forces are caused by the wind of the blast load and the impact is significant on small objects such as piping lines and electrical cable trays. These forces can be calculated according to the Eq. (3.1)

$$F_D = \tfrac{1}{2}\, C_D\, \rho\, v_{gas}^2\, A \qquad (3.1)$$

Where C_D = drag coefficient

ρ = density of gas

v_{gas} = velocity of gas flow

A = projected area of the object normal to the flow direction

Since ρ and v_{gas} are not straight forward and are quite hard to predict, Eq. (3.1) is simplified to the empirical expression as follows (Eknes and Moan (1994)):

$$q_D = C_D \; p(t) \; D \tag{3.2}$$

Where q_D = line load on pipe

p(t) = maximum overpressure time-history

D = outer pipe diameter

3.2.3.3 Missile load

The subsequent effects of drag loads are missile loads. Missiles are considered to be all kinds of flying objects as well as fragments caused by the rupturing of equipment. The equation for missile loads originated from drag forces Eq. (3.1) and can be described as follows:

$$F_{Missile} = \tfrac{1}{2} C_D \; \rho \; (v_{gas} - v_{missile})^2 A \tag{3.3}$$

Where $F_{missile}$ = drag force on the missile

$v_{missile}$ = velocity of the missile

Tan and Simmonds (1991) (quoted by Eknes and Moan (1994)) correlated maximum gas velocity ($v_{g\max}$), duration of the gas flow ($t_{g\max}$) and mass of missile to empirical parameter α for calculating the peak velocity.

$$\alpha^2 = \tfrac{1}{2} \rho \, C_D \, A \, v_{g\max} \frac{t_{g\max}}{M} \tag{3.4}$$

Where $v_{g\max}$ = maximum gas velocity

M = mass of the missile

$t_{g\max}$ = duration of the gas flow.

Then the peak velocity of the missile is written as:

$$v_{missile} = v_{g\max} \left[1 - \frac{\sqrt{2}}{\alpha} \tan^{-1} \left(\tanh \frac{\alpha}{\sqrt{2}} \right) \right] \tag{3.5}$$

3.2.4 Hazard, safety and structural performance

The appreciation of hazard assessment shall be performed prior to deciding which assets are to be protected and the determination of safety levels to be applied on the working areas of the installation. The essential elements for hazard assessment should include hazard identification and characterisation (severity/location), consequence modelling (possible effect and specifying appropriate safeguard) and probabilistic risk assessment (discussed in section 3.2.1)

Hazard can also be defined based on the most vulnerable, and the likelihood of escalation effects by blast loads. There is also a possibility that the damaged assets could pose further hazards to human beings, the implication being that they can cause injury and possibly death. Human responses to blasts can be divided into 3 categories (Smith and Hetherington (1994) and Gruss (2006)):

i. Primary injury
Due to direct exposure and severe injuries are likely to the abdomen (internal organs) and ear drum

ii. Secondary injury
Due to impact by missiles. Possible laceration, penetration and blunt trauma

iii. Tertiary injury
Due to displacement of the entire body;

While Fire and Explosion Guidance Part 0 (2003) under hazards management, defines incidents within 4 categories of general accidents :

i.. Catastrophic – multiple death

ii.. Fatal – single death and or multiple injuries

iii. Severe – single severe injury and or multiple minor injuries

iv. Minor – at most single minor injury

Table 3.2

Effects of overpressure on human

Overpressure – bar*	Damage
0.03	Temporary loss of hearing
0.35	Threshold for eardrum rupture
0.4	Minor lung damage
1.0	Severe lung damage
3.0	Low mortality rate
7.0	High mortality rate

*Baker et al. (1983), Smith and Hetheringtin (1994), and Crawley and Grant (1997)

Nevertheless, the injury to human beings must be minimised as low as possible since most human body parts are irreplaceable. Table 3.2 relates injury to the level of overpressure while Table 3.3 summarises the effects of blast escalation on equipment.

From these tables, a deduction can be made that, although priority in design accentuates the performance and integrity of a structural system, containment of blast escalation must not be overlooked in order to avert additional substantial damage.

Table 3.3

The hazards and the possible escalation effects on assets and structures

Components	The weakest parts	The effects
Vessels (separators, scrubbers etc.), heat exchanger etc.	Attached piping lines and instrumentation units, and structural supports	Drag load, relative displacement, missile load and further leakage.
Piping lines, valves, tanks, launcher/receiver etc.	Structural supports	Drag load, missile load, further leakage and possible failure of a system.
Electrical cables and trays, motors, gas meter, pump, blower, solar panel etc.	Structural supports	Drag load, missile load, back-up power failure.
Safety system (backup generator, firewater, escape ways, separation wall, temporary refuge etc.)	Attached piping lines, connections and structural supports	Loss control of equipment, drag load, missile load and further leakage.
Structural components (secondary and primary members)	Connections and supports	Failure of supports and compartmentalisation, and large relative displacement. Collapse of the whole system.

3.2.5 Performance and demand levels

In non-technical terms and from a regulator's perspective, the objective of performance based design for explosions is mainly focused on life safety and damage to the environment. On the other hand, the operator/owner may define performance as objectives or statements of the desired installation behaviour subjected to a specified severity of explosion. As there is always an element of subjectivity (most of the times are related to costs and schedule) to evaluate the regulator's demands against the operator requirements, especially for quantifying the design work, the concept of multi-level performances is introduced. The resistance of the structural system is investigated according to the defined performance levels and then results are transformed into a presentable conclusion which links the engineering perspectives and the requirements of stakeholders.

In order to define performance levels, consequence events need to be identified at the outset. The degree of consequences may vary from one installation to another depending on the type of platform, its location and the regulator's requirements. Unlimited cases of consequence events can be idealised but in this present study the consequence events are proposed as four events. These events are the functional, operational, life safety and failure/near collapse, all of which can have major impacts on design and cost. Similarly, the explosion levels are simplified to four levels; frequent, occasional, rare and remote. The expected responses of the topside structural system with respect to each performance level are proposed as follows:

a. Functional

Level 1	major interruption to daily work routine but shut down of platform is not required
Level 2	daily work routine can be resumed after inspection is made
Level 3	daily work routine can be resumed immediately

Fatality is intolerable and very minimum damage to the equipment and other inventories. All structural supporting systems are intact.

b. Operational

Level 1	significant loss of reservoir and total shut down for repair.
Level 2	temporary shut down or low volume of production for the flow-lines.
Level 3	localised damage events, minimum impact on operation or public interest.

Fatality is intolerable. Minor damage to equipment is acceptable and within the economics of repair. The supporting structural systems require inspection before resuming operation.

c. Life Safety

Level 1	loss of life and health/safety implications for the general public
Level 2	serious injury and minimum health/safety implications for the general public.
Level 3	minor injury to personnel and no health/safety implications for the general public.

Injury is acceptable but fatality is intolerable. The damage on equipment is major with high costs to repair and loss of some structural supporting systems.

d. Failure/ Near Collapse scenario

Level 1	potential well flows, likely result in sea contamination and environmental problems.
Level 2	production shut down, sea contamination can be controlled.
Level 3	production shut down, contamination is limited on topside area only.

Fatality is tolerable. The damage on equipment and supporting systems is very significant. Costs to repair are beyond economic reasons and platform can be decommissioned completely.

Relatively, very little data is available to link between the load damage level and the structural performance level. This is due to the fact that it is the Client's policy not to reveal any design information, especially to its rival companies, furthermore the cost for development of QRA study is quite enormous and time consuming. In the absence of a QRA study or past history, we propose a Performance based design level for topside structures of offshore installations as shown by Figure 3.4. The basis of our proposal is on the following references, Baker et al. (1983), Chen and Han (1991), Evans (1994), Smith and Hetherington (1994), Crawley and Grant (1997), Corr et al. (1999), Vinnem (2000), Yasseri (2002) and (2003a), Bakke and Hansen (2003), Carter et al. (2003), Fire and Explosion Guide Part 0 and 1(2003), and 2 (2006), API RP 2FB (2006), Louca and Mohamed Ali (2007), Bjerketvedt et al. - Gas Explosion Handbook[11]:

i. The structural layout on the deck level is quite typical from one platform to another. The stringer beams (secondary beams) are commonly spaced 1000 mm - 1200 mm apart, while equipment is seated on dedicated beams which are directly supported by the primary beams. Other design considerations include; the pre-service conditions (load-out, lifting and sea transport) and operation conditions inclusive of maintenance must also be accounted for in design. The configuration for the primary beams is usually made consistent with the arrangement of stringer beams/equipment supports for facilitating fabrication work. As blast load will mostly first impinge on secondary members due to a large surface area, upsizing of primary members may not make any significant change to the performance level if the blast load path of the structural configuration is not well addressed.

Performance/ Occurrence	Functional	Operational	Life Safety	Failure/Collapse
Frequent Prob. **10%** in ***n*** years **or** Annual Freq. **< 10^{-2}** Performance acceptance **0.25 bar** < Pr. < **0.75 bar**	**High risk and fatality is intolerable** **Recommended for design**	High risk and fatality is intolerable (x)	High risk and fatality is intolerable (x)	Medium risk and fatality is intolerable (x)
Occasional Prob. **5%** in ***n*** years **or** **10^{-2}** < Annual Freq. < **10^{-3}** Performance acceptance **0.75 bar**< Pr. < **1.25 bar**	High risk and fatality is intolerable (+)	**High risk and fatality is intolerable** **Recommended for design**	Medium risk and fatality is intolerable (x)	Low risk and fatality is tolerable (x)
Rare Prob. **1%** in ***n*** years **or** **10^{-3}** < Annual Freq. < **10^{-4}** Performance acceptance **1.25 bar** < Pr. < **2.0 bar**	High risk and fatality is intolerable (+)	Medium risk and fatality is intolerable (+)	**Medium risk and fatality is intolerable** **Recommended for design**	Low risk and fatality is tolerable (x)
Remote Prob. **0.1%** in ***n*** years **or** **10^{-4}** < Annual Freq. < **10^{-6}** Performance acceptance **2.0 bar** < Pr. < **4.0 bar**	Medium risk and fatality is tolerable (+)	Medium risk and fatality is tolerable (+)	Low risk and fatality is tolerable (+)	**Low risk and fatality is tolerable** **Recommended for design**

Notes and Notations : a. Prob. = Annual Probability; Annual Freq. = Annual Frequency; Pr. = Pressure; *n* = design life of a platform.
b. (+) - stringent design and will incur extra costs ;
c. (x) – Not acceptable for a new designed topside structure. For existing platforms, requires consent from stakeholders

Figure 3.4

The proposed performance based design level for typical topside structures

ii. The study by Vinnem (2000) which was based on 25 years of data from offshore installations on the North sea area (the UK, Norway and Holland) reveals that most incidents of blast overpressure are less than 0.2 bar for a return period of 110 year and 0.5 - 1.0 bar for return period of 1428 year compared with platform design service in the range of 30 – 50 year. The generalised damage level for secondary members studied by Louca and Mohamed Ali (2007) of typical topside structure subjected to a hydrocarbon explosion is in the range of 0.66 bar to 1.0 bar while the developed chart in section 8.3 by Bjerketvedt et al. - Gas Explosion Handbook[11] illustrates that a serious explosion usually occurs in the range of 0.5 bar to 1.0 bar. For these reasons, under functional and operation performance levels, overpressure load due to hydrocarbon explosions is proposed not to exceed 1.25 bar as an upper bound limit.

iii. Practically, under life safety performance, adequate safe routes must be available for carrying injured personnel leaving the safe temporary refuge to abandon the platform. Most equipment on the platform will be heavily damaged above 1.4 bar (Bjerketvedt et al. - Gas Explosion Handbook[11]) where structure members should at least able to sustain this condition within allowable deformation. Therefore, overpressure under life safety is proposed not to exceed 2.0 bar as an upper bound limit.

iv. Designing structural primary members for overpressure of more than 4 bar for collapse will be beyond the economic reason. At this pressure, primary members will be very massive in size. Furthermore, there will be nothing to protect as most equipment is expected to fail and the anticipated mortality rate is 100 percent (Table 3.2).

From the proposed performance level given in Figure 3.4, moving to the right farthest from the recommended design cell will involve substantial repair, unsafe and unacceptable fatalities for a new platform. Conversely, moving to the left farthest from the recommended design cell will result in a very safe and stringent design.

In terms of structural performance, if the integrity of the structural system is being unfulfilled, the operation on the platform is certainly unsafe and unacceptable. This is because the components of the system must be adequately supported by load bearing structural members which are usually the primary members. To complement the design, interactions between the secondary members are required for which they are designed to provide stability for primary members. Thus, the degree of resistance between primary and secondary components must be distinguished as summarised in Table 3.4; theoretically and ideally, secondary members will initiate and deform much more than primary members thus minimising the load transferred to them.

Table 3.4

The expected structural performance levels against blast load of topside structures

Performance	Primary structural members	Secondary structural members	Remarks
Functional	Neither damage nor deformation is allowed	Insignificant damage	All systems on topside are operable immediately. Repair is not required.
Operational	Insignificant damage (not exceeding yield) for main members and connections	Marginally to reach yield or just surpass yield level	Minor damage, all systems are operable and repair work can be executed at anytime.
Life safety	Deformation is allowed up to 50% loss of carrying capacity	Deformation is allowed up to 75% loss of carrying capacity	Significant damage, not safe, systems' failures and structural entities require major repair.
Failure/ Near Collapse	Deformation is allowed up to 75% loss of carrying capacity.	Deformation can reach 100% loss of carrying capacity	Loss of structural integrity and repair is totally impractical.

3.2.6 The definition of risk

The risk inherent in offshore installations involves evaluating the conditions of explosions and the consequences of their occurrence. The assessment of risk is necessary for supporting criteria when making decisions and for highlighting shortcomings in the preventative method, which must be balanced with costs. Therefore, it is crucial that the process of risk assessment is evaluated by qualified and experienced professionals.

In the proposed performance based design level (Figure 3.4), we define the risk on offshore installations as follows:

a. High risk where engineers must consider all aspects of blast effects in the design. The details must be diligently designed so that the structural integrity is guaranteed safe to the desired performance level. Equipment and other inventories are comprehensively protected and they are expected to be working under normal conditions after the explosions.

b. Medium risk where engineers will consider the key elements for maintaining the state of stability and integrity of the structural system i.e. supports and connections. Deformation and minor damage on both structural members and equipment are allowed.

c. Low risk where most entities under the system are damaged and total economic loss results.

In the study by Yasseri (2003a), the author has quantified the relationship between design explosion recurrence and the total cost, which includes engineering and repairs as shown by Figure 3.5. The study concludes that designing for intermediate recurrence (medium risk) gives a reasonable balance risk-cost compared to designing for low recurrence (low risk). For high recurrence (high risk), despite the fact that initial cost is high at the early design stage, total costs remain about the same because failure costs are minimised towards the end.

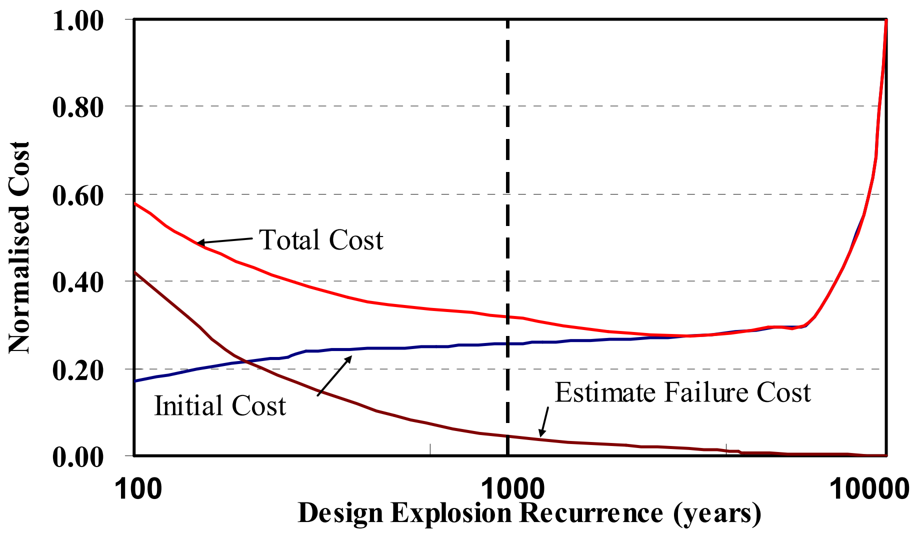

Figure 3.5

The normalised cost against the estimated recurrence of explosions

3.2.7 Design tools and analysis

The complexity of topsides and design methodology are the prime factor for the selection of design tools and analysis. Figure 3.6 summarises the structural analyses for blast loads.

The simplest model, an equivalent single degree of freedom, SDOF, is appropriate for simple structures and sometimes can be a handy method for determining the response of isolated cases of a local structural member.

As deck space areas are usually compactly occupied by inventories (equipment and piping lines), a meaningful multi-degree of freedom model is required for idealizing proper load distribution in order to obtain an accurate response of the structure.

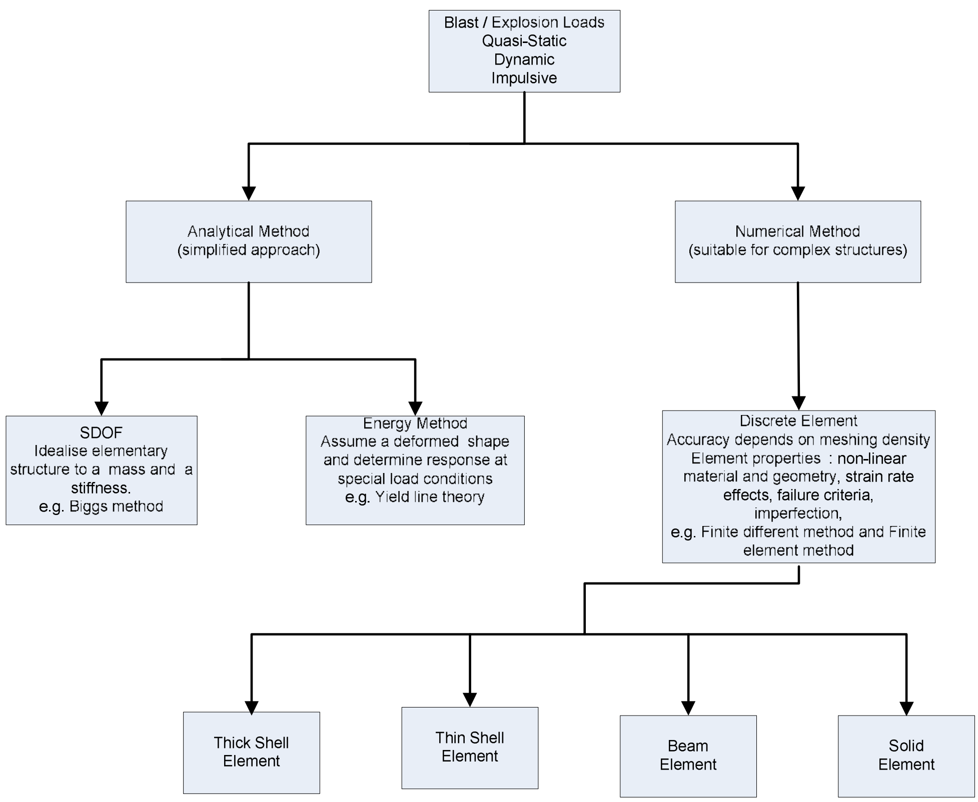

Figure 3.6

The typical blast analysis method

Another simplified approach is energy method, which approximates solutions by considering strain energy as potential energy. The potential energy is then balanced with the total work done for deforming each part of the structural elements. Solutions to these methods are usually in partial differential equations, which can be solved either by manual calculations or spreadsheets.

Evolving computer technology and commercially available structural analysis software packages using finite elements, for example ANSYS, ABAQUS and NASTRAN, facilitate complex structures to be analyzed rigorously in 3-D. The detailed model can lessen the design demand by relaxing loads and the redistribution of bending moments, especially in joints that minimise costs and repair schemes. Despite the advantages, factors such as quick assessment, uncertainties of loads, the high cost of software and the need for experienced users sometimes make the simplified method more preferable than using sophisticated software packages. Regardless of the method employed, the process of structural analysis plays an important role for determining the performance of the whole system be it either component based or at a global level.

For various economic reasons, certain structural components of the high risk structures can not be designed to remain a hundred percent elastic for blast resistance because the occurrence of the explosion is only once, or at most a few times in its design life period. Primary structural members are recommended to remain elastic or alternatively will be proportioned to the development of ductile behaviour for sufficient capacity during load transfer.

On the other hand, allowing plasticity on secondary structural members and plates to develop membrane forces allows more energy absorption. Under performance based design for serviceability, the design for both primary and secondary structural members should also meet the performance level in operational cases.

3.2.8 Mitigation

Mitigation of topside structures to improve the performance can be categorised in two parts; the structural and the non-structural components.

For the structural part, mitigation may involve a review of the applied overpressure and its return period to a more realistic load level, placing barrier walls to protect other structural elements reported by Louca et al. (2004), implementing compartmentalisation on non-hazardous areas to separate and minimize explosive loads, strengthening measures, for example additional structural members for load sharing and reducing displacement, as was investigated by Boh et al. (2005) and Louca and Mohamed Ali (2007), new additional steels on existing structural members for improving ductility and strength studied by Soleiman et al (2007) and some research studies mentioned in chapter two.

For the non-structural part, the input of process plant from multi-disciplines has to be re-visited which may require relocation of some equipment or the installation of additional control measures such as many more emergency shutdown valves, an increased number of gas detectors, extensive coverage of deluge systems and implementing artificial ventilation.
Sometimes, the proposed method of mitigation for non structural works may not be practical due to the large area to be covered or the constraint in space. As a result the penalty is always strengthening the structure itself. Unless not required by other load conditions, strengthening on structural members should cater for loads caused only by explosions for optimum design. The guidelines on prevention and mitigation of explosions are reasonably well documented by Fire and Explosion Guidance Part 0 (2003) which has incorporated some recent findings.

Having a similar structural configuration but additional inventories will normally result in an increase in the probability of blast occurrences. Spreading new loads to more supports (close to uniform distributed load) will improve the performance of structural members besides strengthening. These loads will have to be transferred to supporting columns through connections. A weaker connection with insufficient web thickness will yield below the required strength (under-strength curve) as shown in Figure 3.7 of TM 5-1300 (1990) while strong but less ductile connections will fail before reaching the permissible rotation (unstable). Under similar principles to the design approach against seismic loads, the performance of the connection in blast design must also ensure adequate strength, stiffness and rotation capacity for transmission of shear, axial and bending moment.

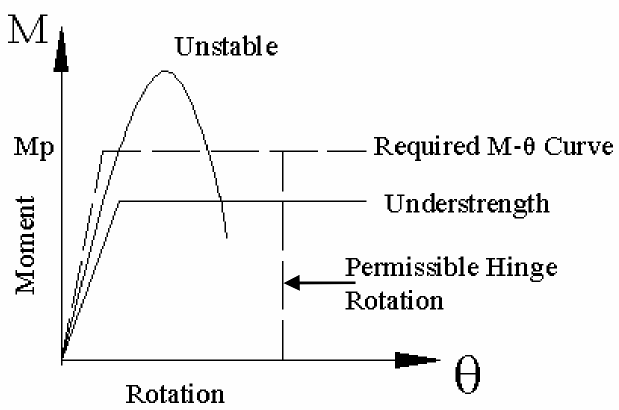

Figure 3.7

The behaviour of moment – rotation at a connection

3.2.9 The admissibility of performance based in offshore design

The principles of performance based design presented in this thesis are brief and are not meant to be an exhaustive study, but rather to provide an overview of the approach. A wide spectrum of performance based design approaches can be further extended to other design events. Due to the uniqueness of the offshore installations, there are many challenges ahead. The installations are not only to be built based on reservoir capacity and process plant requirements, but their design must also assimilate the surrounding topography and be balanced with the ecology. Hence, performance based design method is the appropriate approach to deal with this kind of scenario and engineers endeavour to deliver new techniques that should be able to quantify the integration of this method, at both component and system level, as requisite requirements which satisfy the stakeholders.

3.3 The design procedure

In the second part of this chapter, the guidelines on Performance based design are presented with an aim to demonstrate the practical use in the structural design of offshore installations. Although the involvement of structural engineers in the study of quantitative risk assessment is minimal, the results from the study are pertinent in determining the criteria for performance level. While some results are practical to implement, some are impractical and impose unreasonable demand levels on the structures. A unanimous decision must be reached prior to design work being commenced (refer to remarks under step 2).

3.3.1 The simplified step by step design guidelines

Step 1. – Establish performance criteria and objectives

Define the level to be implemented for asset protection and life safety. The safety standard performance should identify; (a) potential over-pressure/blast load, (b) escape routes, (c) escalation effects, (d) availability of temporary refuge, (e) level of functionality before and after blast scenario.

Demarcation of hazardous areas due to blasts on the platform shall be determined by qualified professionals. Structural engineers will propose structural framings for supporting the proposed layout whereby selection of preliminary sections of structural members should at least satisfy the design requirement in both the operational and pre-service conditions.

Step 2 Establish loading types

Identify potential sources of explosions, strength of the blast and the possible load profiles (i.e. rectangular or triangular pulse shapes). Computational Fluid Dynamics (CFD) methods such as FLACS, EXSIM and AutoReaGas are probably the most practical methods to simulate the possibilities of explosions accurately at a cost of increased CPU and modelling times.

Important remarks

Step 1 and step 2 require structural engineers to communicate with other disciplines, especially the process engineers. The proposed performance based design level (Figure 3.4) can be used as an indicative reference when impractical design values are proposed. Before commencing with the design, getting approval from the operator is necessary so that issues of risk, as well as levels for protection, are vividly addressed for all parties involved.

Step 3 – Determine the first fundamental period (T_N).

Determine the period T_N which gives the maximum displacement or bending moment. This can be done by solving the modal equation of motion or any simplified method such as a single degree of freedom method developed by Biggs (1964), Eq. (3.6)

$$T_N = 2\pi\sqrt{\frac{K_{LM}M_T}{k}} \tag{3.6}$$

Where K_{LM} = load-mass transformation factor

M_T = total mass

k = equivalent spring of the system

By knowing the value of T_N, the probable governing domain of response can be determined from the ratio of t_d/T_N.

Step 4 - Conduct Analysis and Design Check

In the front end engineering design (FEED) and the conceptual design stage; a simplified method can be used as a quick check for sizing-up sections of structural components. At this stage, members can be designed to the level of yield and not to exceed the maximum of ductility ratio more than 2 unless modelling of the structure is properly established. This stage can be considered as basic check for verifying the acceptability against the design premise.

In the detailed design, a reliable weight control report can be used as a tool for justifying load factors to be adopted in the analysis. With the assumption that ninety percent of structural design has been completed and a hundred percent of the inventories have been finalised, the proposed load factors tabulated in Table 3.5 are recommended for the blast design. The Figures in the table are not meant to be a definitive list; other load factors may be used at the discretion of responsible engineers or operators. On existing platforms, site surveys and a comparison of structural framings to as-built drawings should be made. The weight of equipment should be thoroughly checked for each level on the platform against the layout plan and the supplied vendor data.

Table 3.5

The proposed design load factor for blast analysis

Loads	Design Factor	Remarks
Structural self-weight and appurtenances	1.0	Structural members shall meet the performance required in pre-services and operational conditions
Equipment	1.0	Consider 50 percent of liquid weight
Piping lines and electric cables	1.10 to 1.20	Consider 50 percent of liquid weight
Environmental load	0.0	Wind and wave loads not required for consideration
Live load	0.5 to 0.75	0.75 seismic design, API RP2A LRFD (1993)
Blast load	1.0	90 percent confidence level

For main primary members which support the structural system, provided that they do not buckle and the estimate of displacements do not compromise escape routes or clearance of equipment, strength based checks are recommended. This is to prevent catastrophic collapse of the whole system and ensure adequate load transfer to supports. API RP FB allows a maximum utilisation factor of not greater than 2.0 and 2.5 for compression and tension respectively.

To ensure that beams and built-up sections will attain full plasticity and behave to the desired ductility at plastic hinge location, TM 5-1300 (1990) and AISC-WSD (1991) specify for rolled I and W shapes under compression, width-thickness ratio for flanges not to exceed the values given in Table 3.6.

Table 3.6

[1]Limits of $b_f/2t_f$

F_y (MPa)	$b_f/2t_f$
248	8.5
289	8.0
311	7.4
345	7.0
380	6.6
414	6.3
449	6.0

[1]It is worth noting that the above limiting values are from American design codes upon which most offshore designs are based. Similar codes can also be used e.g. Eurocode 3 (2005) and mentioned by Gardner and Nethercot (2005) where the above classification is equivalent to class I and II cross sections.

For boxed girders, the compressed flanges are limited by $\frac{b_f}{t_f} \leq \frac{500}{\sqrt{F_y}}$ where b_f is the longitudinal distance between connecting welds or bolts (F_y in MPa).

Similarly, for web, the depth-thickness ratio shall not exceed the value given by Eqs. (3.7) and (3.8)

$$\frac{d}{t_w} = \frac{2842.8}{F_y}\left[1 - 1.4\frac{P}{p_y}\right] \ when \ \frac{P}{P_y} \leq \ 0.27 \qquad (3.7)$$

$$\frac{d}{t_w} = \frac{1773.3}{F_y} \ when \ \frac{P}{P_y} > \ 0.27 \qquad (3.8)$$

Where P_y = plastic axial load (static yield stress multiplies by cross-section area)

P = the applied compressive load

For connections, a weaker connection fails by rupturing while a very stiff connection fails due to a brittle facture. Thus, a well designed connection is a connection that meets its performance, is able to distribute excessive load and rotation to adjacent members (members can experience some deformation) with only little or no impact on its integrity and capacity.

For secondary members, such as deck plates, large deformations can be allowed to develop and therefore by taking advantage of the membrane forces, provided that no weld failure is anticipated at the connection to top flanges of supporting stringer beams. Higher ductility ratio (μ) can be applied on plates because the deformed deck plates are easy to replace moreover deformation of deck plates prevents a further escalation of damages to other structural members.

To ensure the development of membrane action, the connections and supporting structural members must have adequate resistance; it is essential that stringer beams should therefore be designed with a ductility ratio (μ) lower than plates.

Structural members of a truss system which consist of columns/braces and girders/beams are not directly exposed to blast loads because the ratio of exposed surface area is far less than equipment, piping lines and deck plating. This is an important fact that distinguishes seismic design from blast design. Blast loads first impinge on secondary structures, and then loads are transmitted via several connections to the truss system while seismic loads act on truss systems where the severity of the effects depends on damage to the truss system itself. In the performance objective for the level near collapse, the truss system must have capacity not only to support topside loads but also must be able to resist the escalation effects. Therefore, it will be appropriate to let the truss systems remain at the upper bound elastic limit (close to yield) as long as serviceability can be achieved. Additional tie-backs or diagonal bracings certainly will be useful for stability in the post blast event.

Step 5 Drawings and design review

Analyses conducted in step 4 shall be documented together with detailed design calculations. Special drawings need to be generated to illustrate the anticipated overpressure with respect to the affected and safe zone areas. New strengthening and resizing of sections shall be transferred onto fabrication drawings with notes for reference of design work for the future. All work done shall undergo design review by qualified professionals or independent checking for evaluating and ensuring that the design work has been conducted within the standards of industrial practices and details shown on drawings are workable.

Step 6 Fabrication and quality control

On-site, fabrication of structures must adhere strictly to the designed structural drawings. Fabrication sequences and installation methods should be reviewed by engineers. Development of non-destructive test (NDT) drawings for welding maps shall be evaluated based on the critical joints by both designers and welding engineers

Step 7 Mitigation work on existing platform

The initial phase of mitigation should start with a feasibility study before embarking on a full scale retrofit. Compilation of data, including design specifications, as-built drawings and vendor supplied records would enable engineers to make an early evaluation of structural performance. The proposed strengthening shall be based on the principle of minimum interruption to the platform operation and existing components of the affected zones. Site survey is necessary for confirming the feasibility and workability of the proposed method.

3.4 The design example of deck flooring.

To demonstrate the concept of performance based design for offshore installations, the deck plates on a typical topside structure are selected for our case study. The presence of deck plates, which are widely spread on topside deck levels, absorb more energy during deformation compared with other structural components, are simple to analyze and the response is straightforward. These are the reasons for selection in this study, Mohamed Ali and Louca (2007b).

The case study

A deck plate located in the potential area of explosions on an offshore installation is to be designed for a 10 kN/m^2 live load. The plate is to be supported by stringer beams spanning 4.0 m long and spaced 1.0 m apart. Fillet welds are to be applied continuously under the deck plate for connection to the support beams.

Step 1

The proposed performance based design objective by Figure 3.4 will be used for defining the performance of the deck plates. A typical deck plan and details are given in Figure 3.8.

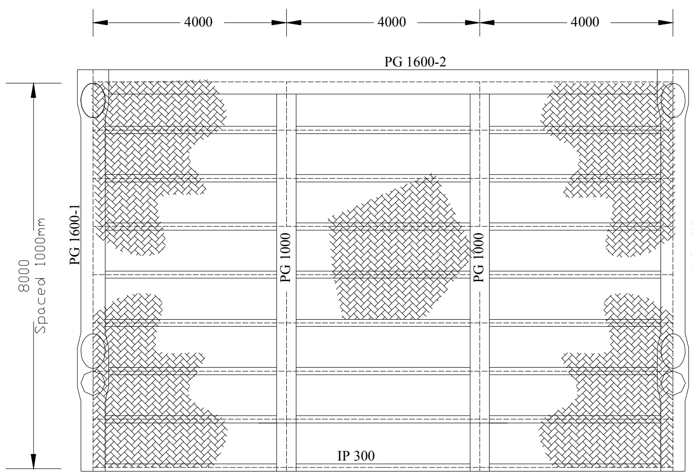

a. Plan view
Nominal deck plate size = 4000 mm x 1000 mm

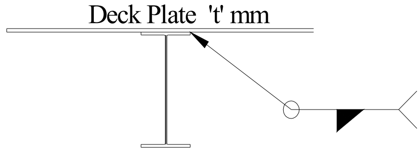

b. Deck plate connection
Continuous all round fillet welds between flanges and bottom plate

Figure 3.8

Plan View – A partial of deck framing
The deck plates are supported by IP 300 beams spaced at 1000 mm apart

Table 3.7

The results of static analysis

(Preliminary investigation with live load and performance based design for serviceability condition)

Design check	**Thickness of Plate**			**Remarks**
	t_p=8 mm **b/t_p = 125**	**t_p=10 mm** **b/t_p = 100**	**t_p=12 mm** **b/t_p = 83**	
ϕ_1	0.00330	0.00186	0.00110	Under service condition, the considered plates are within elastic limits
$\phi_{1(yield)} = \frac{\varepsilon_{yield}}{z\ 8a^4\ b^2}$	< 0.0102 (elastic)	<0.0081 (elastic)	<0.0068 (elastic)	
ϕ_2	$-6.56978\text{x}10^{-7}$	$-2.07942\text{x}10^{-7}$	$-7.23684\text{x}10^{-8}$	Small in-plane displacement
ϕ_3	$-2.46752\text{x}10^{-8}$	$-7.81002\text{x}10^{-9}$	$-2.71806\text{x}10^{-9}$	Small in-plane displacement
Out-plane displacement *δ (mm)* *(*allowable *l/240=4.2mm)*	3.303 (SL -ok)	1.866 (SL -ok)	1.096 (SL-ok)	Serviceability limits : l/240 (industry) l/200(N-001) l/360 (AISC)
$\varepsilon_x\ (1x10^{-6})$ Max	26.43	18.58	13.16	At long span (ls)
$\varepsilon_y\ (1x10^{-6})$ Max	422.83	297.35	210.5	At short span (ss)
$\sigma_x(MPa)$	28.58	20.10	14.23	At long span (ls)
$\sigma_y(MPa)$	95.25	66.99	47.42	At short span (ss)
$\sigma_{vms}(MPa)$ (Von Mises)	84.66 (ss) 5.29 (ls) 42.60(mid) (ok)	59.54 (ss) 3.72 (ls) 29.60(mid) (ok)	42.15 (ss) 2.64 (ls) 21.21 (mid) (ok)	Allowable stress $\leq 0.75F_y$ *(industry)* *0.75*248=* *186MPa*

$$\sigma_{vms} = \sqrt{\sigma_x^2 + \sigma_y^2 - \sigma_x\sigma_y + 3\sigma_{xy}^2} \qquad \sigma_x = \frac{E}{1-\nu^2}\left(\varepsilon_x + \nu\varepsilon_y\right) \qquad \sigma_y = \frac{E}{1-\nu^2}\left(\varepsilon_y + \nu\varepsilon_x\right)$$

Since plate is elastic, the effects of membrane and lateral displacements are insignificant, hence ε_x *and* ε_y are calculated based on thin plate theory for pure bending:

$$\varepsilon_x = -z\frac{\partial^2 w}{\partial x^2} \quad \varepsilon_y = -z\frac{\partial^2 w}{\partial y^2}$$

To start with the design, the deck plate is assumed to be 10 mm thick.

Applying appropriate load factors (Table 3.5), preliminary checks under service load condition are as follows:

Design load = 1.15 x Self-weight + 1.0 x Live load
= 1.15 x 7.850 x 0.01 x 9.81 + 1.0 x 10 = 10.885 kN/m^2
(factor 1.15 for self-weight to account for change in plate thickness)

The dimensions of the plate to be analysed are: a = 2.0 m, b = 0.5 m and the plate thicknesses to be considered are 8 mm, 10 mm and 12 mm. Adopting the proposed analytical method discussed in chapter 4, the results from the static analysis are tabulated in Table 3.7 which concludes that all selected plates satisfy operational requirements.

Step 2

The overpressure load used in this design is adopted from a case study developed by Yasseri and Menhennett (2003). The topside weight is about 23,000 tonnes, supported by an 8 legged fixed jacket in 125m depth of water.

The Quantitative Risk Assessment (QRA) study was conducted on the defined hazardous activities of the utility area, which was separated by the blast walls. The straight line shown in Figure 3.9 is a summary of a linearised line representing the distribution of explosions recurrence against overpressure. As can been seen from the graph, at high over pressure, the cumulative value of recurrence is low, which results in a higher return period.

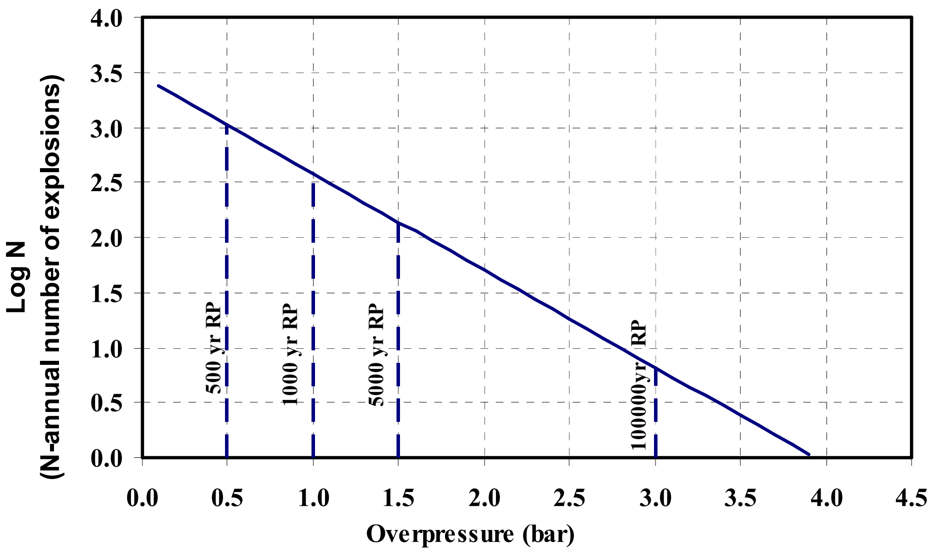

Figure 3.9

Relationship of recurrence and overpressure

(QRA – a case study from Yasseri and Menhennett (2003))

Assuming that the shape of overpressure-duration is an isosceles triangular pulse, the duration t_d is now determined from Figure 3.10 which is derived from a CFD simulation study. Similar to recurrence distribution, the plotted curve is the result of regression analysis on the scattered data from the CFD study.

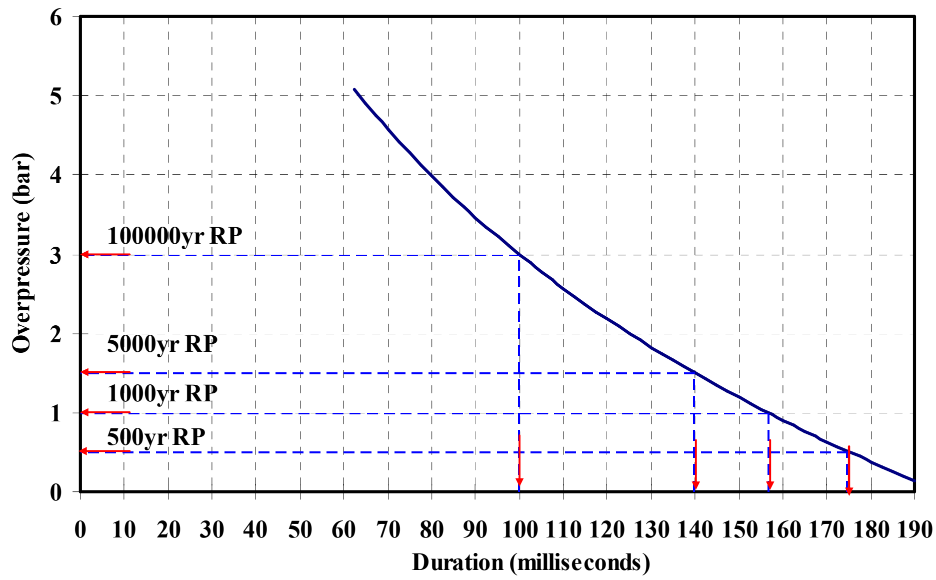

Figure 3.10

Mean duration of overpressure

Adopting performance levels as defined in Figure 3.4 and magnitudes of the overpressure from this case study, Table 3.8 summarises the expected demand levels for deck plates.

Table 3.8

The definition of performance levels for the deck plate

Designated design case	Probability, Return period	Expected Demand Level	Overpressure, Duration
(a)	10 % (500 years return period)	Fully functional High risk and low damage is expected.	0.5 bar, t_d = 175 ms
(b)	5 % (1000 years return period)	Operational High risk and minor structural damage.	1.0 bar, t_d = 157 ms
(c)	1 % (5000 years return period)	Life safety Significant structural damage and repair works are required for operation to resume	1.5 bar, t_d = 140 ms
(d)	0.05 % (100,000 years return period)	Near collapse Substantial damages. All system are lost and repair is impractical	3.0 bar, t_d = 100 ms

<u>Step 3</u>

Applying equation Eq. (3.9) (Eq. 4.29 from chapter 4) to calculate the natural period for a rectangular plate with fixed supports, the governing domain of responses can be evaluated. From Table 3.9, when live load is considered, except for cases when t_d are 175 ms and 157 ms for 12 mm thick plate, all cases are found to be in the dynamic loading domain regime.

$$T_N = \frac{2\pi}{\omega_n}, where\, \omega_n = \sqrt{\frac{63\,D}{m\,a^4\,b^4}\left(\frac{a^4}{2}+\frac{b^4}{2}+\frac{2}{7}(ab)^2\right)} \qquad (3.9)$$

Table 3.9

The ratio of t_d/T_N and the response domains

Thickness T_d	8mm Plate		10mm Plate		12mm Plate	
	No Live load	With Live load	No Live load	With Live load	No Live load	With Live load
175 ms	7.88	**1.84**	9.86	**2.64**	11.83	3.44
157 ms	7.08	**1.70**	8.85	**2.37**	10.61	3.08
140 ms	6.31	**1.52**	7.90	**2.10**	9.46	**2.75**
100 ms	4.50	**1.08**	5.63	**1.51**	6.70	**1.97**

Note :

N-004 Norsok (1998) Impulsive domain $\mathbf{t_d/T_N < 0.3}$

Dynamic domain $\mathbf{0.3 < t_d/T_N < 3}$

Quasi-static domain $\mathbf{3 < t_d/T_N}$

The thicker the plate, the smaller the natural period T_N because T_N is proportional to mass, without a live load. All plates fall under quasi-static conditions.

Step 4

Similar to step 1 and adopting simplified analysis (chapter 4), three equations of motions with time-dependent generalised coordinates $\phi_1(t)$, $\phi_2(t)$ *and* $\phi_3(t)$ in terms of partial differential equations are solved using Maple by a numerical approach adopting the fourth order of the Runge-Kutta method. The results give the maximum values for the three generalised displacement functions, which are then used to calculate the strain and the stress. The maximum normal stress is predicted by combining the strain due to pure bending and the membrane strain at which the shear strain is zero.

Results from the analyses

As can been seen from Table 3.10, the out-plane displacements with overpressure loads have exceeded the serviceability limit shown by Table 3.7. When the applied overpressure is increased, the displacements and predicted ductility ratios continue to rise. However, when the applied overpressure exceeds the performance at the level of 5000 year return period at 1.5 bar as shown in Figure 3.11, the slope of the ductility ratio decreases gradually, illustrating that plasticity is no longer concentrated at the centre supports and that it has begun to spread to other areas of the plate, especially for an 8 mm thick plate. The slopes for 10 mm thick and 12 mm thick plates do not show any significant change compared with 8 mm thick plates and they are responding quite consistently until the applied overpressure has reached the maximum 3 bar. Comparing responses based on calculated ductility ratio, maximum strain and Von Mises stress, 10 mm thick plate is recommended for topside deck plate for the following reasons:

a. <u>Functional 0.5 bar return period in 500 years</u>

10 mm thick plate can still be considered elastic although ductility has exceeded 20 percent with live load. It is highly likely that temporary equipment will come with a support frame which spans between the beams, and this load will be transferred to the beams rather than the plates. An 8 mm thick plate has exceeded more than 40 percent of the elastic limit while 12 mm thick plate is still elastic.

b. <u>Operational 1.0 bar return period in 1000 years</u>

At this level, all plates have yielded. Plasticity is quite apparent for the 8 mm thick plate as the ductility ratio has 70 percent exceeded elastic. The differences of ductility ratios between the 8 mm thick plate and the 12 mm thick plate against the 10 mm thick plate are not significant, 4.9 percent and 11.1 percent respectively. Similarly, in terms of stress and strain, the differences are 7.5 percent and 11.4 percent. Therefore, a selection of the 10 mm thick plate (the middle thickness) is quite reasonable.

c. <u>Life safety 1.5 bar return period in 5000 years</u>

The ductility ratio for the 8 mm thick plate has reached twice the yield limit while the 10 mm thick plate and 12 mm thick plate remain below 2. The estimated maximum strain is in the range of 0.22 percent to 0.26 percent. It is highly likely that at this stage localised ruptures have occurred along the supports as the Von Mises stress exceeded 500 MPa (the ultimate stress) while the 10 mm thick plate and 12 mm thick plate are still below 500 MPa. If only 75 percent of live load is considered effective (Table 3.5) the maximum Von Mises stress for the 10 mm thick plate is estimated at 476 MPa, which is below the welding strength of 483 MPa for electrode E70. Thus, connections between the supports for the 10 mm thick plate and 12 mm thick plates are still intact.

d. <u>Near collapse 3.0 bar return period in 100,000 years</u>

The predicted strains in all selected thicknesses i.e. 8 mm, 10 mm and 12 mm plates have exceeded twice the strain at yield, with a maximum 0.33 percent (theoretical ε_{yield} is assumed 0.13 percent). All plates are expected to fail by rupture at supports.

Table 3.10

The result and summary of dynamics analysis solved using MAPLE[42]

Design check	Case	8 mm Plate		10 mm Plate		12 mm Plate	
		No LL	With LL	No LL	With LL	No LL	With LL
Out-plane displacement δ_{max}	(a)	9.36	14.32	6.85	9.83	4.61	6.70
	(b)	13.37	17.32	10.22	13.19	7.71	9.74
	(c)	16.00	20.29	12.76	15.56	10.20	11.79
	(d)	21.41	25.62	18.51	20.92	15.26	16.78
Ductility $\mu = \frac{\delta_{max}}{\delta yield}$	(a)	0.92	**1.41**	0.84	**1.21**	0.68	0.99
	(b)	**1.32**	**1.70**	**1.26**	**1.62**	**1.14**	**1.44**
	(c)	**1.60**	**2.00**	**1.57**	**1.91**	**1.51**	**1.73**
	(d)	**2.12**	**2.52**	**2.28**	**2.57**	**2.25**	**2.48**
$\varepsilon_x (1x10^{-6})$	(a)	74.86	114.58	68.50	98.26	55.33	80.49
	(b)	107.02	141.79	102.16	131.91	92.53	116.94
	(c)	128.02	162.35	127.62	155.64	122.51	140.25
	(d)	171.97	204.95	185.08	209.20	183.14	201.31
$\varepsilon_y (1x10^{-6})$	(a)	1197.80	1833.29	1095.94	1572.14	885.51	1287.78
	(b)	1712.28	2268.68	1634.63	2110.56	1480.54	1870.98
	(c)	2048.26	2597.60	2041.85	2490.24	1960.09	2244.06
	(d)	2751.56	3279.23	2961.29	3347.26	2930.25	3322.88
$\sigma_x (MPa)$	(a)	80.95	123.90	74.07	106.25	59.82	87.03
	(b)	115.72	153.32	110.47	142.64	100.06	126.45
	(c)	138.43	175.55	137.99	168.30	132.47	151.66
	(d)	185.96	221.62	200.13	226.22	198.03	217.67
$\sigma_y (MPa)$	(a)	269.83	412.99	246.89	354.16	199.42	290.10
	(b)	385.73	511.08	368.24	475.46	333.53	421.49
	(c)	461.42	585.17	459.98	560.99	441.56	505.53
	(d)	619.86	738.60	667.10	754.22	660.11	725.59
$\sigma_{vms} (MPa)$ (Max Von Mises)	(a)	239.83	367.08	219.44	314.79	177.24	257.85
	(b)	342.85	454.26	327.30	422.59	296.45	374.62
	(c)	410.12	520.11	408.84	498.62	392.47	449.32
	(d)	550.94	656.60	592.94	670.22	586.72	644.91

Load and duration

(a) P_{max} = 0.5 bar, t_d = 175 ms, **(b)** P_{max} = 1.0 bar, t_d = 157 ms,

(c) P_{max} = 1.5 bar, t_d = 140 ms, **(d)** P_{max} = 3.0 bar, t_d = 100 ms.

Calculation of strain

$$\varepsilon_{Total} = \varepsilon_{Bending} + \varepsilon_{Membrane}$$

$$\varepsilon_{x-Total} = \left[-z\left(\frac{\partial^2 w}{\partial x^2} + v\frac{\partial^2 w}{\partial y^2} \right) \right] + \left[\left(\frac{\partial u}{\partial x} \right) + \frac{1}{2}\left(\frac{\partial w}{\partial x} \right)^2 \right]$$

$$\varepsilon_{y-Total} = \left[-z\left(\frac{\partial^2 w}{\partial y^2} + v\frac{\partial^2 w}{\partial x^2} \right) \right] + \left[\left(\frac{\partial v}{\partial y} \right) + \frac{1}{2}\left(\frac{\partial w}{\partial y} \right)^2 \right]$$

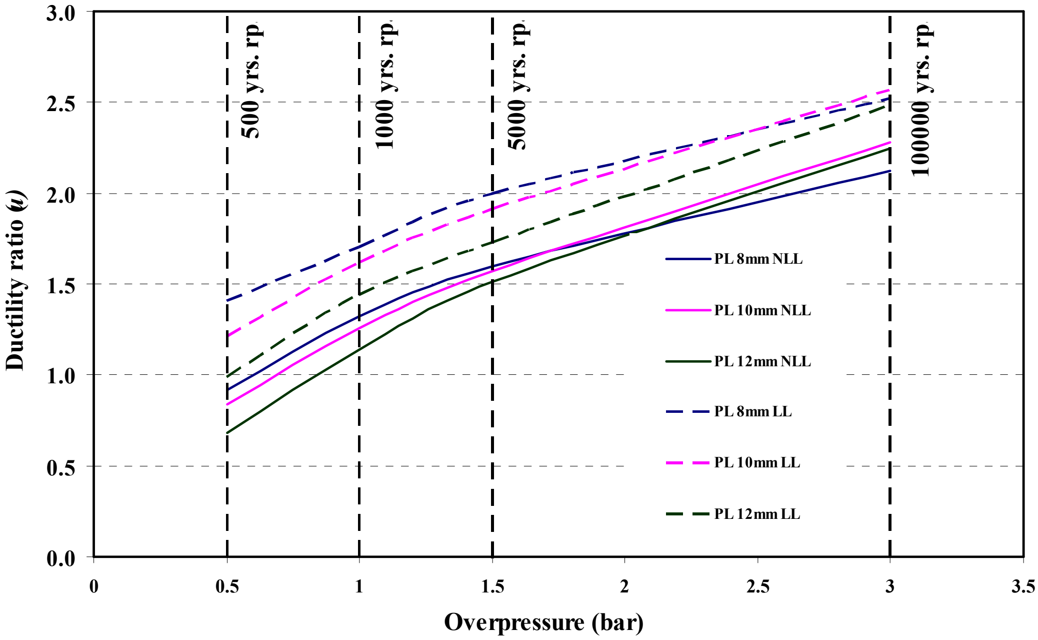

Figure 3.11

The deck plate performance against estimate ductility ratio

(NLL - No live live, LL – With live load)

Comparing with working stress design (WSD)

Applying the same magnitude of blast load, the deck plate is checked using WSD methodology (API RP 2A - WSD (2000)) with a one-third increase in allowable stress. The final plate result is rounded to the next highest thickness. As can be seen from Table 3.11, the saving of steel material is quite significant from the minimum 30 percent (functional) to the maximum 180 percent (near collapse). Under a collapse scenario, using a 28 mm thick plate is impractical; not only it is too heavy but it also requires very strong stringer beams. This domino effect on other structural components will result in a massive topside structure, and the installation of the structure offshore may be impossible. The results also show that, although the methodology offers a safe (not reaching yield) structure, it is extremely cumbersome to convince the client of the acceptance and implementation in design.

Table 3.11

Summary of plate design based on WSD methodology

Performance Level	Plate Thickness	Maximum Strain (%)	Utilization Ratio	Percentage of saving based on PBD
Functional	13	0.095	0.93	30
Operational	17	0.090	0.94	70
Life safety	20	0.114	0.92	100
Near Collapse	28	0.105	0.95	180

Step 5.

The details of the 10mm plate as deck flooring and the affected areas for blast protection shall be transferred to the design drawing accompanied by notes which explain the design performance level for review by the owner and regulatory body.

Step 6.

The feedback from fabrication yard to design office in relation to changes of equipment load and support configuration shall be advised to the responsible engineer. Re-analysis may be required for the 10 mm thick plate for ensuring that the performance level is within the limit.

3.5 Conclusion

A performance based design level of blast resistance (given by Figure 3.4) is proposed. In the absence of a QRA study, the proposed performance level that is based on the analysis of a typical topside structure and the statistical evidences of the factual explosion and empirical data can be adopted in topside structure design.

The study has demonstrated that implementing a performance based approach in design, and following the proposed guidelines, the expected capacity (resistance) of the designed component is much more coherent than the existing design approaches, although the procedures require additional checks. The approach has also facilitated communication between designers and other stakeholders, in particular the owner, as non-technical terms could be used for representing engineering judgement.

Under performance based design, the 10 mm thick mild steel plate is recommended for deck plates of a typical topside structure. The maximum resistance capacity is estimated at 1.5 bar for life safety, after which rupture at supports is predicted.

In the plate analysis, deformation of the supporting beams is not considered. Thus, when assessing a single structural component, a lower bound of ductility ratio is recommended. From the analysis, rupture at supports is anticipated when the ductility ratio is about 2, which falls under moderate ($2 \leq \mu \leq 4$, Table 3, Louca and Mohamed Ali (2007) for repairable damage and interruption to production with operations resuming after repair and replacement. Thus, when evaluating a complete structural system in which stiffness and combined responses from other structural components are included, it is reasonable to apply an upper bound ductility ratio.

Chapter Four

A Simplified Analytical Model for the Deck Plate of Offshore Topsides

4.1 Introduction

Deck plates on the topsides of offshore installations, which are typically fabricated from mild flat steel, not only serve as deck flooring but are also used for protection against weather, the overspill of liquid and as demarcation of hazardous areas. The plates are laid on top of supporting beams and continuous fillet welds are applied at the interfaces between the deck bottom plates and top flanges of the beams. With these connections, the boundary conditions of the deck plates can be regarded as fixed supports. The welded connections also improve the lateral stability by integrating structural components at the deck level as one large panel which is needed for resisting skew loads during pre-service operations such as lifting and sea transportation.

Possessing a larger surface area compared to other structural members on a topside, the deck plates are highly likely to be the first structural components to be pounded by the blast load. This scenario certainly provides an advantage to the structural system because of the behaviour of plate systems. With the right boundary conditions, it allows large deformations to develop that result in less energy being transferred to other main structural members which are supporting permanent loads. Consequently, this will potentially reduce damage to primary joints and other structural members.

The study of plate behaviour is a well researched field and only key aspects are highlighted in this introduction. Historically, engineers had their own rules of thumb for determining load carrying capacity before the first mathematical expression on membranes was introduced by Euler in 1766. This was followed by other mathematicians/ engineers who had associated the plate response with governing criteria such as aspect ratio, slenderness ratio, shape and boundary condition. Timonshenko and Krieger (1959) and Szilard (2004) provide some classical solutions for estimating maximum deformation under static and linear elastic conditions with various boundary conditions, while the Biggs method[10], idealizes the plate with load history to an equivalent system (single degree of freedom) using transformation factors for maximum response.

Nurick and Martin (1989) reviewed and summarised the development of plate studies subjected to impulsive load by others and concluded that incorporating transverse and lateral displacements would result in close approximation with experiments. Schleyer et al. (2003) and (2004), conducted experiments on mild steel clamped plates subjected to pulse pressure and proposed an elastic-plastic analytical method with pre-determined non-linear spring at the plate edges.

On the contrary, based on the assumption of rigid plastic, Amdahl (2005) combined a portion of the plate with T-stiffener as an equivalent asymmetrical I beam profile. While the method is acceptable for assessment of the support, it is slightly conservative in design as the middle deformation of plate is being ignored.

Although a number of methods have been proposed ((Biggs (1964), Jones (1971), Nurick and Martin (1989), Schleyer et al. (1998), Yasseri (2004), Amdahl (2005)) with some in complex formulations for plate analysis subjected to overpressure, very few have looked into their practical uses in industry whereby the deck plates should be regarded as structural components that hold important roles in reducing damage from spreading to other structural components as well as for protection of non structural components. A Performance Based methodology discussed in chapter three is one of the approaches that can be used to satisfy this dual purpose.

The primary objective of the present study is to simplify the analysis method which currently looks complicated, though they are actually straightforward and simple formulae. Although sophisticated software is available, such as finite element software and high-tech computer systems which definitely make calculation easy and even quicker, they are costly and require experienced users. In the proposed method, by considering a simple deformed shape function for a plate which any shape of deformed functions can be chosen as long as they meet the kinematic boundary conditions, basic parameters such as the first fundamental period, the static and dynamic displacements, and the static displacement at yield can easily be evaluated and becomes handy for preliminary sizing of deck plates.

The present study on the fixed supported plate employs energy method, which is based on the proposed simplified non-linear method for a simply supported plate by Louca and Wadee (2002). Then the solutions to the derived partial differential equations are solved numerically by simple programming code using mathematical software called Maple.

4.2 The plate boundary conditions and selected deformed functions

Consider a rectangular flat plate with dimensions 2a by 2b, density of *ρ,* Young's modulus *E,* plate flexural rigidity *D* ($Et_p/\left[12(1-\nu^2)\right]$) and thickness of t_p. The kinematics boundary conditions for the plate with fixed supports as shown in Figure 4.1 can be written as follows:

$$when\ x = \pm\, a, \quad u,\, w\ and\ \frac{\partial w}{\partial x} = 0 \tag{4.1}$$

$$y = \pm\, b, \quad v,\ w\, and\ \frac{\partial w}{\partial y} = 0 \tag{4.2}$$

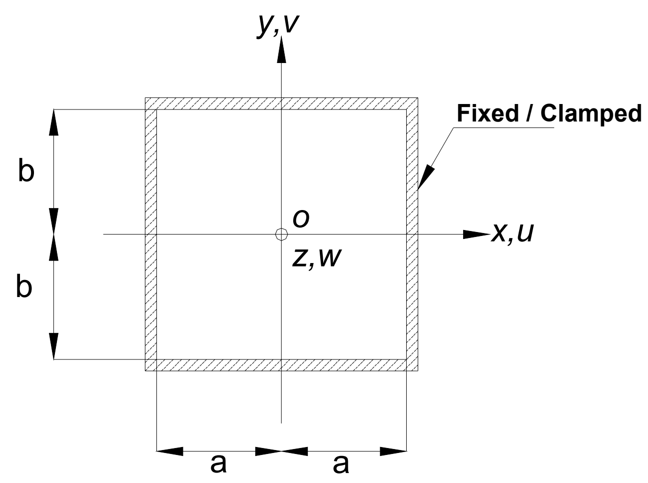

Figure 4.1

A fixed rectangular plate (a ≥ b)

The three selected shapes of the generalized deformed functions *u*, *v* and *w* which are time-dependent, simple, straightforward for generation of derivatives and integrals; are introduced in x, y, z directions respectively. They are given by Eqs. (4.3), (4.4) and (4.5) which satisfy the boundary conditions given by Eqs. (4.1) and (4.2) as well.

Several analyses were performed at the early stages of the model development using an increasing number of time-dependent variables for determining the efficiency of the proposed functions. However, the analyses became quite complicated and the result showed only a marginal improvement; less than 5 percent in displacement. In order to keep the model simple such that it is of value for preliminary design, it was decided only three variables were necessary i.e. $\phi_1(t)$, $\phi_2(t)$ and $\phi_3(t)$.

$$w(x,y,t) = (a^2 - x^2)^2 \, (b^2 - y^2)^2 \; \phi_1(t) \tag{4.3}$$

$$u(x,y,t) = x \; (a^2 - x^2) \; (b^2 - y^2) \; \phi_2(t) \tag{4.4}$$

$$v(x,y,t) = y \; (a^2 - x^2) \; (b^2 - y^2) \; \phi_3(t) \tag{4.5}$$

where

$\phi_1(t)$ = time-dependent generalized coordinates out-plane displacement in z-direction

$\phi_2(t)$ = time-dependent generalized coordinates in-plane displacement in x-direction

$\phi_3(t)$ = time-dependent generalized coordinates in-plane displacement in y-direction

The first two terms for *w* in Eq. (4.3) are even functions which will vanish at supports as well as its first derivatives, while the first two terms for *u* and *v* in Eqs. (4.4) and (4.5) are odd functions, which will also vanish at supports.

In order to find the approximate solutions for *u*, *v* and *w* and by the law of virtual work, which states that the change in internal strain energy must be equal to the work done by external forces during virtual distortion on the plate, the equation for this equilibrium in terms of energy can be written as:

$$\delta U \; = \; \delta W_D + \; \delta W_{IN} + \; \delta W_C \tag{4.6}$$

Where $\delta U = \dfrac{\partial U}{\partial \phi_i} \, \delta\phi_i$ = a change in internal strain energy;

the combined energy due to membrane and bending

$\delta W_D = \dfrac{\partial W_D}{\partial \phi_i}\delta\phi_i$ = a change in virtual work done by external load *P(t)*

$\delta W_{IN} = \dfrac{\partial W_{IN}}{\partial \phi_i}\delta\phi_i$ = a change in virtual work done by inertia forces

$\delta W_C = \dfrac{\partial W_C}{\partial \phi_i}\phi_i$ = a change in virtual work done by damping forces

It can be shown that the work done by inertia forces can be written as:

$$\delta W_{IN} = -\frac{d}{dt}\left(\frac{\partial K_E}{\partial \dot{\phi}_i}\right)\delta\phi_i + \left(\frac{\partial K_E}{\partial \phi_i}\right)\delta\phi_i \qquad (4.7)$$

where notation δK_E = a change of kinetic energy.

Because kinetic energy is a function of velocity instead of displacement the second term will vanish:

$$\left(\frac{\partial K_E}{\partial \phi_i}\right) = 0, \quad \text{therefore} \quad \delta W_{IN} = -\frac{d}{dt}\left(\frac{\partial K_E}{\partial \dot{\phi}_i}\right)\delta\phi_i \qquad (4.8)$$

Assuming that the effect of damping is very minimum for the system, $\delta W_C = 0$. Further manipulation in terms generalized coordinates leaves behind three partial differential equations in the general form of Lagrange's equation, Eq. (4.9):

$$\frac{d}{dt}\left(\frac{\partial K_E}{\partial \dot{\phi}_i}\right) + \frac{dU}{\partial \phi_i} = \frac{dW_D}{\partial \phi_i} \quad where \;\; i = 1,\, 2\, and\;\, 3. \qquad (4.9)$$

4.3 The description of energy terms

In order to solve Eq. (4.9) subjected to blast load, large deflection formulae proposed by Thimonshenko-Krieger (1959) are adapted in the analysis in which both bending and strain stretching are included in the formulation. Applying the appropriate boundary conditions and replacing the variables involved, the energy terms can be simplified as follows:

a. The energy due to membrane strain

The membrane strain energy U_{ms} for the plate which is due solely to stretching at the middle surface is given in the following form:

$$U_{ms} = \frac{Et_p}{2\left(1-\nu^2\right)} \int_{-a}^{a} \int_{-b}^{b} \left[\varepsilon_x^2 + \varepsilon_y^2 + 2\nu\varepsilon_x\varepsilon_y + \frac{1}{2}(1-\nu)\gamma_{xy}^2 \right] dx\,dy \qquad (4.10)$$

and the variable components of strain-displacement relations in terms of deformed function *u*, *v* and *w* for $\varepsilon_x, \varepsilon_y$ and γ_{xy} are given by Eqs. (4.11), (4.12) and (4.13):

$$\varepsilon_x = \frac{\partial u}{\partial x} + \frac{1}{2}\left(\frac{\partial w}{\partial x}\right)^2 \qquad (4.11)$$

$$\varepsilon_y = \frac{\partial v}{\partial y} + \frac{1}{2}\left(\frac{\partial w}{\partial y}\right)^2 \qquad (4.12)$$

$$\gamma_{xy} = \frac{\partial u}{\partial y} + \frac{\partial v}{\partial x} + \frac{\partial w}{\partial x}\frac{\partial w}{\partial y} \qquad (4.13)$$

At this stage in the design, the effect of imperfection on plate is considered not to be significant because it is assumed that the deck plates are to be fabricated within the limit of fabrication tolerances and will follow the industry standard ‘Code of practices’.

b. The energy due to bending

The strain energy of bending is given by the following expression:

$$U_{bs} = \frac{D}{2} \int_{-a}^{a} \int_{-b}^{b} \left(\left(\frac{\partial^2 w}{\partial x^2} + \frac{\partial^2 w}{\partial y^2} \right)^2 - 2(1-\nu) \left(\frac{\partial^2 w}{\partial x^2}\frac{\partial^2 w}{\partial y^2} - \left(\frac{\partial^2 w}{\partial x \partial y} \right)^2 \right) \right) dy\,dx \qquad (4.14)$$

Performing integration by parts for the last term $\iint \left(\frac{\partial w}{\partial x \partial y} \right)^2 dx\,dy$ inside the parenthesis gives the following expression:

$$\iint \left(\frac{\partial^2 w}{\partial x \partial y} \right)^2 dx\,dy = \int \left(\frac{\partial^2 w}{\partial x \partial y} \right) \left(\frac{\partial w}{\partial x} \right) dx - \int \left(\frac{\partial w}{\partial x} \right) \left(\frac{\partial^2 w}{\partial y^2} \right) dy \qquad (4.15)$$
$$+ \iint \left(\frac{\partial^2 w}{\partial x^2} \right) \left(\frac{\partial^2 w}{\partial y^2} \right) dx\,dy$$

Applying $\dfrac{\partial w}{\partial x} = \dfrac{\partial w}{\partial y} = 0$ at the boundary; Eq. (4.14) is now being reduced to:

$$U_{bs} = \frac{D}{2} \int_{-a}^{a} \int_{-b}^{b} \left(\left(\frac{\partial^2 w}{\partial x^2} + \frac{\partial^2 w}{\partial y^2} \right)^2 \right) dy\, dx \tag{4.16}$$

c. Work done (W_D) by the external Loads

The external load by the uniformly applied time- varying pressure *p(t)* on the surface of the plate, which represents the work done to distort the plate can be written as follows:

$$W_D = \int_{-a}^{a} \int_{-b}^{b} p(t)\ w(t)\ dy\ dx \tag{4.17}$$

d. Kinetic energy of the plate

The kinetic energy of the plate is the summation of energies in x, y and z directions, given by:

$$K_E = \frac{1}{2} \int_{-a}^{a} \int_{-b}^{b} \rho\ t_p \left(\dot{u}^2 + \dot{v}^2 + \dot{w}^2 \right) dy\, dx \tag{4.18}$$

where the velocities are given by: $\begin{pmatrix} \dot{u} = \dfrac{\partial u(x,y,t)}{\partial t} \\ \dot{v} = \dfrac{\partial v(x,y,t)}{\partial t} \\ \dot{w} = \dfrac{\partial w(x,y,t)}{\partial t} \end{pmatrix}$

Replacing Eqs.(4.11), (4.12) and (4.13) into Eq. (4.10); substituting the derivatives and integrations from the defined shape functions into the respective formulae of Eqs. (4.16), (4.17), (4.18), and replacing them in Eq. (4.9), gives three non-linear second-order of ordinary differential equations (ODE) which the generalised time-dependent coordinates can be solved numerically by an already built-in differential solver in Maple, (Heck (2003)).

4.4 The first fundamental period, T_N

In deriving T_N, besides the assumption that the plate is an isotropic and homogeneous material, and to simplify calculations, only displacement in the z direction is considered. The assumption is valid as both displacements in-plane directions are very small and will not significantly change the period. The new Langrange's equation analogous to Eq. (4.9) where ϕ is no longer a time dependent coordinate is now used to obtain a simplified modal equation of motion:

$$\frac{d}{dt}\left(\frac{\partial K_E}{\partial \dot{\phi}_1}\right)+\frac{dU}{\partial \phi_1}=\frac{dW_D}{\partial \phi_1} \tag{4.19}$$

Substituting $m=\rho t_p$ as mass per unit area and the first derivative of *w*, Eq. (4.3) (velocity in z direction) into Eq. (4.18); the kinetic energy is given by:

$$KE=\frac{1}{2}\ m\int_{-a}^{a}\int_{-b}^{b}\left(\dot{w}^2\right)\ dy\ dx \tag{4.20}$$

Integrates and simplifies Eq. (4.20):

$$\frac{\partial KE}{\partial \dot{\phi}_1}=\frac{\partial}{\partial \dot{\phi}_1}\left(\frac{32768}{99225}m\dot{\phi}_1^{\,2}\,a^9b^9\right) \tag{4.21}$$

and differentiates against t, Eq. (4.21) becomes:

$$\frac{\partial}{\partial t}\left(\frac{\partial KE}{\partial \dot{\phi}_1}\right)=\frac{65536}{99225}\,m\,\ddot{\phi}_1\,a^9b^9 \tag{4.22}$$

Similarly, the total potential energy, Eq. (4.16) can now be simplified to:

$$U_b=\frac{1}{2}D\phi_1^{\,2}\,a^5\,b^5\left(\frac{32768}{1575}\,a^4+\frac{32768}{1575}b^4+\frac{131072}{11025}a^2b^2\right) \tag{4.23}$$

and differentiates against ϕ_1 gives:

$$\frac{dU_b}{\partial \phi_1}=D\phi_1\,a^5\,b^5\left(\frac{32768}{1575}\,a^4+\frac{32768}{1575}b^4+\frac{131072}{11025}a^2b^2\right) \tag{4.24}$$

The external work done by uniformly distributed load, Eq. (4.17) is given now as:

$$W_D = \frac{256}{225} P(t)\, \phi_1\, a^5\, b^5 \tag{4.25}$$

and differentiates against ϕ_1 gives:

$$\frac{dW_D}{\partial \phi_1} = \frac{256}{225} P(t)\, a^5\, b^5 \tag{4.26}$$

Finally, substitutes Eqs. (4.22), (4.23) and (4.25) into Eq. (4.19) yields modal equation of motion:

$$\ddot{\phi} + \frac{63D}{ma^4b^4}\left(\frac{a^4}{2} + \frac{b^4}{2} + \frac{2}{7}(ab)^2\right)\phi = \frac{71.68}{ma^4b^4} P(t) \tag{4.27}$$

Comparing Eq. (4.27) against a typical modal of equation for a single degree of freedom:

$$\ddot{\phi} + \omega_n^2 \phi = \varphi_{static} P(t) \tag{4.28}$$

where ω_n is the natural frequency and φ_{static} is modal static deflection, therefore the natural frequency of the system can be written as follows:

$$\omega_n = \sqrt{\frac{63\,D}{m\,a^4\,b^4}\left(\frac{a^4}{2} + \frac{b^4}{2} + \frac{2}{7}(ab)^2\right)} \quad or \quad T_N = \frac{2\pi}{\omega_n} \tag{4.29}$$

4.5 The static displacement of a fixed plate

Under static condition, the virtual work done by the inertia forces is zero and, assuming that the damping force is not significant, the total potential energy now is the combination of strain energies by bending U_{bs} and membrane U_{ms}. Eliminating ∂W_{IN} and ∂W_c, Eq. (4.6) can now be simplified to:

$$dU = dU_{ms} + dU_{bs} = dW_D \tag{4.30}$$

Therefore, the revised general form of static equations analogous to the general Lagrange's equation can now be written as:

$$\frac{dU}{\partial \phi_i} = \frac{dW_D}{\partial \phi_i} \tag{4.31}$$

where $\phi_{1,}$ ϕ_2, ϕ_3 are now no longer time dependent but only the generalised coordinates in the directions of z, x and y, respectively. By replacing deformed functions u, v and w into the appropriate equations similar to section 4.3, this will result in three equations which can be solved manually.

To demonstrate the proposed method, an example of a plate with the following properties is considered; E_s = 2.05e^{11} Nm^{-2} ν = 0.3, a = 1.0 m, b = 0.5 m (plate size 2 m x 1m) and t_p = 0.01 m, after the substitution of the plate properties into the equations; leaves behind three equations with three unknown variables which are as follows (e^x = 10^x) :

$$\begin{gathered} 4.18376e^5\phi_1^3 + 5.2837e^5\phi_1\phi_2 + 1.3209e^5\phi_1\phi_3 + 1.4711e^4\phi_1 \\ -3.5555e^{-2}P = 0 \end{gathered} \tag{4.32}$$

$$2.6419e^5\phi_1^2 + 1.6020e^8\phi_2 + 1.3016e^7\phi_3 = 0.0 \tag{4.33}$$

$$6.6046e^4\phi_1^2 + 1.3016e^7\phi_2 + 1.2265e^8\phi_3 = 0.0 \tag{4.34}$$

Solving Eqs. (4.33) and (4.34) gives ϕ_2 and ϕ_3 in terms of ϕ_1

$$\phi_2 = -1.61935e^{-3}\phi_1^2; \quad \phi_3 = -3.66647e^{-4}\phi_1^2 \tag{4.35}$$

Replacing ϕ_2 and ϕ_3 in Eq. (4.32), results in a third degree equation in which only ϕ_1 couples with the external pressure P , Eq. (4.35).

$$4.1747e^5\phi_1^3 + 1.4712\phi_1 - 3.5556e^{-2}P = 0 \tag{4.36}$$

The static displacement of the plate can now be determined by providing the pressure P and considering only the real value of ϕ_1 from the solution of the cubic equation.

When P = 100000 Nm^{-2} (1 bar); $$\phi_1 = \begin{Bmatrix} 0.148588 \\ -0.074294 + i0.2276 \\ -0.074294 - i0.2276 \end{Bmatrix}^*$$

(* - solved using hand calculator)

Substitute ϕ_1 into Eq. (4.3), at x = 0, y = 0 (middle of the plate), the approximate static deflection for plate (t_p = 10 mm thick) = 0.009287 m.

4.6 The static yield limit

Under the performance based design approach, the ductility ratio can be used as an indicator for evaluating the performance level for a component or a system. The ratio is defined as the division of maximum response against the elastic response at yield.

For most materials, the yield point at which plastic strain is noticeable is not obvious. The graphical method, such as the offset method and the tangent method are the two that are usually implemented to approximate the yield point as shown in Figure 4.2, (Chen and Han (1991)).

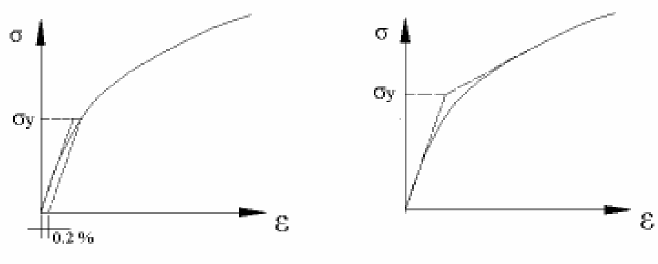

a. Offset Method **b. Tangent Method**

Figure 4.2

Methods for approximating yield point

In the first method, yield point is defined as a intersection between the stress-strain curve and a tangential line at the residual strain of 0.2 percent, while in the second method it is defined as the intersection between the tangential lines of elastic and plastic behaviour.

For a rectangular plate with fixed end boundary conditions, loaded with pressure P, the initial maximum strain at yield (ε_{yield}) occurs in the middle of the longitudinal side supports or at both ends of the shorter span (the first mode) shown by Figure 4.3.

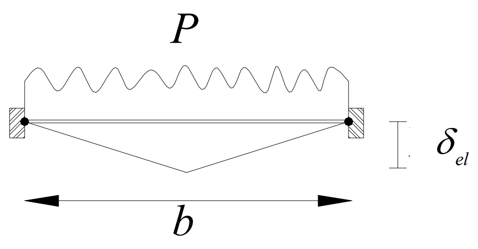

Figure 4.3

Cross section of plate - estimate of elastic displacement at yield , δ_{el}.

(when ε_y at both end supports reach 0.13%)

In the proposed method for approximating static yield displacement δ_{el} , the following assumptions are made:

(a) δ_{el} is the deflection of the plate in the middle at which the assumed strain value reaches 0.13 percent at both ends for a grade of steel where F_y = 248 MPa (different strains should be used for different grades of steel).

(b) ε_x and γ_{xy} = 0 at y = $\pm$ b, therefore the maximum principal strain

$$\varepsilon_{12} = \frac{\varepsilon_x + \varepsilon_y}{2} \pm \sqrt{\left(\frac{\varepsilon_x - \varepsilon_y}{2}\right)^2 + \gamma_{xy}^2} = \varepsilon_y = 0.0013 \qquad (4.37)$$

(c) the whole-cross section at supports becomes plastic when the considered element at the external surface of plate surface reaches the yield limit.

Thus, the total strain at the support is the combination of strains due to the actions of bending, together with membrane, and can be written as follows:

$$\varepsilon_{y-Total} = \varepsilon_{y-Bending} + \varepsilon_{y-Membrane} \tag{4.38}$$

$$\varepsilon_y = \left[z\frac{\partial^2 w}{\partial y^2} \right] + \left[\frac{\partial v}{\partial y} + \frac{1}{2}\left(\frac{\partial w}{\partial y} \right)^2 \right] \tag{4.39}$$

Substitute w and v into Eq. (4.39)

$$\varepsilon_y = \left\{ \begin{array}{c} z\left[8\phi_1 (a^2 - x^2)^2 y^2 + 4\phi_1 (a^2 - x^2)^2 (b^2 - y^2) \right] \\ + \\ \left[\begin{array}{c} \phi_3 (a^2 - x^2)(b^2 - y^2) - 2\phi_3 y^2 (a^2 - x^2) \\ + \\ 8\phi_1^2 (a^2 - x^2)^4 (b^2 - y^2)^2 y^2 \end{array} \right] \end{array} \right\} \tag{4.40}$$

Consider only half of the span such that at the support, x = 0.0, y = b, Eq. (4.40) is now simplified to:

$$\varepsilon_y = -z\ 8\phi_1\, a^4\, b^2 - 2\phi_3\, b^2\, a^2 \tag{4.41}$$

The value of ϕ_3 in terms ϕ_1 can be obtained by using the method discussed under section 4.5. The coefficient of ϕ_1 , *K,* which is a constant for specific plate aspect ratio of a/b is tabulated in Table 4.1.

Table 4.1

Co-efficient *K* ($\phi_3 = -K\,\phi_1^2$)

Ratio a/b	-1 x 10^{-5}
1.0	2.883
1.5	13.457
2.0	36.665
2.5	74.042
3.0	122.931
3.5	176.821
4.0	226.132

Replacing ϕ_3 in terms of ϕ_1 into Eq. (4.41) and re-arranging, Eq. (4.42) is now a quadratic equation for which the roots can be solved by applying standard formula Eq. (4.43)

$$2Ka^2b^2\,\phi_1^2 - z\,8\phi_1\,a^4\,b^2\phi_1 + \varepsilon_y = 0 \qquad (4.42)$$

$$\left(\phi = \frac{-B \pm \sqrt{B^2 - 4AC}}{2A}\right) \qquad (4.43)$$

where $A = 2K\,a^2\,b^2,\ B = -z\,8a^4\,b^2,\ C = \varepsilon_{yield}$

The approximate displacement at yield can be determined by substituting ϕ_1 back into Eq. (4.3).

To validate the proposed method, two sizes of mild steel plates (F_y= 248 MPa) with different thicknesses of 8 mm, 12 mm, 15 mm, 20 mm and 25 mm are selected for comparison. These plates are modelled using ABAQUS CAE and ABAQUS modified Riks Algorithm non-linear analysis (Riks (1979) and Crisfield (1981)) is employed to generate the curve for the middle displacement against the strain at the support. The displacements at yield are determined using the two aforementioned methods; tangent method and by monitoring strain when the strain ε_y reaches 0.0013.

As can be seen from Table 4.2, with the exception of the 8 mm thick plate, the overall results of the present study are close in agreement with the finite element analyses (FEA). It is also interesting to note that when the aspect ratio (a/b) of the plate is increased from 2 to 4, the differences between displacements become quite insignificant. Conversely, as the plate becomes more slender, the present study slightly over-estimates the displacement. The former behaviour is due to the plate behaving more like a beam, while the second behaviour is due the rising number of elements along the support edges, which have also reached yield in FEA.

Table 4.2

Comparison of displacements (δ_{el} mm) at the centre of the plate

a/b = 2 **a/b = 4**	**ABAQUS** **Riks Analysis** ($\varepsilon_{yeild} = 0.0013$)	**ABAQUS** **Riks Analysis** **(tangent method)**	**Present Analytical study** **Eqs. (4.3 and 4.43)**
Pl 2 x 1: 25 mm thk.	3.60	3.25	3.25
20 mm thk.	4.20	4.04	4.06
15 mm thk.	5.68	5.40	5.42
12 mm thk.	6.70	5.90	6.77
10 mm thk.	7.60	6.40	8.12
8 mm thk.	8.48	6.88	10.15
Pl 4 x 1 : 25 mm thk.	3.65	3.40	3.24
20 mm thk.	4.47	4.05	4.04
15 mm thk.	5.63	5.20	5.38
12 mm thk.	6.75	6.20	6.70
10 mm thk.	7.75	6.72	8.00
8 mm thk.	8.53	7.15	9.93

4.7 The analysis of deck plates

Under performance based prescriptive design, most platform operators limit the minimum thickness for deck floor to 8 mm. Deck designers will opt for 10 mm thick mild steel to minimise permanent displacement due to that fact that heavy live loads can cause depression on the plates which leads to water ponding and the collection of over-spilled oil on the deck floor. The deck plates are supported by rows of stringer beams which are typically spaced between 1.0 m to 1.2 m.

In the analysis, two plate sizes are chosen, 2.0 m x 1.0 m and 4.0 m x 1.0 m. The thicknesses of plates is varied based on commercially available sizes from 5 mm, 8 mm, 10 mm, 15 mm, 20 mm and 25 mm. The plates are made from mild steel, F_y= 248 MPa with Young's modulus, $\boldsymbol{E}$ = 2.05 x 10^{11} N/m^2 and Poisson's ratio υ = 0.3.

The time-dependent pressure *P(t)* with equal rise and fall in times (isosceles triangular) is uniformly applied on the plate surface for total duration, t_d = 50 ms. The peak pressure starts from 0.5 bar, 0.75 bar, 1.0 bar and follows with an increment of 1 bar up to maximum pressure of 6.0 bar.

Using the energy terms discussed in section 4.3, computer codes using Maple software is developed for solving the generalised coordinates in both dynamic and static cases.

4.7.1 Classification of deck plates

Table 4.3 summarises the characteristics of the chosen plates. The stocky plates, thickness 15 mm and greater, are found to fall under the quasi-static domain, while plates 10 mm thick lie in between the transition of quasi-static and dynamic domains. The slender plates, 8 mm thick or less, fall into the dynamic domain, for which it is highly likely they will develop membrane strains even for a pressure at lower level.

At the outset of the design stage, it is pertinent to establish the classification of plates as this allows designers to predict the responses which help to affirm the decision on how other structural members will behave.

Table 4.3

Properties and classification of plates

t_d is assumed 50 ms (typical for hydrocarbon gas explosions)
(Impulsive - t_d/T_N < 0.3, dynamic -0.3 < t_d/T_N < 3, quasi-static 3 < t_d/T_N ; N-004 Norsok (1998))

a. Plate 2 m x 1 m

Thickness t_p; Slenderness b/t_p	Period T_N (ms)	Ratio t_d/T_N	Classification
25; 40	6.59	7.58	quasi-static
20; 50	8.24	6.07	quasi-static
15; 67	10.99	4.55	quasi-static
10; 100	16.48	3.03	quasi-static
8; 120	20.61	2.43	dynamic
5; 200	32.97	1.52	dynamic

b. Plate 4 m x 1 m

Thickness t_p; Slenderness b/t_p	Period T_N (ms)	Ratio t_d/T_N	Classification
25; 40	7.10	7.04	quasi-static
20; 50	8.88	5.63	quasi-static
15; 67	11.83	4.23	quasi-static
10; 100	17.75	2.82	Dynamic
8; 120	22.19	2.25	Dynamic
5; 200	35.50	1.41	Dynamic

4.7.2 Analytical responses of deck plates

As shown in Table 4.4, the results indicate that the response of each plate depends on the duration t_d. As the natural period approaches t_d, the anticipated response becomes very significant and may reach the maximum value. Hence, plates less than 10 mm thick show higher dynamic amplification factors (DAF) compared to the 15 mm thick plate and greater.

There are a few cases in which the DAFs are found almost equal to unity, e.g. plate 15 mm thick. This illustrates that the plates are in the lowest region of the DAF curve. Similarly, as the slenderness of the plate is increased, the DAF also becomes significant.

It is worth noting that, although displacement for the plate with greater aspect ratio a/b is higher than the plate with less aspect ratio a/b, the ratios of dynamic against static displacement in both cases are found to be similar. Hence, it can be concluded that the DAF for a plate only depends on the ratio of t_d/T_N and the slenderness ratio b/t_p.

4.7.3 Finite element method

For verification of the proposed simplified method and its accuracy, the deck plates are modelled using ABAQUS CAE Version 6.6 as deformable shell elements (4SR) with 800 and 1600 elements for plates 2 m x 1 m and 4 m x 1 m, respectively. Imperfections in the deck plate are not considered but the steel strain rate (Cowper and Symonds coefficients, D = 40.4 s^{-1} and q = 5 from Jones (1971) and HSE Report 105[76]) is included in the material properties.

Post Notes

New cases are added to incorporate the examiners' comments. The selected cases are for plates of 8 mm and 10 mm thicknesses. In the analysed cases, plastic properties and strain rate were removed in the FEA. These cases are named as FE (elastic).

Table 4.4

Estimates of maximum displacements from the analytical results
(Plates 2 m x 1 m and 4 m x 1m)

Thickness (mm)	Peak pressure (bar)	Static (mm)		Dynamic (mm)		Ratio Dynamic/Static	
		2 x 1	4 x 1	2 x 1	4 x 1	2 x 1	4 x1
25	0.50	0.48	0.56	0.50	0.60	1.04	1.07
25	0.75	0.72	0.84	0.76	0.90	1.04	1.07
25	1	0.97	1.12	1.01	1.20	1.04	1.07
25	2	1.93	2.23	2.00	2.39	1.04	1.07
25	3	2.87	3.32	2.99	3.56	1.04	1.07
25	4	3.80	4.38	3.95	4.71	1.04	1.08
25	5	4.71	5.41	4.88	5.81	1.04	1.07
25	6	5.60	6.41	5.78	6.87	1.03	1.07
20	0.50	0.94	1.09	0.93	1.16	0.99	1.06
20	0.75	1.40	1.63	1.41	1.73	0.99	1.06
20	1	1.88	2.17	1.85	2.29	0.99	1.06
20	2	3.69	4.24	3.61	4.43	0.98	1.04
20	3	5.38	6.14	5.26	6.32	0.98	1.03
20	4	6.94	7.85	6.89	7.96	0.99	1.01
20	5	8.37	9.40	8.47	9.41	1.01	1.00
20	6	9.68	10.79	10.01	10.68	1.03	0.99
15	0.50	2.20	2.54	2.30	2.49	1.04	0.98
15	0.75	3.24	3.72	3.41	3.68	1.05	0.99
15	1	4.23	4.82	4.47	4.82	1.06	1.00
15	2	7.56	8.41	8.28	9.04	1.10	1.07
15	3	10.10	11.07	11.07	12.28	1.10	1.10
15	4	12.13	13.18	12.95	14.45	1.07	1.10
15	5	13.83	14.93	14.44	16.07	1.04	1.08
15	6	15.30	16.43	15.70	17.45	1.03	1.06
10	0.50	5.99	6.61	6.80	7.67	1.13	1.16
10	0.75	7.83	8.52	8.61	9.62	1.10	1.13
10	1	9.29	10.02	9.95	11.07	1.07	1.10
10	2	13.26	14.11	15.25	16.55	1.15	1.17
10	3	15.93	16.85	18.24	19.56	1.15	1.16
10	4	18.01	18.99	20.04	21.56	1.11	1.14
10	5	19.73	20.77	22.60	24.30	1.15	1.17
10	6	21.22	22.31	24.58	26.35	1.16	1.18
8	0.50	8.29	8.90	9.72	10.67	1.17	1.20
8	0.75	10.17	10.84	11.61	12.58	1.14	1.16
8	1	11.63	12.34	12.95	14.02	1.11	1.13
8	2	15.63	16.46	18.58	19.76	1.19	1.20
8	3	18.35	19.27	20.71	22.39	1.13	1.16
8	4	20.48	21.47	24.28	25.62	1.19	1.19
8	5	22.26	23.32	26.19	27.80	1.18	1.19
8	6	23.81	24.92	27.25	29.28	1.14	1.17
5	0.50	11.87	12.45	14.16	14.84	1.19	1.19
5	0.75	13.83	14.48	16.75	17.44	1.21	1.20
5	1	15.37	16.08	18.98	19.73	1.24	1.23
5	2	19.69	20.57	22.98	24.19	1.17	1.18
5	3	22.70	23.69	27.15	28.54	1.20	1.20
5	4	25.08	26.17	29.44	30.07	1.17	1.15
5	5	27.08	28.25	32.48	32.92	1.20	1.17
5	6	28.30	30.07	34.09	35.62	1.18	1.18

i. **The out-plane displacements (z- direction) of the plates**

From the graphs in Figure 4.4, the comparison of displacements evaluated from the analytical approach (AA) of the present simplified method with the finite element analysis (FEA) can be summarized as follows:

a) Plate 25 mm thick, the stockiest plate in the study, compares favourably with FEA for all cases.

b) Plate 20 mm thick compares favourably with FEA up to overpressures of 4.5 bar followed by a significant increase in FEA thereafter.

c) Plate 15 mm thick compares favourably up to 2.7 bar and 3.8 bar for plates 2 m x 1 m and 4 m x 1 m, respectively, showing a steady increase in FEA thereafter.

d) Since the thickness of the two plates is quite close, the response of plate 10 mm thick is comparable to plate 8 mm thick. They are compared favourably with FEA up to 2.6 bar and 3.3 bar for plates 2 m x 1 m and 4 m x 1 m, respectively, showing a steady increase in FEA thereafter.

e) Plate 5 mm thick compares favourably up to 2 bar and 3 bar for plates 2 m x 1 m and 4 m x 1 m, respectively. The development of membrane strain is significant thereafter in FEA whereby a rapidly rising slope exceeds the present study.

f) In most cases, the proposed analytical analysis has slightly over-predicted the displacement before the relevant elements start to deform plastically.

g) For plates of 8 mm and 10 mm thickness without plastic properties in FEA (elastic), the displacements are compared favourably with the proposed analytical analysis.

In conclusion, the results from the proposed simplified method resemble FEA (with elastic-plastic properties) up to a threshold at which plasticity becomes intrinsically controlling of the behaviour of the modelled elements. Although this finding limits the use of the proposed simplified method, the approach has shown a good correlation with FEA with less than 10 percent difference in terms of displacements up to a pressure of 4.0 bar.

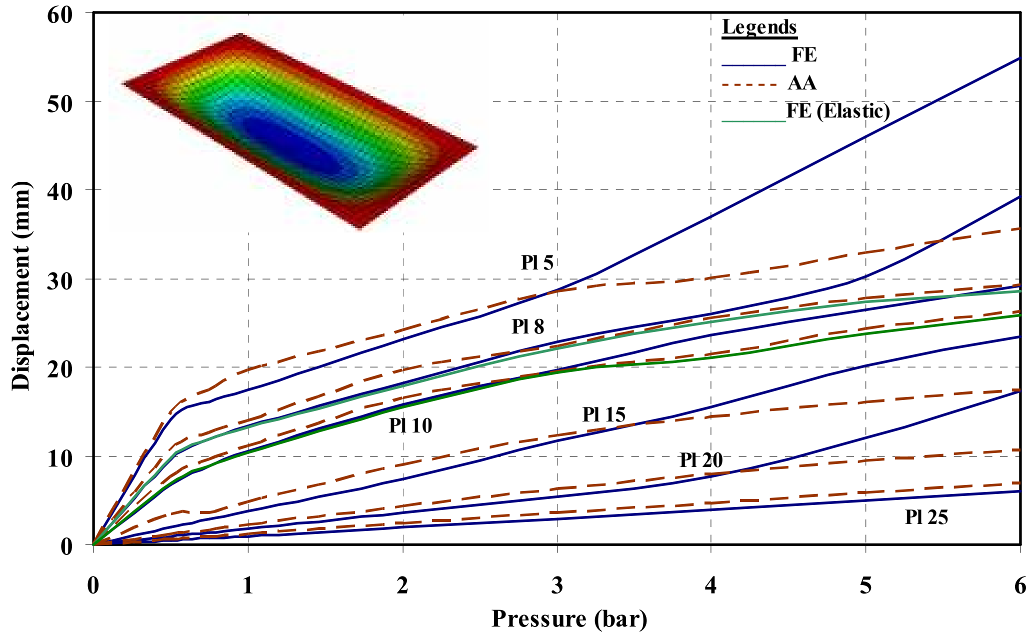

a) Plate 2 m x 1 m, a/b = 2

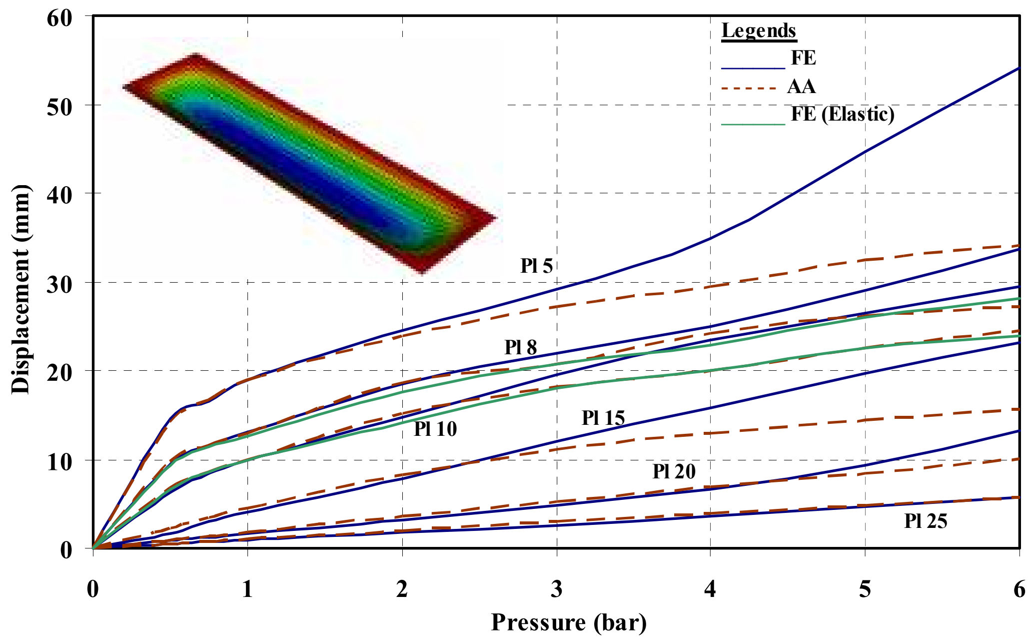

b) Plate 4 m x 1 m, a/b = 4

Figure 4.4

Middle plate displacement – Plates: 2 m x 1 m and 4 m x 1m
(FE –Finite Element , AA –Analytical Analysis)

ii. The strains in longitudinal (x) and transverse (y) directions

Despite the fact that the terms of the generalized displacements *u, v and w* are solved non-linearly and the calculated out-plane displacements are consistent up to maximum 4.0 bar compared to FEA, the comparison of strain is found to be very sensitive to the change of overpressure. Contribution by yielding and propagating of plasticity from deformed elements to other adjacent elements has triggered extensive elongation of elements over the plate area, especially at the supports at higher overpressure. The drastic change of strains and the selected cases influenced by these behaviours are shown in Figures 4.5 and 4. 6.

For plate 25 mm thick, the calculated strains are quite consistent with FEA under all circumstances. For other plates, the consistency of the results ends at a particular point of pressure, which depends on the thickness of the plates. The plotted strain curves also show that the approximate values of strains are always slightly higher than FEA in the transverse direction before a sudden rise. On the contrary, for higher aspect ratio such as plate 4 m x 1 m, the strains in longitudinal direction are found to be slightly lower than FEA. This is not critical as the governing case is the strain along the transverse side supports on which the design will be based.

From Table 4.5, the consistency of strain results between FEA and the present study improves when the aspect ratio equals 4. The effect is more significant on the slender plates 5 mm thick and 8 mm thick because the membrane forces are spreading efficiently over the plate area. Nevertheless, this has no effect on the stocky plates. Thus, the performance of a thin and slender plate can be improved by increasing the aspect ratio a/b.

Table 4.5

The maximum limit of consistency between FEA and AA
(when FEA curves intersect with AA curves)

Plate Thickness (mm)	Plate 2 m x 1m (bar)	Plate 4 m x 1 m (bar)
5	0.95	1.6
8	1.1	1.9
10	1.2	2.0
15	2.5	3.0
20	4.0	4.0
25	6.0	6.0

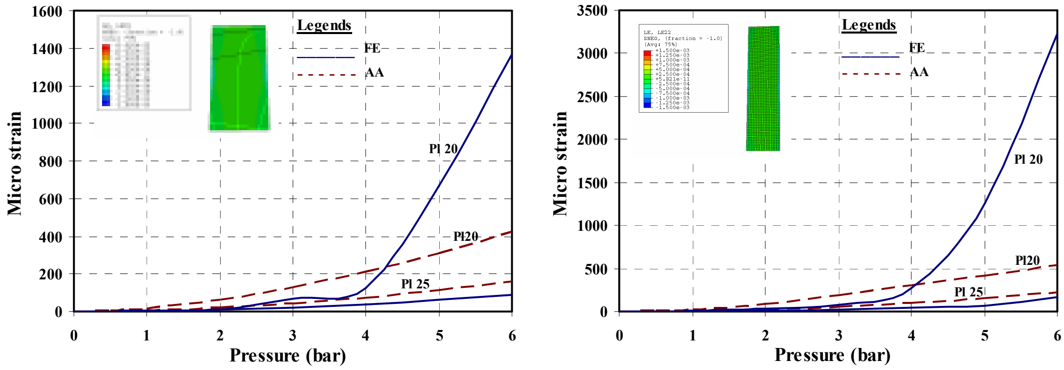

a. b/t_p = 40 and 50, aspect ratio a/b = 2 and 4
The contour profiles (FE) shown are for plate 25 mm, Pr = 6 bar, t = 50 ms

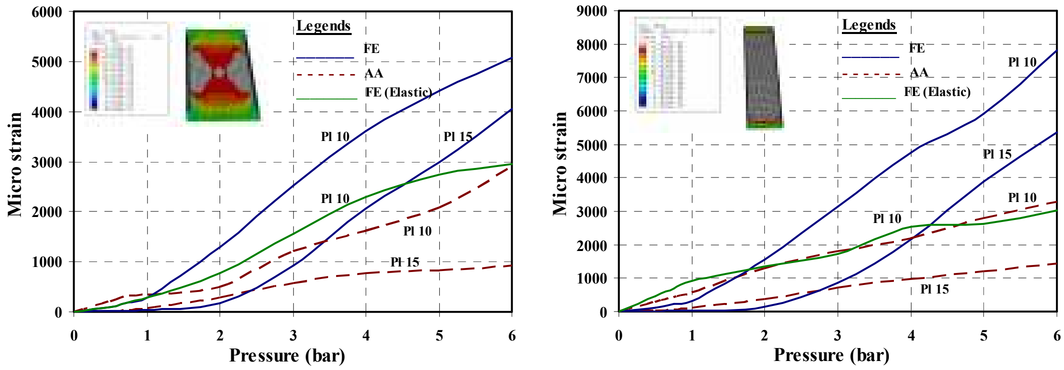

b. b/t_p = 67 and 100; aspect ratio a/b =2 and 4
The contour profiles (FE) shown are for plate 10 mm, Pr = 6 bar, t = 50 ms

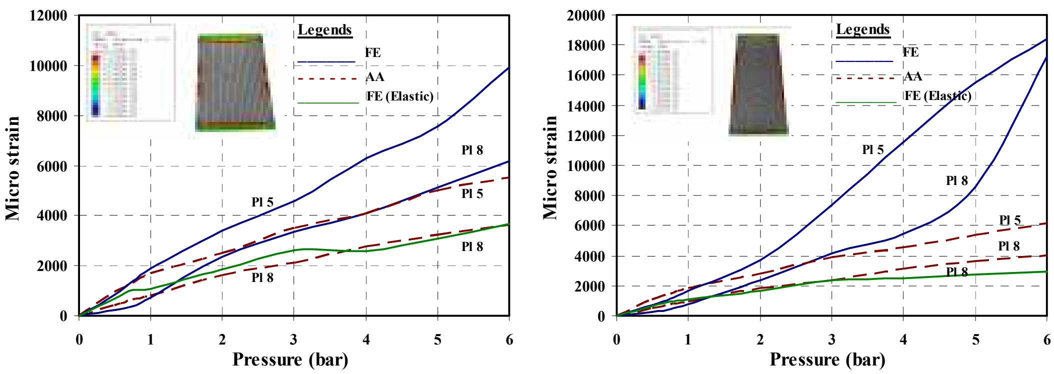

c) b/t_p = 125 and 200; aspect ratio a/b = 2 and 4
The contour profiles (FE) shown are for plate 5 mm, Pr = 6 bar, t = 50 ms

Figure 4.5
Maximum transverse strain ε_y

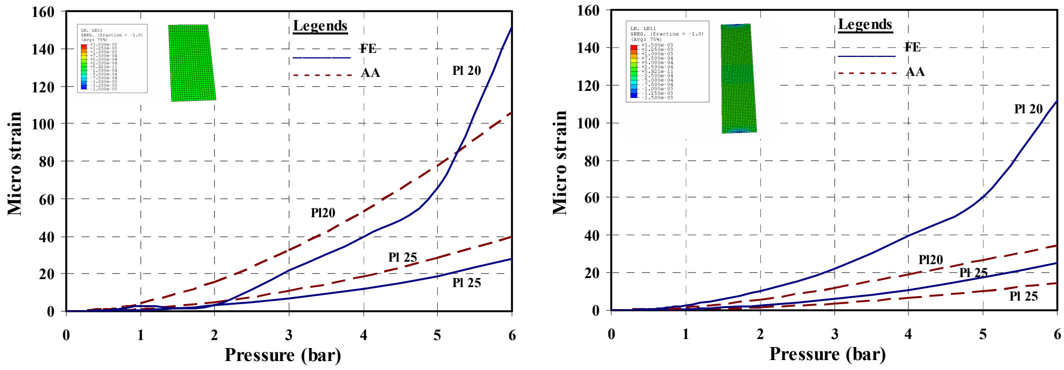

a. b/t_p = 40 and 50, aspect ratio a/b = 2 and 4

The contour profiles (FE) shown are for plate 25 mm, Pr = 6 bar, t = 50 ms

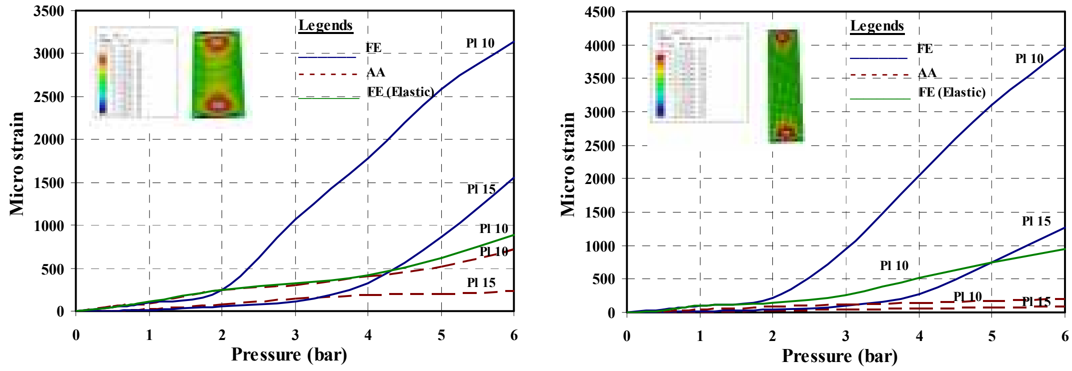

b. b/t_p = 67 and 100; aspect ratio a/b =2 and 4

The contour profiles (FE) shown are for plate 10 mm, Pr = 6 bar, t = 50 ms

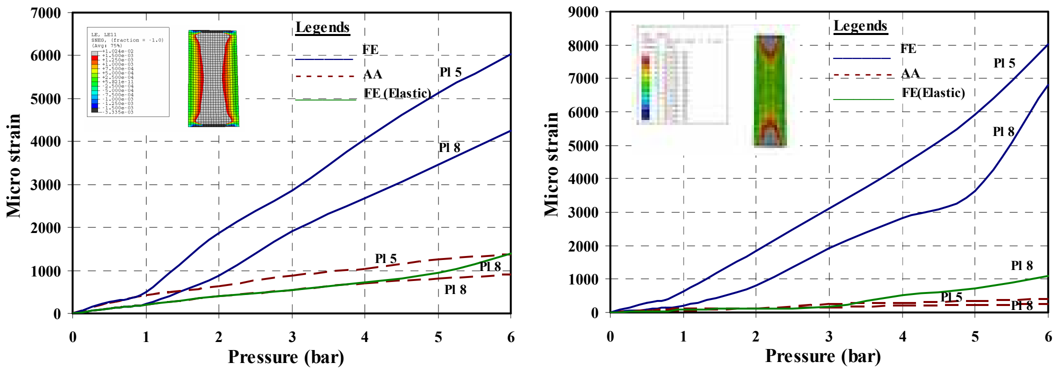

c. b/t_p = 125 and 200; aspect ratio a/b = 2 and 4

The contour profiles (FE) shown are for plate 5 mm, Pr = 6 bar, t = 50 ms

Figure 4.6

Maximum transverse strain ε_x

For the additional cases without plasticity, despite the erratic plotted graphs, responses from FEA (elastic) are close to the proposed analytical method without any sudden jumps at higher pressure.

4.8. Ductility of deck plates

Based upon the formulation derived in section 4.5 for δ_{el}, a summary of ductility ratios is presented in Table 4.6. The shaded cells represent ductility ratios (DRs) that have exceeded 10 percent (4 bar and above) in comparison to the present study (AA) to the FEA which can be explained due to extensive plastic deformation in FEA.

Table 4.6

Ductility of plates, $\mu = \frac{\delta_{max}}{\delta_{el}}$

		Plate 2 m x 1 m						Plate 4 m x 1m					
	t_p (mm)	25	20	15	10	8	5	25	20	15	10	8	5
	b/t_p Pr.	40	50	67	100	125	200	40	50	67	100	125	200
AA	0.50	0.16	0.23	0.42	0.84	0.96	0.92	0.19	0.29	0.65	0.96	1.05	0.91
FE	0.50	0.14	0.21	0.32	0.79	0.93	0.95	0.15	0.23	0.37	0.84	0.95	0.87
AA	0.75	0.23	0.34	0.63	1.06	1.14	1.09	0.28	0.43	0.68	1.20	1.24	1.07
FE	0.75	0.21	0.31	0.55	1.04	1.14	1.07	0.23	0.35	0.54	1.11	1.17	0.99
AA	1.00	0.31	0.46	0.83	1.23	1.28	1.23	0.37	0.57	0.90	1.38	1.38	1.21
FE	1.00	0.28	0.41	0.75	1.22	1.28	1.23	0.30	0.46	0.71	1.31	1.32	1.07
AA	2.00	0.62	0.89	1.53	1.88	1.83	1.56	0.74	1.10	1.68	2.07	1.95	1.49
FE	2.00	0.56	0.80	1.45	1.82	1.82	1.59	0.59	0.90	1.38	1.98	1.80	1.42
AA	3.00	0.92	1.30	2.04	2.25	2.04	1.76	1.10	1.56	2.28	2.45	2.21	1.76
FE	3.00	0.81	1.19	2.21	2.41	2.16	1.89	0.90	1.35	2.17	2.46	2.25	1.77
AA	4.00	1.21	1.70	2.39	2.47	2.39	1.91	1.45	1.97	2.69	2.69	2.52	1.85
FE	4.00	1.11	1.64	2.92	2.89	2.46	2.26	1.19	1.88	2.88	2.94	2.56	2.27
AA	5.00	1.50	2.09	2.66	2.78	2.58	2.11	1.79	2.33	2.99	3.04	2.74	2.03
FE	5.00	1.43	2.29	3.63	3.26	2.85	2.90	1.55	2.97	3.74	3.30	2.98	2.83
AA	6.00	1.78	2.46	2.90	3.03	2.68	2.22	2.12	2.64	3.24	3.29	2.88	2.19
FE	6.00	1.75	3.24	4.28	3.63	3.32	3.52	1.86	4.28	4.37	3.65	3.86	3.38

Notes:
AA - analytical analysis FE – finite element Pr. – pressure in bar

As the area of a plate 4 m x 1 m is twice as great as a plate 2 m x 1 m, on average, theoretically, the ductility ratios of plates 4 m x 1 m should be higher than plates 2 m x 1 m at same level of overpressure. The ductility ratios of stocky plates 25 mm thick remain the least affected with the applied pressure. Plate 20 mm thick shows a sudden jump at 5 bar and thereafter in FEA, illustrates that the plasticity in the plate has occurred locally. Conversely, for plates 15 mm thick and less, the changes of ductility ratios are quite gradual, which can be explained by the uniformly distributed plasticity over the whole area of the plate. In the same fashion shown by the responses of the plate in terms of displacement, the measured ductility ratios also manage to show comparable results between the two analyses; the present proposed analytical method (AA) and the FEA method.

As can be seen from Figure 4.7, the optimum plate thickness in design is when the slenderness of the plate is between 70 and 100 (plates 8 mm, 10 mm and 15 mm thicknesses) whereby the ductility ratio slopes rise moderately until a maximum and slowly reduce its steepness. The selection of plate 25 mm thick and 20 mm thick are quite conservative if they are to be chosen as deck plates as these still possess elastic characteristics even at high pressure, and a sudden jump in ductility ratio (plate 20 mm thick) occurs only at high pressure, while with plate 5 mm thick the change of ductility ratio is erratic due to early development of membrane forces.

Although the determining of δ_{el} will not be straightforward for a complex structure with multi degrees of freedom, ductility ratio values can offer extra information on the state condition of the plate during blast. Moreover, based on ductility ratios, the appropriate slenderness for which suitable design can quickly be decided may involve extra hours in computing times.

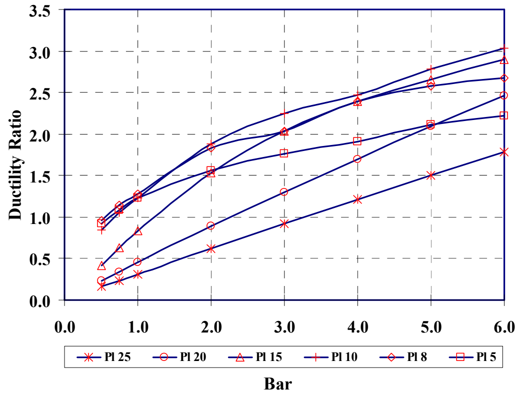

a. Plate 2 m x 1 m
(Analytical analysis)

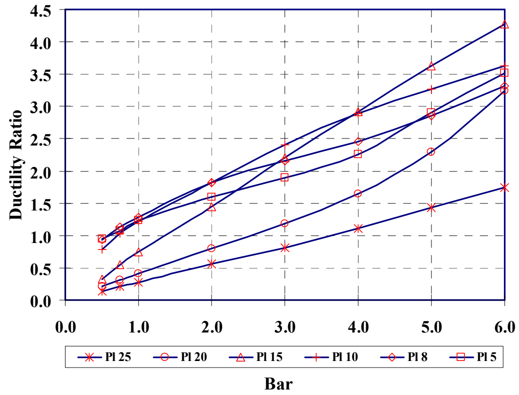

b. Plate 2 m x 1 m
(Finite element)

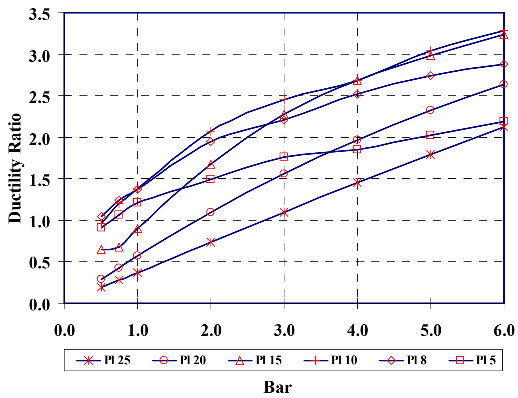

c. Plate 4 m x 1 m
(Analytical analysis)

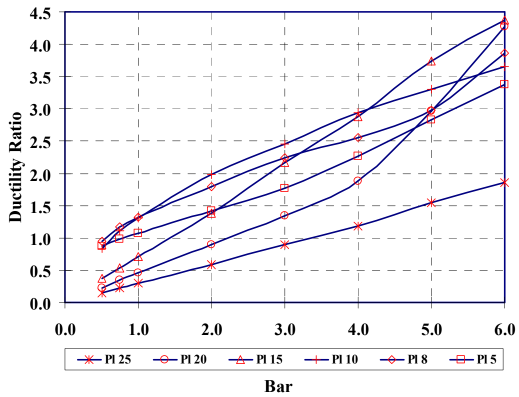

d. Plate 4 m x 1 m
(Finite element)

Figure 4.7

Ductility ratio – pressure

Notes:
Separate plots for clarity between analytical analysis and finite element analysis show plate 8 mm thick, plate 10 mm thick and plate 15 mm thick slopes rising gently until peak and gradually decreasing compared with other plates thicknesses.

4.9 Comparisons with experiment

The present analytical approach (AA) is compared to the experiment result by Schleyer et al. (2003) who conducted several tests on clamped mild steel with different edge conditions and plate stiffening. The selected experiment result is based on plate PLT/1, restrained at edges, no intermediate stiffening with net area exposed to pulse loading being 1.0 m x 1.0 m and, the thickness of plates investigated was 2 mm with an average grade F_y =186 MPa. A total of 60 stud bolts were used to fix the position of the plate ends to the frame and the authors reported an average slip of 1mm as a result of membrane forces. The estimated duration t_d and maximum pressure P_{max} of pulse were 62.83 ms (Figure 4.8) and 1.022 bar respectively, during which a maximum displacement of 44 mm was observed in the out-plane direction.

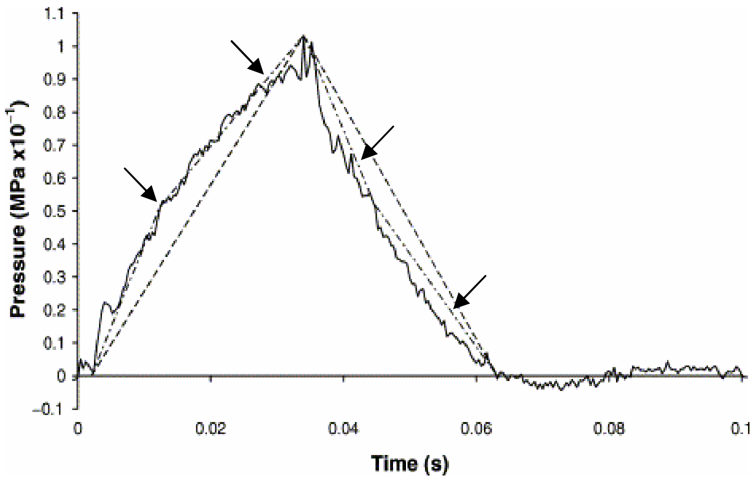

Figure 4.8

Pressure-time pulses – Experiment and linearised curves, Schleyer et al. (2003)
(Arrows show the chosen profile implemented in the analyses)

As shown in Table 4.7, the tested plate is a slender member and falls under the dynamic domain.

Table 4.7

Classification of test PLT/1, Schleyer (2003)

Static yield , δ_{el} (Section 4.5)	40.63mm
Natural period , T_N (Eq. (4.29) for ω_n)	56.43 ms
$\frac{t_d}{T_N}$ (Figure 4. 8, for t_d = 62.83ms)	1.11 (dynamic)
Plate slenderness, b / t_p	1000/2 = 500 (very slender)

4.9.1 The analyses and results

The plate is analysed using the proposed method of the present analytical approach (AA) and FEA with ABAQUS 6.6 as a control case. The plate is modelled with 400 shell elements (S4R) and the edges are specified as fixed.

The results of the maximum displacement between the FEA and AA show a very close agreement, however these values are about half the maximum displacement as reported by Schleyer et al. (2003), Figure 4.9. This is because the effect of slip at the edges as mentioned in the report was not incorporated in the analyses.

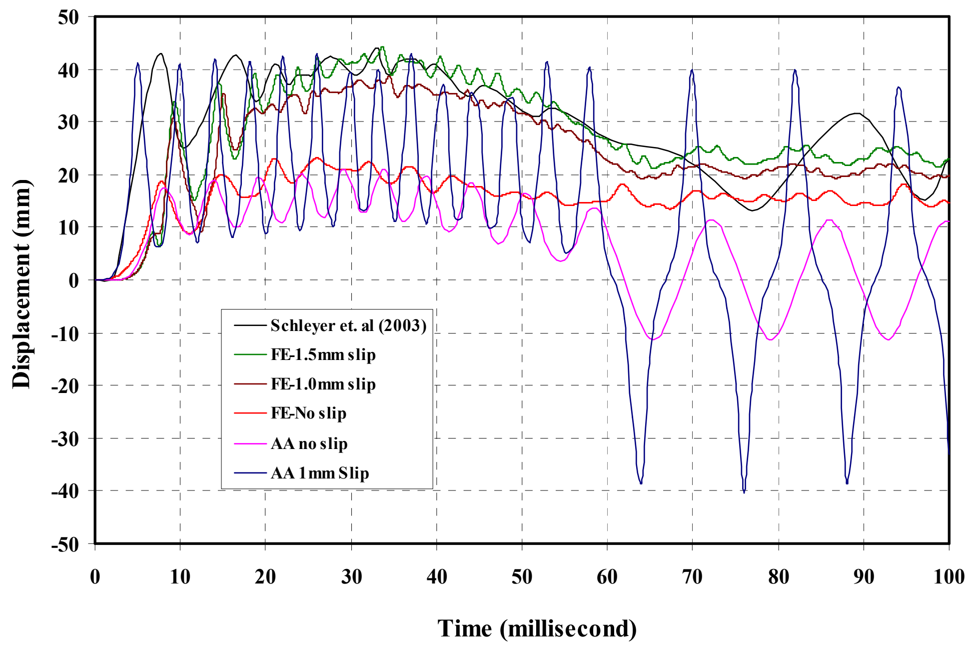

Figure 4.9

The comparison of displacement history at the centre of the plate
(Experiment result Schleyer (2003), ABAQUS Modelling using FE method , the present simplified analytical analysis solved using MAPLE.)

In the new analyses, this effect is incorporated by introducing slip in the boundary option of the input under load module in the FEA as initial step and allows us to propagate in dynamic step , whereas in the present study two new terms were added for u and v, Eqs. (44) and (45)

$$u = x\,(a^2 - x^2)\,(b^2 - y^2)\phi_2(t) - \phi_4\left(\frac{x}{a}\right) \tag{4.44}$$

$$v = y\,(a^2 - x^2)\,(b^2 - y^2)\phi_3(t) - \phi_5\left(\frac{y}{b}\right) \tag{4.45}$$

where ϕ_4 and ϕ_5 represent slips in x and y directions.

As can be seen from Table 4.8, by introducing slip at the plate edges, the maximum displacements for both analytical and finite elements are now quite comparable to the experiment with a ductility ratio just above unity. Similarly, the curves of displacement history with slip (Figure 4.9) shown by both AA and FEA consistently match the experiment within duration t_d. Hence, with minor adjustment in the shape functions, the present simplified method is capable of approximating out-plane displacement accurately which is comparable to the finite element method as well as the experiment.

Table 4.8

The results of the maximum displacements

Experiment / Method	**(mm)**
Experiment	
Schleyer et al. (2003)	44
Analytical Analysis (AA)	
Present study – no slip	21
Present study – introduction of 1mm slip in *u* and *v*	43
Finite Element Analysis (FEA) –ABAQUS	
Original Case – no slip	23
With slip 1mm at boundary	39
With slip 1.5mm at boundary	44
Ductility = 43/40.63 = 1.06	

Despite being able to sustain higher pressure and a low ductility value due to the development of membrane action, the response with too large deformation is certainly not recommended for very thin and slender plates to be part of the topside components, especially for carrying permanent loads. Furthermore, there are substantial piping lines and cables running below the deck floors which will be vulnerable to this impact.

4.10. Conclusion

The proposed method offers an alternative for a simplified analysis to determine the deck plate performance. The method can serve as a handy tool for structural engineers where a quick appraisal can be made, particularly at the outset of the project.

Since the development of strain due to plastic deformation is excluded in the model, the application for deck plate analysis is limited to plates of slenderness less than 125 and a maximum blast pressure of 4 bar. Although this will limit its application, the values are reasonable for effective deck plate design in meeting most of the serviceability and blast resistance issues that are likely to arise.

From the performance based design aspect, ductility ratios can be used as a benchmark to measure the response of topside deck plates. In this study, under the current blast conditions subjected to hydrocarbon explosions, plate slenderness in the range 70 to 100 is recommended for selection of optimum thickness in design.

For efficient energy absorption during a blast, the deck plate with higher aspect ratio is recommended. In this study, uniform strain along longitudinal supports is observed on plate 4 m x 1 m compared with concentration of strain in the middle part of longitudinal supports on plate 2 m x 1 m. The uniform distribution of strain to a larger area will certainly improve the performance level of supporting members.

<u>Response to examiners' comments</u>

"The candidate employed an elastic analysis in the study of deck plates alongside a numerical elastic-plastic analysis and experimental data in which permanent deformation occurred. The examiners were not entirely satisfied that the candidate justified the use of the elastic analysis in the thesis particularly since the analyses were presented in the context of ductility levels for blast resistant design".

Although the proposed analytical method for the deck plate design employed an elastic method, it has included the membrane strain formulation for large displacement that results in output comparable with the finite element method to a certain limit before plasticity becomes significantly dominant in the behaviour. It has been stressed in the introduction of this chapter that deck plates hold prominent roles for other design cases, especially for stability during major operation of topside pre-service conditions i.e. lifting and transportation, where very few studies have looked into this interaction with other structural components. Under normal operating conditions, especially during drilling, many temporary reciprocating machines such as booster pumps and generators are placed on the deck plates. As a result, permanent deformation of deck plates is not allowed due to safety hazards, repair costs and interruption in the process plant.

Despite having its limitations, the proposed method has exhibited a good correlation with finite element analyses at a practical application. It would definitely be a great advantage to design engineers as they are able to approximate initial size and predict deck plate behaviour using a simple method, but the result is equivalent to the finite element method, especially at the outset of the design stage.

Chapter Five

Improving the Ductile Behaviour of Offshore Topside Structures

---

5.1 Modelling a topside structure

The basic criteria in design for offshore installations are to be as simple as possible to construct, as well as being easy and safe to operate. The paramount stage in design is during the conceptual phase when most of the irreversible decisions are made. Firm decision and strong management control will result in minimum re-engineering in order to guarantee a successful project that remains within budget and on schedule. In the past this has been a problem for designing against explosions as possible pressure (P) – time (t) histories given to structural engineers change as the design evolves, generally becoming more severe at later stages.

Due to the fact that offshore installations, especially the topside structures, are potentially subjected to extreme loads more frequently than land based structures, incorporating past experiences in the new design and implementing mitigation work for improving topside structures, are becoming critical issues in design because not only do they change the original concept but could also cause the budget for the project to overrun.

The study presented in this chapter is aimed at demonstrating the application of performance based design for evaluating topside structures and to introduce a novel idea which is simple, cheap and practical for improving the resistance of topside structures to explosions.

In this study, a representative portion of a typical offshore topside structure with primary and secondary structural components was modelled. The assumptions made in developing the model were as follows:

a. The applied blast loadings were in vertical directions (upwards and downwards) and applied as linearised triangular pressure on the deck floors (no temporal or spatial variation accounted for).

b. As the study focuses on response and behaviour of the structure subjected to explosions, only self-weight and blast loads were considered in the analysis.

c. The input of plastic strain (ε_{pl}) and true stress (σ_{true}) were calculated from the nominal plastic-strain data as shown by Figure 5.1 and Eqs. (5.1), (5.2) and (5.3).

$$\varepsilon_{true} = \ln(1+\varepsilon) \quad (5.1)$$

$$\sigma_{true} = \sigma(1+\varepsilon) \quad (5.2)$$

$$\varepsilon_{pl} = \varepsilon_{true} - \sigma_{true}/E \quad (5.3)$$

where ε and σ are the nominal strain and stress from the plasticity data curve.

E = steel Young's modulus.

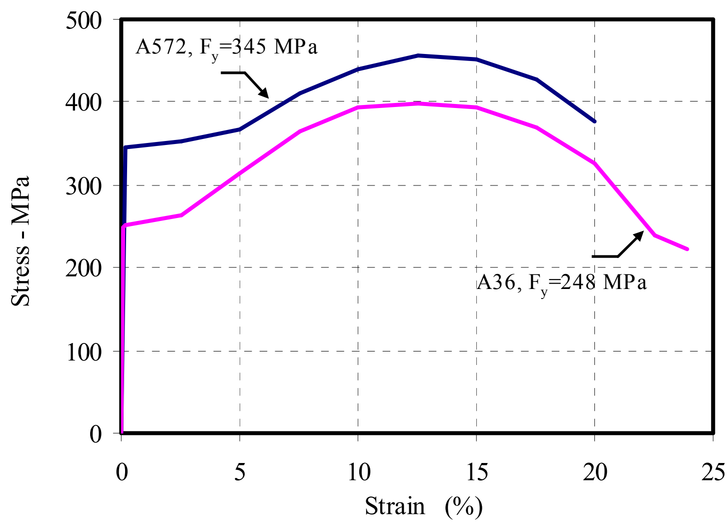

Figure 5.1

Stress strain curves for F_y = 345 MPa and F_y = 248 MPa

d. All connections were fully welded.

e. Minimum gap between structural members were set to 50 mm.

f. The modelled taper for flange plate was set at 1:4 while the haunch gradient was set to 1:1.

g. For a more practical approach and engineering appreciation, all stresses and strains reported were in terms of PEEQ (plastic equivalent strain) and Von Mises (combined stress) as defined by Eqs. (5.4) and (5.6).

$$\boldsymbol{PEEQ = \bar{\varepsilon}^{pl}\Big|_0 + \int_0^t \dot{\bar{\varepsilon}}^{pl}\, dt} \qquad (5.4)$$

where $\bar{\varepsilon}^{pl}\Big|_0$ is the initial equivalent plastic strain and

equivalent plastic strain rate $\dot{\bar{\varepsilon}}^{pl} = \sqrt{\frac{2}{3}\dot{\varepsilon}^{pl} : \dot{\varepsilon}^{pl}}$

The limiting plastic strain from N-004 Norsok standard (1998) given by Eq. (5.5) was used to compare plastic strain at ductility ratios 6 and 20.

$$\varepsilon_{cr} = \mathbf{0.02 + 0.65}\,\frac{t}{l} \qquad (5.5)$$

where ε_{cr} = critical average strain

t = plate thickness

l = length of plastic zone, minimum $5t$

The mesh size of elements varies from a minimum 25 mm square to a maximum 100 mm square, hence the upper limit of plastic strain ε_{cr} (%) of the modelled structural members* were given as follows :

Structural component	ε_{cr} **(%)**
i. Deck Pl 8 mm	7.20
ii. stringer beams IP 300	20.55
iii. plate girder PG 1000	18.25
iv. plate girder PG 1600-1	28.00
v. plate girder PG 1600-2	21.50

(* - refer table 5.1 for full details of structural members)

$$\textit{Von Mises stress} = \sqrt{\frac{3}{2}\, \boldsymbol{S}_{ij}\, \boldsymbol{S}_{ij}} \qquad (5.6)$$

where $\boldsymbol{S}_{ij}$ is the component of stress deviator tensor.

5. 2 The structural configuration of the topside structure

The modelled portion of the topside structure consists of two deck levels, the upper level and the lower level, which are separated 7200 mm apart as shown by Figure 5.2. The two deck levels are inter-connected by two tubulars 508 mm ø 19 mm thick, as vertical and diagonal supports. Below each footprint of the tubular landings on plate girders, 20 mm thick half cut stiffeners from braces 508 mm ø and 650 mm ø are provided for vertical and inclined braces respectively.

Each deck level covers an area of 8000 mm x 6000 mm. The deck plates are made from 8 mm thick plate and supported by secondary structural members IP 300 beams, both of which are mild steel with yield strength, F_y = 248 MPa.

The primary members on the deck level consist of plate girders with two sizes. Plate girder PG 1000 is in the middle of the deck area supports secondary IP 300 beams. Plate girder PG 1600-1 is on the east side of the deck which forms a structural main truss with tubular bracings, while plate girder PG 1600-2 across the deck area serves as an intermediate member which supports plate girder PG 1000 and carries loads from the middle of the deck area back to plate girder PG 1600-1. All plate girders at deck levels are fabricated from high strength steel with F_y = 345 MPa.

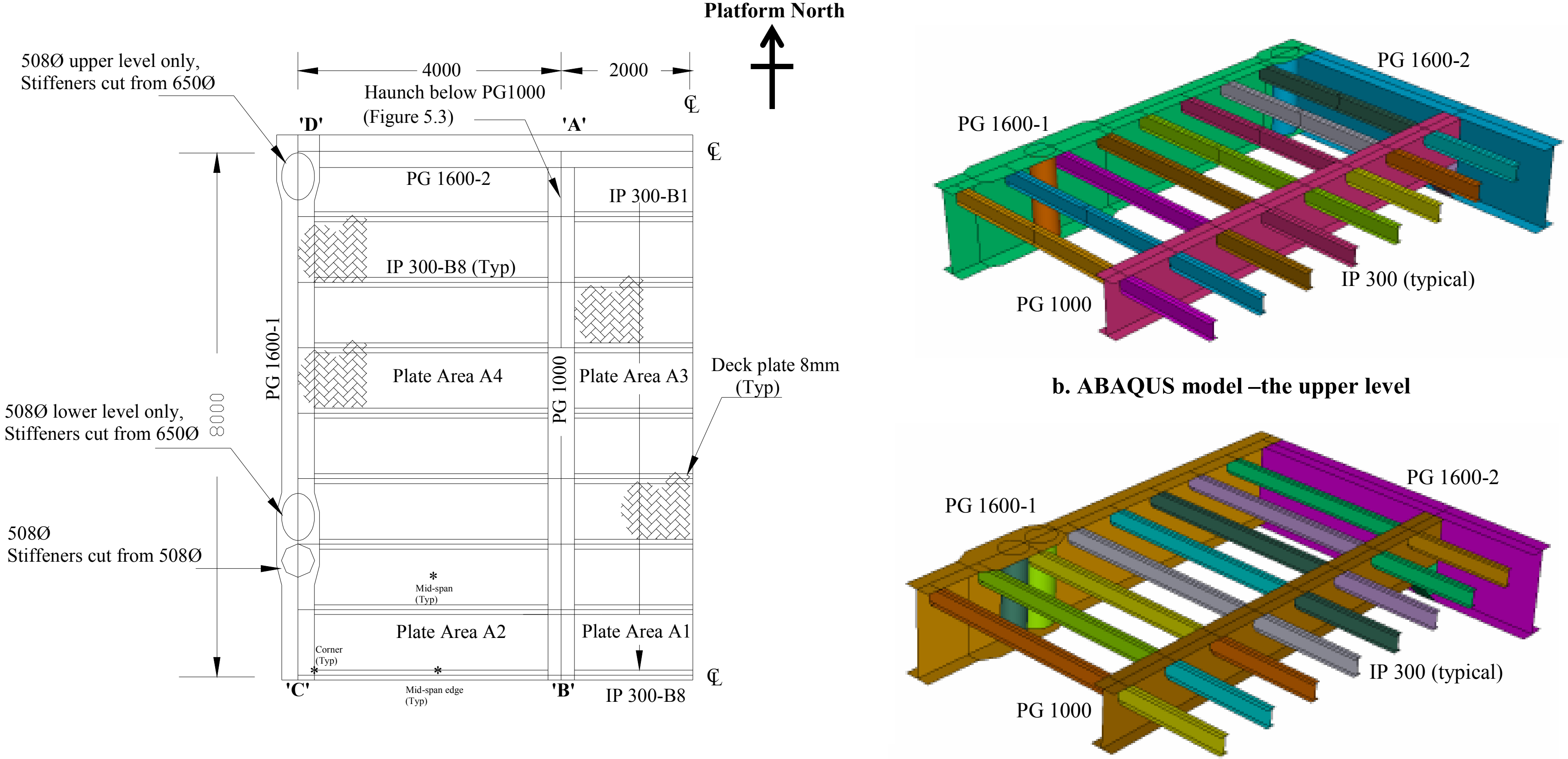

a. Plan View
The upper level is as shown and the lower level is similar.

b. ABAQUS model –the upper level

c. ABAQUS model –the lower level

(Note: Deck plates, bracings and meshing of elements are removed for clarity)

Figure 5.2

The topside structure framing plans and details

5.3 The details and properties of the modelled structural members

The cross sectional properties of the structural members are summarised in Table 5.1 while detailed schemes adopted for modelling the topside structure are given by Figure 5.3.

The finite element model of the topside structure was developed using the finite element package ABAQUS version 6.4[1]. ABAQUS Explicit module was used for the blast load analysis while ABAQUS Implicit module was used for the static analysis. All structural components were modelled as 3-D deformable and quadrilateral shell elements (S4R). The total number of elements was 62618. The meshing size varies from a minimum of 25 mm square to a maximum of 100 mm square. Each instance part was connected to other instance parts using 'tie constraint'. This interaction is equivalent to a fully welded connection which prevents the modelled contact surfaces from penetrating, separating or sliding relative to other surfaces.

In the generated ABAQUS model, the overlapping part of the structural components such as webs, flanges and joints, were trimmed accordingly to represent as-built fabricated connections. The stringer IP 300 beams were sniped at bottom flanges, which is a common practice on offshore platforms for walkway beams because they are designed as simply supported beams and for preventing distortion on primary beams during welding.

Strain rate was specified in the material properties for sensitivity check of the developed topside model. The constitutive relation of Cowper-Symonds Eq.(5.7) is defined based on steel material constants, $D = 40.4 s^{-1}$ and $q = 5$, Jones (1989) and HSE Report 105[76].

$$\dot{\varepsilon} = D\left(\frac{\sigma'_o}{\sigma_o} - 1\right)^q \tag{5.7}$$

where $\dot{\varepsilon}$ = strain rate

σ_o' = dynamic flow stress

σ_o = associated static flow

D and q = constants for a particular material

Table 5.1

The sectional properties of the modelled structural components

Structural components	Min Yield Strength F_y (MPa)	Nominal Depth d (mm)	Nominal Width b_f (mm)	Flange t_f (mm)	Web t_w (mm)	Ix (mm^4)	Zx (mm^3)	Sx (mm^3) (plastic)	Locations/ levels
PG1600-1	345	1600	500	40	25	31657600000	39572000	45640000	Upper and lower levels
PG1600-2	345	1600	500	30	20	24576106667	30720133	35408000	Upper and lower levels
PG1000	345	1000	400	25	15	5825885400	11651770	13134375	Upper and lower levels
IP 300 Structural sections[88]	248	300	150	10.7	7.1	836560000	557000	628000	Upper and lower levels
508 mm ø 19 mm thick	345	-	-	-	-	873766162	3440024.3	4524223.3	Between upper and lower levels
8 mm thick plate as deck plate	248	-	-	-	-				Upper and lower levels
½ cut from 650 mm ø 20 mm thick	345	-	-	-	-				Upper and lower levels
½ cut from 508 mm ø 20 mm thick	345	-	-	-	-				Upper and lower levels
L6x6x5/16 (strengthened case)	248	152	-	-	7.9	5411008	48670		Below IP 300 at supports
IP Stiffener Pl 10 (strengthened case)	248	-	-	-					Below IP 300 at surface of ½ cut 508 ø

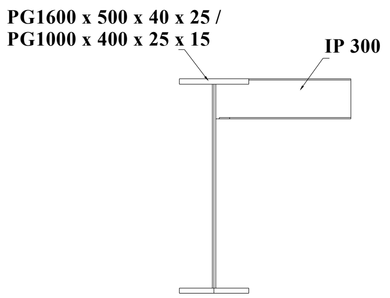

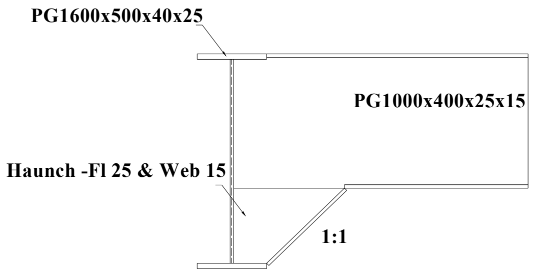

Haunch Details

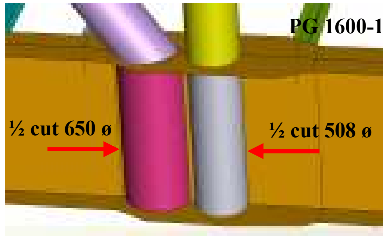

Half cut stiffeners 508 mm ø and 650 mm ø

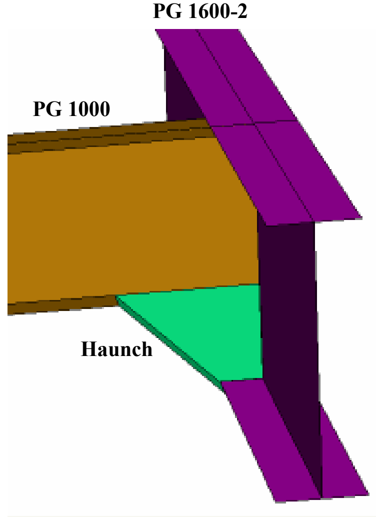

Plate girder PG 1000 with haunch to plate girder PG 1600-2

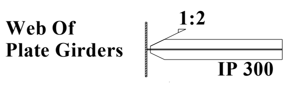

Snipe at bottom flange

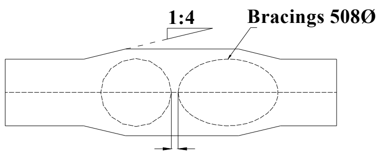

Plate Girder At Bracing Supports

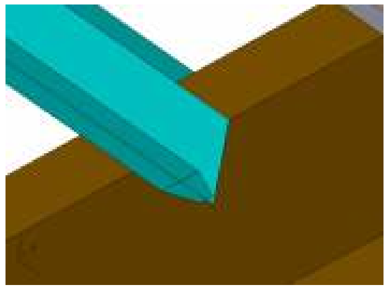

Looking from bottom
Sniped bottom flange of stringer beam IP 300 to plate girder PG 1000

Notes

All connections assume full weld penetration.

Figure 5.3

The structure details: sniped bottom flange, haunch and stiffeners for braces

5.4 The imposed boundary conditions

Structural members with similar configurations and partially simulated in the model were applied with symmetric boundary conditions. The applied boundary conditions on structure members are shown by Figure 5.4 and the restrained directions are summarised in Table 5.2.

Table 5.2

Summary of the imposed boundary conditions

Upper level/ Lower level	Symmetry Boundary Conditions		
	X	Y	Z
Plate girder PG1600-1	not applicable	not applicable	North and south sides
Plate girder PG1600-2	East side only	not applicable	North side 4000 mm from PG1600-1
Plate girder PG 1000	not applicable	not applicable	South side only
8 mm Deck Plate	East side only	not applicable	not applicable
Stringer beam IP 300	East side only	not applicable	not applicable

5.5 The simulation of blast loads

Table 5.3 compares the overpressure load between buildings and offshore installations. The overpressure loads between 0 bar and 1.0 bar are quite common in design for secondary structural members, whilst overpressure loads from 1 bar to 2 bar are implemented for designing structural support members, Bjerketvedt et al.- Gas Explosion Handbook[11]. Based upon exceedance diagram, Yasseri and Menhennett (2003) proposed overpressure load of 0.9 bar and 2.25 bar as the lower and upper level events for hydrocarbon explosions, respectively. With reference to the aforementioned data, the peak pressure implemented in the study was limited to a maximum 2.5 bar.

The blast loads in the model were represented by uniformly overpressure loads with a total duration of 50 ms and the time for peak overpressure was set to 25 ms. The pre-determined natural period of the topside was 73.94 ms, hence the ratio $t_d/T_N = 0.672 < 3$, which can be considered as under the influence of dynamic load regime, N-004 Norsok (1998).

Table 5.3

Comparison of load level for buildings and offshore installations

a. Onshore structures – Buildings
Smith and Rose (2002) and Lees (1996)

Zone	Damage Level (see note)	Maximum overpressure (bar)
A	**Total destruction.** Damaged beyond economical repair.	**> 0.83**
B	**Severe damage.** Partial collapse and failure of Structural members.	> **0.35**
	Brick wall panel, 8-12" thick not reinforced – shearing and flexural.	**0.21 – 0.69**
	Concrete or cinder-block wall panels, 8-12"in thick, not reinforced – shattering of wall	**0.10 - 0.38**
C	**Moderate damage**. Still usable but need repair works.	> **0.17**
D	**Light damages**. Broken windows, light cracks, damaged on wall panels and roofs.	<**0.035**

b. Occurrence events of the North Sea Installations, Vinnem (2000)
The UK, Holland and Norway for 25 years, 1973 to 1997

All events (Total 34 events)	Annual Exceedance Frequency	Acceptance Criteria+	Overpressure (bar)
24	9×10^{-3}	Unlikely*	**< 0.2**
8	9×10^{-3} - 7×10^{-4}	Rare*	**0.2 to 1**
2	7×10^{-4} - 9×10^{-4}	Rare*	**1 to 2**
0	$> 9 \times 10^{-4}$	Rare*	**> 2**

Note :

a. The damage levels for offshore platforms are determined by considering protection for assets and process plant aspects.

b. '*' see also table 2.5 and '+' denotes Fire and Explosion Guidance Part 1 (2003).

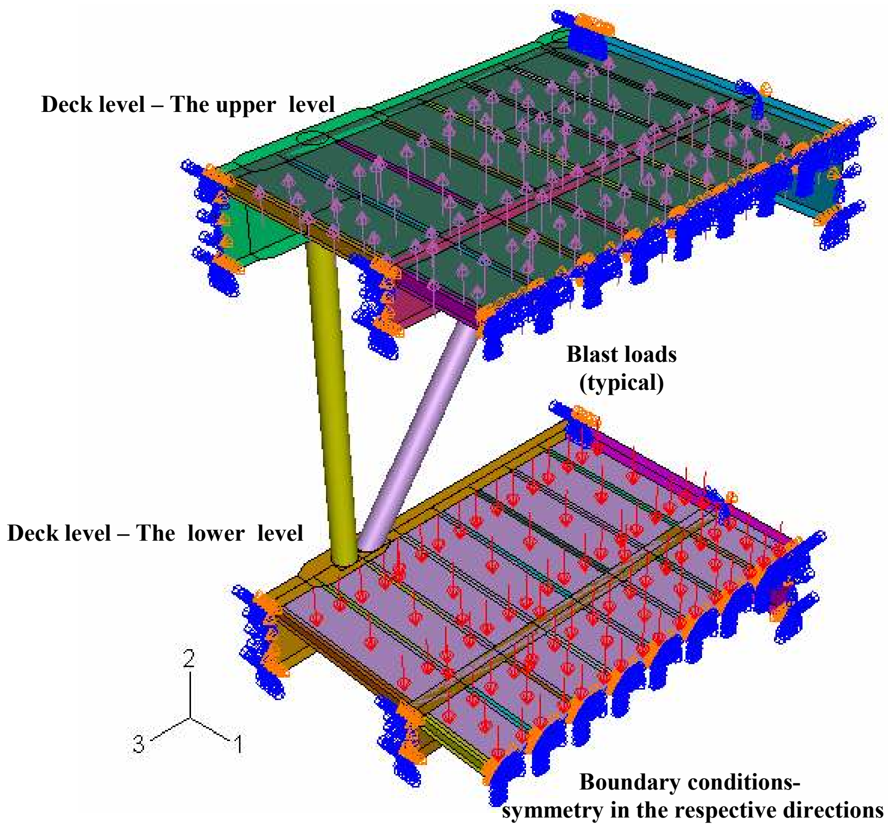

Figure 5.4

The complete analysed model with boundary conditions and directions of the applied blast loads

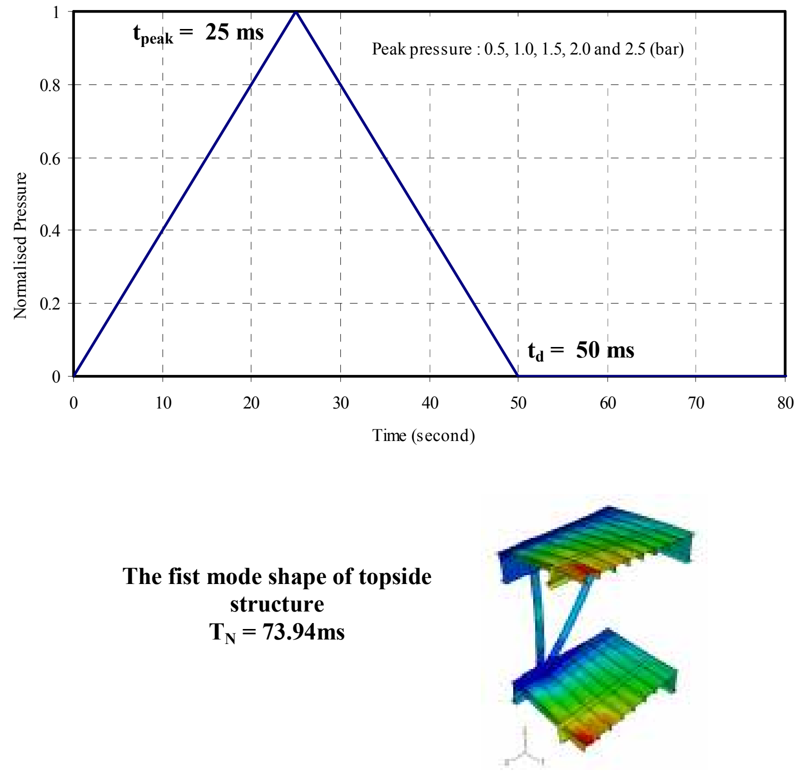

Figure 5.5

Linearised triangular overpressure impulse and the first mode shape

The overpressure loads were applied simultaneously on top of deck plates at the lower level and bottom of the deck plates of the upper level as shown in Figure 5.4. The applied loads were increased by an increment of 0.5 bar in each case until a 2.5 bar of peak pressure, as shown in Figure 5.5. Since no cladding is assumed around the deck, the 508 mm ø braces were to be minimally affected by the vertical overpressures, thus no blast loads were applied on its surfaces.

5.6 The performance level of the topside.

Using Figure 3.1 and the applied load level in section 5.5, the following performance level is proposed for the present topside structure:

i.	Functional	0.5 bar
ii.	Operational	1.0 bar
iii.	Life safety	1.5 bar
iv.	Near collapse	2.0 bar
v.	Total collapse	2.5 bar

It is worth noting that performance levels are determined by the stakeholders of the project. The acceptance of a defined performance level must also comport with the findings from quantitative risk assessment study. In principle, adopting a high performance level will impose additional costs on the project but will minimise repair work should explosions occur.

5.7 The constructed and the proposed mitigation models

Having developed the proper ABAQUS model, two cases of topside were investigated. The first case is called the original case, which represents a typical offshore fabricated deck flooring with sniped bottom flanges at connections for stringer beams (denoted by 'o') while the second case is called the strengthened case, which is a modified form of the original case (denoted by 's').

The second case is considered to be a retrofitting work for improving the performance of an existing installation. In this model, strengthening is proposed for IP 300 stringer beams with angles L 152 x 152 x 7.9 (equivalent AISC size – L 6 x 6 x $\frac{5}{16}$). The angles are welded between undersides of sniped areas of stringer IP 300 beams to webs of plate girders (PG 1000 and PG 1600-1) as shown by Figure 5.6.

The proposed method can be regarded as a simple strengthening because the existing structural configuration remains unchanged, as well as obstruction to the existing facilities on the topside structure is minimal.

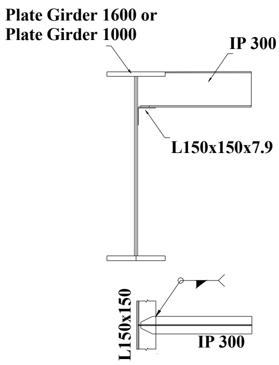

a. Details of sniped bottom with angles

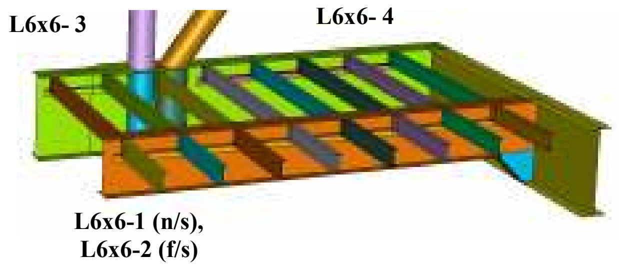

b. The ABAQUS model at the lower level - IP 300 with L150 x 150 x 7.9 mm (similar for the upper level)

Note :
Labels L6x6-1, 2, 3 and 4 denote reference numbers for the angles

Figure 5.6

The strengthened case with L150 x 150 x 7.9 mm

The analyses of the models were executed using the ABAQUS explicit module for dynamic analysis and ABAQUS implicit for the static analysis.

ABAQUS modified Riks algorithm (Riks (1979) and Crisfield (1981)) non-linear analysis was performed for determining the elastic limit of displacement at mid-span and rotational at selected joints of the structural components as was mentioned in section 4.6. By obtaining the maximum response from the topside dynamic analysis, ductility ratio can be calculated as defined by Eq. (5.8):

$$\left\{\begin{array}{l} u = \dfrac{\delta_{\max}}{\delta_{el}} \ \text{for mid-span} \\[2ex] u = \dfrac{\theta_{\max}}{\theta_{el}} \ \text{for end-span} \end{array}\right\} \qquad (5.8)$$

where $\delta \ or \ \theta$ = displacement or rotation at selected node from ABAQUS Riks analysis.

5.8 The validation models

5.8.1 Case I – A simple connection between beam to column

To validate the topside finite element model, the study of two-dimensional (2D) steel column-beam connections by Krauthammer (1999) was referred to. The study was selected because the overpressure load was a gas explosion, the joint between beam to column was a welded connection and the steels used in the experiment were from different grades; all of which resembled the characteristics of the modelled topside.

Although eight cases were presented, only one case was selected as shown in Figure 5.7a, because the other seven cases were devoid of input data.

Figure 5.7b shows the assembly of W 36 x 150 (A36) beam connected to W 14 x 342 (A572) column with 5024 deformable S4R elements using ABAQUS CAE. A tie-constraint interaction was applied between the beam end and the column face, while symmetry boundary conditions were applied on both of the other ends.

It was assumed that the load on the roof panel and the wall panel was uniformly distributed along the main frame. The overpressure loads were linearised, as shown by Figure 5.7c. The column was subjected to overpressure loads of 1.8 bar to 1.0 bar from 0 ms to 1.14 ms and 1.0 bar to 0.0 bar from 1.14 ms to 80 ms while the beam was subjected to overpressure loads of 1.0 bar to 0.0 bar from 0 ms to 80 ms. The analysis was executed using ABAQUS dynamic explicit module.

The comparison is made based on the available results of the maximum stress and strain recorded on the main frame at the connection. The maximum stress on the element predicted by ABAQUS is 318.3 MPa compared with 278.76 MPa from the experiment data. However, the maximum strain on the element predicted by ABAQUS and the experiment data compared favourably well, 0.052 and 0.056 respectively. Although the stress difference can be regarded as insignificant, the inconsistency is probably caused by the material properties. The plasticity data used in the ABAQUS model are extracted from typical stress-strain curves (Figure 5.1) instead of the actual test coupon results (data not available).

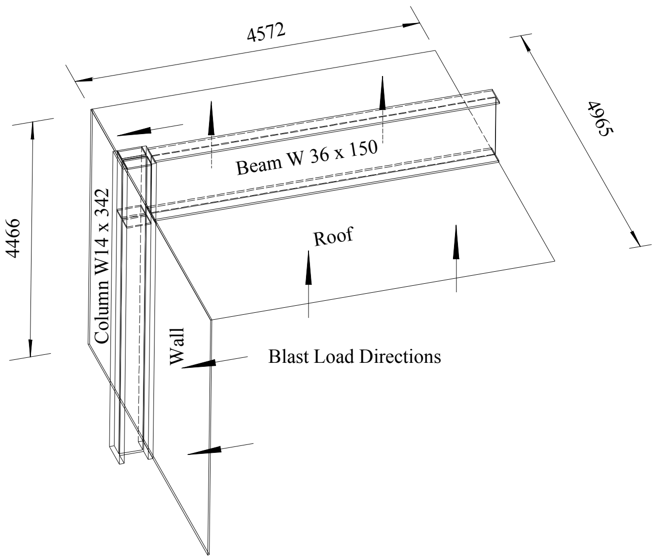

a. Beam to column connection and blast load area

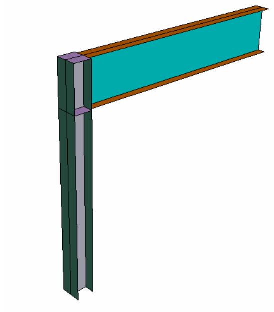

b. The ABAQUS model

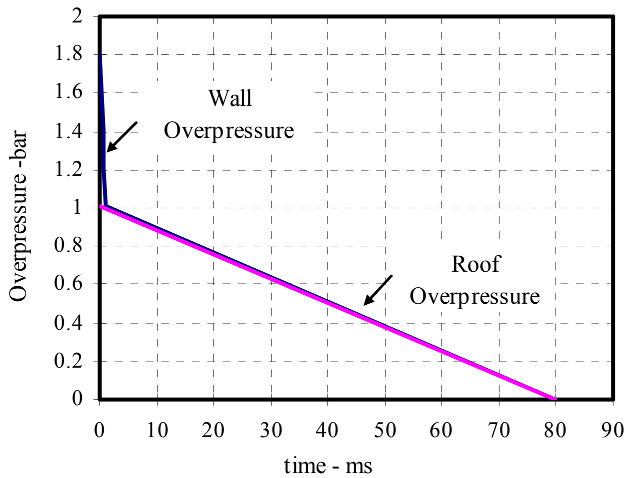

c. Load history of gas overpressure

Figure 5.7

Case I -The validation model case 2D reported by Krauthammer (1999) and ABAQUS model

5.8.2 Case II – A congested connection between beams to column

The second model was created to incorporate comments by the examiners. A three-dimensional (3-D) model connection reported by Krauthammer (1999) was referred to. A similar blast profile and material properties as case I were implemented in the model.

Figure 5.8 shows the assembly of two W 36 x 150 (A36) beams connected to W 14 x 342 (A572) columns with 8330 deformable S4R elements using ABAQUS CAE. Tie-constraint interactions were applied between the beams to column. The end spans were classified as symmetry boundary conditions in the respective directions. Blast loads impacted on roof and walls were assumed equally distributed along the truss frame as described in the literature. The roof was applied with 1.0 bar to 0.0 bar from 0.0 ms to 80 ms while the walls were applied with 1.8 bar to 1.0 bar from 0 ms to 1.14 ms and 1.0 bar to 0.0 bar from 1.1.4 ms to 80.0 ms. The analysis was executed using ABAQUS dynamic explicit module.

Table 5.4 summarises the results from the analysis. The measured stress and displacement at the connection from the ABAQUS model compared favourably with the experiment. However, the measured strains are less than the reported data which was highlighted as a probable failure in the literature. Since the model assumed a full weld penetration, one of the reasons that could result in this inconsistency is due to failure of the welded connection. The result also shows that the beam (Beam 1- W36) welded to the stronger axis of the column deforms more at the connection but less at the mid span compared to the beam (Beam 2 - W36) welded to the weaker axis. In conclusion, despite minor inconsistencies in the results due to failure at the connection, the ABAQUS model is able to predict the response reasonably well to the experiment work.

Table 5.4

Comparison of results at beams to column connection

Structural Components	Max stress (MPa)	Maximum Strain at	Maximum Displacement (mm)	Maximum Displacement at the Middle Span (mm)
Krauthammer (1999) Case 3D	442.98	0.390	172.0	Not available
Beam 1	443.07	0.096	169.03	777.13
Beam 2	437.67	0.078	165.01	887.15

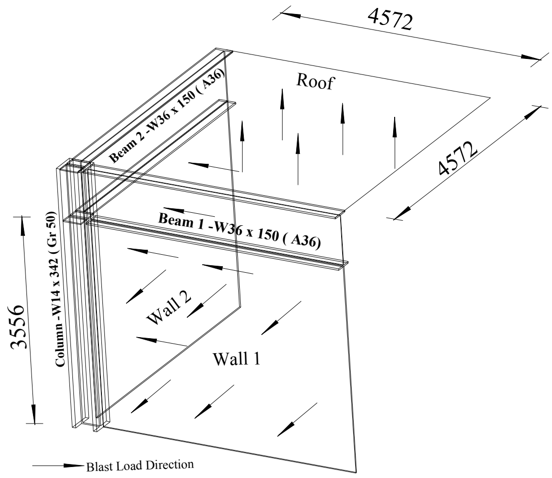

a. Beams to column connection and blast load areas

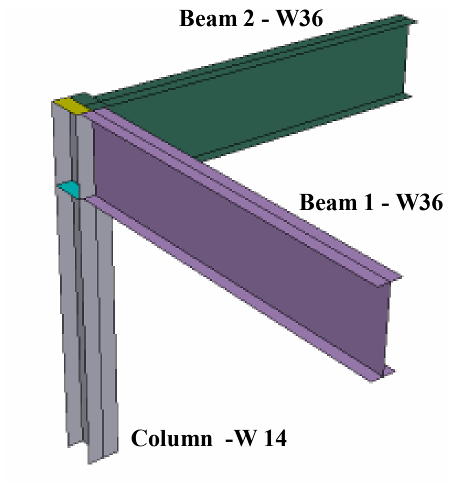

b. The ABAQUS model

c. Stress contour

Maximum stresses are observed occurring at the bottom flanges.

-denotes critical elements

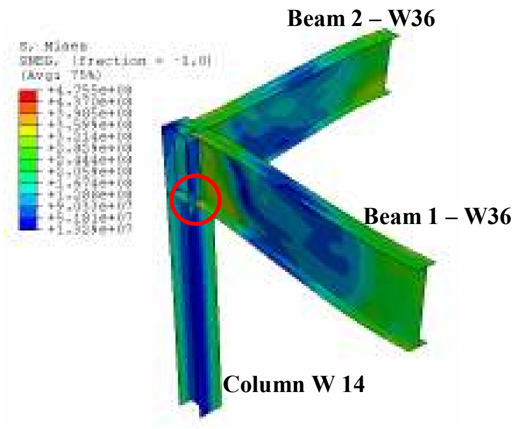

Side view

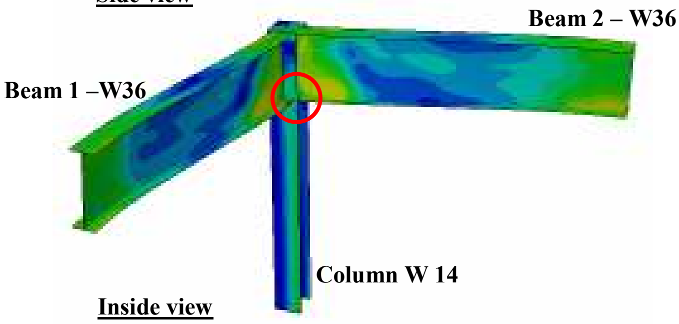

Inside view

Figure 5.8

Case II - The validation model case 3D reported by Krauthammer (1999) and ABAQUS model

5.9 The behaviour and interaction of structural components

5.9. 1 The global response of the topside

Figure 5.9 shows the distribution contours of global displacements between the selected original cases and strengthened cases at maximum deformation when both deck levels were applied with the overpressure load.

In general, the applied overpressure load causes the upper level to displace upwards and the lower level to displace downwards at the maximum response. The maximum points of deflection on the deck levels are observed occurring at the middle span of the plate girder PG 1000.

Figure 5.10 shows displacements at the middle span for plate girders PG 1000 (point 'B' in Figure 5.2a) for the original case, and the strengthened case with L152 x 152 x 7 mm. The plotted displacement curves with strain rates incorporated in the analyses show an insignificant effect on the overall global displacement of the topside. For a comparison, the maximum combined stress and plastic strain for each case with strain rate and without strain rate are extracted from the most critical elements at the four selected cross-sections along plate girder PG 1000 as tabulated in Table 5.5

The extracted data reveal that the elements in elastic condition (4.0 m from support) show a slight drop in stress and strain while the elements which just yield show a relatively small increment in strain. However, a significant increase of stress and strain is observed for the elements at the haunch.

Having modelled structural members according to the actual fabricated sections, the strain rate effect is found to be significant only at areas which have already experienced an extreme strain in the case without strain rate. It is also noticed that the effect of strain rate is highly localized and will be significant only at elements that have reached yield. As the effect of strain rate is found to have a minimum influence on the performance, especially for the global behaviour of the structural system, it is ignored for the remainder of the study.

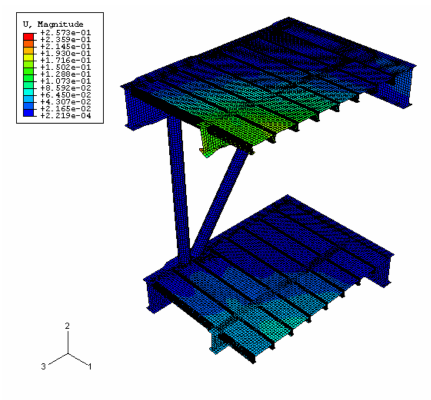

a. Response at 1.0 bar (o)

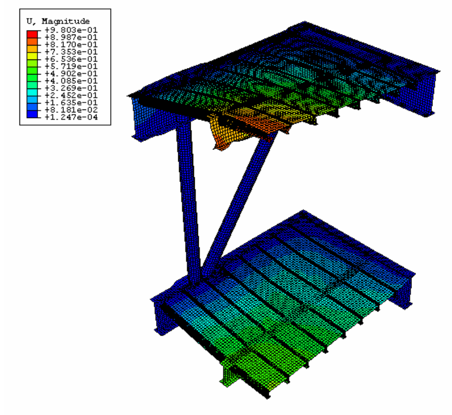

b. Response at 2.0 bar (o)

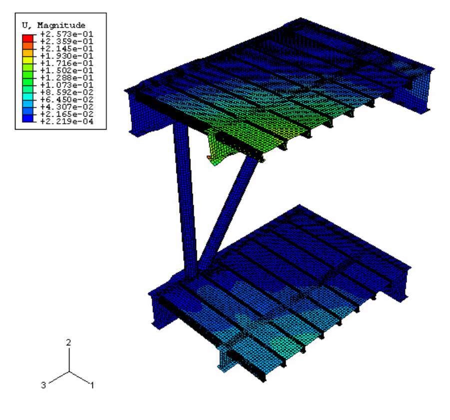

c. Response at 1.0 bar (s)

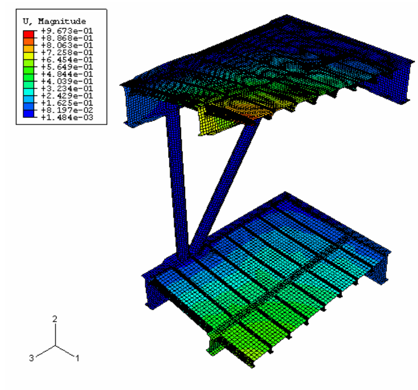

d. Response at 2.0 bar (s)

Figure 5.9

Global displacement of topside structure

Strengthening with angles are found to reduce global displacement by an average of 7.5 percent

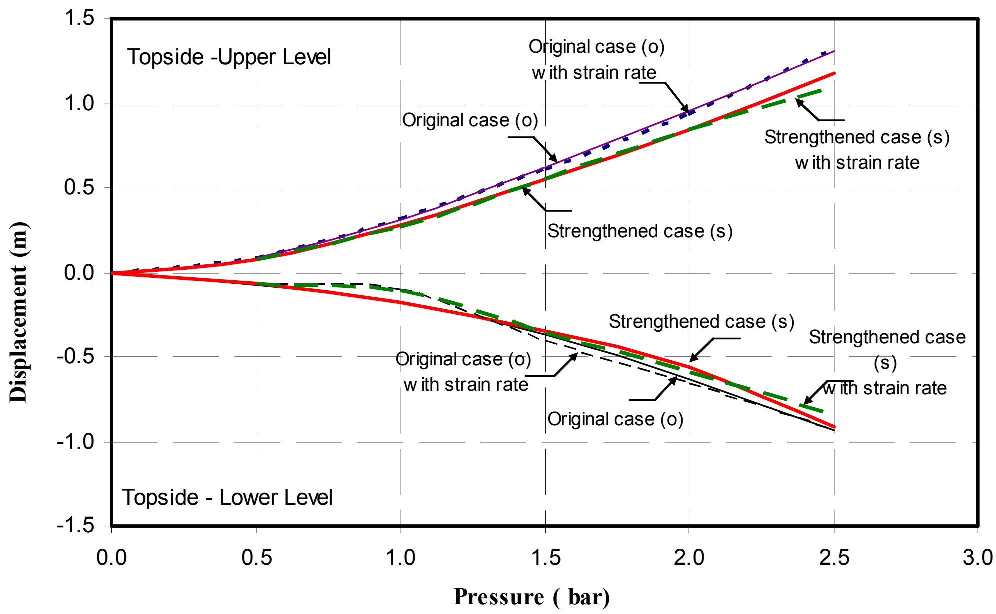

Figure 5.10

Displacements at the middle span of plate girder PG 1000

(with and without strain rate)

In general, for the strengthened case, the maximum middle global displacement is less than the original case by an average of 7.5 percent. The deck framing of the upper level displaces with an average magnitude of 24 percent more than the lower level. This behaviour can be explained by the applied overpressure loads on the surfaces below the upper level which cause the deck plates and beam top flanges to be in tension while the applied overpressure loads on top surfaces of the lower level cause the deck plates to be in tension and beams top flanges in compression which increase the stiffness, resulting in a reduction of the displacement.

From responses of the considered cases, it can be concluded that the proposed strengthening method with angles not only reduces the displacement but also attributes to a uniform load distribution along supporting structural members.

Table 5.5

Plate Girder PG 1000 – The effect of strain rate on maximum stress (MPa) and plastic strain (%).

Stress and Strain / Location		**Pressure = 0.5 bar**				**Pressure = 1.0 bar**				**Pressure = 1.5 bar**			
		O	**O-SR**	**S**	**S-SR**	**O**	**O-SR**	**S**	**S-SR**	**O**	**O-SR**	**S**	**S-SR**
Lower Level σ	a	346.5	346.3	345.8	345.8	457.6	448.0	476.8	486.0	426.4	426.4	488.8	496.2
	b	172.0	109.2	115.0	96.47	172.7	165.0	193.8	164.18	270.6	213.42	267.7	208.5
	c	396.4	438.4	378.9	414.7	506.7	518.5	503.3	518.9	482.3	518.5	478.2	518.7
	d	359.3	360.9	368.2	369.2	360.5	360.7	369.8	368.41	368.8	368.8	386.0	379.4
ε	a	0.22	0.19	0.15	0.14	8.10	7.60	9.10	10.11	6.50	6.51	10.00	13.54
	b	0.00	0.00	0.00	0.00	0.00	0.00	0.00	0.0	0.00	0	0.00	0.00
	c	5.38	7.12	4.74	6.06	10.80	15.06	10.70	12.60	9.50	53.67	9.20	15.44
	d	2.15	2.38	3.41	3.48	2.30	2.3	3.70	3.35	3.50	3.51	5.00	4.71
Upper Level σ	a	211.3	211.20	191.2	189.83	352.8	352.7	349.4	350.3	361.6	361.6	360.4	364.4
	b	141.4	110.83	107.7	96.39	278.9	276.3	299.5	259.4	345.2	342.3	303.6	326.7
	c	362.9	364.5	358.4	359.2	477.6	481.9	489.1	501.63	485.9	485.9	494.2	518.1
	d	439.3	464.0	478.5	518.1	489.6	390.2	440.5	474.4	372.1	372.1	369.1	372.1
ε	a	0.00	0.00	0.00	0.00	1.30	1.26	0.70	0.79	2.40	2.5	3.00	2.86
	b	0.00	0.00	0.00	0.00	0.00	0.00	0.00	0.0	0.00	0.0	0.00	0.0
	c	2.94	2.81	2.05	2.18	10.70	10.93	10.90	10.38	12.10	12.1	12.70	13.07
	d	7.00	8.00	10.00	13.94	9.80	5.14	7.10	8.85	4.50	4.5	3.60	3.90

Legends :
σ = Von Mises
ε = plastic equivalent strain , PEEQ
O = original case
O-SR = original case with strain rate
a = middle span
b = 4.0m from support
S = strengthened case
c = haunch
d = end-span
S-SR = strengthened case with strain rate

5.9.2 Secondary structural component - stringer beam IP 300

Figure 5.11 compares the maximum middle displacements of IP 300 beams, which are represented as bar charts for overpressure 0.5 bar, 1.0 bar and 1.5 bar, while Figure 5.12 shows the displacement history of the beams.

In the original case and the strengthened case, at 0.5 bar, the displacements rise steadily and peak between 40 ms to 50 ms, and are then followed by rebound displacements which occur after 60 ms. Conversely, at 1.0 bar and 1.5 bar, the peak displacements occur at 60 ms and 65 ms respectively, after which a plastic deformation is observed.

As shown by the bar charts, at a low overpressure, the displacements in the strengthened case are less than the displacements in the original case. However, when the overpressure is increased, the beams in the strengthened case, especially the beams towards the centre of the deck area, tend to displace at a higher magnitude than the original case.

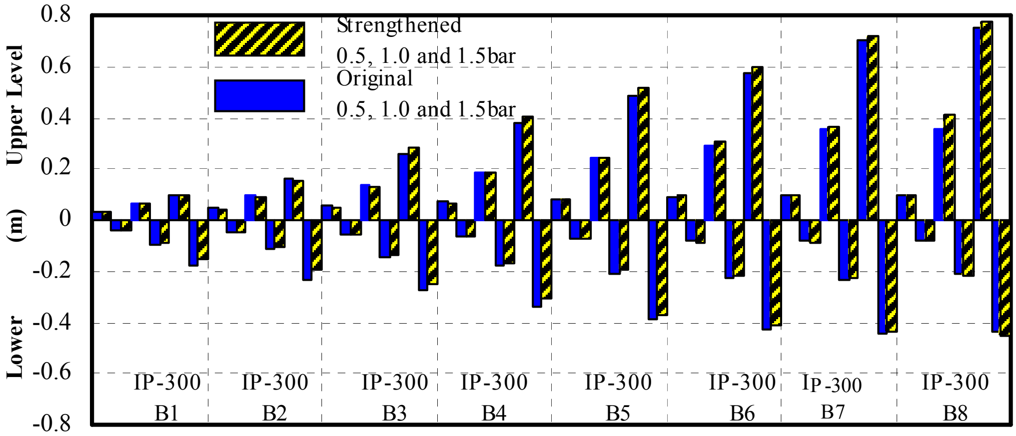

Figure 5.11

Stringer IP 300 Beam: Maximum displacement at the middle span

(B3, B4, B5, B6, B7, B8 beams on the upper level at 1.5 bar in the strengthened cases which are towards the centre of the PG 1000 have exceeded the displacements in the original case. Conversely, B1 to B7 beams on the lower level for the original case displace more than the strengthened case)

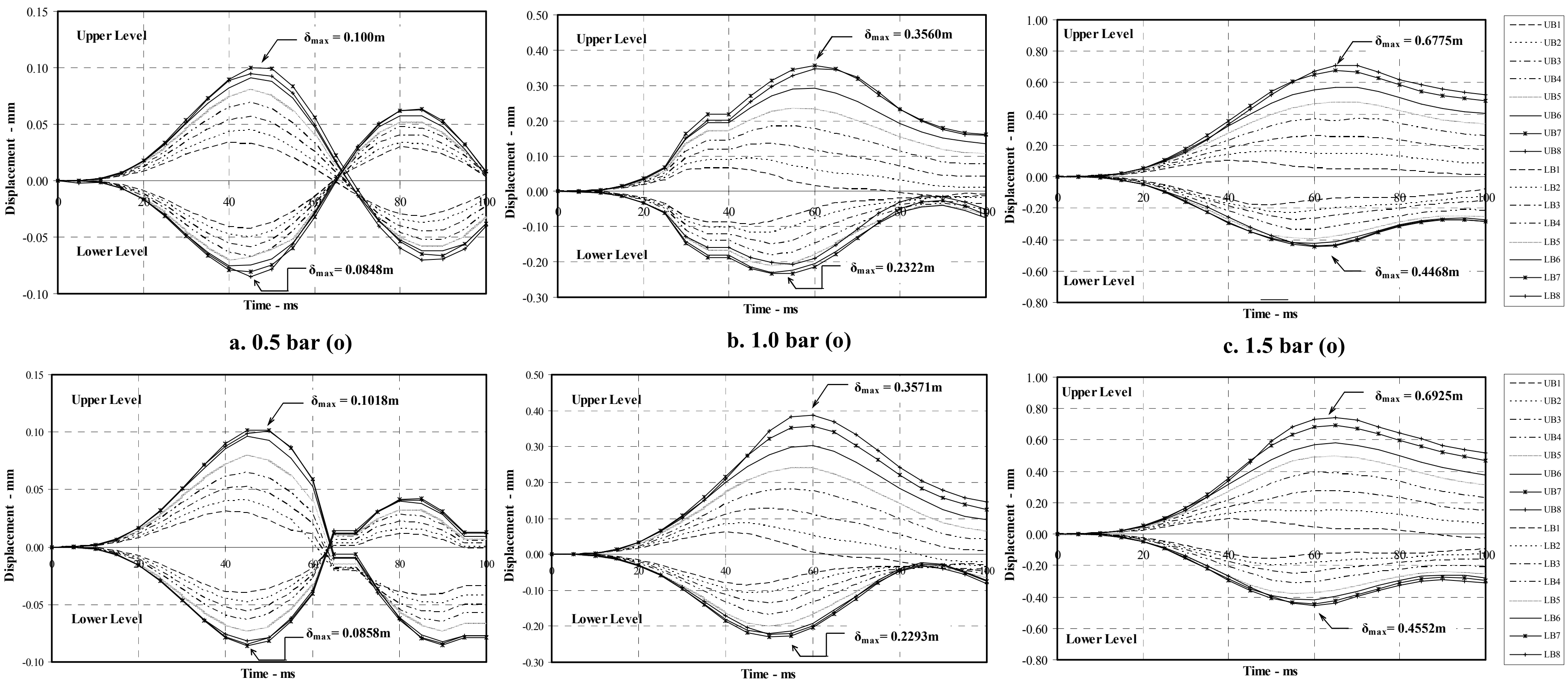

a. 0.5 bar (o) b. 1.0 bar (o) c. 1.5 bar (o)

d. 0.5 bar (s) e. 1.0 bar (s) f. 1.5 bar (s)

Figure 5.12

IP 300 beams - History of displacement

Depending on the load direction, the upper level displacement of IP 300 beam in the strengthened case is higher than the original case because failure at sniped area is overcome by welded angles. On the lower level because the top flange is in compression and restrained by the tensioned deck plates, the behaviour likewise the upper level is observed occurring at 1.5 bar and above.

This behaviour can be explained due to the presence of angles. Strengthening with L150 x 150 x 7.9 mm angles increases stiffness at supports compared with other parts along the IP 300 beams. When the beams are loaded with uniformly distributed load, the mid-span is the weakest point because it has a lower resistance capacity compared with the supports. Therefore, under high overpressure, for IP 300 beams in strengthened cases, the middle span will be the first point to yield.

This behaviour can be further attested by reviewing the stress and strain for beam B8, which is the most overstressed beam located at the centre of deck area on the upper deck level as illustrated by Figure 5.13. The investigated case is for an overpressure equal to 1.0 bar shows a reduction in the magnitudes of Von Mises stress and plastic equivalent strain at the support from 558 MPa to 232 MPa and from 23.6 percent to 0.83 percent in the original case and the strengthened case respectively. Similarly, in the middle span, the combined stress reduces from 312 MPa to 250 MPa while the plastic strain increases from 1.23 percent to 2.61 percent.

The contour plots of the plastic strain shown by Figures 5.13c and 5.13d indicate that the concentration of plastic deformation at the bottom web of the support in the original case whilst distributed plastic deformation over larger areas at the mid-span in the strengthened case. The support strengthened with angles shows a significant reduction in plastic strain by 96.5 percent.

This concludes that strengthening with angles has resulted in the change of stiffness and the pattern of load transfer by triggering elements at the mid span to yield first instead of elements at end supports.

The strain rate profiles based on data acquired at the support and the middle span at 1.0 bar show by Figures 5.13e and 5.13f that in the original case, the support has two peaks: 6.64 s^{-1} just after the maximum applied load ; and 7.46 s^{-1} in the rebound period due to the reaction from the lower level. In the strengthened case, strain rate reduces to 0.33 s^{-1} at the support and becomes more than double at 1.11 s^{-1} at the middle span, which clearly gives an indication that more energy has been consumed for deforming the middle span.

As a result of relocation of yielding and plastic deformation to middle span of IP-300 beams, it reduces damage at connection, consequently increasing the deck global resistant against explosions.

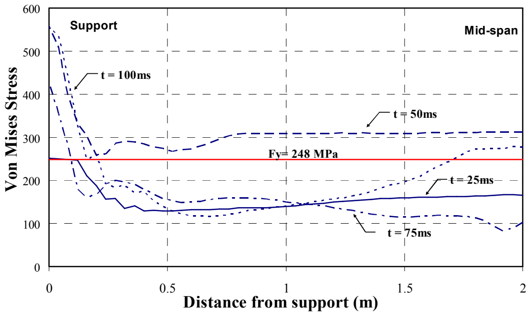

a. Von Mises stress (o)
From the support to the middle span. Higher stress at support with maximum of 558 MPa.

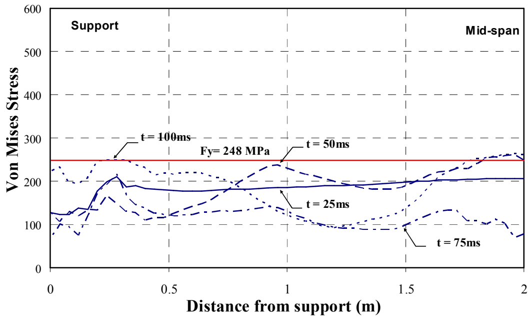

b. Von Mises stress (s)
From the support to middle span. Stress reduces to 232 MPa at support.

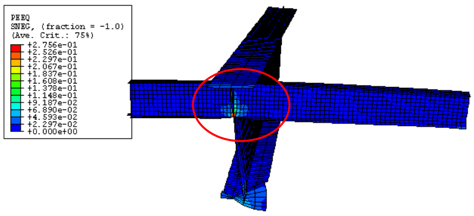

c. Strain (o)
Localised plastic strain at the bottom web at 1.0 bar (o), $PEEQ_{end\ span}$ = 23.6 percent and $PEEQ_{mid\text{-}span}$ =1.23 percent.

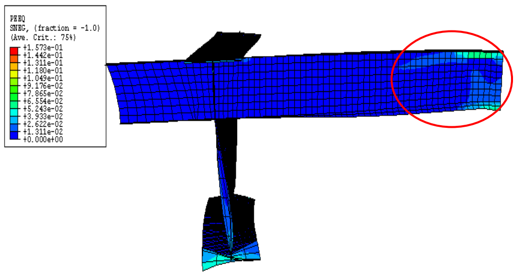

d. Strain (s)
Distributed plastic strain at the middle span at 1.0 bar (s) , $PEEQ_{end\ span}$ = 0.83 percent and $PEEQ_{mid\text{-}span}$ =2.61 percent.

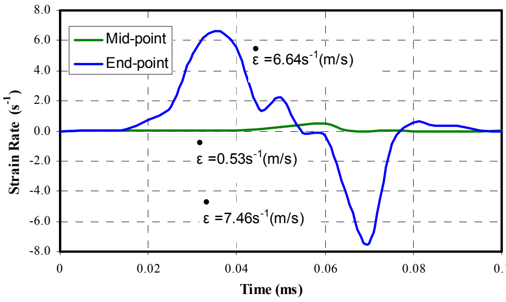

e. Strain rate (o)
Two peaks for the end span because reaction from plate girder PG 1000 in rebound phase while a relatively low strain rate at mid-span.

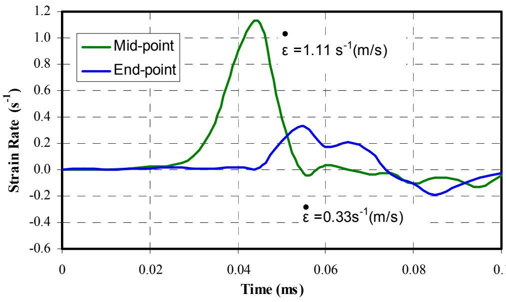

f. Strain rate (s)
Reduced strain rate for the end-span, single peak for the middle span less than the end-span in the original case as deformation is spread to many more areas.

Figure 5.13

IP 300 B8 – Distribution of stress and strain at 1.0 bar
The effect of strengthening relocates yield area from end span (o) to middle span (s), reducing global displacement.

5.9.3 Primary structural component - plate girder PG 1000

As discussed in section 5.9.1, the strengthened case reduces overall displacement in the middle of the deck area as well as plastic strain along the plate girder except at the end span. This is because the modelled L 150 x 150 angles welded to plate girder PG 1000 are terminated 750 mm from the end span.

Figure 5.14 shows the maximum average Von Mises of elements from the top flange to the bottom flange of the plate girder at the mid span and the end span.
At the middle span of the upper level, the stress in the strengthened case is much higher than the original case. This is because the presence of angles increases the stiffness of the plate girder that attracts more out-plane moment from stringer beams. Similar responses are also exhibited by the plate girder at the lower level; however the magnitude is much lower than the upper level (this behaviour was explained in section 5.9.1).

At the end span, where no angles are provided, although there is a significant reduction of stress at 0.5 bar for the lower level as a result of improvement in load distribution along the plate girder by angles, most of the plotted stress curves level off to a magnitude slightly above yield (345 MPa) for overpressure above 1.0 bar. The behaviour can be correlated further by the summary of maximum strain as tabulated in Table 5.5. It is also observed that no plastic deformation of elements at the mid span and 4.0 m from the end-span on the lower level at 0.5 bar. The behaviour can be explained because the action of deck plates in tension provides constraint to top compression flanges of the plate girder PG 1000. However, at the end span, the deck plates and plate girder flanges are both in tension, which result in higher stress and strain compared to the upper level.

On the upper level, the haunch is found to be the weakest point in both the original and strengthened cases. The plastic strains of elements rise to more than double at 1.0 bar but drop slightly at 1.5 bar. The anomaly is the result of failure mechanism at haunch which is in compression buckles earlier than the end span. Moreover, the sudden change of cross section has caused stress to concentrate in the transition area which leads to a higher strain at haunch but a drop at the end span. On the lower level, the stress and plastic strain are less than the upper level at 0.5 bar due to the fact that the bottom flange is in tension, which can sustain higher longitudinal stress. From these response modes, a summary can be made that the haunch detail and the distance of bottom flange extension beyond the haunch point are the two key parameters for controlling failure mechanism at the connection.

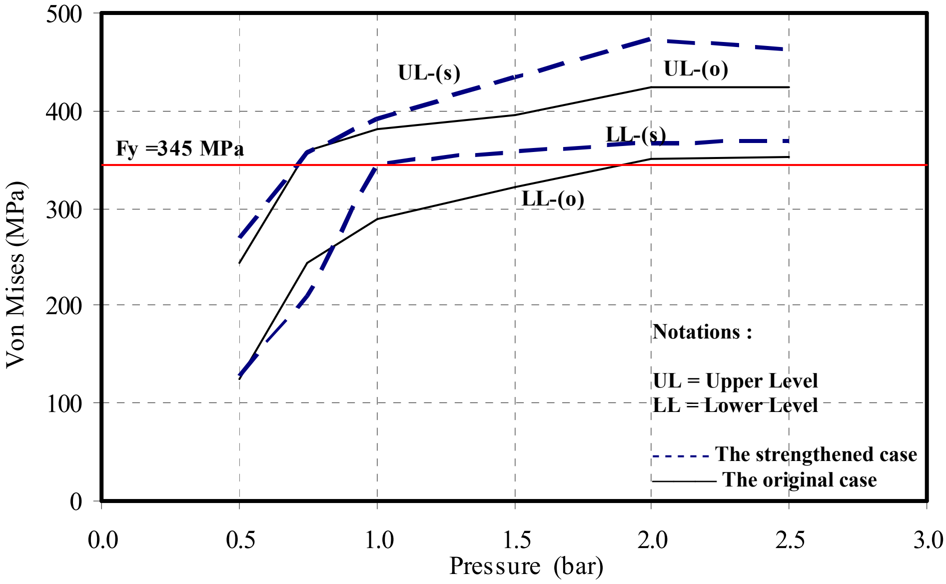

a. Mid span

High stress in strengthened cases due to more out-plane moments from stringer beams

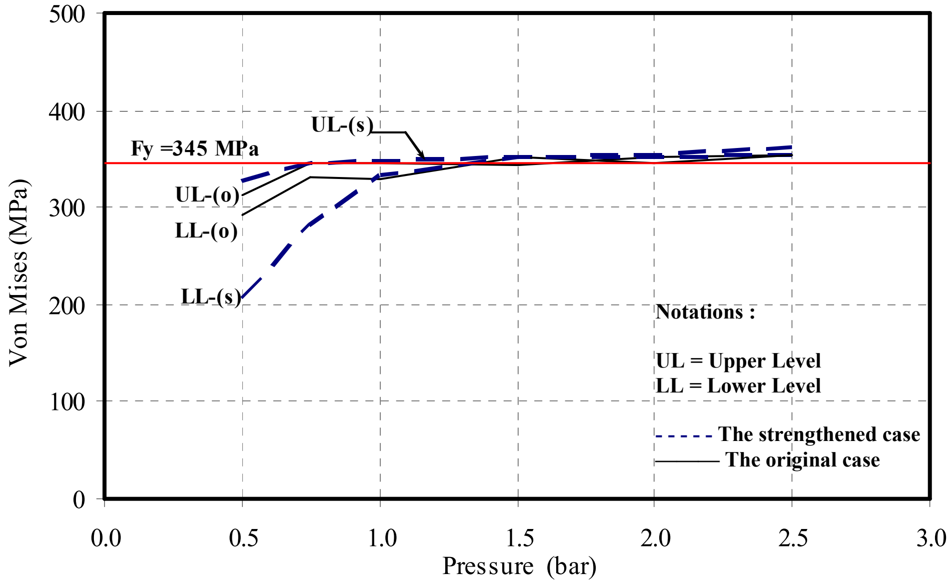

b. End span

Since no strengthening is made at the end span, the stresses at overpressure above 1.0 bar are almost equal.

Figure 5.14

Plate Girder PG 1000 Maximum average stress across the section

5.9.4 Primary structural component - plate girder PG 1600-2

Due to the fact that these plate girders are not directly exposed to blast loads, their responses can be divided into two stages: the first stage, within the explosion period (t_d), and the second stage, the rebound period (after t_d). Most overstressed elements of the plate girder are caused by local failures which concentrate at the support joints in both the original and strengthened cases as shown by Figure 5.15.

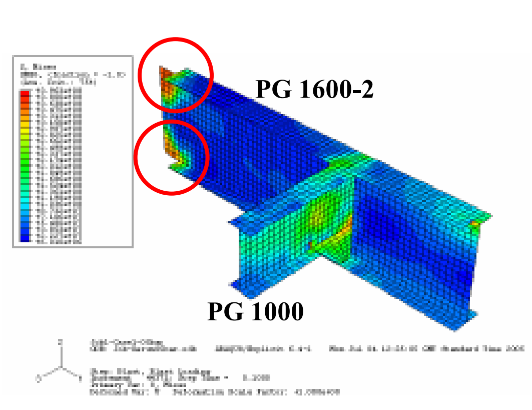

a. Upper level Von Mises at 0.5 bar (o)

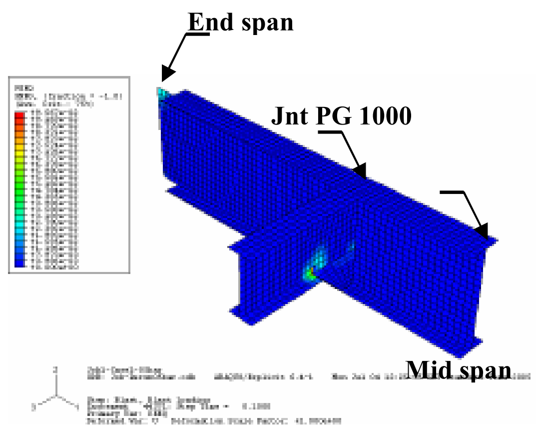

b. Upper level PEEQ at 0.5 bar (o)

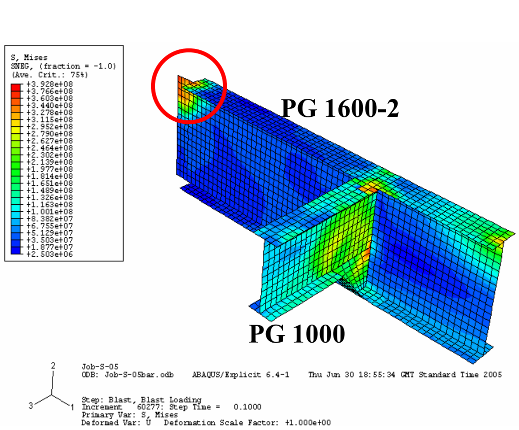

c. Upper level Von Mises at 0.5 bar (s)
(Reduce overstressed areas)

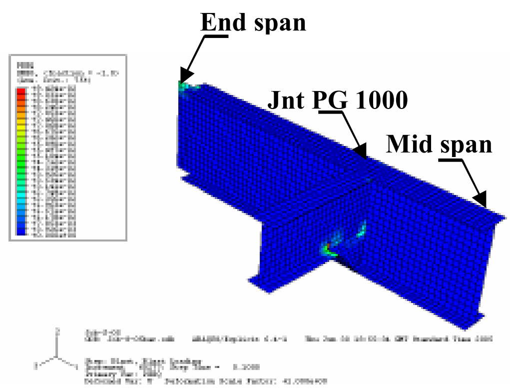

e. Upper level PEEQ at 0.5 bar (s)
(Less overstrained areas)

Figure 5.15

Plate girder PG 1600-2– The stress and strain contours

Table 5.6

Plate Girder PG 1600-2 – Maximum stress (MPa) and plastic strain (%)

Position of elements Plate Girder PG 1600-2		Pressure = 0.5bar		Pressure = 1.0bar		Pressure = 1.5bar	
		Original	Strength	Original	Strength	Original	Strength
Upper Level σ	Bottom web end-span	347.06	51.67	*295.33	90.63	348.05	106.80
	Top web end-span	351.37	371.53	*350.21	*370.36	*352.72	398.50*
	Bottom flange at joint	208.09	188.17	332.09	314.79	345.86	345.56
	Top flange at joint	301.70	252.40	343.58	327.96	345.26	341.89
	Bottom web at mid-span	212.41	211.05	323.93	343.35	346.52	346.40
	Top web at mid-span	236.52	260.53	260.54	261.24	301.45	325.66
Upper Level ε	Bottom web end-span	0.70	0.00	0.13*	0.00	0.67	0.00
	Top web end-span	1.32	3.93	1.07*	*3.75	*1.26	*5.56
	Bottom flange at joint	0.00	0.00	0.03	0.02	0.17	0.12
	Top flange at joint	0.00	0.00	0.02	0.02	0.10	0.06
	Bottom web at mid-span	0.00	0.00	0.01	0.01	0.23	0.27
	Top web at mid-span	0.00	0.02	0.00	0.01	0.08	0.07
Lower Level σ	Bottom web end-span	372.20	518.54	*360.70	464.86*	*363.91	*434.30
	Top web end-span	123.65	149.48	188.88	326.32	237.79	266.15
	Bottom flange at joint	335.55	346.76	325.72	276.32	345.45	345.95
	Top flange at joint	345.43	345.74	*345.19	*348.45	*345.71	*346.47
	Bottom web at mid-span	217.51	196.90	345.15	323.68	348.83	346.46
	Top web at mid-span	199.17	170.39	345.29	344.56	346.99	348.67
Lower level ε	Bottom web end-span	4.16	14.36	*3.06	*8.92	*3.23	*7.37
	Top web end-span	0.00	0.00	0.00	0.00	0.00	0.00
	Bottom flange at joint	0.02	0.34	0.08	0.04	0.28	0.27
	Top flange at joint	0.08	0.41	*0.15	*0.70	*0.39	*0.25
	Bottom web at mid-span	0.00	0.00	0.05	0.00	0.59	0.23
	Top web at mid-span	0.00	0.00	0.08	0.01	0.36	0.72

* A drop in stress and strain due to yielding at haunch.

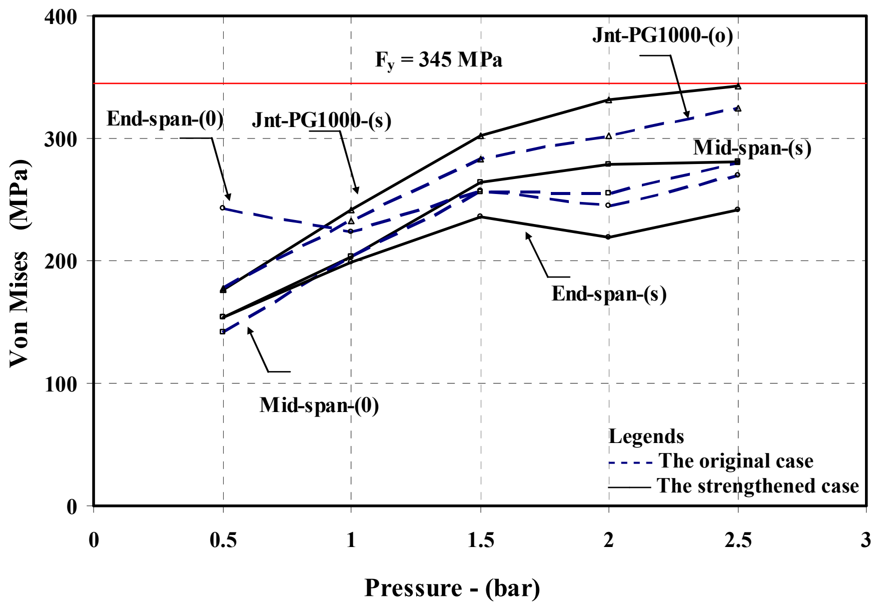

a. The upper level

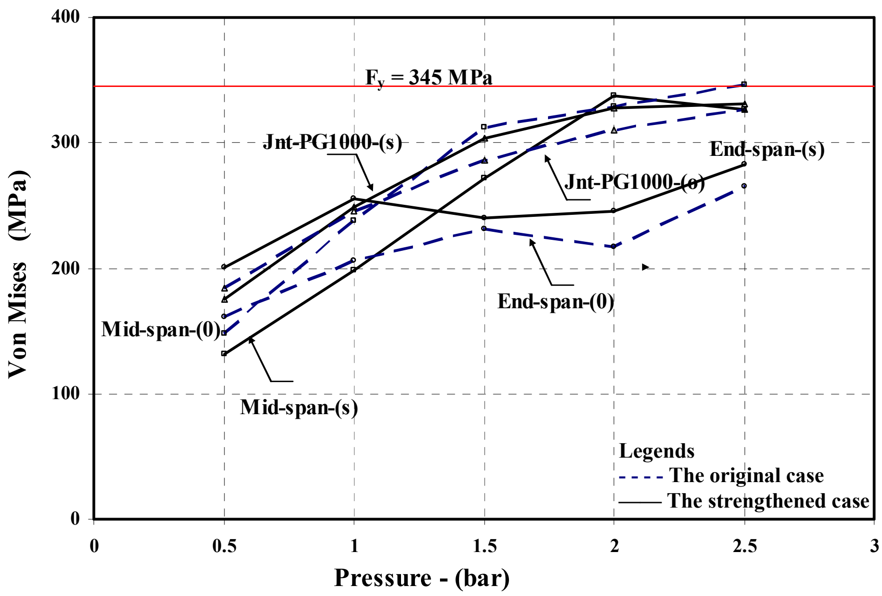

b. The lower level

Figure 5.16

Plate girder PG 1600-2 Maximum average stress across the section

Details of stress and strain at the selected critical points are reported in Table 5.6. From this table, although plasticization concentrates on a few elements, the maximum of average stress across the selected points is below theoretical yield of the steel as shown by Figure 5.16. This case can be classified as local joint failure. One possible solution for mitigation can be achieved by increasing the plate thickness.

Another interesting finding that can be seen from the table for Figures marked with an asterisk '*' is caused by the effect of stress concentration at the haunch between 0.5 bar and 1.0 bar. With propagation of yielding to many more elements at haunch, this causes a further reduction in stress and strain for plate girder PG 1600-2 at end span.

Table 5.7 shows displacements of the main support points of the structural framing at the end span of plate girder PG 1600-2 (pt. 'D') and the vertical support by tubular 508 mm Ø (pt. 'C').

Table 5.7

Comparison of maximum displacements (mm) between the middle span PG 1600-1 and end span connection PG 1600-2 to PG 16001-1.

Pressure (bar)		(o) Pt D		(o) Pt C		(s) Point D		(s) Pt C	
		(t <t_d)	(t>t_d)	(t <t_d)	(t>t_d)	(t <t_d)	(t>t_d)	(t <td)	(t>t_d)
0.5	U	+6.2	-9.6	+3.5	-7.4	+4.2	-18.9	+1.7	-16.9
	L	-11.9	+6.3	-6.9	+3.7	-14.8	{nil}	-16.8	(nil)
1.0	U	+20.3	-16.6	-6.6	-16.9	+7.7	-41.5	+3.1	-38.2
	L	-21.2	{nil}	-16.5	+7.5	-35.2	{nil}	-39.6	+3.5
1.5	U	+15.4	-14.4	+9.3	-12.7	+7.4	-54.7	+5.3	-52.7
	L	-25.1	{nil}	-12.7	+10.7	-50.4	{nil}	-52.7	+5.3
2.0	U	+19.1	-9.3	+12.6	-11.4	+12.3	-64.9	+6.5	-63.6
	L	-27.6	{nil}	-9.2	+14.3	-59.1	{nil}	-62.6	+6.7
2.5	U	+24.1	{nil}	15.2	Nil	+14.5	-73.4	+8.0	-73.5
	L	-31.0	+8.2	nil	+21.1	-69.5	{nil}	-70.9	+8.5

Note :

1. – and + denote downwards and upwards displacements respectively
2. U and L denote upper level and lower level respectively
3. {nil} - denotes displacement less than maximum in the first stage or no reverse displacement during rebound period

On the upper level, within the first 50ms (t_d), displacements in the strengthened case are less than in the original case. However, within the rebound period, displacements in the strengthened case have exceeded the original case.

On the lower level, the responses are opposite, with higher displacements in the first stage and lower displacements in the second stage. These behaviours are caused by the angles L150 x 150 and, the diagonal 508 mm ø brace which supports the plate girder at the end span of the upper level.

In the strengthened case, energy from the blast loads are consumed to deform IP 300 beams at the middle span and their reactions are then uniformly distributed along the plate girders PG 1600-1 and PG 1000 by angles which reduce displacement on the upper level in the first stage. In the second stage, the end span support of PG 1600-1 is being pulled by the tensioned diagonal braces because of overpressure loads from the lower deck. Hence, this increases displacement downwards.

Likewise on the upper deck with uniform load distribution but without a diagonal support, the displacement in the strengthened case is higher in the first stage but less in the second stage compared with the original case on the lower level. It is also interesting to note that strengthening with angles L152 x 152 reduces in terms of relative displacements between the main supports (C and D) by 10 to 80 percent. This finding is beneficial for sensitive equipment which requires adjustment at the support bases after explosions.

5.9.5 Primary structural component - plate girder PG 1600-1

Figures 5.18 and 5.19 show the effect of strengthening on the stress and strain distribution contours for the plate girders, while Table 5.8 reports the average values of maximum stress and strain calculated from top flange to bottom flange based upon four selected sections as shown in Figure 5.17.

For plate girders PG 1600-1, responses are dependent on the reactions of plate girder PG 1600-2 and tubular braces 508 mm ø. As can been seen from Table 5.8, the stress and strain at supports in the strengthened case are found to be less than the original case except at the end span support of the lower level. The former response is due to uniformly distributed load caused by angles and more deformation in the middle span of IP 300 beams. The latter response is because the end span of the lower level has no brace support.

Table 5.8

Plate Girder PG 1600- 1 - Maximum Stress and Strain

Position of Elements		**0.5 bar**		**1.0bar**		**1.5bar**		**2.0bar**		**2.5bar**	
		(o)	**(s)**	**(o)**	**(s)**	**(o)**	**(s)**	**(o)**	**(s)**	**(o)**	**(s)**
Upper level Von Mises stress (MPa)	BF-S5	34.9	25.2	47.2	44.8	56.7	56.7	75.1	73.7	128.2	120.0
	TF-S5	39.0	27.9	59.4	39.5	70.6	73.5	87.8	94.3	113.7	107.3
	BF-ES6	170.3	42.9	90.2	56.2	120.2	73.1	145.0	92.8	218.7	123.3
	TF-ES6	214.7	111.1	345.1	118.7	346.4	143.3	245.1	168.9	327.9	290.5
Upper level Plastic equivalent strain (%)	BF-S5	0.00	0.0	0.0	0.0	0.0	0.0	0.0	0.0	0.0	0.0
	TF-S5	0.00	0.0	0.0	0.0	0.0	0.0	0.0	0.0	0.0	0.0
	BF-ES6	0.00	0.0	0.0	0.0	0.0	0.0	0.0	0.0	0.0	0.0
	TF-ES6	0.00	0.0	0.2	0.0	0.4	0.0	0.0	0.0	0.08	0.0
Lower Level Von Mises stress (MPa)	BF-S5	102.3	90.4	164.8	151.0	180.5	188.0	214.3	208.8	208.3	219.9
	TF-S5	105.1	73.7	165.4	123.4	192.1	151.7	185.6	179.4	279.3	206.2
	BF-ES	320.7	325.0	345.3	345.1	345.3	345.4	350.7	347.6	346.4	347.6
	TF-ES	256.6	345.4	343.3	344.2	346.5	349.5	347.6	348.7	345.7	348.9
Lower level Plastic equivalent strain (%)	BF-S5	0.0	0.0	0.0	0.0	0.0	0.0	0.0	0.0	0.0	0.0
	TF-S5	0.0	0.0	0.0	0.0	0.0	0.0	0.0	0.0	0.0	0.0
	BF-ES	0.0	0.0	0.08	0.06	0.17	0.18	0.83	0.38	0.51	0.40
	TF-ES	0.0	0.2	0.04	0.34	0.21	0.67	0.38	0.64	0.27	0.57

Note :

1. BF/TF -S5 – Bottom/Top flange at joint 508Ø stiffeners, BF/TF-ES6 Bottom/Top flange End span 650Ø stiffeners
2. BF/TF -ES – Bottom /Top flange end span (no support).

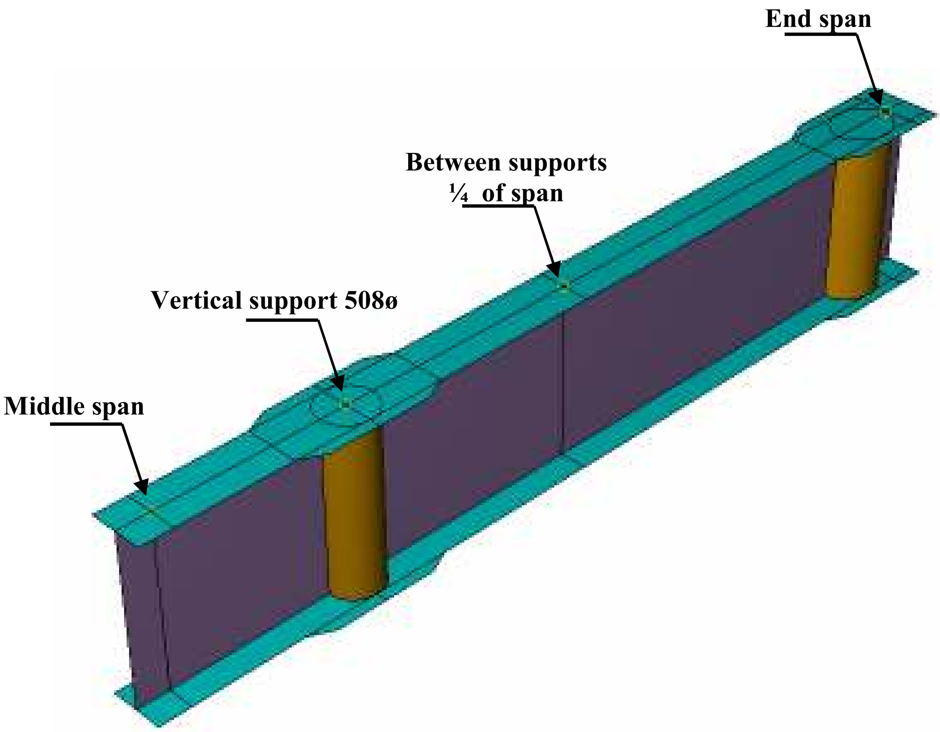

Note:

The critical part of the plate girder PG 1600-1 is the end span that connected to plate girder PG 1600-2. The end span receives more loads compared to other parts because the contribution of loads which are mostly originating from the central deck area. The situation is much more critical for the lower level with no brace support and stiffener.

Figure 5.17

Plate Girder PG 1600-1: The selected cross section

As can be seen from Figure 5.20, although a small number of elements have slightly exceeded yield locally, the average maximum stresses over the cross section are found to be remained below theoretical yield up to 2.5 bar. Without the diagonal support at the lower deck, the increase in stress is quite consistent with the increase in pressure up to 1.5 bar.

At 1.5 bar, the maximum stress at the end span and between 508 ø drops slightly lower than 1.5 bar because more energy is being used to deform many more elements of other structural members (PG 1000 and IP 300) which have already reached yield state in the strengthened case. With average stress below 345 MPa, it can be concluded that globally, plate girder is able to withstand the overpressure up to 2.5 bar.

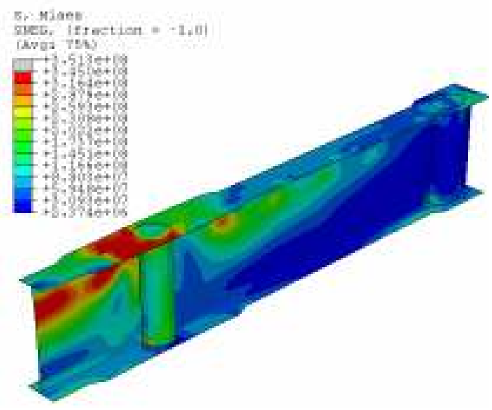

a. The original case - Von Mises

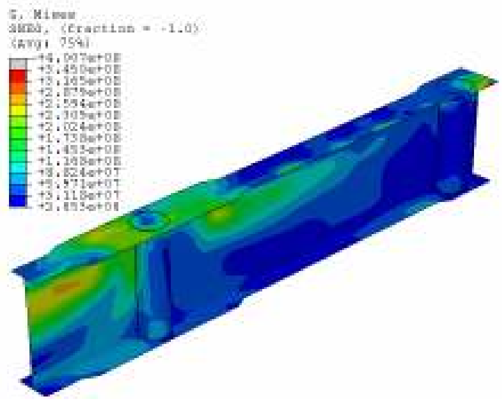

b. The strengthened case – Von Mises

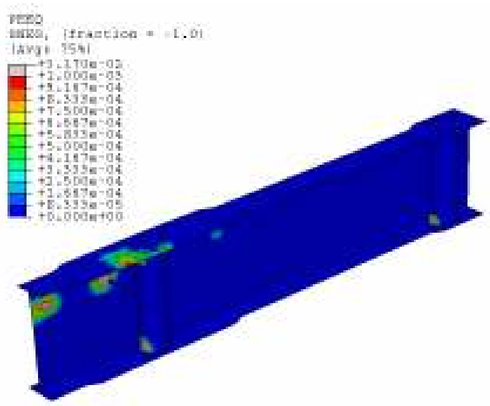

c. The original case – Plastic strain

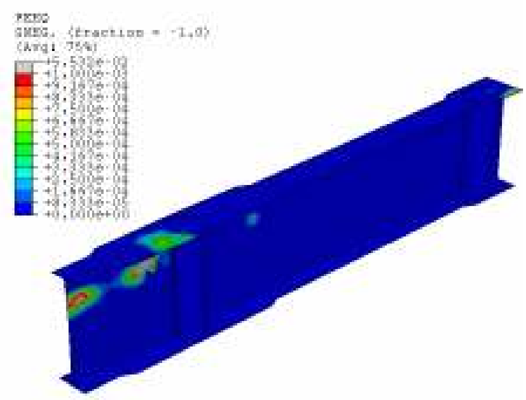

d. The strengthened case – Plastic strain

Note:
A high localised stress and strain at the end span due to loads from PG 1600-2 but other areas on the plate girder experienced less strain and strain because of the angles in the strengthened case. Localised stress and strain can also be seen at the bottom of stiffeners in the original case while they have diminished in the strengthened case.

Figure 5.18

Plate Girder PG 1600-1 Stress and strain distributions on the upper level at 1 bar

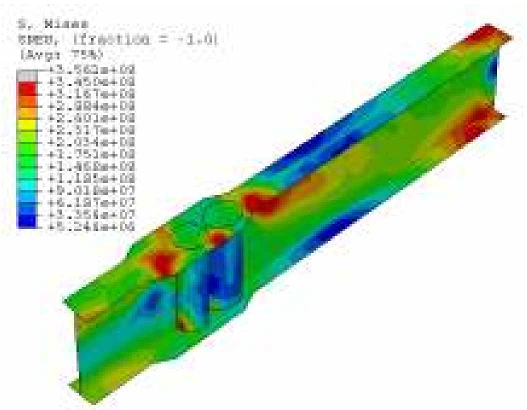

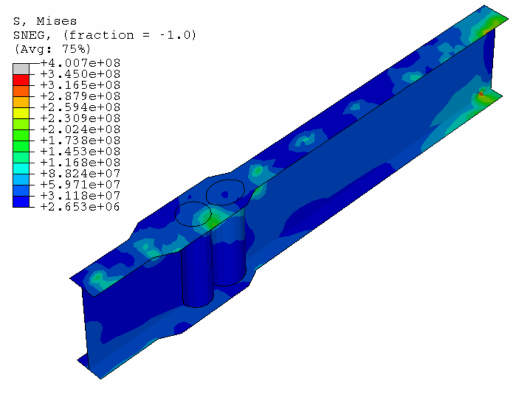

a. The original case - Von Mises

b. The strengthened case – Von Mises

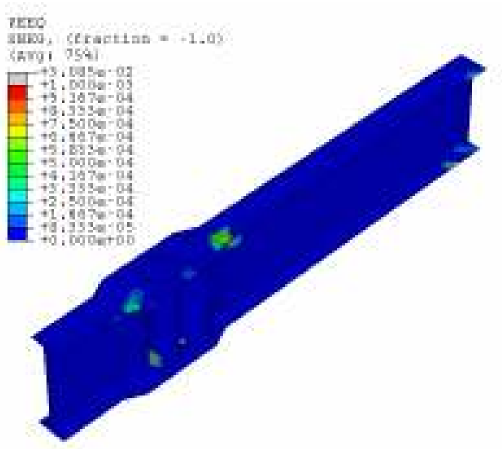

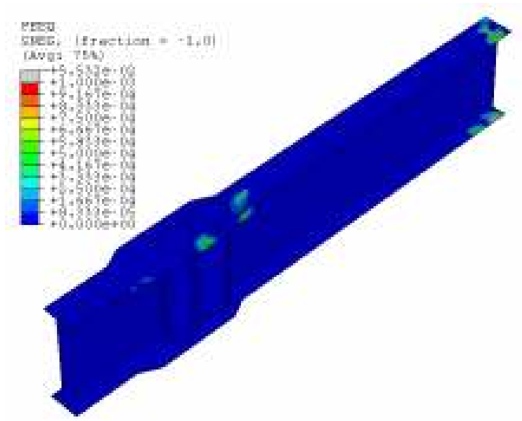

c. The original case – Plastic strain

d. The strengthened case – Plastic strain

Note:
Although the average stress and strain are much lower in the strengthened case compared with the original case, locally the end span remains highly stressed as mentioned in Figure 5.17 because more loads are coming from PG 1600-2 and no brace support as the upper level.

Figure 5.19

Plate Girder PG 1600-1 Stress and strain distributions on the lower level at 1 bar

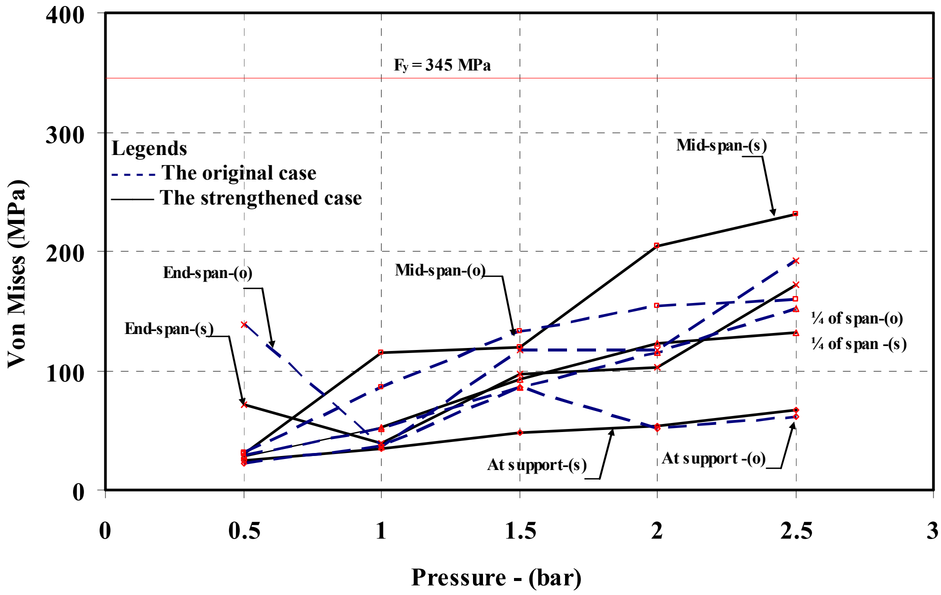

a. The upper level

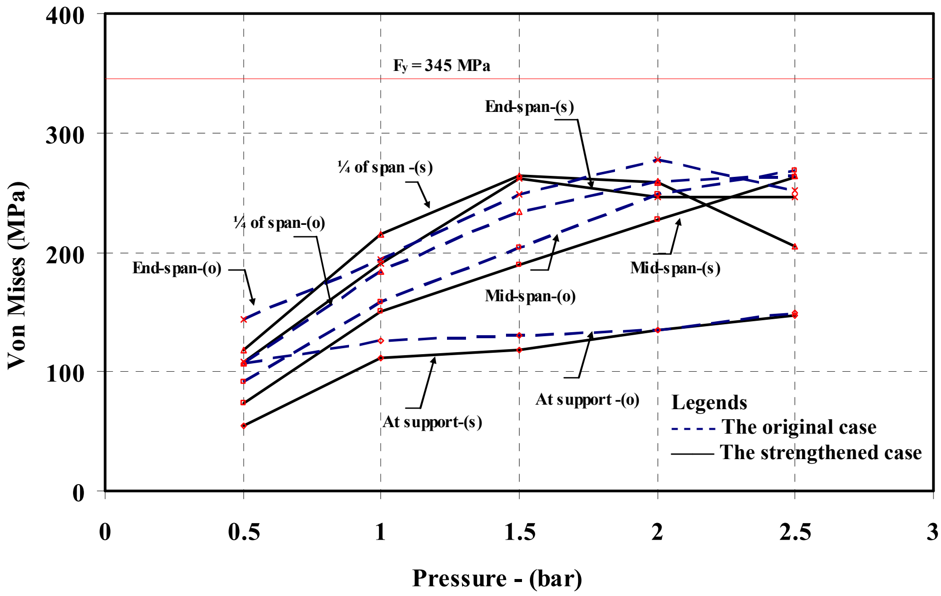

b. The lower level

Note:
Stress reduces at brace supports (508 mm ø) for both the upper and lower levels in the strengthened case. Because there is no support at end span of the lower level, stress is higher in between the brace support (508 mm ø) and end span.

Figure 5.20

Plate girder PG 1600-1 Maximum average stress across the section

5.9.6 Secondary structural component 8 mm thick deck plate

Four deck plate areas as shown by Figure 5.2a are selected. The basis of the selection is based on distance to major joints and load travel path. The descriptions for these areas are as follows:

Area A1:	located in the middle of the model for maximum relative displacement
Area A2:	on the west side close to vertical support 508 ø for maximum membrane action
Area A3:	at one quarter of span length, minimum influence from major supports.
Area A4:	the middle between two main supports (bracings).

Because the support is very much stiffer than the deck plate, some deck plates will not exhibit their actual responses but they will be influenced by responses of stiffer members that could lead to local failure. The deck plate close to main support is expected to displace less than the deck plate in the middle of deck area. However, when the applied overpressure reaches to a stage for development of membrane strain, the deck plate close to support will show a sudden and significant response as exhibited by deck areas A4 and area A2 as shown by Figure 5.21 in the original case of the upper level. The effect of strengthening allows more deformation in the middle span of IP 300 stringer beams which results in more deformation and higher stress shown by Figure 5.22 in the strengthened case. Similar response is also observed on the lower level but the magnitude in terms of displacement and stress is less compared to the upper level because the stringer beam flanges are in compression (as was explained in section 5.9.2).

Table 5.9 summarises the maximum stress and strain for each of the selected areas. In general the deck plates for both deck levels remain elastic below 1.5 bar. At 2.0 bar, the deck plates close to the plate girder 1600-1 are experiencing higher stress and strain compared with the deck plates in middle. It is noted that the measured strains have approximately doubled in magnitude between 1.5 bar to 2.0 bar. However between 2.0 bar to 2.5 bar some plates are showing lower stresses (area A3 and A4) than 1.5 bar but the strains continue to rise with the overpressure. This indicates that plastic deformation has dominated the plate behaviour with many more elements are about to reach the maximum threshold.

Based upon maximum plastic strain at 2.0 bar and also the response at 2.5 bar, it can be concluded that the upper limit of pressure for optimum design of 8 mm thick mild steel deck plate 4.0 m x 1.0 m should not exceeded 2.0 bar.

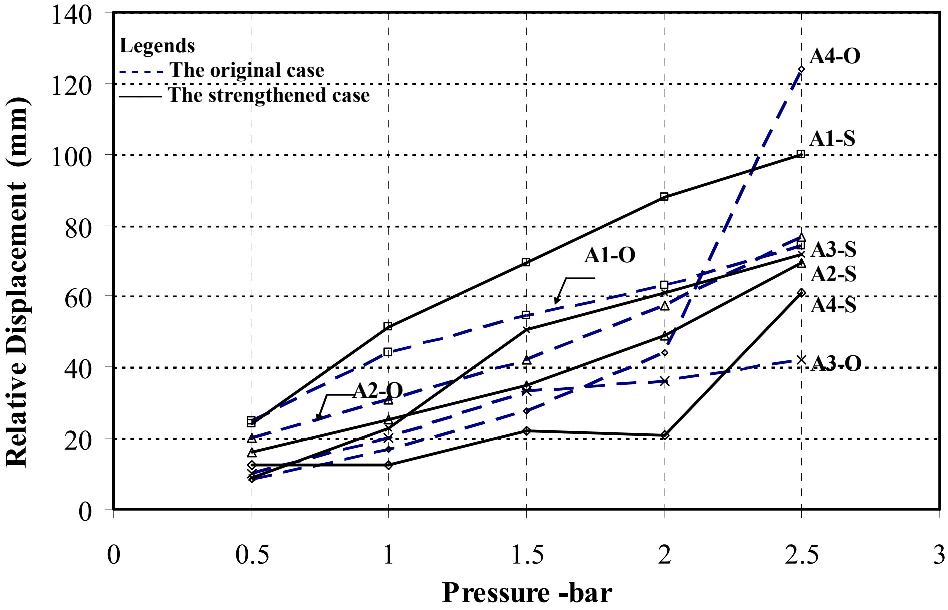

a. The upper level

Area A4 is closer to a truss frame while area A1 is in the middle of deck area. The graph rises steadily for area A1. However, a slow rising at the beginning followed by a sudden rise after 2 bar as a result of influence from the truss for area A4.

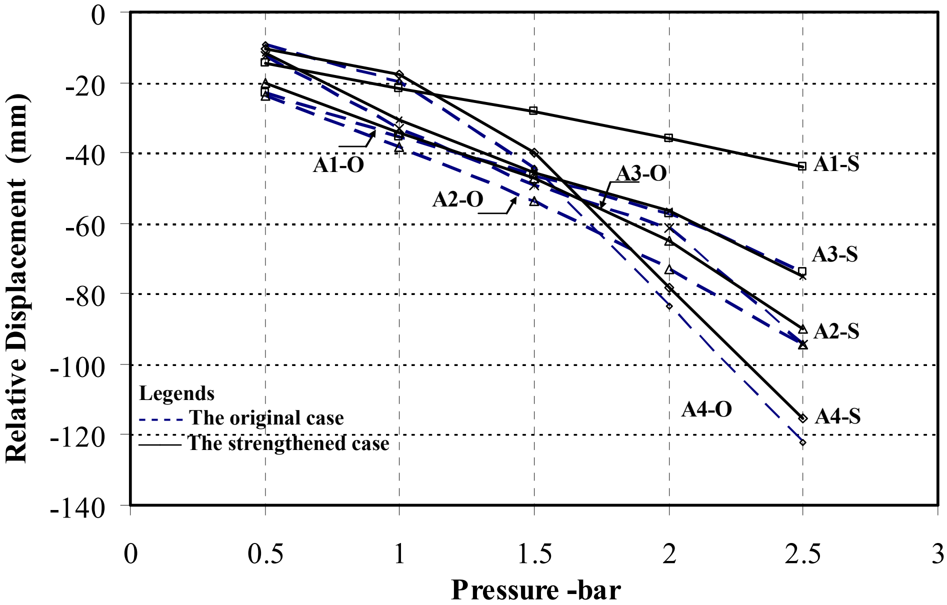

b. The lower level

Likewise the upper level, because the deck plate is in tension while the top flange in compression less displacement for area A1 compared with the upper level. Area A2 and area A4 are close to the truss while area A3 is nearer to plate girder PG 1600-2 .

Figure 5.21

8 mm thick deck plate – maximum displacement in the middle area

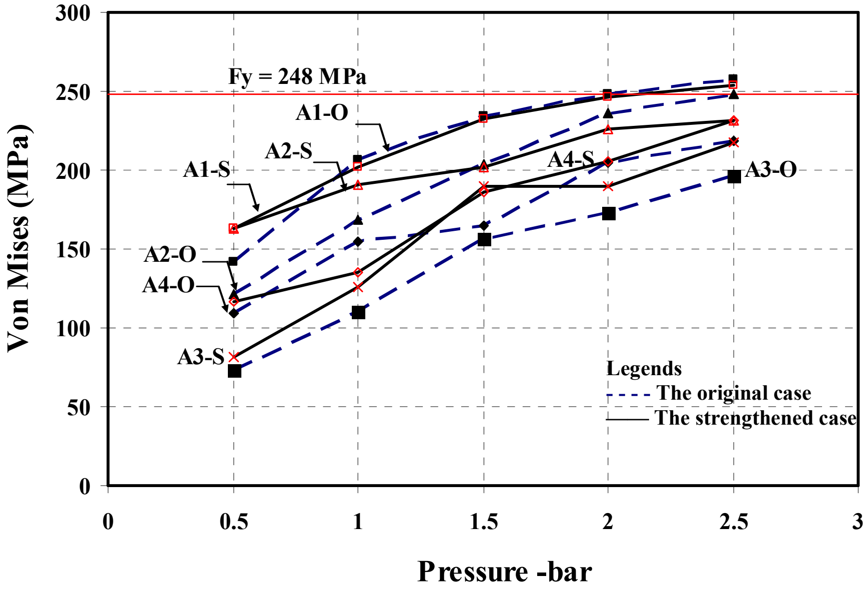

a. The upper level

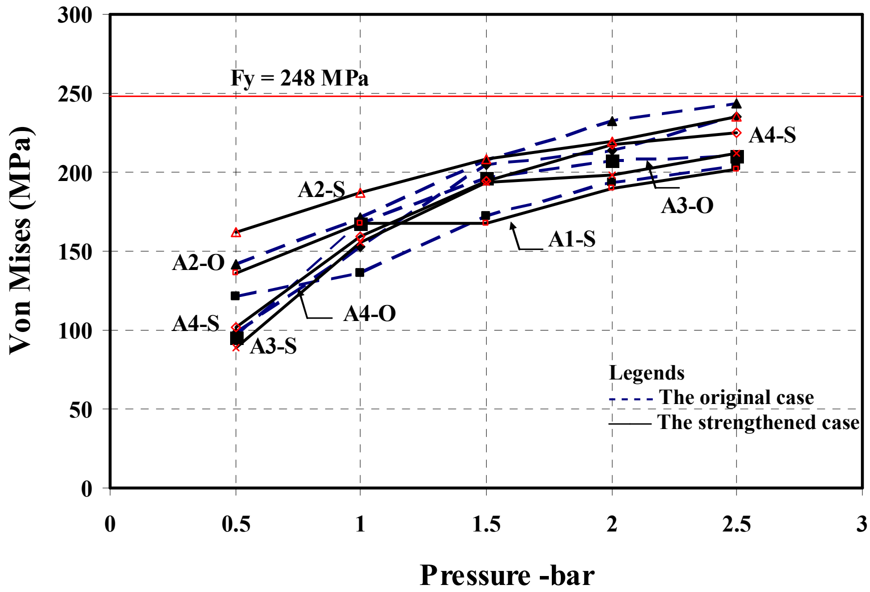

b. The lower level

Note:
The strengthened case shows higher stress compared to the original case as much more deformations of elements are occurring in the middle span as a result of the welded angles to bottom flanges of IP 300 beams.

Figure 5.22

8 mm thick deck plate – maximum stress in the middle area

Table 5.9

8 mm thick deck plate - Maximum stress and strain

Locations of elements	**Pressure (bar)** 0.5	1.0	1.5	2.0	2.5
Von Mises UL-A1-O	122.70	186.37	223.53	237.00	234.68
Von Mises UL-A2-O	126.33	171.95	206.11	241.54	**248.72**
Von Mises UL-A3-O	78.60	112.73	139.32	173.00	208.10
Von Mises UL-A4-O	74.41	110.96	171.53	**248.86**	***243.26***
PEEQ UL-A1-O	0.00	0.02	0.03	0.04	0.09
PEEQ UL-A2-O	0.00	0.01	0.03	0.07	**0.15**
PEEQ UL-A3-O	0.00	0.00	0.00	0.00	0.01
PEEQ UL-A4-O	0.00	0.00	0.00	**0.17**	0.12
Von Mises UL-A1-S	126.52	158.96	185.31	211.75	227.08
Von Mises UL-A2-S	105.71	162.65	191.66	222.04	245.92
Von Mises UL-A3-S	78.03	117.43	230.28	***197.62***	***208.08***
Von Mises UL-A4-S	76.82	113.24	176.91	244.76	251.73
PEEQ UL-A1-S	0.00	0.00	0.02	0.04	0.07
PEEQ UL-A2-S	0.00	0.00	0.02	0.08	0.10
PEEQ UL-A3-S	0.00	0.00	0.03	0.03	0.04
PEEQ UL-A4-S	0.00	0.00	0.00	0.10	**0.28**
Von Mises LL-A1-O	101.33	126.26	155.92	165.33	182.88
Von Mises LL-A2-O	146.44	187.89	227.53	247.05	**248.76**
Von Mises LL-A3-O	100.71	163.32	184.08	205.83	214.90
Von Mises LL-A4-O	102.92	203.10	245.68	**249.38**	**250.39**
PEEQ LL-A1-O	0.00	0.03	0.09	0.14	0.20
PEEQ LL-A2-O	0.00	0.03	0.06	0.13	**0.26**
PEEQ LL-A3-O	0.00	0.01	0.04	0.07	0.11
PEEQ LL-A4-O	0.00	0.00	0.07	**0.29**	**0.50**
Von Mises LL-A1-S	123.45	153.52	151.96	156.33	235.83
Von Mises LL-A2-S	130.75	182.41	208.87	243.82	247.69
Von Mises LL-A3-S	110.44	172.38	188.47	194.03	232.57
Von Mises LL-A4-S	101.60	213.02	247.79	**250.35**	**251.47**
PEEQ LL-A1-S	0.00	0.02	0.05	0.05	0.09
PEEQ LL-A2-S	0.00	0.02	0.06	0.12	**0.21**
PEEQ LL-A3-S	0.00	0.00	0.02	0.04	0.08
PEEQ LL-A4-S	0.00	0.00	0.19	**0.53**	**0.72**

Note :
Figures in bold denote the stress that has exceeded the theoretical yield at 248 MPa
Figures in italics denote enlargement of plasticity area and extensive development of membrane strain.

.

5.9.7 The strengthening component - angle L152 x 152 x 7.9

Responses shown by the angles are dependent on the behaviours of plate girders and stringer beams. Table 5.10 summarises the maximum stress and strain. At 0.5 bar, all angles are still elastic. At 1.0 bar there is small amount of plastic deformation (PEEQ = 0.02 percent) although the stress is 50 percent below the theoretical yield. Comparing this strain with IP 300 (maximum PEEQ = 0.83 percent) at the support, it can be concluded that the local strain on stringer beams has been distributed uniformly on the angles. Consequently, this has reduced the global deflection as was discussed under section 5.9.1. It is also observed that the most critical location in strengthening is the angle (L6x6-4) close to vertical brace 508 mm ø that exceeds yield stress at 2.5 bar while others remain below 248 MPa.

Similar to the behaviour of deck plates, the Von Mises stresses for angles at the lower level are always less than the upper level because the top compression flanges of IP 300 stringer beams are restrained by the tension deck plate.

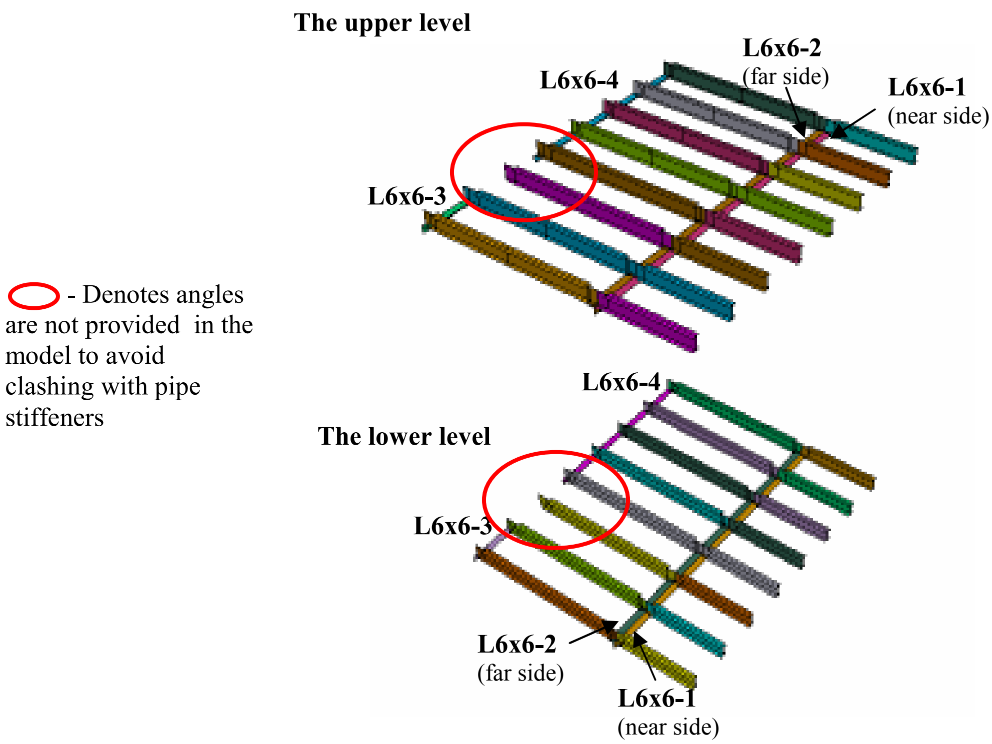

Figure 5.23

The positions of angles on the deck

Table 5.10

L152 x 152 x 7.9 - Summary of maximum stress and strain

Angle L6 x 6	**Pressure (bar)**				
	0.5	**1.0**	**1.5**	**2.0**	**2.5**
UL-VM-1	78.12	109.75	134.3	154.05	178.02
UL-VM-2	71.17	106.08	131.5	150.16	176.089
UL-VM-3	48.04	123.77	195.61	227.71	**251.62**
UL-VM-4	33.81	64.22	113.99	160.19	201.74
UL-PE-1	0.00	0.02	0.03	0.05	0.07
UL-PE-2	0.00	0.02	0.03	0.05	0.07
UL-PE-3	0.00	0.02	0.04	0.10	**1.21**
UL-PE-4	0.00	0.00	0.01	0.03	0.09
LL-VM-1	69.66	113.17	151.39	189.54	200.30
LL-VM-2	84.02	120.70	164.31	192.94	202.64
LL-VM-3	56.13	104.28	151.90	202.88	220.51
LL-VM-4	57.35	107.56	159.94	199.89	221.25
LL-PE-1	0.00	0.02	0.03	0.05	0.10
LL-PE-2	0.00	0.02	0.04	0.05	0.11
LL-PE-3	0.00	0.01	0.03	0.07	0.13
LL-PE-4	0.00	0.01	0.03	0.06	0.13

Notes

UL – Upper level ; LL – Lower level

VM - Von Mises (MPa); PE denotes PEEQ (%)

5.10 Ductility ratios in relation to the performance level of structural components

A single damage level cannot be used to represent the whole structural system because blast loads will usually first impinge on the secondary structural components such as plates, wall, cladding or equipment surfaces. These are then transferred to the supporting primary structure system and finally to the foundation. To simplify these complications, generalized damage levels (Table 5.11) are introduced and limited to the normalised estimates of ductility ratios based on displacement at mid–spans and rotations at end-spans for the structural members on the upper level of the deck, which is the worst case in the study. The limiting strain ε_{cr} Eq.(5.5) is used as a reference to monitor strain derived from finite element analyses.

As shown in Table 5.11, the strengthened cases with angles L150 x 150 improve deck plate ductility by an average of 22 percent, 49 percent and 17 percent at corner, mid-span edge and mid-span, respectively compared with the original cases. When the applied overpressure reaches 1.0 bar, ductility ratio remains below 20. At 1.5 bar, the ductility ratio at the corner is the first one to exceed 20 in both cases while ductility ratio remains below 20 at 2.5 bar for the strengthened case at the middle area of plate and the edge (longitudinal side) of the middle span.

For the stringer IP 300 beam, significant improvement is observed at the end-span by an average of 61 percent because angles are welded to sniped bottom flanges and ductility ratio remains below 20 at 2.5 bar, while the middle span improves by 23.9 percent and exceeds ductility ratio 20 after 2.0 bar in the strengthened case.

For the plate girder PG 1000, ductility ratio at the middle span in the strengthened case improves steadily until the pressure equals 1.0 bar. However, when the pressure is greater than 1.0 bar, ductility ratio in the original case is less than the strengthened because of the rupture of some elements at the haunch. Similarly, at the end-span, ductility ratio has increased by more than triple after 1.0 bar but remains below the original case.

For the plate girder PG 1600-1, the ductility ratio in the middle span varies erratically because the effect of vertical braces 508 mm ø, which are connected to the lower level. However, in the strengthened case, angles L150 x 150 improve the load distribution resulting in lower ductility ratio at the end span. For the plate girder PG 1600-2, although ductility ratio at the middle span shows significant improvement with a lower magnitude, the end span shows a marginal increase of ductility.

Table 5.11

Summary of average ductility ratios for structural components

Pressure/Locations	0.5bar (o)	0.5bar (s)	1.0bar (o)	1.0bar (s)	1.5bar (o)	1.5bar (s)	2.0bar (o)	2.0bar (s)	2.5bar (o)	2.5bar (s)
8mm plate mid span	1.73	1.49	4.55	3.78	8.92	7.29	13.98	11.46	20.53	16.07
8mm plate edge mid span	3.89	2.09	10.25	6.93	15.64	9.05	23.53	9.83	31.80	12.04
8mm plate corner	4.19	3.30	15.15	11.68	29.02	24.54	41.33	32.29	53.60	40.59
IP 300 mid span	2.49	1.95	7.18	5.59	14.41	11.08	23.28	17.76	34.59	25.17
IP 300 end span	2.86	1.02	9.92	3.60	18.89	6.78	23.64	9.67	25.44	12.26
PG 1000mid span	3.44	2.94	12.48	10.12	17.01	20.46	26.75	31.60	52.61	43.59
PG 1000 end span	3.05	2.24	9.36	4.33	18.76	14.47	31.14	241.4	38.59	29.54
PG 1600-1mid-span	1.27	1.59	2.14	1.82	3.10	2.75	3.37	4.15	8.12	7.28
PG 1600-1 end span	3.34	1.00	5.46	1.76	8.09	2.57	12.73	4.27	23.32	7.73
PG 1600-2 mid span	1.77	1.40	3.28	2.73	4.65	3.38	6.02	5.85	11.56	10.82
PG 1600-2 end span	1.20	1.33	1.96	2.10	2.31	2.56	6.51	6.78	21.44	22.77

Note : Ductility ratio $\mu = Y_{max}/Y_{el}$ (mid-span) or θ_{max}/θ_{el} (end-span)

This is owing to additional bending moment coming from IP 300 beams with angles. The average difference is less than 8 percent and does not affect the overall performance.

5.10.1 The damage level at $\mu = 6$ and $\mu = 20$

With reference to ductility ratio μ = 6 which is considered the highest damage level in design by Yasseri (2005) for preventing collapse of the whole structure system while ductility ratio u = 20 which structural members are deemed to fail by TM 5-1300 (1990) and Scheler et. al. (1991), the generalized pressures are determined and correlated to interpolated strain tabulated in table 5.11. Due to the fact that the structural members are modelled as shell elements, average values are normalized based on each element of the cross-section for representing deformation at the selected positions as well as for simplifying the results globally. Therefore, when ductility ratio μ = 20 for end-span, rotation will not necessarily equal 12 degree because the behaviour at end-span is under the influence of responses and stiffness of the other connected members. However, the table will be beneficial for predicting areas and connections which require further improvement for resisting explosions.

It is noted that for all structural members, the maximum final strain as highlighted in the table when damage level μ = 20 have not exceeded the critical strain ε_{cr} as defined by N-004 Norsok (1998).

<u>8 mm thick deck plates</u>

From the table, the corner of the deck plate has the lowest pressure of 0.60 bar when the damage level is 6. At this pressure many areas of the deck plates are still in elastic condition (section 5.9.6). A higher damage level can be implemented for more deformation in plates which can help reduce damage on supporting structures.

<u>Secondary members</u>

As for the IP 300 beam, at damage level of 6, a significant increase of pressure from 0.77 bar to 1.38 bar and a significant drop of plastic strain from 8.57 percent to 0.004 percent for end support in the strengthened case. This finding is consistent with middle span displacements whereby at 1.5 bar more than 60 percent (Figures 5.10 and 5.11) of the beams start to yield and the displacements in the strengthened case have exceeded the displacements in the original case.

Table 5.12

Estimate of pressure with reference to the highest design damage level u = 6 and members to fail u = 20

The structural components	Original $\mu = 6$ Pressure (bar)	Original $\mu = 6$ PEEQ (%)	Strengthened $\mu = 6$ Pressure (bar)	Strengthened $\mu = 6$ PEEQ (%)	Original $\mu = 20$ Pressure (bar)	Original $\mu = 20$ PEEQ (%)	Strengthened $\mu = 20$ Pressure (bar)	Strengthened $\mu = 20$ PEEQ (%)
Dk Pl 8mm (ε_{cr} = 7.20)[b]								
mid-span	1.17	0.021	1.32	0.071	2.46	0.046	> 2.5	0.200
edge mid-span	0.67	0.031	0.93	0.081	1.78	0.108	>2.5	0.300
Corner	0.60	0.330	0.70	**0.469**	1.17	0.680	1.32	**0.955**
IP 300 (ε_{cr} = 20.55)[b]								
mid-span	0.89	1.133	1.04	2.350	1.82	1.278	2.15	6.300
end-span	0.77	**8.570**	1.38	0.004	1.62	**15.48**	>2.5	2.440
PG1000 (ε_{cr} = 18.25)[b]								
mid-span	0.67	3.083	0.76	**4.730**	1.65	**9.330**	1.48[a]	6.236
end-span	0.82	0.420	1.08	1.172	1.55	1.860	1.79	2.613
PG1600-1 (ε_{cr} = 28.00)[b]								
mid-span	2.28	0.209	2.30	**3.310**	> 2.5	1.310	> 2.5	**1.500**
end-span	1.10	0.002	2.25	0.001	2.3	0.128	> 2.5	0.150
PG 1600-2 (ε_{cr} = 21.50)[b]								
mid span	1.98	0.532	2.10	1.679	>2.5	2.56	>2.5	2.85
end span	1.94	5.901	1.90	**6.100**	2.45	15.45	2.41	**17.32**

Notes :
1. '> 2.5' bar denotes that the analysis was performed with the maximum pressure up to 2.5 bar and strain values are taken from 2.5 bar.
2 [a] – Due to rupture at haunch [b] – see assumptions made in section 5.1

<u>Primary members</u>

For plate girders PG 1000 and PG 1600, both plate girders show an increase of overpressure in the strengthened case compared with the original case except at the condition where deformation at haunch becomes critical on plate girder PG 1000. Haunch detailing is crucial for ensuring deformation away from the main joint, i.e. if the bottom flanges of the incoming member are extended beyond the haunch point, plastic deformation will first occur at the flanges of the connection rather than the haunch.

5.11 Discussion

5.11.1 Loading direction and load travel path

The load direction and load path are two prominent factors for determining the behaviour and response of a structural member. Typically, the topsides of offshore installations are designed for loads which are under the influence of gravity and the combination of lateral loads due to environmental loads. However, in explosions, the generated frontal waves propagate in all directions, which impose overpressure loads on obstructed surfaces. As shown in the study, having been restrained by the tensioned deck plates on top compression flanges of stringer IP 300 beams, globally increases the stiffness, thus the deck lower level is less sensitive than the deck upper level although the two deck levels are similar in the structural configuration.

As explosion occurs over a very short duration as impulse load, exposed structural members will respond instantly. Structural members which are not directly exposed, but on the load travel path, will respond at a delayed stage. The expected responses will be the combined reactions from exposed members and their own stiffness as exhibited by plate girders PG 1600-2.

5.11.2 Strengthened case with L150 x 150 x 7.9

The introduction of angles L150 x 150 at supports for both ends of stringer IP300 beams profoundly increases the efficiency of bending moment and shear transfer to primary members (plate girders) as well as resistance of plates and stringer IP 300 beams against blast loads on both deck levels.

The new configuration induces stringer beams to react with first yielding at mid-span by flexural rather than first shear failure at both end supports, thus minimising further damages to plate girders. However, strengthening at supports has changed connection to fully restrained which attracted additional out-plane bending moment to plate girders. At the same time, angles L150x150 have increased the stiffness of plate girders which also reduced displacement.

5.11.3 Structural configuration and connection

Structural members designed for providing resistance against explosions must be directly connected to supports. This is for preventing damage on the non-exposed members which can escalate unnecessary damage to other non-affected members.

The analysis has shown that spreading of plastic and failure of haunch elements have resulted in the reduction of stress and strain at the joint of the end-span. This detailing can be a mechanism for stopping further overstressing and for maintaining the joint within the design damage level.

5.11.4 Detailing of structural members

Typically on offshore installations, stringer beams or secondary members are designed as simply supported or partially restrained supports whereby the bottom flanges of beams at supports are removed or sniped. As a result, the contribution of stiffness to the main structural framing is often assumed to be not significant, hence these secondary members are not modelled in the analysis.

For large designed topsides, sniping bottom flanges of stringer beams minimize welding work and weld distortion on primary members as well as representing a great saving in fabrication cost. However, in partially restrained conditions (no welding at bottom flanges), bottom webs at sniped areas are the weakest point and these beams usually fail due to shear.

As shown in the analysis, in the worst condition of the upper level for stringer IP 300 beams, the end-span fails at a pressure about 1.62 bar (when ductility ratio u = 20) in the original case while in the strengthened case at 2.5 bar, ductility ratio still remains under 20 and yielding of the beams first to occur at the mid-span. This concludes that retrofitting work with angles L150 x 150 x 7.9 increases the blast resistance by relocating yield areas from end span to mid-span.

Although a haunch on a primary structural member can be developed as a mechanism for minimising the effects of explosions on other structural members, they should be designed carefully to avoid a concentration of stress which can cause catastrophe collapse. As shown by responses of some structural members (PG 1600-2 and PG 1000) in the analysis, local failures are commonly anticipated at joints when loads are transferred to other members. Hence, any strengthening and mitigation works should emphasise the efficiency of load transfer in reducing load to the repaired area.

5.12 Performance level and ductility ratio

5.12.1 Components based performance level

At ductility ratio of 6, the plastic strain shown in table 5.12 at the middle span for the stringer IP 300 beam in the strengthened case is approximately twice compared with the original case. For the end span, the plastic deformation is almost negligible in the strengthened case compared with the original case. The overpressure on IP 300 beam has increased from the lowest value of 0.77 bar (functional) to 1.04 bar (operational). This concludes that resistant capacity by the IP 300 beam has been improved and failure at supports has been prevented.

Similarly, at ductility ratio of 6, although still under functional performance; with angles, the overpressure for plate girder PG 1000 improves from 0.67 bar to 0.76 bar while the deck plate improves form 0.60 bar to 0.7 bar. For plate girder PG 1600, which is the primary component, improves from functional performance at 1.10 bar to near collapse performance at 2.3 bar with angles.

Finding by Vinnem (2000) reveals that for the North Sea sector, 70.6 percent from the total occurrence of explosions are less than 0.2 bar, 23.5 percent between 0.2 bar to 1.0 bar, 5.9 percent between 1.0 bar to 2.0 bar and none for overpressure greater than 2.0 bar. This is a useful finding for benchmarking the present overpressure on plate girder PG 1000 and stringer IP 300 beams. With overpressure ranging from 0.67 bar to 0.82 bar for plate girder PG 1000 and 0.77 bar to 0.89 bar for IP 300 beam (without strengthening) at ductility ratio of 6, these Figures can be regarded as the highest damage level, although in terms of defined performance levels they are just slightly below operational. Conversely, secondary members such as plates should allow for a higher damage level (greater than 6) compared to other structural components so that plates will consume more energy and yield earlier than other components.

5.12.2 Global based performance level

Based on the criteria proposed in section 5.6, the current performance levels of the present structural system are summarised as follows:

	Original case	Strengthened case
Functionality 0.5 bar	Although main frame plate girder PG 1600 is still intact but repair work requires that primary member plate girder PG 1000 (μ = 3.34) and inspection to evaluate secondary members (deck plate, μ = 4.19). Platform shut down required for short period and may interrupt daily routine works.	Minimum damages, with repair can be done at any convenient time. Requires inspection on deck plates (μ = 3.30) and PG 1000 (μ = 2.94). Platform shut down is not necessary and minimum interruption to daily routine works
Operational 1.0 bar	Major repair for plate girder PG 1000 which supports the walkway (heavily damaged, μ =12.5) although the main frame still intact. Loss of equipment support. Secondary members need replacement. Requires longer period for platform shut down.	Repair required at mid span plate girder PG 1000 (μ = 10.12). Some plates might have been damaged and may require replacement. Inspection requires for IP 300 beams. Main framing is still intact with short period of platform shut down.
Safety 1.5 bar	Repair work is unlikely because rupture of deck plate and loss of support for IP 300 beam and plate girder PG 1000 hence escape route can not be guaranteed. Main framing is damaged and platform must be shut down.	Substantial damage and repair work is possible but at a high cost. The main frame plate girder PG 1600 is still intact (μ = 2.75) and the structural integrity is within the limits (no connection failure). Escape route is estimated 25 percent safe (no facture yet on IP 300 connection). Platform shut down is required to minimize the blast escalation effects.
Near	Almost all components fail, main	Failure on deck plate and plate girder

collapse 2.0 bar	frame plate girder PG 1600 is 40 percent to collapse.	PG 1000. IP 300 beam is about 50 percent to rupture at supports and major deformation at mid span. Plate girder PG 1600 (μ = 4.27) is still intact but some damages. No safe escape route.
Total Collapse 2.5 bar	All structural components fail. ($\mu > 20$)	Almost all components fail, main frame plate girder PG 1600 is 65 percent to collapse.

5.13 Concluding Remarks

In the performance based design methodology, a ductility ratio of 6 can be regarded as the upper bound damage level for primary structural members exposed directly to blast loads at which none of the modelled finite element structural members have exceeded critical strain (Eq. (5.5)). However, for primary structural members which are the structural truss system, moderate values ($2 \le \mu < 3$) should be adopted in order to prevent premature failure at the connections.

The study has shown that improvement in modelling allowing a higher damage level than 6 can be adopted for secondary members such as plates. Although the relationship between responses of structural members and sensitivity at connections are complex, defining damage level in terms of ductility simplifies the description of performances for a structural system.

The configuration of structural framing for new topside designed for hydrocarbon explosions should be arranged for a direct exposure to the overpressure blast load. Reactions resulting from responses of structural members have to be transferred to the designated supports in the shortest possible load path. Shortening the load travel path will prevent unnecessary damage occurring to other structural members. Similarly, a selection of options for mitigating blast resistance on any existing topside caused by an explosion will become more acute if the sensitivity of the structural system is not thoroughly checked.

The study has highlighted the weakness of sniped bottom flanges of stringer beams which is commonly practiced for cost saving and minimizing defect on primary members. The proposed strengthening method with angles (L152 x 152 x 7.9) improves the performance level of the deck by the relocation of yield areas to mid spans of sniped beams at component level. The angles also help to distribute the load uniformly which reduces the global displacements as well as meeting the performance level up to near collapse.

The fundamental detailing of connections must not allow components of the structural members in its vicinity to yield. As shown in the present study, the provision of haunches can be a mechanism for preventing damage at a joint while with a considerable amount of strengthening for IP300 beams at supports relocates the plastic hinge from end-span to mid-span.

Chapter Six

Strengthening Beam to Beam Connection for Blast Resistance on Topside Structures

6.1 The connection of primary structural members on typical topside structures

A connection for load transfer is formed when at least a single or more than one, of the structural members that carry loads are joined together to a point on a support member. As most connections serve as intermediate points during load transfer to foundations, the ductility at connection plays an important role for ensuring effective load transfer and preventing collapse. Hence, structural support members must have sufficient capacity and stiffness at least similar or greater than structural load carrying members.

In a beam to column connection, the easiest or possibly simplest method without changes in structural detailing can be improved by having a beam with yield strength lower than a column. The advantage of this method is due to the fact that the beam is allowed to deform at the same magnitude because displacement is independent of yield strength while stiffness at the connection remains the same and is not affected because there is no increase in sectional properties. The first yield will occur in the beam instead of the column. Alternatively, connections can also be improved by having additional plates attached to beam flanges as discussed by Chen et al. (2003) and Sabuwala et al. (2005). The existence of a cope hole or access hole during welding may also affect the performance of connection as highlighted by Ricles et al. (2002) while improper welding procedures potentially allow seepage of hydrogen that can induce brittleness and encourage cracks in welds as reported by Dubina and Stratan (2002) and is summarised in Table 2.7.

On offshore structures, especially for topside structures, the load path during operational cases which can be classified as static load, commences with loads imposed on deck floorings i.e. either on grating panels or deck plates. These loads are then carried by secondary structural members, usually stringer beams (typical depth of 200 mm to 300 mm), which are supported by primary structural members. Supports for equipment are designed separately and seated on their own support beams. The positions of support beams are usually adjusted to share the loads between other primary beams. Alternatively, equipment supports or support stools are adjusted to sit directly on existing primary structural members. The primary structural members will then carry all loads to other primary members, or they may form part of the main framing of the structural system where loads are transferred to final supports or foundation points. Failures on structural members are highly likely along the load path when the loads have exceeded the theoretical Euler's column load.

The blast load path is equivalent to static load path but the blast damaging effect is more prominent on the first members in contact with the load, usually the secondary members. Therefore, ensuring the integrity of primary members and connections are important so that secondary members can achieve the designed damage level and reactions can smoothly be transferred to supports.

The main connections for primary structural members that can be found on topsides are as follows:

a. Vertical main columns (very large in size) with incoming horizontal and diagonal members welded around the column circumference. This type of connection is usually found at deck legs with enlarged ring flanges. The connection can be categorized as the strongest joint on the topside as most loads will be transferred through this point to piles or foundation supports.

b. In the middle of a truss system with a concentration of diagonal braces landed on the top and bottom flanges of a truss beam. The truss beam is usually fabricated with extended flanges or a portion of built-up plate girder and stiffened by flat plates or half cut pipes as load bearing stiffeners.

c. Load carrying beams (primary beams) to truss beams or plate girders.

The first and the second connections are shown in Figure 6.1. They are the basic constituents of the structural main truss system that should be designed to be robust and must not experience any premature failures under all kinds of load scenarios.

The third connection is the vast majority of connections found on topsides in which most connections can be grouped. The beams from this group support loads from stringer beams, deck floorings and equipment. Under an extreme blast load condition, these beams are allowed to deform at moderate level as long as escape routes are passable and safety is guaranteed. Hence, it is paramount that these beams have sufficient capacity not only to be able to absorb as much energy as they can during deformation but also able to support other inventories that they have been designed for after explosion events.

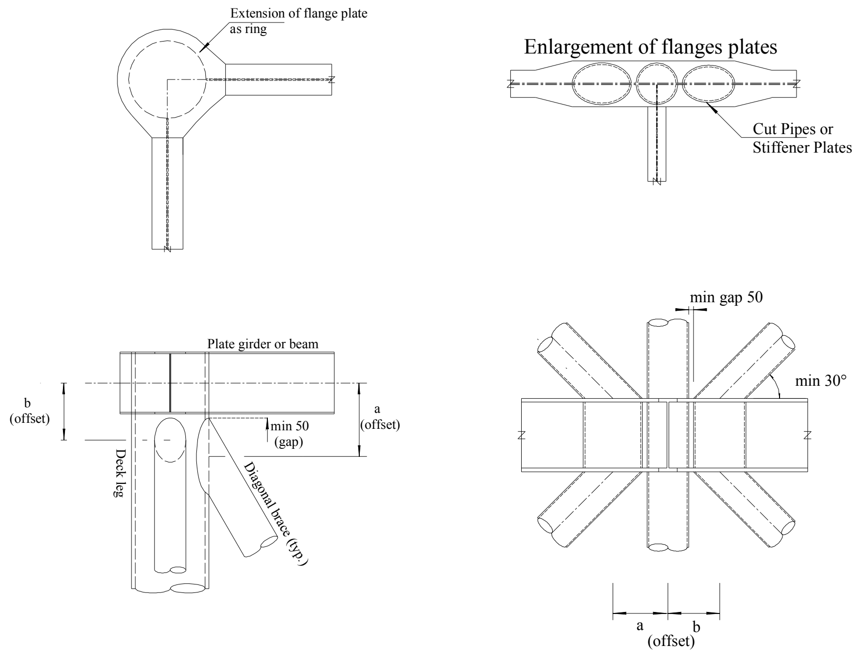

a. Connection at deck leg

b. Congested connection at middle truss

Figure 6.1

Common main connections on topside structures

Offsets on members must not be ignored and should be incorporated in the design. A gap of minimum 50 mm for avoiding overlapping of welds is usually adopted. Bigger gaps are preferred in fabrication but this will increase the offset distant as well as the bending moment. API RP 2B recommends the offset not to be more than 305 mm or D/4 (D is the diameter or overall depth of the incoming structural member) whichever smaller. All incoming braces must at least achieve a minimum 30^{o} inclined angle for ensuring sufficient access area during welding.

6.2 The study of beam to beam connections

The aim of this study is to mitigate existing beam to beam connections for better resistance to blast loads. The proposed approach should be a simple strengthening method; an efficient and workable solution such that minimum interruption to the daily activities on the topside occurs.

Tables 6.1 and 6.2 summarize connection details for beam to beam, many of which are commonly found on topside structures. Basically, they can be divided into two cases based on the overall depth of beams. Case I represents beams with equal depth, while case II represents beams with different depths. The control case in this study is defined as a connection with no steels added at the connection except for a simple back-up stiffener to account for the depth difference of the incoming beam.

6.2.1 Case study I - beams with equal depth

The selected beam on which the load is to be applied is an I beam IP 600 while the beam to support the load carrying beam is also an I beam IP 600. The case study is summarised by Table 6.1 while connection details for each case are given in Figures 6.2 to 6.4.

Case IB emphasizes the cope holes that are created for full access of welding and the effect of having additional plates at the end span. On the other hand, case 1C looks into the strengthening of the support beam rather than the beam which is applied with a blast load.
In case ID-1 and case ID-2, neither modifications are made nor are plates added at the existing connection. However, the beams are interconnected by new diagonal tubular members between the supports to the middle span. The tubular section is selected because it has a symmetric cross section in all axes. Slotted gusset plates at ends of tubular serve as a dual purpose. The first purpose serves as a vertical stiffener for transferring shear to flanges while the second purpose serves as an intermediate between the beam and the pipe, and load transfer in terms of axial load. The combined tubular with end gusset plates is easy to fabricate and install offshore

because the over length gusset plates can simply be trimmed for site adjustment.

Table 6.1

Connection of beams with equal depth

Case	Descriptions
IA	As a control case and a typical standard connection with full penetration weld between flanges and fillet weld between webs (Figure 6.2)
IB-1	The extended wing plates are welded to the beam flanges which are flushed bottom and top. The added plates are equal in thickness as the beam flange. 20 mm cope holes are created at corners for avoiding overlapping welding on existing welds as well as for ensuring complete access to accommodate a full weld penetration (Figure 6.3)
IB-2	Similar to case 1B-1 but no cope holes.
1C-1	The extended wing plates are provided on both sides of the support beam.
ID-1	Consider as a mitigation case where load to deform the beam is shared in tension by a single horizontal brace with gusset plates at both ends. One end is connected to the middle of the beam while another end is connected a stronger point. Both sides of the gusset plate are applied with fillet welds which are equivalent to a full penetration weld (Figure 6.4).
ID-2	Similar to case ID-1 but with double diagonal braces.

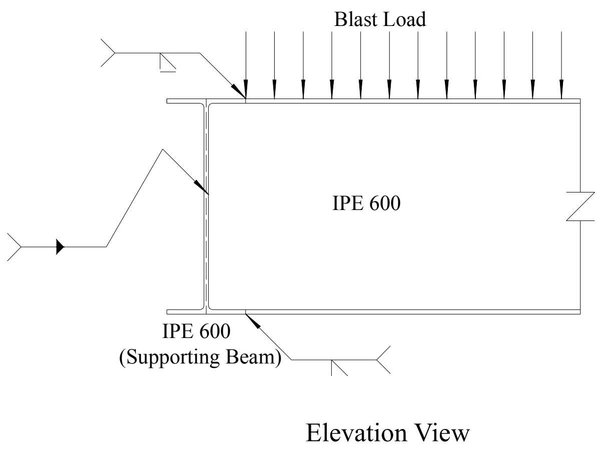

Figure 6.2
A typical connection for primary beams with equal depth
Double bevel full weld penetration for plate with thickness ≥ 25 mm.

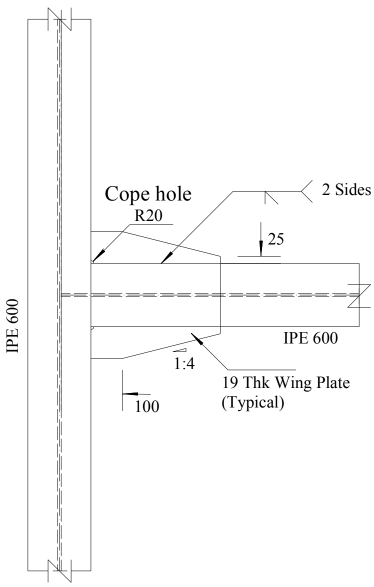

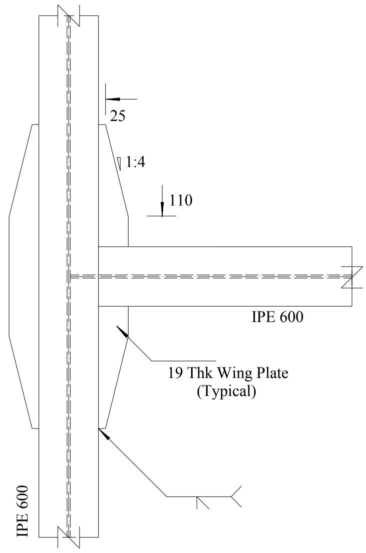

a. Case IB

Case IB-1 as shown and with cope holes

Case IB-2 similar without cope holes

b. Case IC

Figure 6.3

Case IB and case IC –
Detail strengthening on the existing beam to beam connection.

<u>Notes</u>

Strengthening in case IB focuses on end span that is equivalent to cover plate method in beam to column connection.

Strengthening in case IC involves strengthening the support beam and end span.

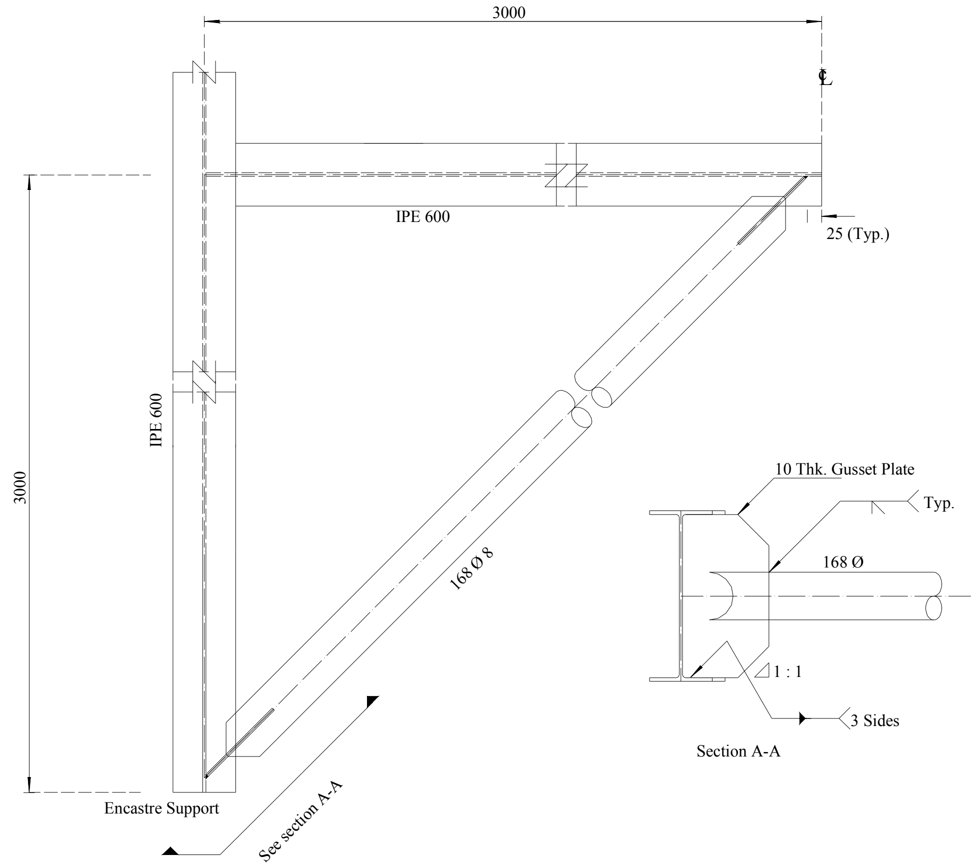

Figure 6.4
Case ID- Existing connection with proposed diagonal braces.

<u>**Notes**</u>

Connection ID-1 and ID-2

No strengthening is made at the existing connection. The new bracing is offset to half depth of the beam and slotted through with gusset plates at ends. The gusset plates are vertical stiffener plates followed by the brace orientation. Both pipe ends can be assumed as a partially restrained condition because only top and bottom are welded to the plate for which only axial force can be transferred.

6.2.2 Case II – beams with different depths

The selected beam to carry blast load is I beam IP 600 beam while the supporting member is plate girder PG 1000 (1000 mm (depth) x 400 mm (width) x 25 mm (t_f)x 15 mm (t_w)). Table 6.2 summarises the considered cases in the study while details for each connection are shown by Figures 6.5 to 6.7. Case IIA is a control case, being the simplest, and is a common connection on topside for different depths. Case IIB and case IIC are implemented for saving material and cost as well as to control weight increase. Case IID and case IIE are originally from case IIA and case IIC respectively, neither modifications are made nor are steels added at the existing connection. The approach is similar to case ID which allows sharing of some loads in terms of tensile load through the diagonal tubular brace.

Table 6.2

Connection of beams with different depths

Case	Descriptions
IIA	Control case considered as no strengthening except for vertical stiffener plates at the bottom flange (near side) and backup (far side), Figure 6.5a.
IIB-1	Typical haunch details tapered 1: 4 slope with extended bottom flange. No welding is performed between bottom flanges to the web, Figure 6.5b.
IIB-2	Similar to detail IIB-1 but the bottom flange is removed at which the haunch is terminated.
IIC-1	Similar to detail IIB-1 but the tapered slope is 1:1 with extended bottom flange to the web, Figure 6.6
IIC-2	Similar to detail IIC-1 but the bottom flange is removed at which the haunch is terminated.
IID-1	Case IIA with single diagonal brace, Figure 6.7.
IID-2	Case IIA with double diagonal braces.
IIE-1	Case IIC-1 with single diagonal brace, Figure 6.7.
IIE-2	Case IIC-2 with 1 pair diagonal braces.

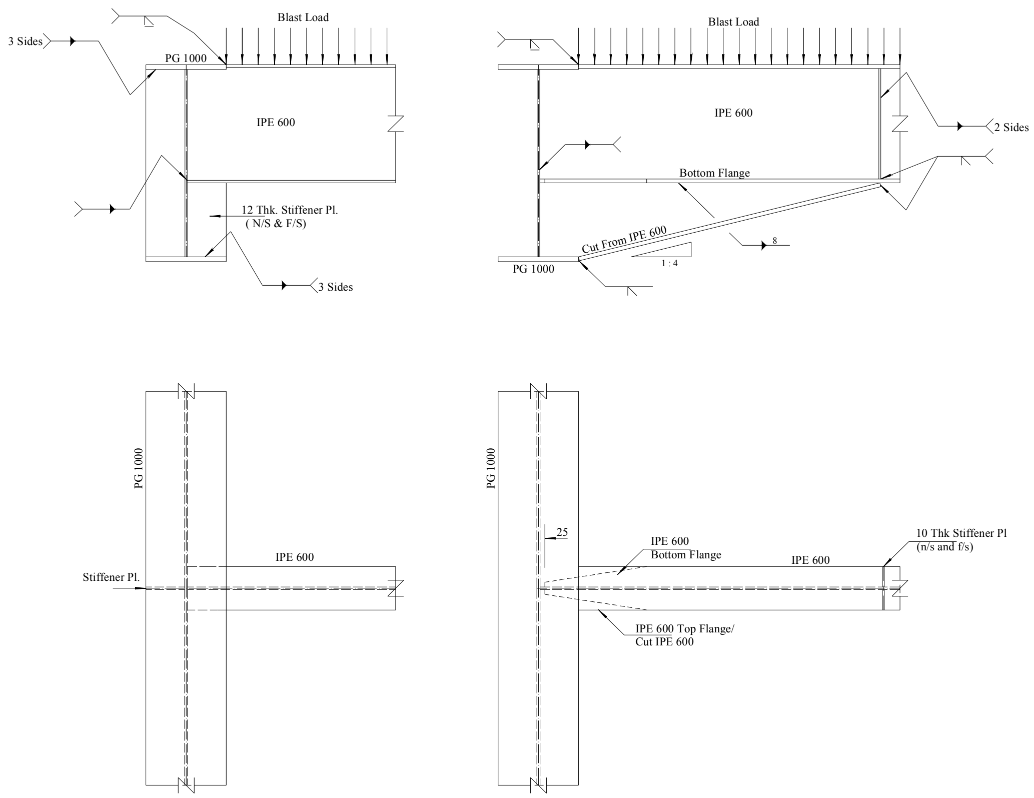

a. Case IIA **b. Case IIB**

Figure 6.5

Case IIA and case IIB – Connection of beams with different depths

(Plate girder PG 1000 : 1000 x 400x 25x 15)

<u>Notes</u>

Connection IIA (control case)

IP 600 is joined to a plate girder PG 1000 with a stiffener plate to make up the depth difference. Another stiffener plate is provided on the far side as backup to counter the axial force from the bottom flange of IP 600.

Connection IIB

Similar to type IIA connection, the makeup of depth difference is made from a cut of IP 600 with tapered slope of 1:4. The incoming bottom flange of IP 600 is trimmed and no welding is made to the plate girder web. Only a pair of stiffeners is provided at the transition point (before the haunch) of the beam.

As an alternative, the bottom flange is removed to represent a fabricated built-up portion with similar properties to IP 600 beam but greater depth than the plate girder.

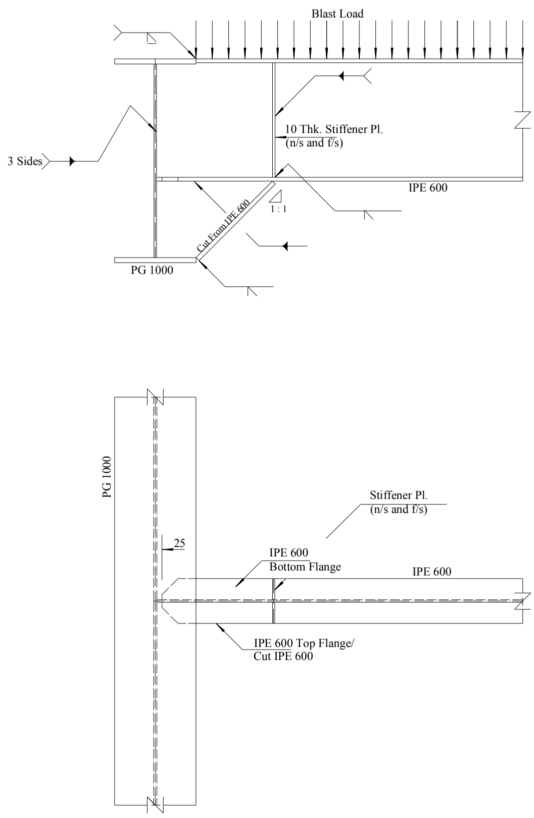

Case IIC

Figure 6.6

Case IIC – Connection of beams with different depths

Notes

Similar to case IIB, the make up of depth difference is made from a cut of IP 600 beam but the tapered slope is changed to 1:1. The incoming bottom flange is trimmed and no welding to the web. Only a pair of stiffeners is provided at the transition point (before the haunch) of the beam.

As an alternative, the bottom flange is removed to represent a fabricated built-up portion with similar properties to IP 600 beam but greater depth than the plate girder.

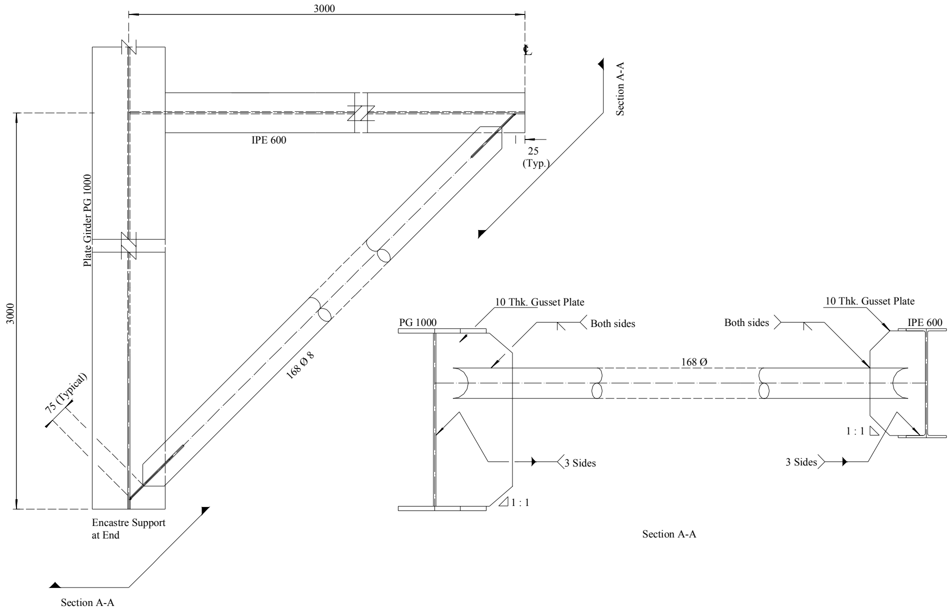

Figure 6.7

Case IID and case IIE
Existing plate girder to beam connection with different depths and the proposed diagonal brace

<u>Notes</u>

The connection between IP 600 to plate girder PG 1000 is similar to case IIA or IIC for case IID and IIE, respectively. The bracing is offset to half depth of the IP 600 beam (as reference line) and both ends are slotted through with gusset plates. The gusset plates are actually stiffener plates with extended wing. Both ends of the tubular can be assumed as partially restrained because only top and bottom are welded to the plate for which only axial force can be transferred.

6.3 The development of ABAQUS model for beam to beam connections

The behaviour at connections was investigated by modelling the aforementioned structural members in case I and case II using the finite element program ABAQUS version 6.6. It was assumed that the validation model used in chapter 5 is also applicable in this study.

All structural members in the model were treated as shell elements (S4R) with an average mesh size of 25 mm square. Cowper Symonds formula (Eq. (5.7)) for strain rate was incorporated into the analysis with no imperfection considered. Only half of the span length for the beam exposed to blast load was considered (3000 mm long) with a symmetric boundary at the middle span. The support beam was assumed to be a continuous beam, restrained at every 6000 mm in both horizontal and vertical directions; therefore a fixed support was assumed at both ends

In order to maintain the consistency of responses, all steels were specified as mild steel with minimum yield strength of 245 MPa. The top surface area of the beam was divided into few partitions so that the same amount of overpressure as the control case would be applied on the beam. Neither stringer beams nor deck plates were modelled so that the anticipated deformation was solely due to the response of the modelled beam and plate girder.

The applied load on the beam was equivalent to the applied load which covered an area of 3000 m by 6000 m with two specific peak overpressures of 1.0 bar and 2.0 bar for a duration t_d = 50 ms. The overpressure of 1 bar was selected because IP 600 is about to fail (measured ductility just over 20) as in the control case IA and to evaluate the effectiveness of mitigation work, while 2 bar overpressure was considered an extreme case whereby total damage and collapse of the beam were expected.

6.4 The analysis results of ABAQUS connection model

In each analysis, deformations to structural members were monitored at middle span and connection while stress and strain were monitored in middle span, connection and support point. A separate ABAQUS modified Riks algorithm non-linear analysis was performed to determine deformation at yield using the tangent method discussed in section 4.6.

6.4.1 Response of beam connection: Case I - with equal depth

Table 6.3 summarises deformations at the middle span and the connection while Figure 6.8 shows distribution of stress contour along the structural members.

For case IB, in which extension plates are welded at the end span of IP 600 beam, the new built-up shows small improvement compared with control case IA where the displacement is reduced by an average of 1 percent. The result also shows that leaving cope holes (20 mm radius) and doing nothing after welding, slightly reduces deformations at the mid span and the end span compared to the case without cope holes. This is the advantage of having cope holes as not only full penetration of weld can be achieved but no extra welding is required to close the gap.

As a result of the end span extension, the connection is much stiffer compared to the control case IA. The method has slightly increased rotation by an average of 0.95 percent. The average ductility ratios at mid span and end span reduce by 0.6 percent and 3.5 percent respectively at 1 bar. However, at 2 bar, ductility ratio increases by 0.6 percent at the middle span but reduces by 13.8 percent at the end span.

For case IC in which strengthening is made by enlarging the flanges of the support IP 600 beam, deformations (i.e. in middle span deflection and end span rotation) are reduced by averages of 5.6 percent and 3.0 percent at 1 bar and 2 bar in comparison to the control case IA, respectively. This signifies that strengthening of the support beam is much better than the end span extension.

Furthermore, some reasonable capacity at the connection ensures the load carrying beam can consume much more energy and deformation along the beam as it is distributed more evenly. Likewise in case IB, ductility ratio at middle span is slightly higher by 0.7 percent but lower at end span by 22.2 percent compared with the control case IA.
From the outcome of cases IB and IC, it can be deduced that although physical rotation is greater than the control case at higher overpressure as a result of new build-up at the end span, lower ductility ratio is anticipated at the end span and less deformation at the middle span. This indicates minimum damage and structural members can sustain a higher load than control case 1A.

Case ID is related to the sharing of responses by having braces connected at the middle span. With double bracings, it is observed that deformations are reduced by averages of 55.3 percent and 59.4 percent at 1 bar and 2 bar in comparison with the control case respectively. The braces share the blast loads mainly by axial tensile force and help to distribute the load quickly to the support points and subsequently suffer some damage at the connection to gusset plates as shown in Figure 6.8.

With a single tubular, deformations are reduced by an average of 21.4 percent and 33.0 percent at 1 bar and 2 bar respectively. While the magnitude of ductility ratio for a single brace is larger than the case with double braces, this configuration shows better results than the four aforementioned cases without braces.
Both deformation and ductility ratio reduce substantially in the double diagonal braces case. Ductility ratios reduce by 46.6 percent and 52.8 percent for end span and middle span at 1 bar respectively; at 2 bar the reductions are 78.9 percent and 51.4 percent, respectively.

Under extreme high overpressure, it can be concluded that having double diagonal braces is preferred to a single brace because the performance and stability of structural members can be improved remarkably.

Table 6.3

Case I (equal depth) - The response and ductility ratio

Case	Normalised Response				Ductility Ratio			
	Middle span deflection		End span rotation		Middle span		End span	
	1 bar	2 bar	1 bar	2 bar	1 bar	2 bar	1 bar	2 bar
IA(Control case)	1.000[a]	1.000[b]	1.000[c]	1.000[d]	7.42	53.03	9.73	75.82
IB-1	0.988	0.881	1.002	1.017	7.35	53.32	9.38	65.21
IB-2	0.992	0.887	1.009	1.018	7.40	53.37	9.40	65.47
I C	0.926	0.823	0.944	0.970	7.27	53.40	8.52	59.02
I D-1	0.786	0.670	0.814	0.939	6.08	50.19	9.24	61.40
I D-2	0.447	0.406	0.477	0.212	3.50	11.15	5.20	36.82

a = 210.80mm b = 1642.94mm c = 4.62° d = 33.04°

a, b, c and d are the magnitudes of displacement and rotation in the control case. The actual magnitude for other cases can be determined by multiplying the ratio with the actual response in control case.

Case I A
Control case
Δ_{max} = 210.80 mm
θ_{max} = 4.62°

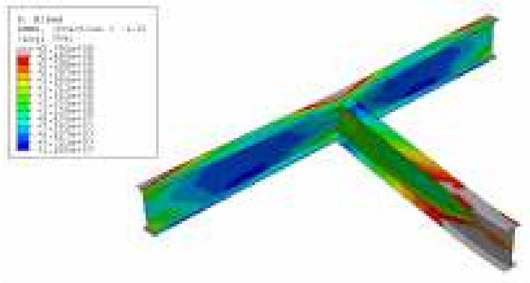

Case IB-2
Extended plates at joint increase stress on support beam
Δ_{max} = 209.14 mm
θ_{max} = 4.66°

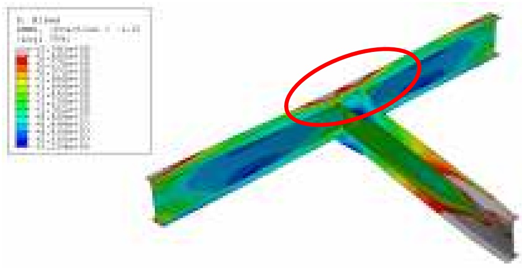

Case IC
Enlargement of flanges reduces and moves the yield areas away from the joint
Δ_{max} = 195.11 mm
θ_{max} = 4.36°

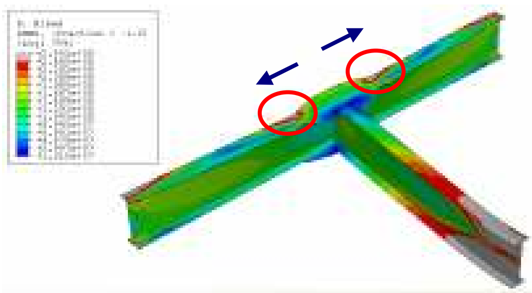

Case ID-2
Stress concentrates much more at middle span and gusset plate - pipe bracing
Δ_{max} = 94.14 mm
θ_{max} = 2.20°

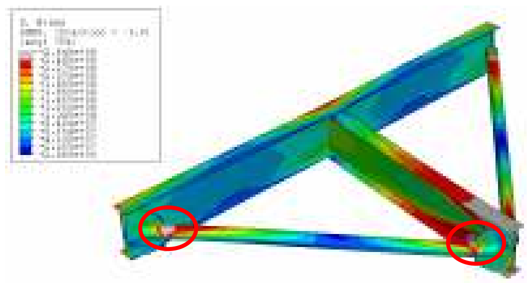

Figure 6.8
Case I - Stress contour at maximum deformation for 1 bar

6.4.2 Response of beam connection: Case II - with different depths.

Generally, under the same load magnitude, responses by structural components with different depths are lesser than structural components with equal depths because the supporting beam is much stiffer than the IPE 600 beam. The summary of deformations is tabulated in Table 6.4 while Figures 6.9 and 6.10 show distribution of stress contour along the structural members.

With haunch at the support to make up the depth difference reduces displacement at the mid-span with an average from 5.6 percent to 8.0 percent at 1 bar compared to control case IIA with only stiffener plates. However, at 2 bar, the deformation is observed as slightly higher from 4.4 percent to 14.4 percent. The shorter haunch with tapered ratio of 1:1 showed lesser displacement at 1 bar but higher displacement at 2 bar compared with the longer haunch with tapered ratio of 1:4.

In terms of ductility ratio, both case IIB and case IIC show higher values at the end spans by 12.5 percent and 8.5 percent respectively, compared to case IIA. In the middle span, case IIB-1 (with extended bottom flange), ductility ratio increases by 3.8 percent while cases IIB-2, IIC-1 and IIC-2 ductility ratio reduces with an average of 5.8 percent.

This anomaly can be explained by the variation of sectional properties along the beam. At overpressure 1 bar, for steep and short distance haunch, the drastic change of sectional properties occurs close to the support. Therefore, almost all sections along the beam will resist blast load equally, which results in less deflection. On the other hand, for less steep and longer distance haunch, the change of sectional properties is gradual and occupies almost a quarter of the span length. As the weakest section is the middle span, much more deformations are expected to occur and concentrate at the middle span rather than other positions along the beam.

At overpressure 2 bar, the deformation along the beam with shorter haunch (same cross-section) is quite extensive compared with the beam with longer haunch (varies cross-section), thus the deformation for the shorter haunch is much more than the deformation for the longer haunch. A similar behaviour is also observed when the redundant bottom flange is removed.

Having a single brace connected between the middle span and the support, at 1 bar the middle span displacements are reduced with averages of 9.1 percent and 15.5 percent while at 2 bar the averages are 4.8 percent and 6.9 percent for case IID and case IIE respectively.
With double diagonal braces, a substantial amount of reduction is noticed similar to the equal depth case I with double braces. The average reductions are 34.6 percent and 38.1 percent at 1 bar, and 49.8 percent and 50.3 percent at 2 bar.

For case IID-1, single brace induces unbalanced torsional moment therefore higher rotation and displacement compared with case IID-2, IIE-1 and IIE-2. While ductility ratio of case IID-1 is the highest at the mid span among the connections with braces, case IIE-1 has the highest ductility ratio at the end span. This can be explained by the yielding of some elements as the end span for case IID-1 which is weaker and less stiffer than case IIE (refer Figure 6.10). Generally, the average reductions with braces are 11.4 percent and 36.5 percent at 1 bar, and 5.1 percent and 50.2 percent at 2 bar for end span and middle span respectively.

Comparing case I (equal depth) and case II (different depth), although the overall performance improves significantly in case II because the support is much stiffer and stronger, the percentage of reduction is more or less equal in both cases except for the cases with braces. This proves that shortening the load path, while at same time allowing deformation on new structural members (tubular) which are initially not included in the original design, remarkably improves the performance of beam to beam connection.

Table 6.4

Case II (different depths) - The response and ductility ratio

Case	Normalised Response				Ductility			
	Mid span deflection		End span rotation		Middle span		End span	
	1 bar	2 bar	1 bar	2 bar	1 bar	2 bar	1 bar	2 bar
IIA (Control Case)	1.000[a]	1.000[b]	1.000[c]	1.000[d]	3.85	52.48	2.53	34.09
IIB-1	0.944	1.003	0.913	0.945	3.91	56.58	2.86	39.86
IIB-2	0.939	1.044	0.913	0.982	3.79	57.54	2.83	40.96
IIC-1	0.924	1.099	0.913	1.026	3.56	57.84	2.67	40.44
IIC-2	0.920	1.144	0.907	1.042	3.53	59.88	2.56	39.65
IID-1	0.909	0.952	0.920	0.948	3.53	50.39	2.18	30.24
IID-2	0.654	0.502	0.702	0.528	2.51	26.31	1.95	19.76
IIE-1	0.845	0.931	0.863	0.918	3.29	49.22	2.53	36.18
IIE-2	0.619	0.497	0.652	0.506	2.38	26.01	1.78	18.59

a = 69.06mm   b = 942.08mm   c = 1.61°   d = 21.68°

a, b, c and d are the magnitudes of displacement and rotation in the control case. The actual magnitude for other cases can be determined by multiplying the ratio with the actual response in the control case.

Case II A

Control case, with single bottom stiffener and no haunch

Δ_{max} = 69.06 mm

θ_{max} = 1.61°

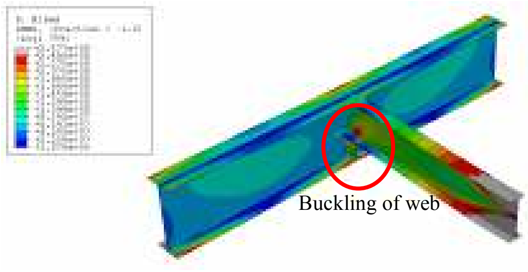

Case IIB-1

Haunch tapered 1: 4 and extended bottom flange

Δ_{max} = 65.16 mm

θ_{max} = 1.47°

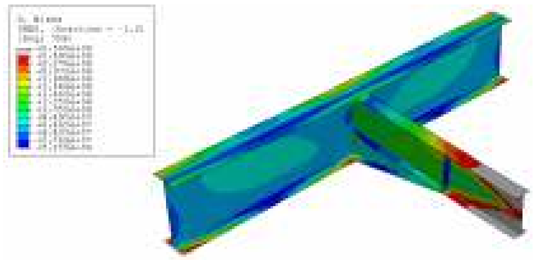

Case IIB-2

Haunch tapered 1:4 and removed bottom flange

Δ_{max} = 64.82 mm

θ_{max} = 1.47°

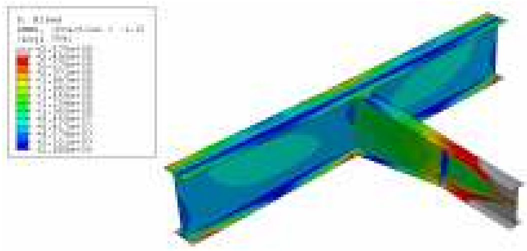

Case IIC-1

Haunch tapered 1:1 and extended bottom flange

Δ_{max} = 63.78 mm

θ_{max} = 1.46°

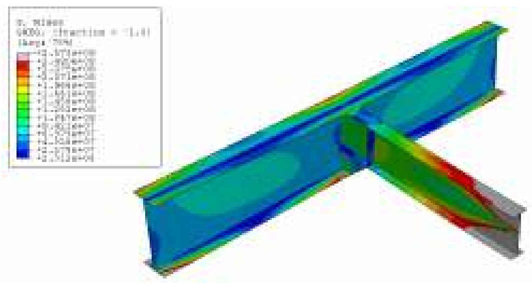

Case IIC-2

Haunch tapered 1:1 and removed bottom flange

Δ_{max} = 63.49 mm

θ_{max} = 1.46°

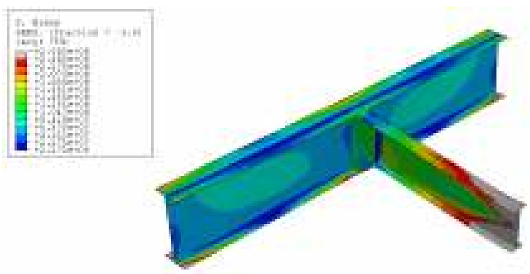

Figure 6.9

Case II -Stress contour at maximum deformation for 1 bar (part 1)

Case IID -1

Control IIA with a single diagonal brace

Δ_{max} = 58.37 mm

θ_{max} = 1.39°

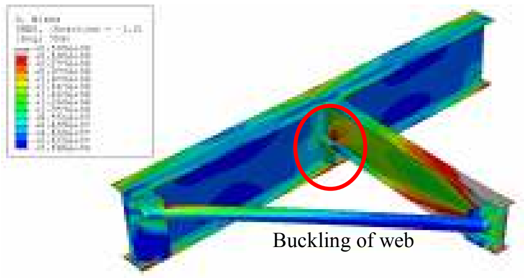

Case I1D-2

Control case IIA with double diagonal braces

Δ_{max} = 42.77 mm

θ_{max} = 1.05°

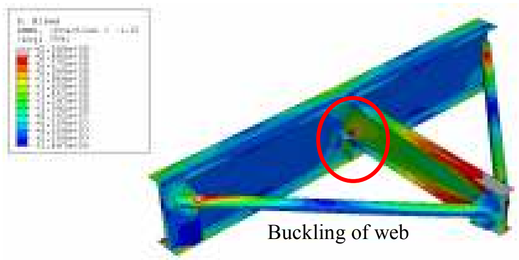

Case IIE-1

Case IIC-2 and a single diagonal brace

Δ_{max} = 62.77 mm

θ_{max} = 1.48°

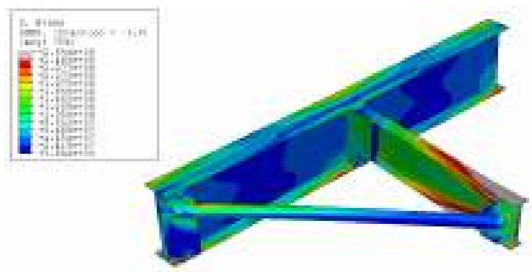

Case IIE-2

Haunch tapered 1:1 and extended bottom flange

Δ_{max} = 45.17 mm

θ_{max} = 1.13°

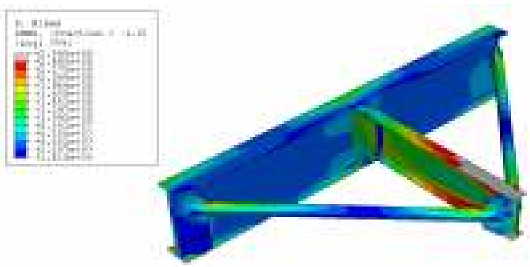

Figure 6.10

Case II -Stress contour at maximum deformation for 1 bar (part 2)

6.4.3 The distribution of stress and strain for the analysed connection models

The maximum stress and strain at selected critical points of the modelled beam and plate girder are monitored and tabulated in Tables 6.5 and 6.6. The stress and strain are extracted from the analyses with 1 bar. At each of the selected points, strain rate is plotted to correlate with ductility ratios calculated in sections 6.4.1 (case with equal depth) and 6.4.2 (case with different depth).

6.4.3.1 Case I - connection with equal depth

As can been seen from Figures 6.8 and Table 6.4, generally the connection with a pair of diagonal braces (case ID-2) shows a reduction of stress and strain at all selected points compared with control case IA.

At the connection between beam and beam, the most significant improvement is observed for case IC with flange extension on both sides in which stresses are reduced by 28.5 percent on the support beam and 36.0 percent at the end span. However, stress concentration on the support beam with maximum value of 250 MPa is observed to occur immediately at which the added flange plates are terminated. Despite having the lowest stress and strain at the connection, case IC has the highest stress and strain at the support (position 1). This can be explained by the fact that the stiffer joint carries more loads than the weaker joint.

Case IB (plates are added only at end span side) relatively shows a small amount of improvement with a less than average 6 percent compared to case IIA, except at the end span by 37.5 percent because the end span is much stiffer and can transfer more moments to support the beam.

In terms of strain rate as shown by Figure 6.12, case ID-2 shows the most stable and smooth plotted curves. However, the lowest strain rate is observed for case ID-1 (with single brace) that can be explained by graph 6.11 The graph shows case ID-1 has the higher strain than case ID-2 after 50 ms. At 15 ms, case ID-2 rises rapidly and reaches a plateau at 35 ms while case ID-1 rises steadily and reaches a plateau at 45 ms. By having a single brace connected to the middle span, it creates additional torsional moment. The torsional moment is then shared by the beam and the gusset plate where deformation is spread to a large area in the middle span. However, with double braces, deformation is shared by two gusset plates and the middle portion of I beam. As the gusset plates are in symmetry, deformation is more likely to be restricted at the middle span hence the load is transferred to supports more efficiently compared to case ID-1. This results in lower strain but higher strain rate in case ID-2.

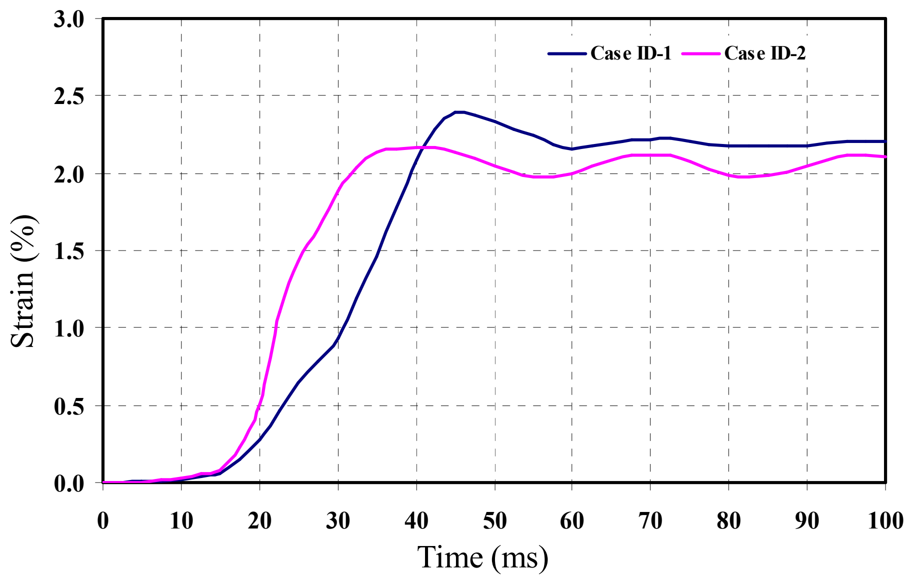

Figure 6.11

History of strain for case ID with diagonal brace(s)

Steep gradient for double diagonal braces

6.4.3.2 Case II –connection with different depths

With the haunch at the end span of IP 600 beam increases stiffness and hence significantly reduces stress and strain as shown by case IIB and IIC in Table 6.6 compared with case IIA. Despite the average reduction for stress being 47.8 percent at position 2B, the strains at positions 2A and 1 have increased by an average of more than 100 percent than case IIA.

In the middle span, the connection with haunch at position 3 shows insignificant reduction of stress with an average of 2 percent less than case IIA. Reduction of strain at the plate girder support (position 1) is expected and gives better results than case I because of a bigger cross section than IP 600.

For single braces in cases IID-1 and IIE-1 which are similar to case ID-1, the end support is found to experience higher strain because the presence of torsional moment as explained for the case with equal depth. The overall performance amongst the studied connections, case IIE-2 shows the best result compared with all the considered cases.

In terms of strain rates, case IIB-1 (Figure 6.13- (b)) longer haunch with extended bottom flange has the highest strain rate at almost all locations and behaves erratically compared with other considered cases. This is due to the fact that with longer haunch and extended bottom flanges, the beam has a stronger section than other structural members. Therefore, many section elements are still below yield and behaving elastically during the blast period.
Case IID-1 and case IIE-1 (single brace) show the lowest strain rate (Figure 6.13 – (f) and (h), and likewise case ID-1 with same depth as was discussed in section 6.4.3.1.

From the discussed results, it can be summarised that although the performance of the connection with haunch is better than without haunch, having double braces without haunch provides better results than with haunch. When the slope of the haunch is too gentle, the strengthened member becomes very stiff and deformation concentrates locally at the weaker section of the middle span. In terms of ductility ratio, the difference is not significant compared with the shorter haunch especially at the end span. Therefore, the choice of having a haunch for strengthening against blast load should be given careful consideration. Strengthening with longer haunch not only significantly increases stiffness at the joint but also could attract new additional loads. On the other hand, connection with double braces proves to provide better performance whether without haunch or with haunch as exhibited by case IID-2 and IIE-2.

Table 6.5

Case I (equal depth) - The maximum stress and strain

Location / Case	1 Strain %	1 Stress MPa	2A Strain %	2A Stress MPa	2B Strain %	2B Stress MPa	3 Strain %	3 Stress MPa
IA	0.31	249.4	0.16	248.8	0.00	170.6	4.09	292.5
IB-1	0.31	249.4	0.39	250.1	0.00	102.9	3.32	269.2
IB-2	0.27	243.0	0.44	250.6	0.00	110.2	3.43	280.5
IC	0.51	250.9	0.00	178.0*	0.00	79.0	3.80	288.8
ID-1	0.13	248.6	0.37	249.9	0.00	187.5	4.28	301.5
ID-2	0.10	248.2	0.04	248.0	0.00	89.0	2.60	268.0

Note :
* after the extended flange plate PEEQ= 0.43, VMS = 250.3 MPa

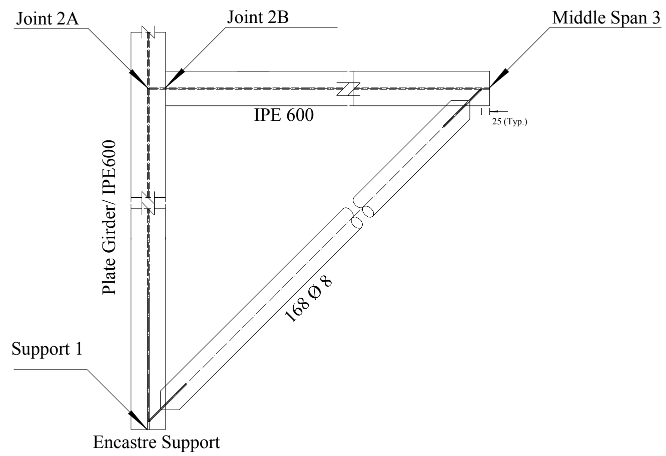

The selected positions

Table 6.6

Case II (different depths) - The maximum stress and strain

Location	1		2A		2B		3		Web at 2B	
Case	**Strain %**	**Stress MPa**	**Strain %**	**Stress MPa**	**Strain %**	**Stress MPa**	**Strain %**	**Stress MPa**	**Strain %**	**Stress MPa**
IIA	0.10	248.2	0.04	240.0	0.06	248.3	1.62	257.2	0.05	248.3*
IIB-1	0.16	249.3	0.09	248.5	0.00	118.0	1.50	256.4	-	-
IIB-2	0.19	249.4	0.23	249.3	0.00	143.8	1.67	257.4	-	-
IIC-1	0.24	249.3	0.17	248.6	0.00	133.4	1.60	256.9	-	-
IIC-2	0.23	249.2	0.22	249.3	0.00	122.7	1.57	257.0	-	-
IID-1	0.17	249.0	0.06	248.3	0.00	227.4	1.70	257.1	0.04	247.9*
IID-2	0.09	248.5	0.00	219.4	0.00	77.4	1.52	256.7	0.02	246.3*
IIE-1	0.18	249.0	0.04	248.2	0.00	177.1	1.47	256.4	-	-
IIE-2	0.08	248.1	0.00	207.1	0.00	74.5	1.34	255.9	-	-

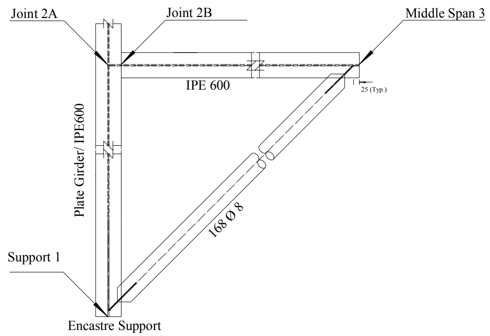

The selected positions

*** Cases IIA and IID without haunch**

Web at the bottom flange with higher stress because bending moment is transferred through a small area on the stiffener. See Figures 6.9 and 6.10.

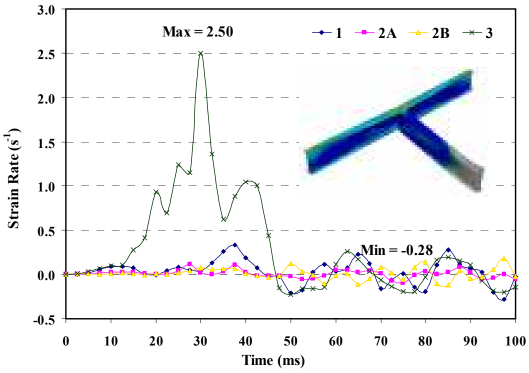

a. Case IA

Control case

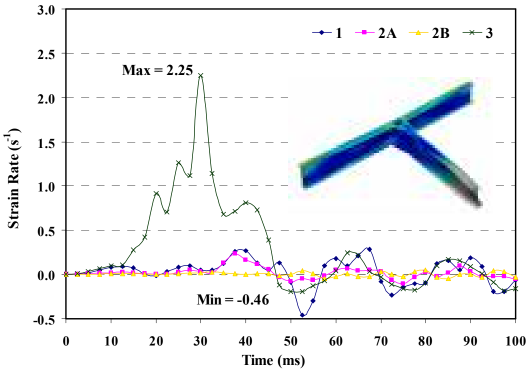

b. Case IB-1

Extended plates with cope holes

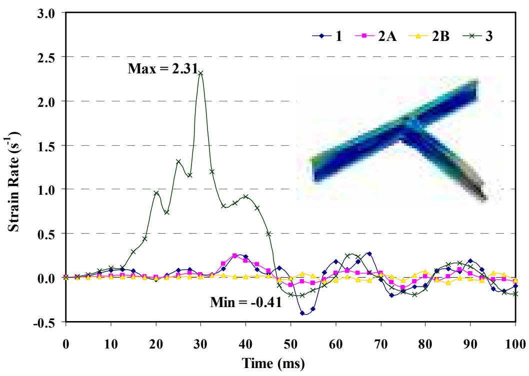

c. Case IB2

Extended plates without cope holes

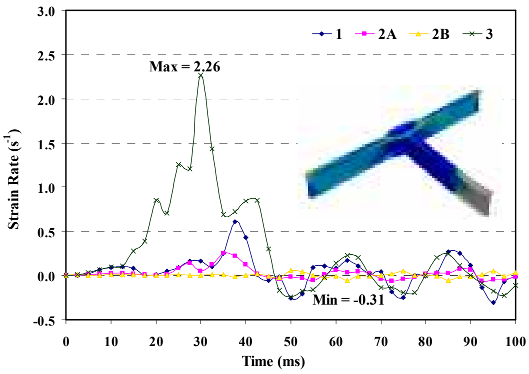

d. Case IC-1

Extended flanges at the support beam

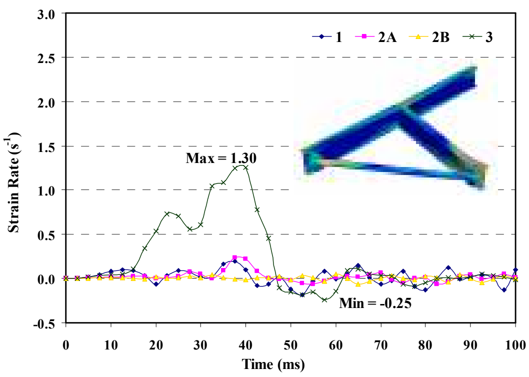

e. Case ID-1

Case IA with a single diagonal brace

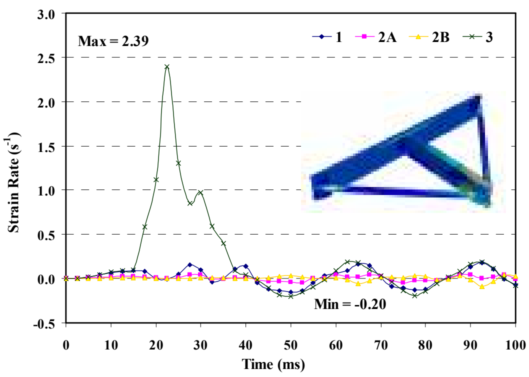

f. Case ID-2

Case IA with a pair of diagonal braces

Figure 6.12

History of strain rate for case I

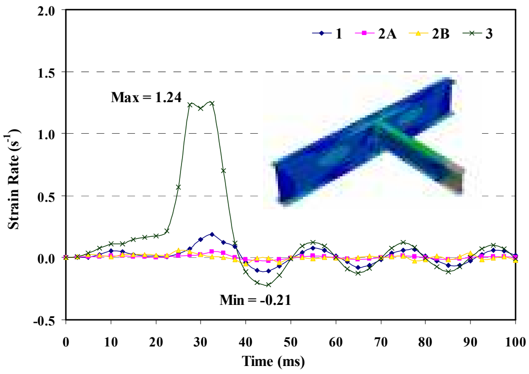

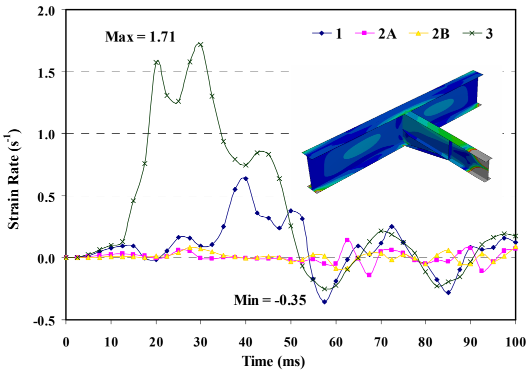

a. Case IIA

Control case

b. Case IIB-1

Tapered haunch 1:4

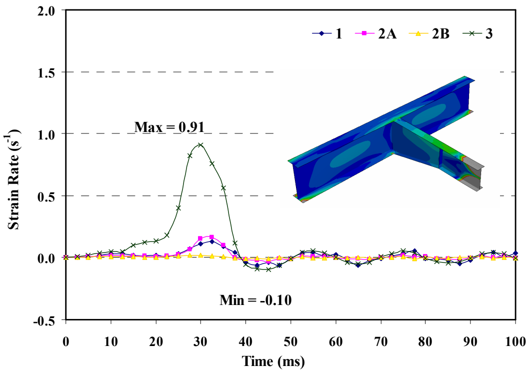

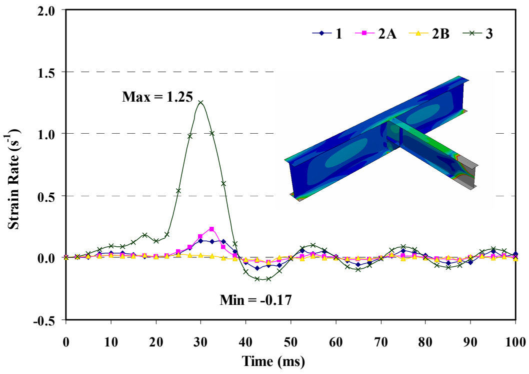

c. Case IIB-2

Tapered haunch 1:4, removed bottom flange

d. Case IIC-1

Tapered haunch 1:1

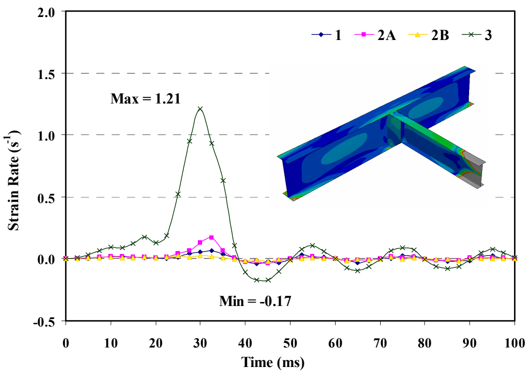

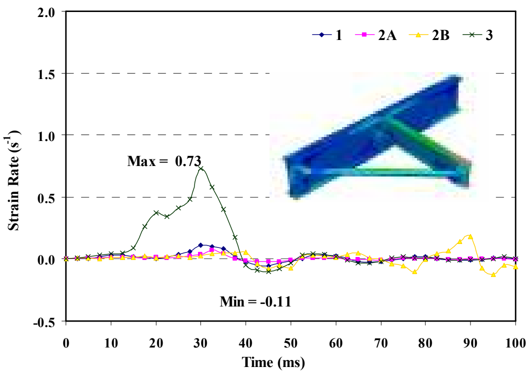

e. Case IIC-2

Tapered haunch 1:1, removed bottom flange

f. Case IID-1

Case II-A with single diagonal brace

Figure 6.13

History of strain rate for case II (Part 1)

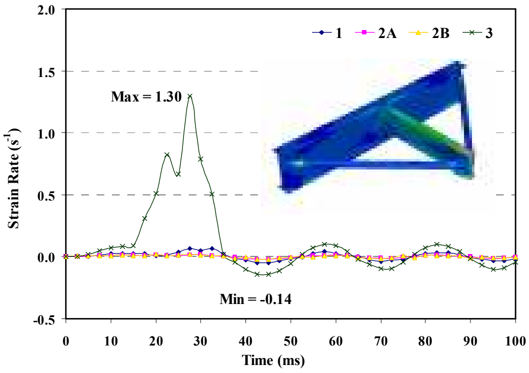

g. **Case IID-2**

Case IIA with a pair of diagonal braces

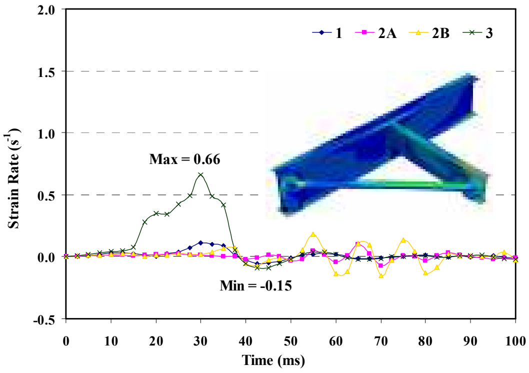

h. Case IIE-1

Case IIC-2 with a single diagonal brace

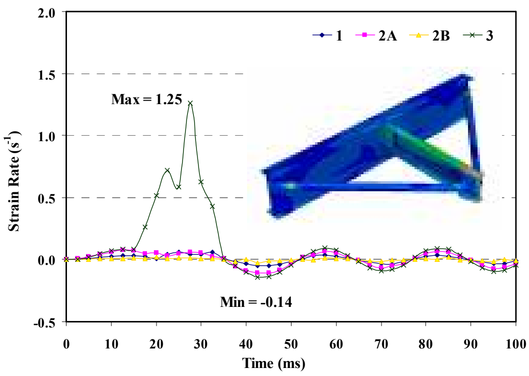

i. Case IIE-2

Case IIC-2 with a pair of diagonal braces

Figure 6.13

History of strain rate for case II (Part 2)

6.5 The development of an ABAQUS topside structure model with horizontal diagonal braces

To demonstrate the effectiveness of horizontal diagonal bracings for improving beam to beam connection on the topside, the topside ABAQUS model which was developed for the original case discussed in chapter five is incorporated with four diagonal braces of 168 mm ø 8 mm thick and 13 mm thick plate of 600 mm width as gusset stiffener plates at each deck level. The gusset plates are slotted through the tubular centreline by a distance of 500 mm. A gap of 50 mm between structural members is adopted while an offset of 500 mm from the bottom of the deck plate to the centre of tubular is implemented to clear IP 300 stringer beams. With stiffness less than IP 300 (comparison of second moment of inertia: 168 ø, I_{xx} = 1290 cm^4, IP 300, I_{xx} = 8356 cm^4), theoretically tubular braces are expected to suffer more deformation than other structural members. All new steels used in the model are set to mild steel (F_y = 248 MPa). The placement of braces on the deck level and its justification are summarised as follows:

Brace B1- Connects the middle span plate girder PG 1000 to vertical support tubular 508 mm ø for reducing displacement at the middle deck

Brace B2 - For shortening the load travel path along PG 1000 and for transferring some loads to support tubular 508 mm ø. The brace also acts as backup for incoming B4 on the far side as well as for balancing incoming B3.

Brace B3 - The function of this brace is similar to B2 for shortening the load travel path as well as sharing the load to inclined tubular 508 ø. On the lower level, the brace will improve the stability at the corner between plate girders PG 1600-2 and PG 1600-1 which has no support.

Brace B4 - Connects the middle span of plate girders PG 1600-2 to PG 1000 for improving connection at the end span of plate girder PG 1000.

All braces can be considered in pairs at the meeting points; B1 and B2 braces at support of tubular 508 mm ø, B2 and B3 braces at a quarter span of plate girder PG 1000 towards north, B3 and B4 braces are at the same meeting point of B2 and B3 while the other ends are connected to plate girder PG 1600-2.

a. The upper Level

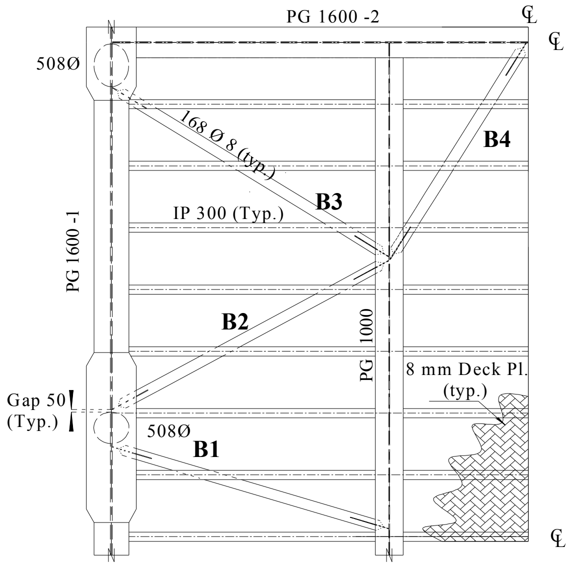

168 ø braces are offset 500 mm below deck level for clearance against IP 300 beams.

b. The ABAQUS topside model

(For clarity of the horizontal diagonal braces, the instance of deck plates is suppressed)

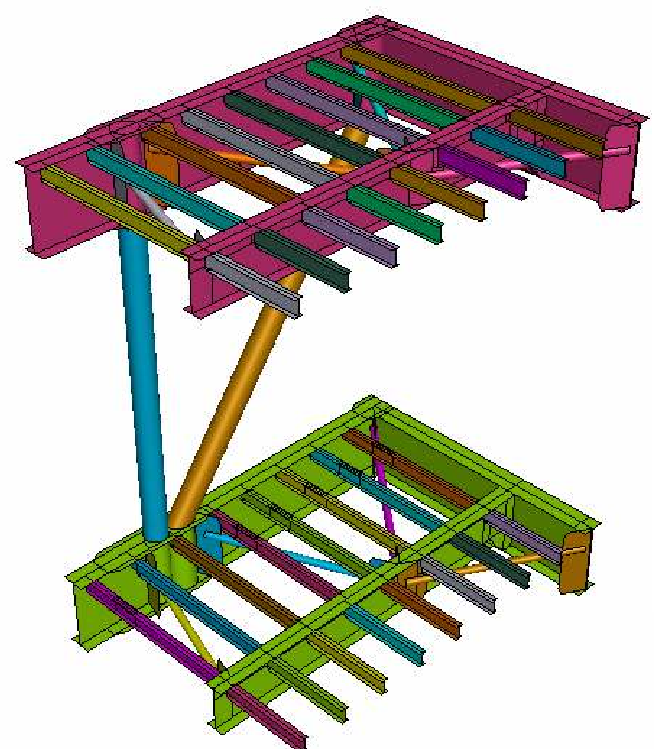

c. The lower Level

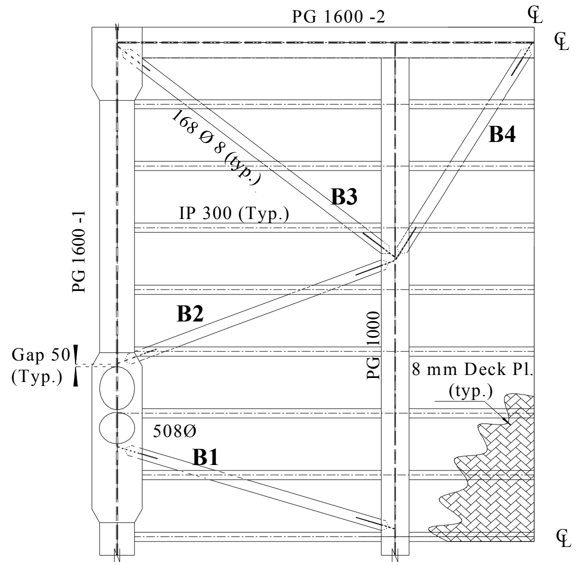

168 ø braces are offset 500 mm below deck level for clearance against IP 300 beams.

Figure 6.14

Topside structure with horizontal tubular bracings

The revised structural arrangement with new braces is shown by Figure 6.14. From the drawing, it is worthwhile noting that each brace connection should have an extended wing plate for effective spread of loads. As the effect of stress concentration is localised and the present study emphasizes improving global performance of primary members at the connection, this detail is not updated in the present ABAQUS model.

To compare with the original case, a similar magnitude of blast loading will be applied to the topside with the maximum blast load equal to 2.5 bar. The result of the new model with horizontal diagonal braces will be marked as "(b)" throughout this chapter.

6.5.1 The overall global response of topside structure

As can been seen from Figure 6.15, the overall global displacement in the present model is much lower than the original case. At pressure 0.5 bar and below, the difference is not significant as most structural members are still elastic with maximum percentage of 14.6 and 10.4 for the upper level and the lower level, respectively. When the pressure is increased above 0.5 bar, the average reductions of displacement are 33.26 percent and 14.36 percent for the upper level and lower level, respectively. Although these reductions are much higher and give a better result than the strengthened case with angles (7.5 percent), the proposed mitigation required more careful planning as the placing of diagonal braces under the deck level is not straightforward. The braces may potentially clash with the existing piping lines.

As can also been seen from Figure 6.16, the distribution of deformation where the braces are installed are quite uniform and widely spread within the area along the structural members, especially for elements from the middle span of plate girder PG 1000 to the intersection joint of braces B2, B3 and B4.

It is also observed that the responses of IP 300 beams in this model are akin to the original case whereby stringer beams are found mostly overstressed and overstrained at supports with sniped bottom flanges. The behaviour and response of IP 300 beams are not the interest of the present study because it has been discussed reasonably in chapter five.

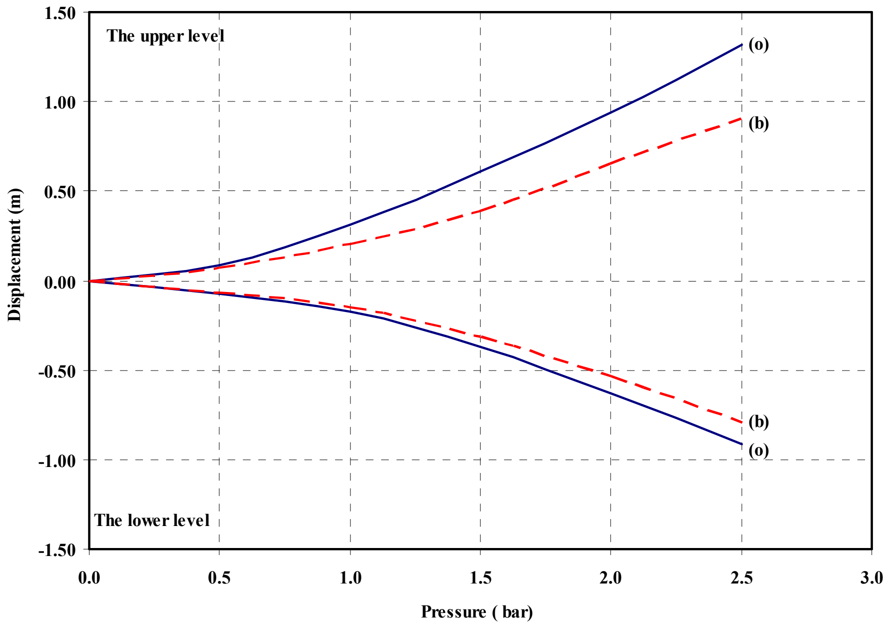

Figure 6.15

Maximum global displacement at middle span PG 1000

(o)— original case (b) ----- with bracings

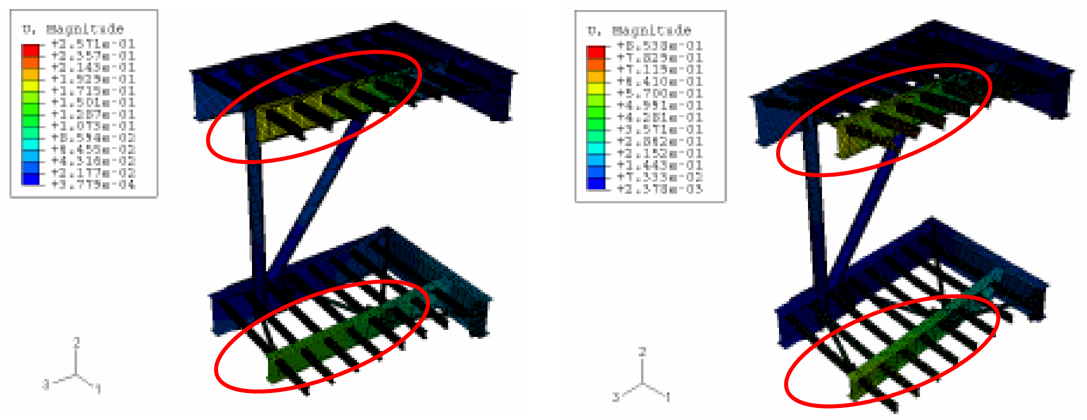

a. 1.0 bar **b. 2.0 bar**

Denotes uniform deformation is restricted between the braces.

Figure 6.16

The topside responses at 1.0 bar and 2.0 bar

(the deck plates are suppressed for clarity of other structural members)

As no strengthening is made at the support, the normalised ductility ratio from chapter five is also applicable in the present study and will be used to justify the performance of the topside in section 6.7

6.5.2 Primary member plate girder PG 1000

Table 6.7 summarises the maximum stress and strain of elements at four control points. The most overstressed elements on this structural member are the elements near the vicinity where new braces are joined (joint/ 4m from support). This is due to the fact that the location is initially part of the plate girder and is not designed to become a connection which must be given serious attention if new structural members are to be added. The stressed elements are found to be concentrated at the edge of flanges where gusset plates of braces are welded to the plate girder.

Table 6.7
PG 1000 Maximum stress and strain (Topside structure with bracings)

	Location/Pressure (bar)	0.5	1.0	1.5	2.0	2.5
	Upper level					
Stress	Middle span	328.17	352.99	351.24	399.26	487.63
MPa	Joint/ 4m fr. support	518.00	507.33	518.54	518.54	518.54
	Haunch	344.50	354.67	392.07	444.12	473.72
	End span	322.96	352.21	347.55	360.34	355.60
	Upper level					
Strain	Middle span	0.00	1.68	1.87	5.56	9.80
%	Joint/ 4m fr. support	4.23	18.40	43.33	71.63	51.16
	Haunch	0.36	1.98	5.20	7.49	9.33
	End span	0.02	0.70	0.80	2.52	2.46
	Lower level					
LL	Middle span	345.90	347.28	343.92	358.09	360.81
Stress	Joint/ 4m fr. support	345.06	346.68	345.30	345.95	346.82
MPa	Haunch	350.37	444.71	512.44	518.54	518.54
	End span	312.50	346.60	353.55	361.49	362.90
	Lower Level					
Strain	Middle span	0.15	0.47	0.01	1.20	2.54
%	Joint/ 4m fr. support	0.00	0.41	0.20	0.26	0.39
	Haunch	0.80	9.32	11.40	14.23	12.70
	End span	0.00	0.48	1.40	2.40	3.60

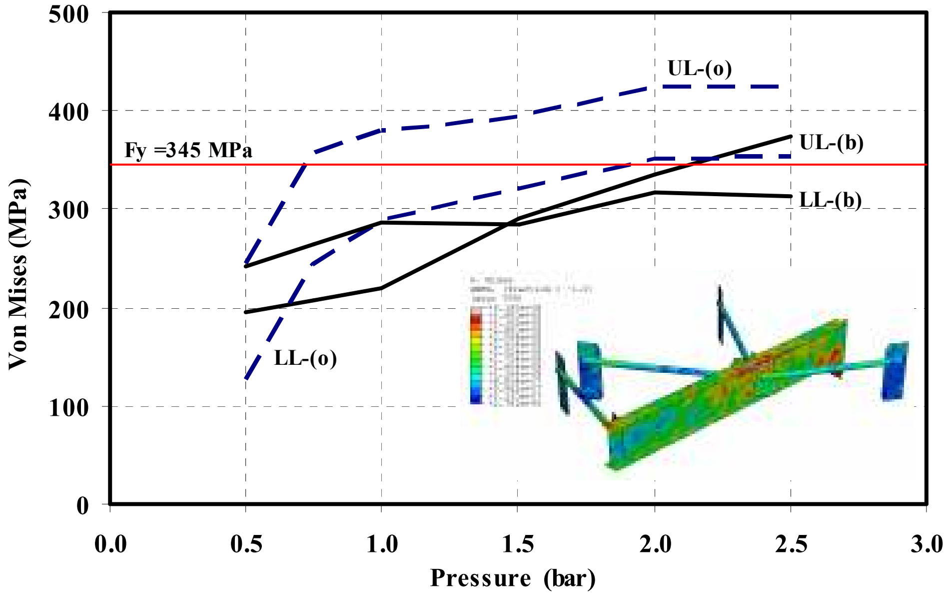

a. The middle span

(The stress contour shown is for the upper level at 1 bar)

“o” denotes the original case while ‘’b” denotes the case with bracings

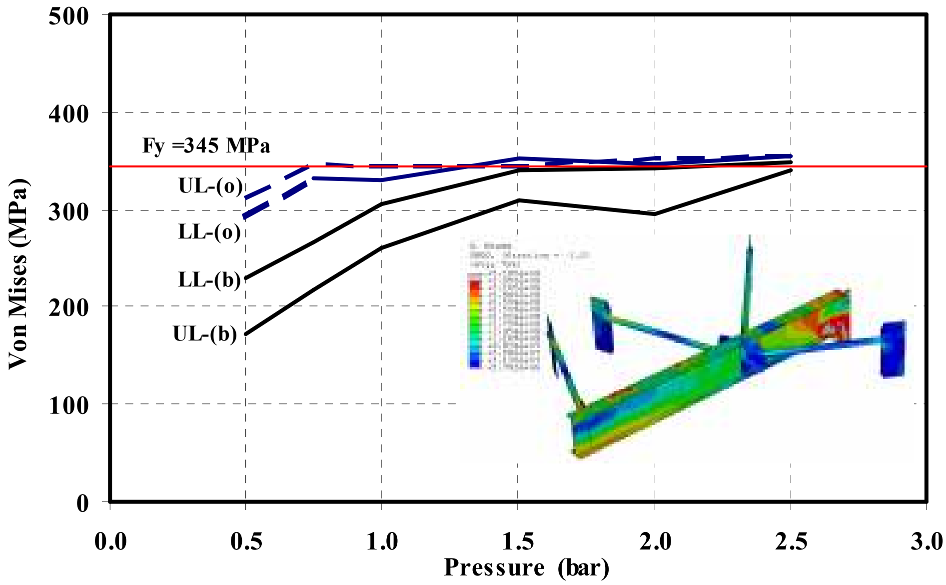

b. The end span

(The stress contour shown is for the lower level at 1bar)

“o” denotes the original case while ‘’b” denotes the case with bracings

Figure 6. 17

Plate girder PG 1000 Maximum average stress across the section

Nevertheless, having bracings shows a marked reduction in displacement as well as the average maximum stress as shown by Figure 6.17.

When the stress and strain values in Table 6.7 (with bracings) are compared to Table 5.4 (the original case and the strengthened case with angles), on the upper level the improvement is observed at many positions except at the new joint, which is 4 m from the end support where braces B2, B3 and B4 intersect. On the lower level, similar responses are also observed at the new joint but a significant reduction at the end span. All responses are dependent on load direction, load travel path and support location, many of which were discussed in chapter five.

Although horizontal bracings manage to reduce displacement by shortening load travel path and sharing some load in terms of axial, the behaviour mode exhibited by the plate girder resembles the original case and the strengthened case. This is based on the fact that the maximum deformation is observed in the middle span, while the existence of stress concentration is still occurring at the haunch. Thus, the finding can be used to justify the current in-place operating condition of topside structure is not affected if new braces are to be installed on the topside.

6.5.3 Primary member plate girder PG 1600-2

As was highlighted in chapter five, because the plate girder is an intermediate support with minimum exposure to blast loading, the status of its response is dependent on the reaction of plate girders PG 1600-1 and PG 1000. Having brace ‘b3’ connected between the end span to plate girder PG 1000 remarkably reduces both stress and strain at the end span as tabulated in Table 6.8 compared with the original case. This gives a good indication as damage on the main truss can be minimised. However, the presence of brace ‘b4’ to balance brace ‘b3’ that connects the middle span to plate girder PG 1000 has carried some deformation loads from plate girder PG 1000 to plate girder PG 1600-2 causes an increase of stress and strain in the middle span and at the joint of incoming plate girder PG 1000.

Table 6.8

PG 1600-2 Maximum stress and strain (Topside structure with bracings)

	Location/ Pressure (bar)	0.5	1.0	1.5	2.0	2.5
	The upper level					
Stress	Bottom Web end span[a]	91.50	146.58	192.88	250.31	312.88
(MPa)	Top Web end span[a]	273.93	303.144	334.70	337.74	345.32
	Bottom flange at joint[c]	253.88	346.97	351.38	359.12	357.75
	Top flange at joint[c]	319.02	365.58	347.17	354.77	360.20
	Bottom web at mid span[c]	265.66	345.00	345.57	347.70	347.82
	Top web at mid span[c]	187.61	338.67	329.43	332.43	343.79
	The upper level					
Strain	Bottom Web end span[a]	0.00	0.00	0.00	0.00	0.00
(%)	Top Web end span[a]	0.00	0.00	0.00	0.04	1.23
	Bottom flange at joint[c]	0.00	0.15	1.16	2.50	4.58
	Top flange at joint[c]	0.00	3.40	0.07	1.47	2.30
	Bottom web at mid span[c]	0.00	0.02	0.14	0.67	0.77
	Top web at mid span[c]	0.00	0.00	0.00	0.04	0.1
	The lower Level					
Stress	Bottom Web end span[b]	83.41	148.15	161.86	180.35	190.02
(MPa)	Top Web end span[b]	153.07	325.23	372.67	479.09	518.54
	Bottom flange at joint[c]	319.24	346.50	349.74	354.20	357.37
	Top flange at joint[c]	343.78	348.78	359.70	370.19	420.43
	Bottom web at mid span[c]	235.54	346.20	349.46	351.72	353.22
	Top web at mid span[c]	198.62	336.90	347.12	348.87	349.85
	The lower level					
Strain	Bottom Web end span[b]	0.00	0.00	0.00	0.00	0.00
(%)	Top Web end span[b]	0.00	0.00	4.17	10.25	13.32
	Bottom flange at joint[c]	0.00	0.18	0.76	1.43	1.86
	Top flange at joint[c]	0.00	1.80	2.27	4.12	6.38
	Bottom web at mid span[c]	0.00	0.25	0.70	1.07	1.31
	Top web at mid span[c]	0.00	0.00	0.03	0.69	0.84

Note

[a] – Significant reduction in terms of stress and strain as a result of load sharing

[b] – No diagonal support at end span but is influenced by both plate girders PG 1000 and PG 1600 at higher load above 1.0 bar.

[c]- At 1.0 bar and above, the strain is higher than the original and strengthened cases due to load sharing with plate girder PG 1000.

As can been seen in Figure 6.18, the end span shows the lowest average stress compared with the middle span and the joint to plate girder PG 1000 for the upper level and the lower level. It is also worth noting that on the upper level, the middle span has the highest average stress while on the lower level the highest stress is exhibited by the joint to plate girder PG 1000. This behaviour is due to there being no direct support at the end span on the lower level. With the introduction of tubular braces, deformations experienced by plate girders PG 1600-1 and PG 1000 are stabilized with some loads being transferred to plate girder PG 1600-2. Therefore, it can be summarised that placement of bracings should not only be based on strong points but also the availability of load paths en route to direct supports should also be accounted for. Often, designers may opt for similar structural configuration to facilitate fabrication for every deck level. However, lack of understanding during the period of blast and misjudgement of brace positions will unintentionally weaken the existing structural members instead of improving the connection.

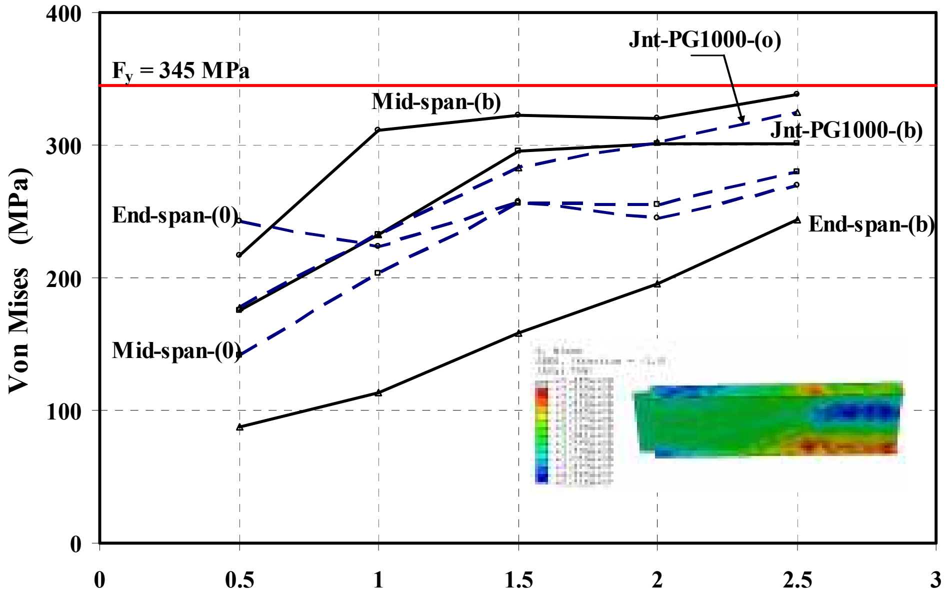

a. The upper level

(The stress contour shown on the plate girder is at 1 bar)

"o" denotes the original case while ''b" denotes the case with bracings

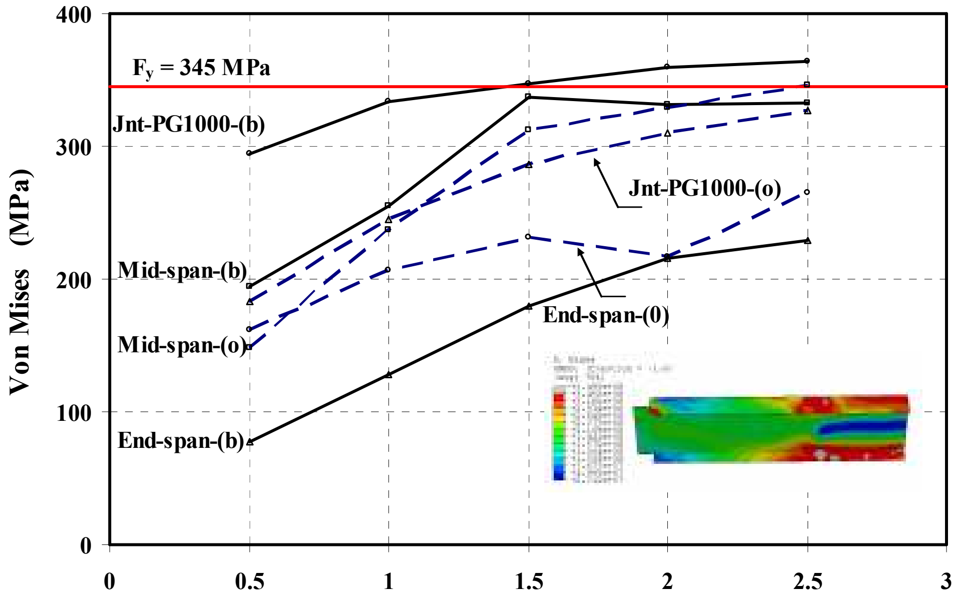

b. The lower level

(The stress contour shown on the plate girder is at 1 bar)

"o" denotes the original case while ''b" denotes the case with bracings

Figure 6.18

Plate girder PG 1600-2 Maximum average stress across the section

6.5.4 Primary member plate girder PG 1600-1

From Table 6.9, there is a significant stress difference between the top flange and the bottom flange of the plate girder compared with the original case, especially on the upper level. The substantial stress build-up can be explained by braces being welded to the plate girder which are in tension in order to maintain the stability as the middle deck area and plate girder PG 1000 are displaced upwards. At the same instance, top flanges of stringer beams and deck plates at connections to the plate girder are also in tension, which worsens the situation. Therefore, a highly localised stress concentration in the flange of PG 1600-1 is observed to which the diagonal braces are welded, as shown by Figure 6.8.

Table 6.9

PG 1600-1 Maximum stress and stress (Topside structure with bracings)

	Location/Pressure (bar)	**0.5**	**1.0**	**1.5**	**2.0**	**2.5**
	The upper level					
Stress	508Bottom flange	40.80	102.616	290.32	129.20	221.72
(MPa)	508 Top flange	484.39	518.53	518.54	464.29	518.54
	End span bottom flange	71.98	112.67	147.70	286.61	321.27
	End span top flange	190.59	347.07	298.22	304.18	338.94
	The upper level					
Strain	508Bottom flange	0.00	0.00	0.00	0.00	0.00
(%)	508 Top flange	16.12	29.70	21.95	22.21	26.443
	End span bottom flange	0.00	0.00	0.00	0.00	0.00
	End span top flange	0.00	3.36	0.01	0.00	0.07
	The lower level					
Stress	508Bottom flange	105.84	180.35	205.76	243.09	251.47
(MPa)	508 Top flange	134.76	342.06	345.19	338.83	345.57
	End span bottom flange	177.92	333.56	343.12	289.26	345.60
	End span top flange	317.83	415.38	349.31	439.03	513.75
	The lower level					
Strain	508Bottom flange	0.00	0.00	0.00	0.00	0.00
(%)	508 Top flange	0.00	0.00	0.00	0.04	0.00
	End span bottom flange	0.00	0.00	0.04	0.00	0.11
	End span top flange	0.00	8.30	3.24	8.38	12.42

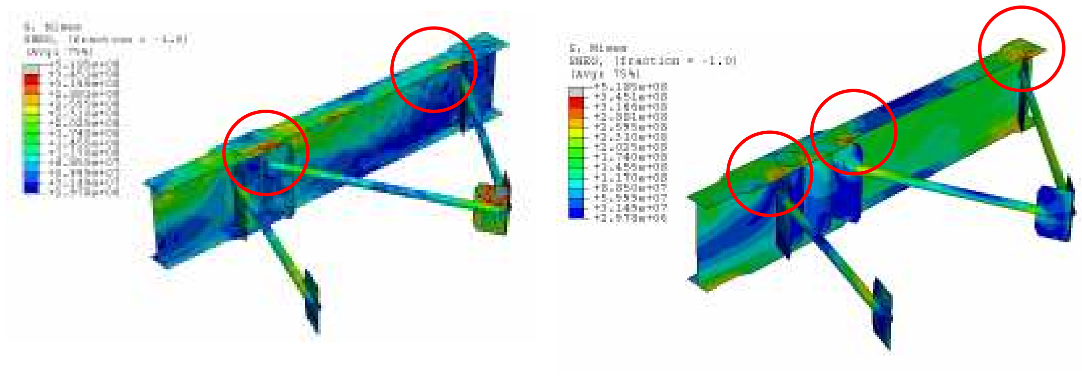

a. The upper level **b. The lower level**

- Localised overstressed

Figure 6.19

PG 1600-1 The distribution of stress contour at 1.0 bar

As can be seen from Figure 6.20, although the average of maximum stresses for the model with tubular bracings is below the yield limit, most stresses are much higher than the original case. This is caused by tubular horizontal bracings, which carry some loads during deformation of plate girder PG 1000 to supports. The effect reduces the stress on plate girder PG 1000 (Figure 6.17) while at the same time increases the stress on plate girder PG 1600.

Between the deck levels, the upper level has lower average stress compared with the lower level. It is also observed that although high stress is anticipated in tubular bracings, the behaviour mode at selected critical positions on the plate girder is almost like the original case. Thus, similar to plate girder PG 1000, the effect of having bracings for improving connection can be concluded to have relatively minimal contribution to stiffness in the plate girder itself.

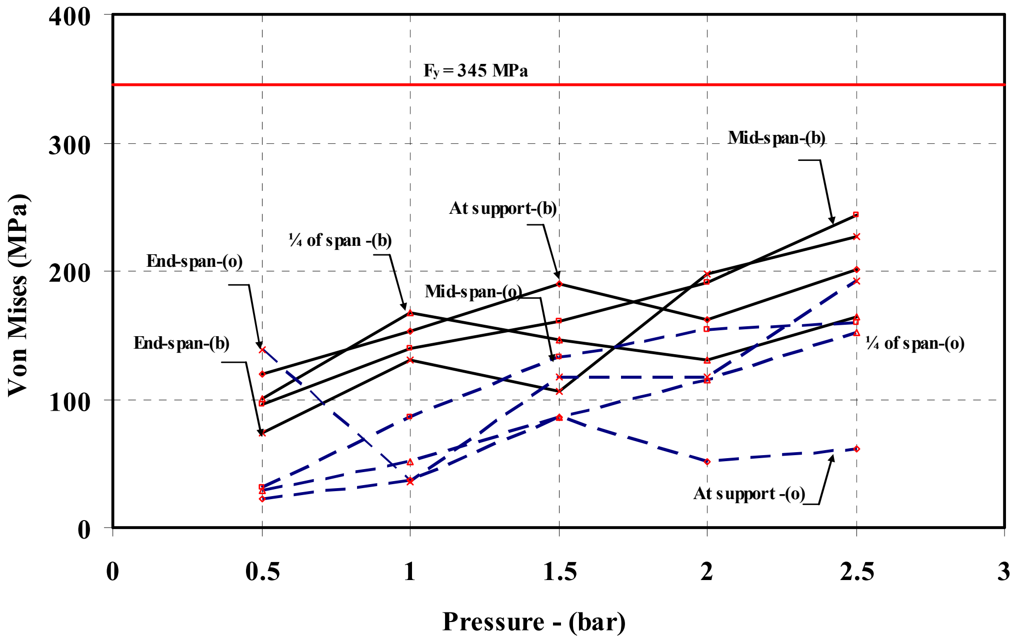

a. The upper level

"o" denotes the original case while ''b" denotes the case with bracings

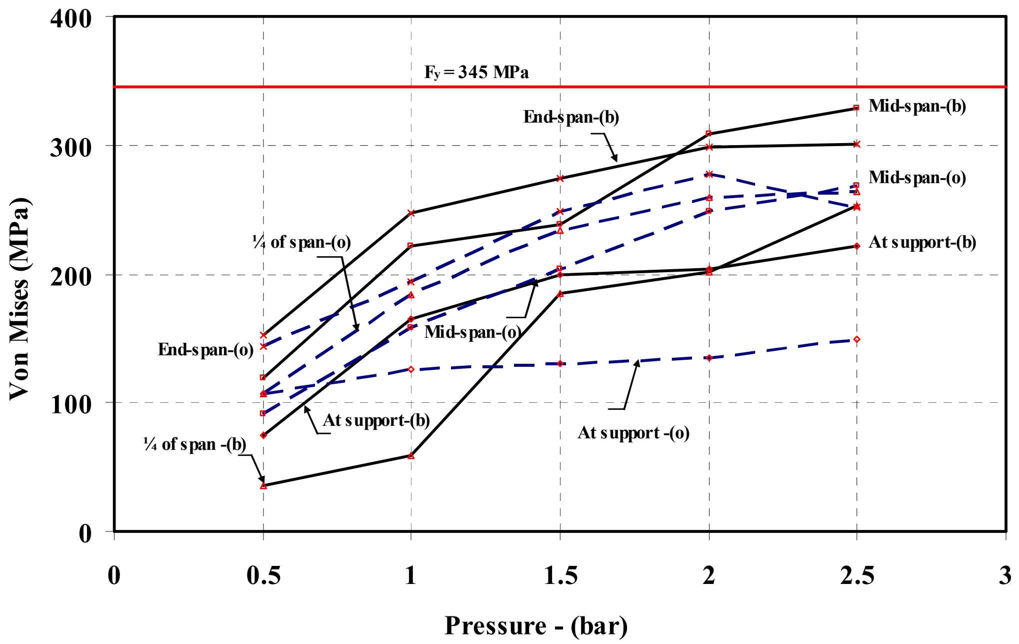

b. The lower level

"o" denotes the original case while ''b" denotes the case with bracings

Figure 6. 20

PG 1600-1 Maximum average stress across the section

6.6 Ductility ratios of primary members

Table 6.10 lists the ductility ratios which can be used to describe the performance of structural components while Table 6.11 summarises the damage level which can be used to evaluate the global performance of the topside. Most selected control points show a significant reduction compared with the original case, while there is no case that the damage level has exceeded 20 for all primary members. The finding asserts that placement of diagonal horizontal braces improves connections on the deck as well as the topside global performance.

Table 6.10

Ductility ratios of primary structural components

(PG 1000, PG 1600-1, PG 1600-2)

Pressure (bar) **Locations**	**0.5**	**1.0**	**1.5**	**2.0**	**2.5**
PG 1000					
UL- mid span	0.823	2.291	4.306	7.317	10.144
LL- mid span	0.725	1.679	3.506	6.000	8.822
UL- end span	0.605	2.273	2.241	4.728	9.560
LL- end span	0.633	3.075	6.633	9.824	14.800
UL -¼ span (4m from joint)	0.744	1.890	2.211	6.088	8.851
LL -¼ span (4m from joint)	0.785	1.780	1.951	5.763	8.411
PG-1600-1					
UL- end span	0.494	0.899	1.272	2.079	3.714
LL- end span	0.752	1.429	1.943	4.250	7.331
UL- support 508 ø	1.106	3.460	2.615	4.096	7.243
LL- support 508 ø	0.583	1.104	1.262	1.714	2.344
UL- ¼ of span	2.105	3.860	5.194	7.576	11.654
LL – ¼ of span	1.750	3.594	4.849	6.550	8.004
PG1600-2					
UL- end span	0.059	0.613	0.124	0.171	0.389
LL- end span	0.056	0.246	0.281	0.564	0.834
UL-mid span UL	0.704	0.858	1.223	1.507	2.828
LL- mid span LL	0.812	1.528	1.278	3.296	5.668

For purposes of comparison, Table 5.10 in chapter five will be used as a reference to assess the performance of primary structural members. The summary of the comparison is listed as follows:

Plate girder PG 1000

At 0.5 bar in the present study with bracings, the average ductility ratio of below unity indicates that on average the plate girder PG 1000 is still elastic and approximately 17.7 percent less to reach yield based on the highest ductility ratio in the middle span of the upper level. Hence, major repair work is not required. On the other hand, in the original case, the plate girder is moderately damaged (highest μ = 3.44). The strengthened case with angles is 14.5 percent less than the original case.

At 1.0 bar, moderately damage level is observed at end span (highest μ = 3.075) in the present study with bracings. While in the original case (highest μ = 12.48) as well as the strengthened case at mid span (μ = 10.12) ductility ratios have surpassed damage level 6, the end span of the strengthened case is still intact (μ = 4.33). Repair in the present study may not be required but inspection at the end span should be carried out to assess the extent of damage.

At 1.5 bar, extensive damage for both the original case and the strengthened with angles but in the present study with bracings major repair is required only for the end span on the lower level (μ = 6.63).

At 2.0 bar and above, total collapse and beyond repair are anticipated for the original case and the strengthened case with angles, however the present study with bracing is about 26 percent to collapse.

Gas Explosion Handbook [11], stated that most equipment is expected to severely damage at 1.4 bar. At 1.5 bar only the end span of the lower level has marginally surpassed damage level of 6 while other control points are below 5. Therefore, it can be concluded that supports for equipment are still intact meaning this increases the safety level as hazard caused by support failure has been minimised.

PG 1600-2

The loads experienced by plate girder PG 1600-2 are originally blast loads from plate girder

PG 1000 and plate girder PG 1600-1. Having two pairs of diagonal braces placed on the deck framings enormously reduces loads on the plate girder thus significantly increases capacity against blast load. On average, the end span of plate girder for both the upper level and the lower level are elastic up to 2.5 bar in the present study with tubular bracings while in the original case and the strengthened case, ductility ratios have surpassed the damage level of 6 at 2.0 bar. From 1.0 bar to 1.5 bar, the middle span is expected to suffer minimum damage as average ductility ratios remain below 2 (highest μ =1.278). At 2.5 bar, likewise the end span, ductility ratio remains below 6 but quite close to the realm of severe damage.

Similar to plate girder PG 1000, by having simple tubular bracings across the plate girders, unnecessary damage to structural members not exposed to blast load can be averted as well as the potential collapse scenario of the whole structure.

Plate Girder PG 1600-1

Comparing the ductility ratio at 2.5 bar, neither the present study with bracings nor the strengthened case with angles has exceeded damage level 20. In the original case, only the end span of plate girder has exceeded 20.

While all ductility ratios in the strengthened case remain below 10 up to 2.5 bar, only a single position in the present study with braces i.e. at one quarter span on the upper lever has exceeded damage level 10. In addition, these points both on the upper level and the lower level of PG 1600-1 are the two only control points which have shown an increase of ductility ratios higher than ductility ratios in the original case and the strengthened case with angles. As shown in Figure 6.20, the middle area between the two supports experiences higher stress compared to the original case although ductility ratios at the supports reduce significantly. Factors that contribute to this response can be explained by the offset distance of braces to supports and centreline of PG 1600-1, and the combination of loads from plate girder PG 1000. In the original case and the strengthened case, the loads are transferred from one beam to another through a connection. However, in the present study with diagonal braces, some loads are shared between main primary structural components i.e. plate girders PG 1600-1 and PG 1000 (discussed earlier for plate girder 1600-2).

Table 6.11

Damage level 6 and 20 (Topside structure with bracings)

Primary structural components	μ = 6		μ = 20	
	Pressure	**PEEQ**	**Pressure**	**PEEQ**
PG 1000 (ε_{cr} = 18.25)				
UL- mid span	1.78	2.57	> 2.50	*5.28
LL- mid span	2.00	1.95	> 2.50	*2.05
UL- end span	2.13	0.75	> 2.50	*1.46
LL- end span	1.41	0.76	> 2.50	*2.56
UL -¼ span (4m from joint)	1.99	2.63	> 2.50	*16.50
LL -¼ span (4m from joint)	2.05	2.05	> 2.50	*2.64
PG-1600-1 (ε_{cr} = 28.00)				
UL- end span	> 2.50	0.02	> 2.50	*0.02
LL- end span	2.28	0.19	> 2.50	*0.22
UL- support 508 ø	2.30	0.20	> 2.50	*4.50
LL- support 508 ø	> 2.50	0.13	> 2.50	*0.13
UL- mid span	1.67	0.91	> 2.50	*2.02
LL - mid span	1.84	2.38	> 2.50	*2.34
PG1600-2 (ε_{cr} =21.50)				
UL- end span	> 2.50	0.00	> 2.50	*0.00
LL- end span	> 2.50	0.10	> 2.50	*0.10
UL-mid span	>2.50	0.30	> 2.50	*0.30
LL- mid span	>2.50	0.64	> 2.50	*0.64

Notes
> 2.50 denotes pressure is greater than 2.50 bar
* denotes the strain is based on pressure at 2.50 bar.

Thus, plate girder PG 1600-2 in the present model, which is not exposed to blast load but acts as an intermediate support, will experience less load compared to the original case. This behaviour can also be used to explain why a significant reduction of ductility ratios is observed at the end span of PG 1600-2 at both deck levels that remain below unity even at 2.5 bar. The introduction of offset is unavoidable in the present ABAQUS model especially for the existing topside structure as there is a number of existing components scattered on the deck to be avoided from clashing with structural members. Large offset distance from centreline causes eccentricity which imposes additional torsional moment on the plate girder. Hence, the combination of these two effects will increase deformation as well as ductility ratio in the middle span.

6.7 Defining the global performance level of the topside structure

Applying performance based design methodology as discussed in chapter three, and comparing with the result of chapter five (section 5.12.2) the revised performance levels of the topside with horizontal braces based upon the ductility of main primary members are summarised as follows:

Performance level	Case with horizontal tubular bracings
Functionality 0.5 bar	All primary members are intact. Operation can continue as normal and platform shutdown is not required. No repair work is expected.
Operational 1.0 bar	All primary members are intact. Operation can continue as normal and platform shutdown is not required. No repair work is expected on primary members. Inspection is required to assess damage in the middle of PG 1600-1 (μ = 3.86). **Note :** At this load level, based on the original case without angle strengthening, replacement of secondary structural members IP 300 is required.
Safety 1.5 bar	Primary members are expected to damage moderately. Temporary platform shut down is

	required to access the PG 1600-1 and PG 1000 probably with some minor repairs. Safety passage can be guaranteed if IP 300 beams are strengthened with angles.
<u>Near collapse</u> 2.0 bar	PG 1000 is 51 percent to collapse and PG 1600-1 is 62 percent to collapse while PG 1600-2 is moderately damaged
<u>Total Collapse</u> 2.5 bar	No total collapse is expected as all primary members have ductility ratios less than 20. However, severe deformation at the intersection of braces (μ = 16.50, average plastic strain = 16.50 percent) on plate girder PG 1000.

6.8 Concluding remarks

The consequence of mitigation to improve structural connections against blast loading should be carefully studied. Designers should broaden the scope of design by noting the effect of secondary structural components. The proposed mitigation probably works satisfactory as a single component. However, when it is combined with the responses of other structural members, the effects may cause them to perform appallingly from their original condition.

The findings in this chapter are listed as follows:

a. **<u>Diagonal brace for improving beam to beam connection</u>**

With proper placement of diagonal braces on the structural framing plan, ductility ratios at the connections of plate girders PG 1000 and PG 1600-2 have improved significantly and are able to sustain higher overpressure loads from 0.82 bar (the original case) and 1.08 bar (the strengthened case with angles) to 1.41 bar on the lower level and 2.13 bar and on the upper level at damage level 6.

While ductility ratios on most members show a significant reduction, stresses of the main supporting plate girder PG 1600-1 increase significantly due to offset distance from the main support points. Offset distances are sometimes unavoidable on existing structures because there a number of equipment or structural members to be cleared from obstructions and impacts during the blast period.

The ideal case for placing braces is to have a pair of braces at mitigation point so that it eliminates additional torsional moment at connections as a result of imbalance forces.

For a case with different depth, brace offsets shall be adjusted to match the centrelines of both structural members instead of using a single reference line of the least depth. This effect has been illustrated by the responses of plate girders PG 1000 to PG 1600-1 where one end of the brace was adjusted to match the centreline of plate girder PG 1000 while the other was offset upward 300 mm from the centreline of PG 1600-1. Although this was a simplified fabrication detail and installation method, more loads were attracted to the top flange compared with the bottom flange. Combining this impact with sniped bottom flange encourages local stress concentration to form on primary members.

b. <u>The effect of secondary members</u>

When the analysis is performed separately under blast conditions, it has been shown that ignoring secondary members such as deck plates and stringer beams will lead to a scenario in which some behaviours of main primary member are overlooked and the shortcomings are not fully apprehended for further study. Severe localised flange distortion due to stress concentration is observed on the beam, at which gusset and stringer beams are welded in the new model, whereas in the simple model severe responses are only noticed at support and middle span. The concentration of overstressed on the gusset plate can be overcome by having short angles welded both side of the gusset plate to plate girder for efficient load distribution as being demonstrated with sniped bottom flange.

c. <u>The extension of wing plate or the enlargement of plate at the end span</u>

For a beam to beam connection, the extension of wing plate on the support beam is recommended as not only yielding is relocated away from the connection but also it is able to reduce the out-plane moment. Having additional plates welded to end span relocates yield away from the connection similar to column to beam connection, however the method is unable to reduce the out plane moment on the support beam.

d. <u>The choice cope hole or no cope hole.</u>

The modelled cope hole size is 20 mm in radius, a typical size implemented during fabrication for full access of welding which can be left as it is. The effect of having cope holes on the structural performance is found to be insignificant in the present study. However, further study is required to determine the optimum size to account for the effect for other loads such from pre and in-service conditions.

e. <u>The haunch detailing</u>

Under blast condition, a shorter haunch will experience greater rotation at the end span but less displacement while longer a haunch will experience less rotation at the end span but greater displacement in the middle span. The choice of the haunch in design must be balanced with the cost of fabrication as well as the weight of the topside.

It has been highlighted in chapter five that a haunch could be devised for a mechanism which could prevent further damage to the support. A gentle slope, such as 1: 4, can be considered conservative as it requires high load to deform the transition point to yield before the end span can be saved. A steep slope such as 1:1, the yield at transition is too close to the end span as has been demonstrated in the present model and also the original model. For optimum design, it is recommended the haunch slope 1:2 is the lower bound and 1: 3 as the upper bound limits.

It is common practice that the haunch is fabricated from the cut of the same beam. Therefore, the bottom flange of the haunch is extended up to the face of the plate girder face. No welding at the interface is performed to avoid distortion on the web of the support member. However, for a newly fabricated plate girder, the bottom flange should not be extended to minimise welding and a weight increase. It has also been shown that having neither an extended bottom flange closer to neither the connection, nor a totally removed flange can improve ductility ratio. However, it is worth noting that the disadvantage of having an extended bottom flange encourages stress concentration to occur at the tip where the flange is terminated. The behaviour has been demonstrated by case IIA, case IIB-1 and case IIC-1.

Chapter Seven

Inventories on the Topside Structure

7.1 Introduction and typical inventories

Topside structures consist of two main components: inventories and structural components. The inventories are supported and they occupy spaces provided by structural members. The proportion of inventories for a typical topside structure is approximately in the range of 45 to 60 percent of the total topside dry weight. The inventories can further be divided into a few main individual systems as follows:

a. Gas oil separation facilities – pumps, vessels, launchers, receivers etc.
b. Gas compression and injection facilities – compressors, vessels, electric motors, risers, heat exchangers, dryers, scrubbers, coolers etc.
c. Power generation distribution systems – generators, electrical cables, distribution boards, instrument bulks, electrical bulks etc.
d. Utility system - firewater pumps, control room, emergency power, life boat, lifting cranes, communication facilities storage etc.
e. Safety and protection system - blast barrier walls, emergency shut down valves, water deluge system etc.
f. Living quarters / helideck for workers' accommodation and helicopter landing-inclusive backup fuel storage, fire fighting system, potable water system, sewerage system etc.

All the aforementioned inventories are dependent upon the process plant. A full production and drilling platform at a remote location with a large reservoir capacity typically contains most facilities, while a platform located in a marginal field may just contain the very minimum of facilities whereby crude oil, gas and impurities from the reservoir are channelled through riser pipes to another platform with full facility or are pumped back to an onshore terminal for further processing.

Space and weight are two main issues in the design of offshore topside structures. These design constraints will determine the final cost and availability and whether the topside structure can be fabricated onshore, transported on an appropriate barge as well as the feasibility of being installed offshore.

As a result, most offshore platforms carry a large amount of equipment but it is held in a small and compact space as operators demand that they recoup their substantial investment in a very short period of time. Thus, this leads to congestion and confinement amongst inventories on the topside structure, which eventually increases the severity of damage should there be an explosion.

While others such as Scheler et al. (1991) and Medonos and Rogers (1998) have conducted research work modelled on the effect of blast based upon a very crude module model that included only main primary truss members, relatively very few have looked into a proper topside model with complete structural elements and inventories.

It is has been acknowledged in some studies that although smaller inventories on topside structures, for examples piping lines and cables, are less likely to experience a significant damage compared to major inventories such as vessels because of smaller surface areas, the impact of losing its supports due to drag loads will eliminate a few critical systems on the topside structure, such as the control and fire fighting system.

Therefore, the aim of the study presented in this chapter primarily concentrates on assessing responses of equipment with respect to the behaviour of structural components, so that a guideline can be established to assist engineers in legislating a procedure which is not only for protecting the equipment and improving structural integrity but also for reducing risk to personnel.

7.2 The ABAQUS model with equipment

Using the model developed in chapter five for a typical topside structure, the ABAQUS topside model is now extended to a bigger scale whereby the symmetry section on the south side in the original case (Figure 5.2) is now extended to another 8000 mm ,while the east side is extended to another 6000 mm. Hence, the analysed model covers an area of 16000 mm by 12000 mm on each deck level.

The extended plate girder PG 1000 is now supported by boxed girder BG 1600. On the east side of the platform, the structural configuration is similar to the original model however a new diagonal brace 610 mm ø is added to connect between the upper level and the lower level. Two deck legs 2000 mm ø with enlarged ring flanges at each of the deck levels on the south side are modelled to suit the incoming plate girders PG 1600-1 as well as the incoming diagonal braces 610 mm ø.

Figure 7.1 shows the new deck framing for the upper level and the lower level. The stringer beams IP 300 with sniped bottom flanges are spaced at 1000 mm apart. Despite its weakness at the bottom flange, as was discussed in section five, the connection is adopted in the new model because this is a common detail for the topside.

Table 7.1 lists all new structural members added in the new ABAQUS model.

Table 7.1

New structural components for ABAQUS model with equipment

	Structural members	Size Depth x Width Thickness	Yield Strength (MPa)	Location
a.	Boxed girder BG 1600	1600 mm x 1200 mm t_f = 50 mm t_w = 30 mm	345	South side to support plate girders PG 1000
b.	Pipe 2000 mm ø	t = 40 mm	345	Deck legs
c.	Pipe 610 mm ø	t = 19 mm	345	Diagonal braces
d.	Channel C 100	100 mm x 40 mm t_f = 8 mm	248	Along the deck legs and below the upper deck. As supports and hangers for fire water pipes 114 mm ø
e.	Stiffeners for boxed girder BG 1600	1600 mm x 800 mm t = 30 mm	345	Backup for incoming plate girder PG 1000
f.	Flat bar	t = 3 mm	248	Hangers for cable trays

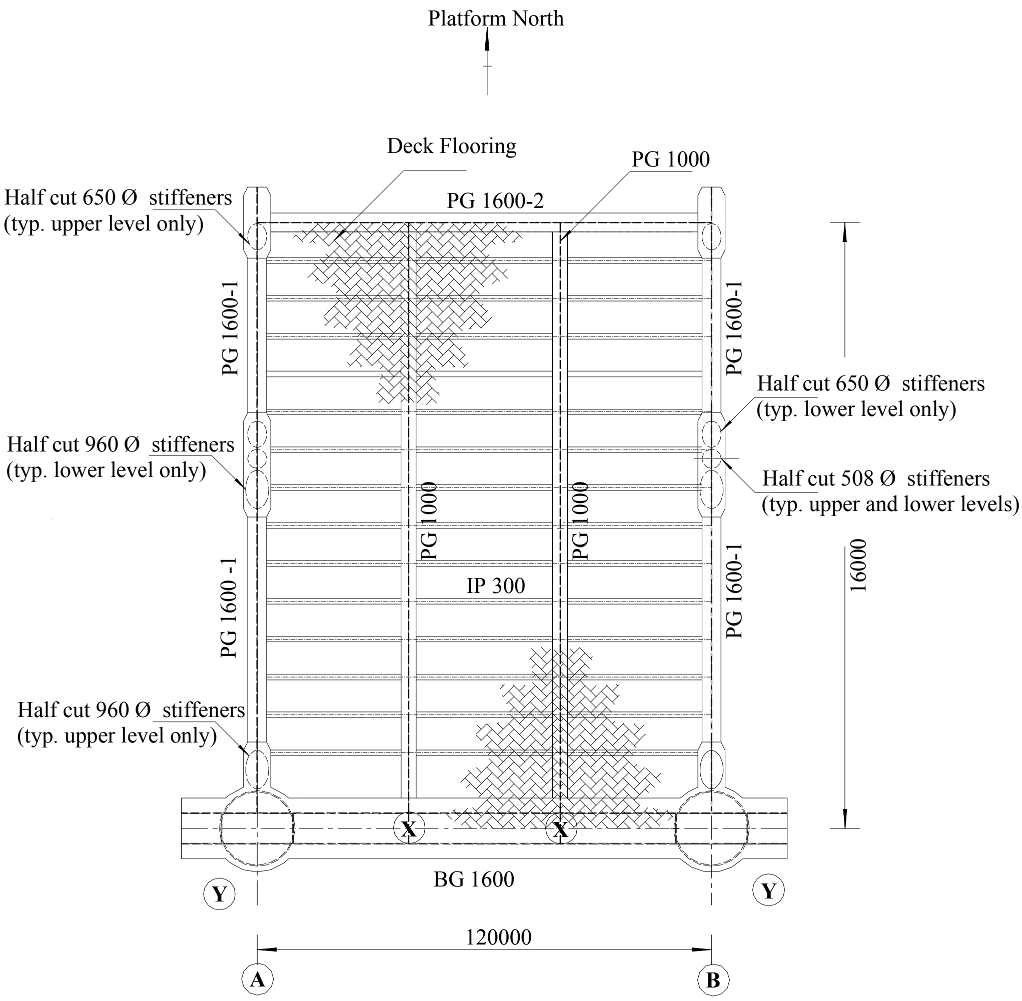

Figure 7.1

Topside deck framing plan

<u>Notes:</u>

The modelled deck area in the new ABAQUS model is 12000 mm x 16000 mm. All stiffeners for pipe bracings are made from 19 mm half cut pipes and placed exactly on the far side of brace foot prints.

X 30 mm thick flat plate stiffeners are provided for the incoming plate girder PG 1000 which inside the boxed girder BG 1600

Y A combination of two 30 mm thick flat plates and two cut of pipe 2000 ø mm are used as internal stiffeners inside the boxed girder at deck legs.

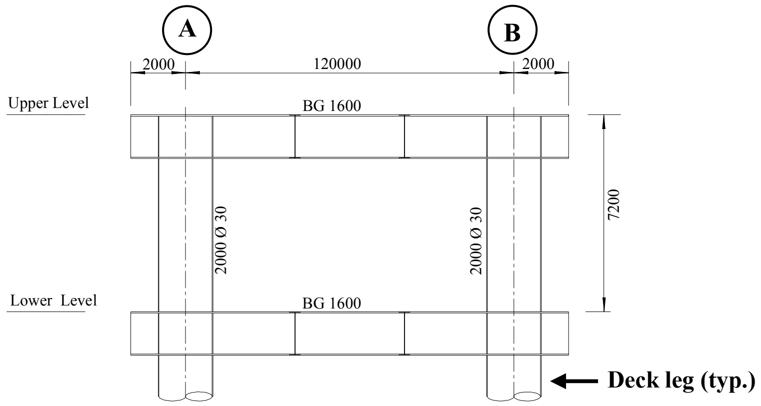

a. Looking towards north

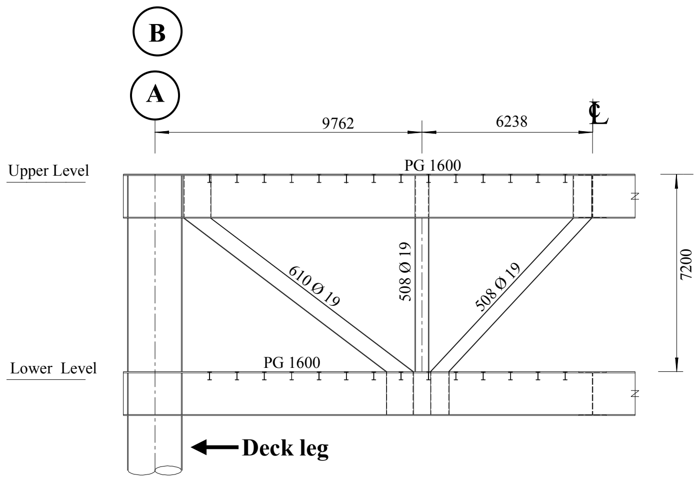

b. Looking towards east

Figure 7.2

Elevation framings

Notes

Gap of 50 mm is maintained between structural members.

The bottom portion of the deck legs are extended 2000 mm below the lower deck for supporting fire water lines and for specifying boundary conditions.

As shown by Figure 7.2, the new south side structural members are now a major truss consisting of boxed girders BG 1600 and deck legs 2000 mm ø. They are designed to be strong and robust members because the deck legs must remain elastic and absorb much more energy than any other structural members in order to prevent total collapse of the platform under all design load conditions.

Despite being available in various sizes, the shape of most equipment on the topside is equivalent to a cylinder. Therefore, in order to reduce the time taken to execute the analysis and to eliminate some constraints of computer usage, the modelling of equipment is selected based on surface area and height from the deck level. Large exposed surfaces attract more blast load while the higher the equipment from the deck level, a higher bending moment is expected to be generated at supports. Hence, only major equipment with a typical shape is adopted and no equipment skids are modelled. However, the equipment is adjusted so that its supports either directly sit on structural members or are hung below the deck level. A stool, which is an intermediate support, is provided under the equipment for better load distribution.

Table 7.2 provides details of the modelled equipment while Figures 7.3 and 7.4 show the location of equipment on the deck. Most major equipment is located on the lower level because it is well protected from environmental loadings and operational extreme loads. Hence, it is reasonable to assume that potential leaks or hydrocarbon explosions will be contained within this region

The placement of equipment on the deck level is arbitrarily assumed and indicative as long as there is no clash with existing structural members. Small fittings which are attached to the equipment are not modelled and it is assumed that these fittings will follow a similar response to the modelled equipment.

Table 7.2

The modelled equipment (inventories) on topside structure.

Equipment	Quantity	Location on the topside structure	Support conditions
Firewater lines 114 mm ø 5 mm	2	1200 mm below the deck upper level, 1200 mm towards the inner deck area of the east and west sides from row A and row B. Along the deck legs, 500 mm clearance is given between 114 mm ø pipes and deck legs.	C 100 channels hang pipes below the deck. Along deck legs, the pipes are cantilevered support. The channels are welded to deck stringer beams IP 300 and deck legs pipe 2000 mm ø. The pipes are assumed 75 percent full with sea water
Launcher and receiver, size 610 mm ø 12 mm thick., and 406 mm ø 12 mm thick., with transition cone.	1	On the lower level 1200 mm from row A of west side of the platform. The height is 550 mm from deck level to centreline of launcher/receiver.	The supports are adjusted to sit on two IP 300 stringer beams with stools to make up the height difference. It is assumed that the launcher and receiver are at 75 percent full with fluid.
Cable tray 600 mm wide and 200 mm height	2	1000 mm below the deck upper level, 550 mm from centreline of row A east and row B west.	Flat plate 3mm as hangers and welded to IP 300 stringer beams.
Vertical vessel 2000 mm ø x 4000 mm (high)	1	East side on the lower level, 3000 mm from row B and 4000 mm from plate girder PG 1600-2	Supported by three IP 300 stringer beams. Two more IP 300 cross beams are added in between the beams. The vessel is assumed 75 percent full with fluid.
Horizontal vessel 3000 mm ø x 6000 mm (long)	1	2500 mm form the centreline of the boxed girder (south side) and centre between plate girders PG 1000.	Sit on 2500 mm wide stools and welded to plate girders PG 1000 on the deck lower level. The vessel is assumed 75 percent full with fluid.

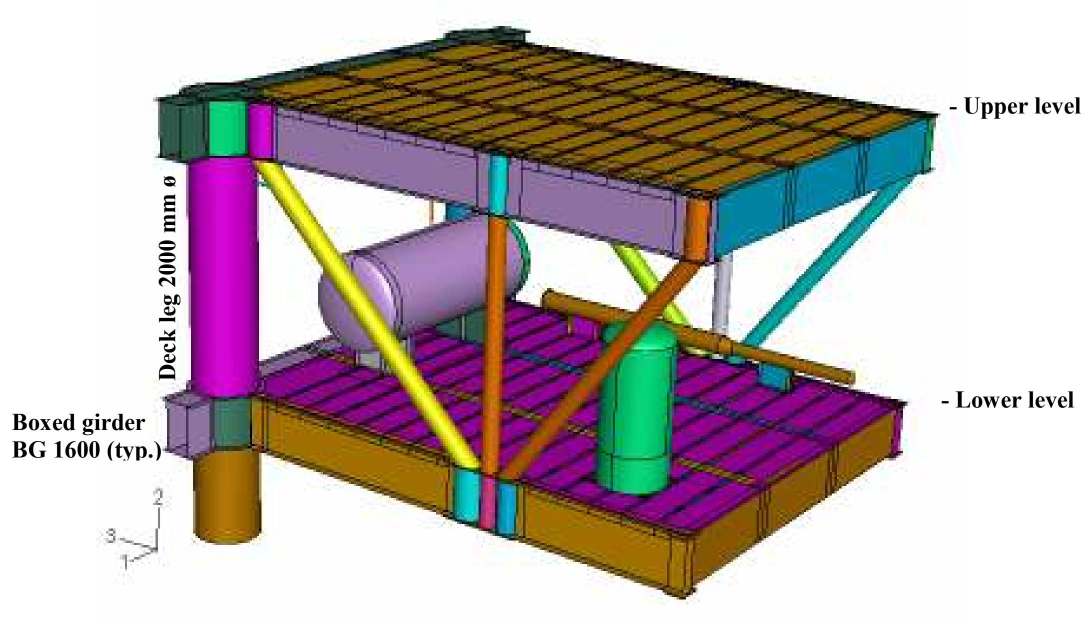

a. A complete ABAQUS model with equipment

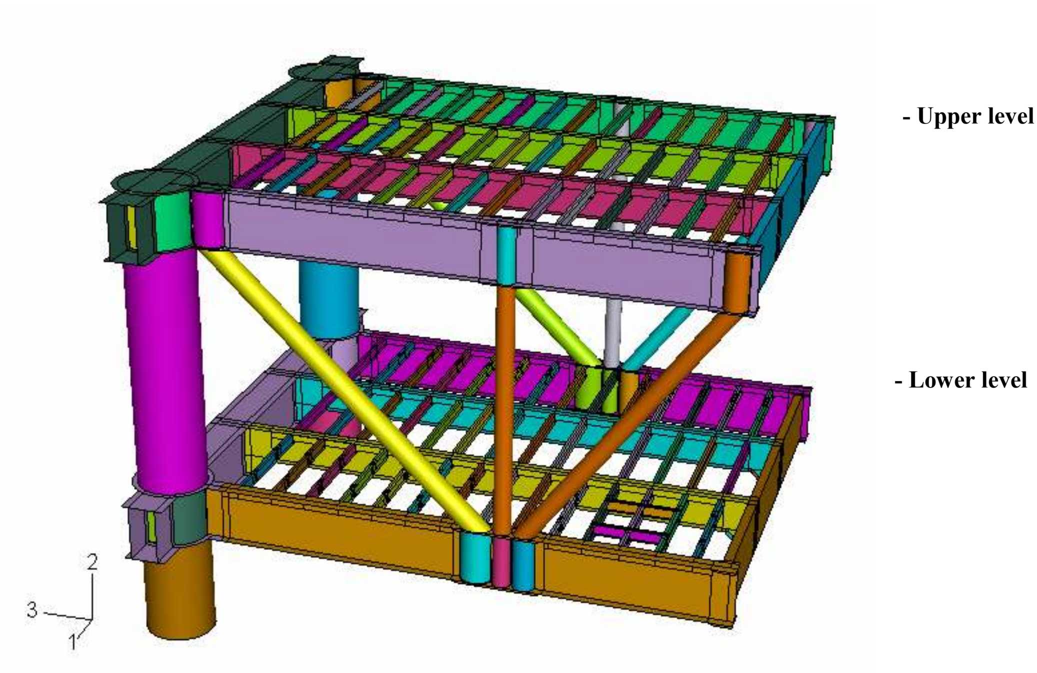

b. The modelled structural components

Equipment and the deck plates are omitted for clarity of other structural members

Figure 7.3

The new ABAQUS Model

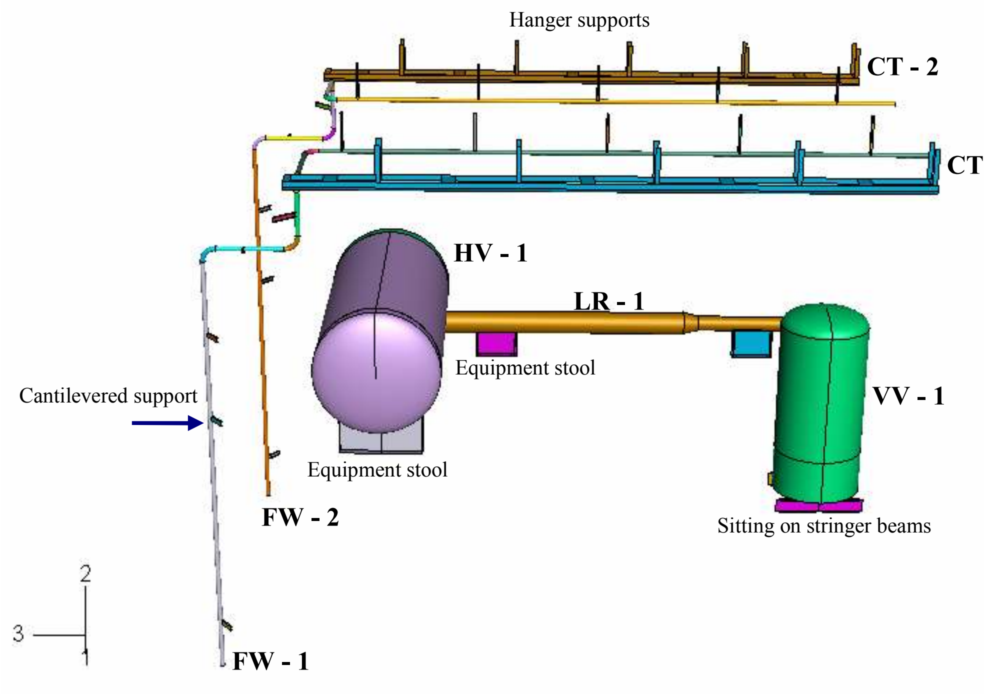

Figure 7.4

The modelled equipment with supports

<u>Legends</u>

FW – 114 mm ø firewater

LR – 610 mm ø and 406 mm ø launcher and receiver

CT – 600 mm wide cable tray

VV – 2000 mm ø vertical vessel

HV – 3000 mm ø horizontal vessel

<u>Note:</u>

All structural components are omitted for clarity of equipment.

7.3 The weight of equipment, natural period and duration of the applied load

7.3.1 The weight of equipment

The equipment was modelled similar to the modelling of structural components. High strength steel (F_y = 345 MPa) was specified for vessels and launcher / receiver while mild steel was specified for cable trays and firewater lines. The density of equipment was adjusted to account for the assumption made that equipment was 75 percent full of fluid except for the electrical cable tray. The summary of factors applied in the analysis is given by Table 7.3. The calculation of the derived factor is enclosed in appendix A.

Table 7.3

Increase factor for equipment weight

Equipment	Mass (kg/ m^3)
Horizontal vessel	20645.5
Vertical vessel	15229.0
Cable weight (5.0 kg/m)	10597.5
Launcher/ Receiver	15150.5
Firewater line	13973.0

7.3.2 The response mode

Frequency analysis using an ABAQUS static module was performed to determine the natural period as a result of modelling the deck leg, boxed girder and new equipment.

Table 7.4 lists the natural period based upon the first 10 modes and each response of topside structure is demonstrated graphically, as given by Figure 7.5a to Figure 7.5e.

Table 7.4

The first ten modes of responses by primary members

(local deformation by deck plates is omitted)

Mode	T_N (ms)	Responses
1	63.20	Twisting of the upper level and the lower level framings close to deck legs.
2	68.97	Maximum displacement in vertical direction in the middle of deck areas.
3	80.81	The framings for the upper lower and the lower level move vertically in the opposite direction.
4	88.92	Lateral displacement of primary members, plate girders PG 1000 displace towards east side.
5	89.21	Lateral displacement of primary members for plate girders PG 1000 both on the upper level and the lower level while deck framings displace downwards.
6	91.30	Lateral displacements of primary members, plate girders PG 1000 displace in opposite direction on the upper level.
7	91.52	Lateral displacement of primary members, plate girders PG 1000 displace towards each other on the lower level.
8	92.45	Lateral displacement of primary members, plate girders PG 1000 displace in one direction.
9	133.85	Topside structure is twisted and displaced upwards.
10	137.09	Topside structure is twisted and horizontal displacement of equipment.

As can been seen from Figure 7.5a, the second mode T_N = 68.97 ms resembles the first mode of the topside model in chapter five where T_N = 73.94 ms. Hence, it can be justified that modelling a portion of topside provides a response which is also comparable to a bigger scale model. The lower natural period in the current model compared to the previous model can be explained as a result of additional masses from equipment. Almost all mode shapes show a distortion at the bottom flange of plate girders PG 1000. This can be explained by the fact that the top flange is restrained by deck plates while the bottom flange is unstrained and free to move sideway.

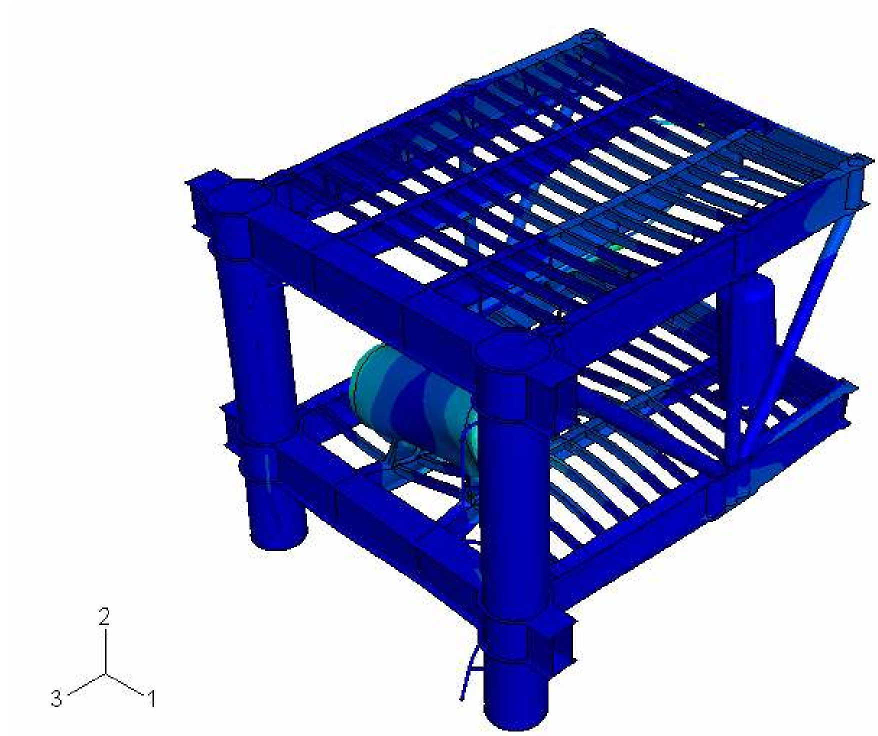

a. Mode no. 1, T_N = 63.20 ms

The deck framing plan at lower level is twisted at the horizontal vessel supports. The upper level on average displaces downwards while the lower level displaces upwards.

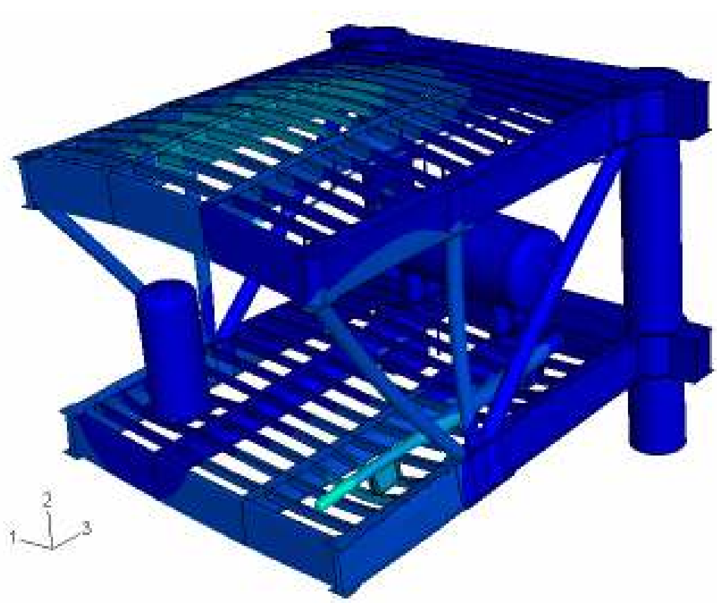

b. Mode no. 2, T_N = 68.97 ms

The response resembles a behaviour subjected to explosions, the upper level displaces upwards while the lower level displaces downwards. The maximum response profoundly concentrates in the middle of deck areas both on the upper level and the lower level.

Figure 7.5a

The response modes of topside structure

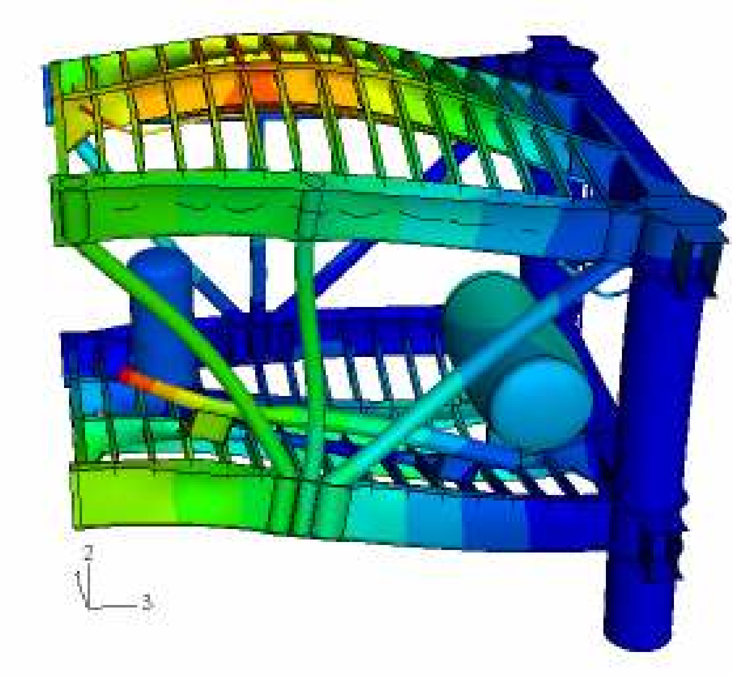

c. Mode no. 3, T_N = 80.81 ms

The response resembles a behaviour subjected to explosions during rebound period. While the upper level displaces upwards and a portion of the lower level displaces downwards, the middle area of the lower level displaces upwards as a result of pulling forces from braces.

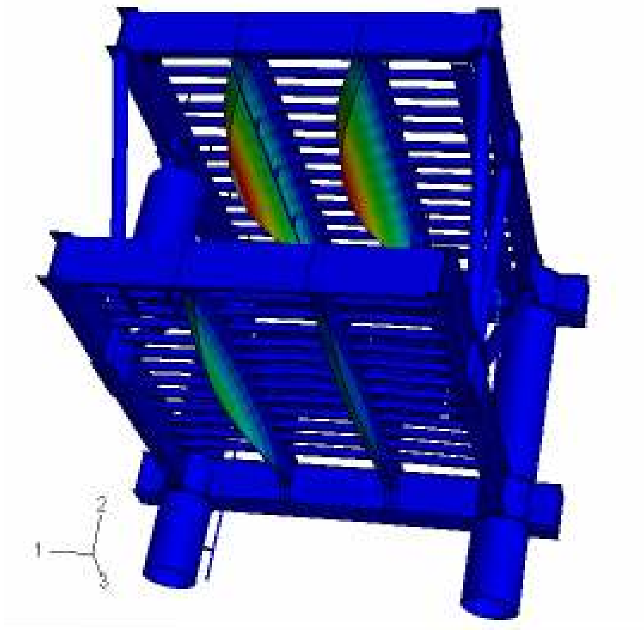

d. Mode no. 4, T_N = 88.92 ms

Distortion of plate girders at bottom flanges. The webs and bottom flanges bend sideway in the same direction.

Figure 7.5b

The response modes of topside structure

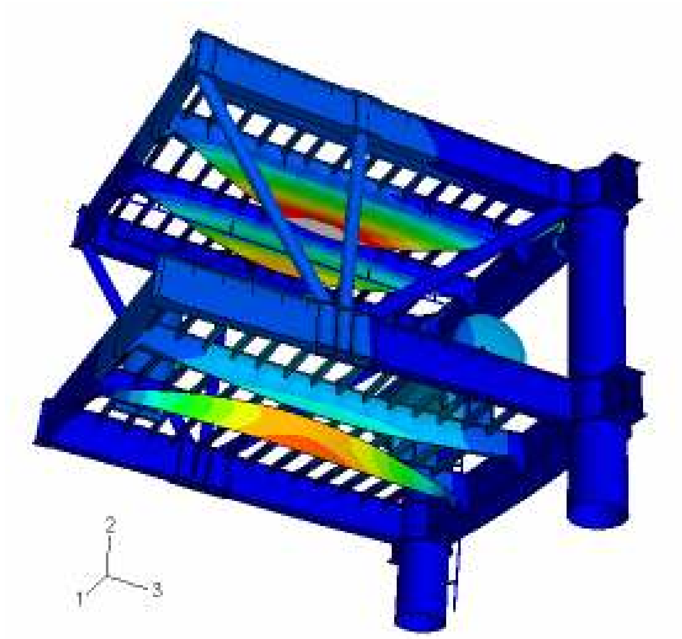

e. Mode no. 5, T_N = 89.21 ms

Distortion of plate girders PG 1000 at the bottom flanges; the upper level displaces to the west side while the lower level, the plate girders displace in opposite direction but towards to each other.

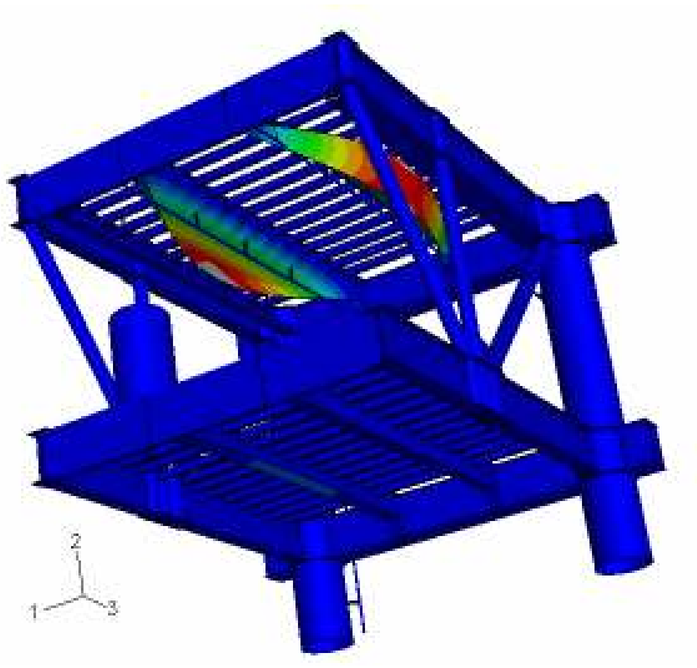

f. Mode no. 6, T_N = 91.30 ms

Distortion of plate girders PG 1000 at bottom flanges of the upper level that displaces in opposite direction.

Figure 7.5c

The response modes of topside structure

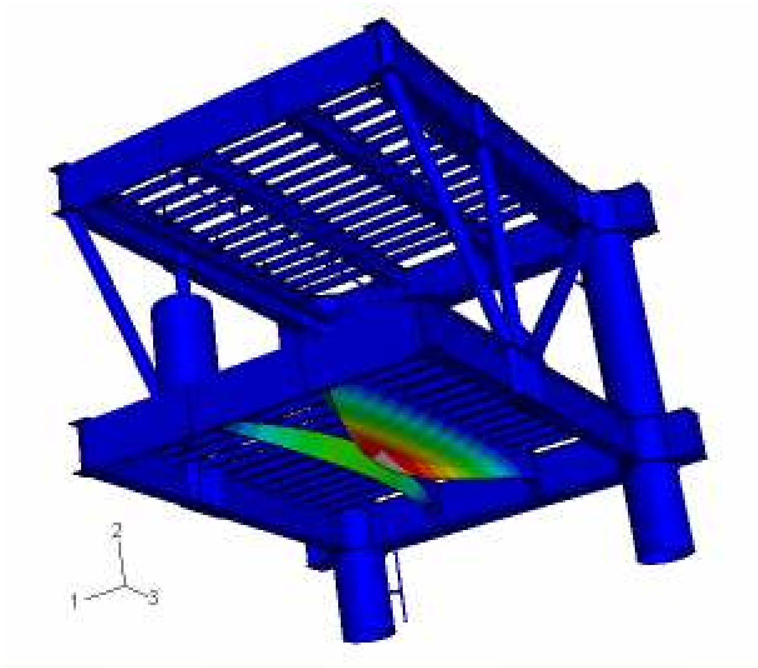

g. Mode no. 7, T_N = 91.52 ms

The distortion at the bottom flanges of plate girders PG 1000 at the lower level. The bottom flanges displaces in opposite direction but towards to each other.

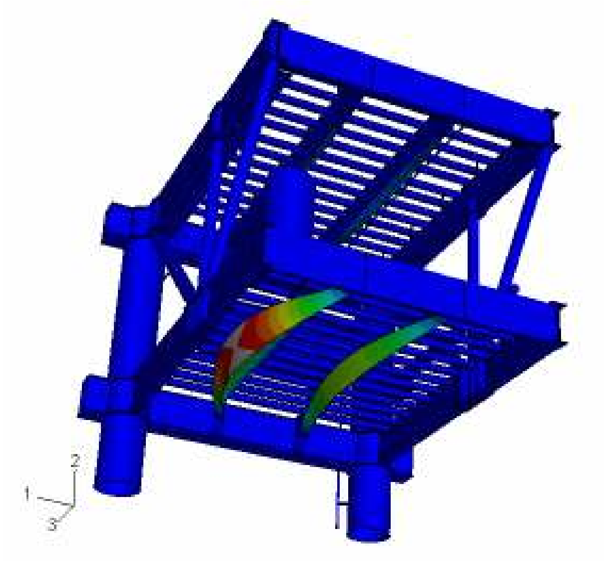

h. Mode no. 8, T_N = 92.45 ms

The distortion at the bottom flanges of plate girders PG 1000 at the lower level. The bottom flanges displace to the west side.

Figure 7.5d

The response modes of topside structure

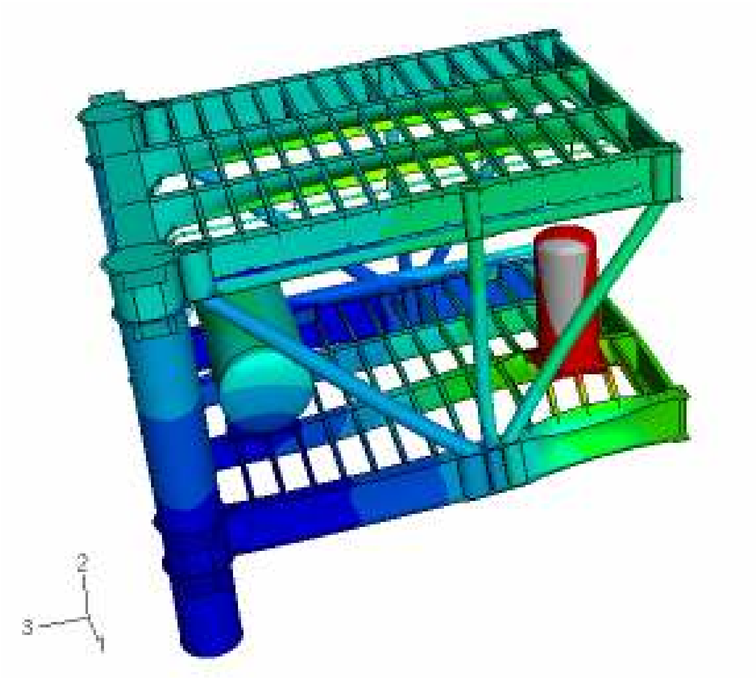

i. Mode no. 9, T_N = 133.85 ms

Similar to mode no. 3 however, deformation concentrates between plate girders PG 1000 and PG 1600-1 that carried loads from the vessels.

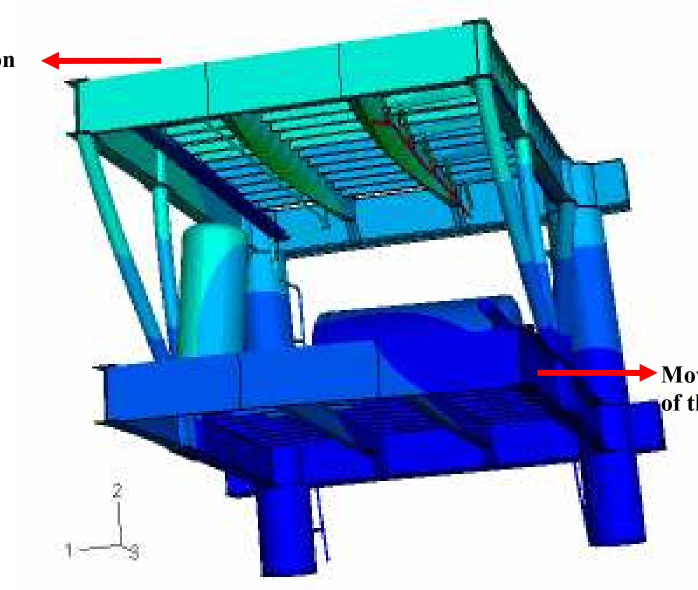

j. Mode no. 10, T_N = 137.09 ms

The upper level framing displaces to the east side while the lower level displaces to the west side.

Figure 7.5e

The response modes of topside structure

7.3.3 The applied loads on topside structure

The loads applied in the ABAQUS model were divided into three categories:

i. Self weight of structural components and equipment.

ii. Live load of 10 kN/m^2 is applied on deck clear areas. The live load represents loads which are temporarily placed on the deck level during maintenance or drilling period. They may consist of backup pumps, generators, cables, drilling equipment etc.

iii. Blast loads from hydrocarbon explosions

To optimise disk space and eliminate unnecessary errors, all loads are defined in ABAQUS explicit module. This is done because while reading static deformation to specify as pre-defined loads in ABAQUS explicit module from database of ABAQUS static module, the size of input data has exceeded the capacity that can be handled by a 32 bit machine.

The static loads (self weight and live load) are applied as a gradual rising load, starting from zero to maximum in duration of three times of the topside natural period (210 ms) which is equivalent to the quasi static condition. The blast profile, which is similar to blast profile defined in chapter five, is adopted at the end of this period. The combination of these loads is given by Figure 7.6.

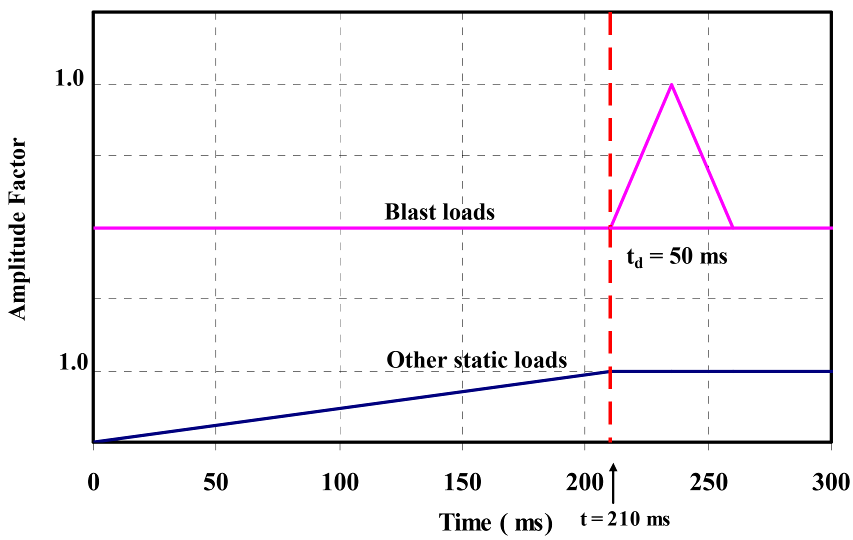

Figure 7.6

The load profile for blast loads and static loads.
(**Note:** The rising time of static loads is three times that of the first mode period)

The blast loads were applied on the relevant exposed areas as given by Figure 7.7. The load areas are defined as follows:

a. The lower level and the upper level. Areas below equipment were excluded, such as the horizontal and vertical vessels
b. Longitudinal surfaces for both the vertical and horizontal vessels.
c. Longitudinal surface of launcher and receiver.

The blast load direction on the deck level was applied vertically, while on the equipment the load was applied perpendicular to the surface. Because of small exposed surfaces, no blast load was applied either on cable trays or firewater lines.

a. Exposed surfaces for blast loads

1. Below deck plates of the upper level.
2. Bottom flanges IP 300 beams and plate girder PG 1000.
3. Top deck plates of the upper.
4. Half surface areas on vessels and launcher / receivers.

b. Open area for live loads

1. Top deck plates of the upper level.
2. Top deck plates of the lower level.

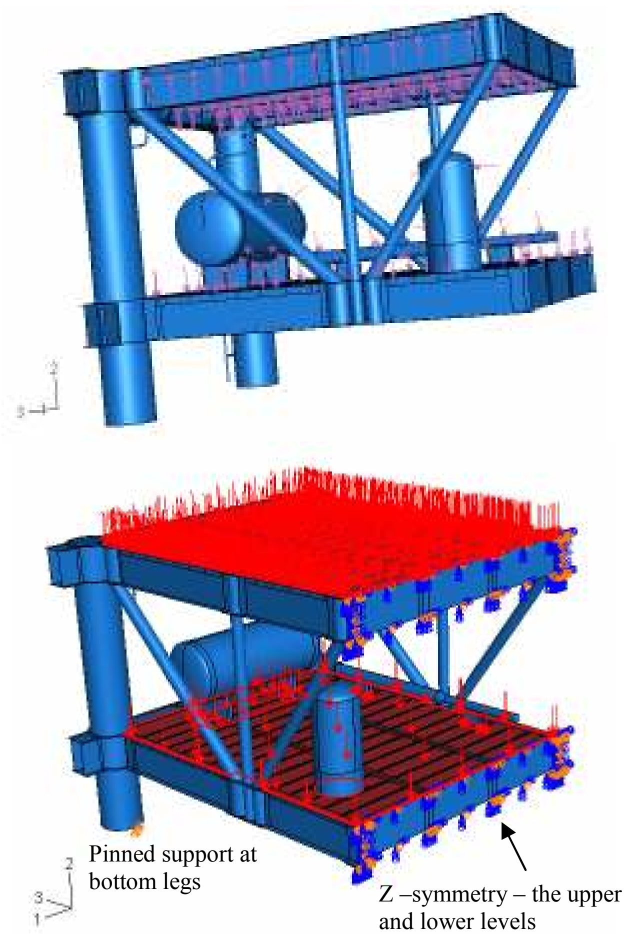

Figure 7.7

The applied loads and directions

7.4 Boundary conditions and load cases

7.4.1 The model boundary conditions

The boundary conditions for the present model are much simpler than the previous model which left only symmetry boundary conditions on the north side as symmetry in z direction for the upper level and the lower level. At connection to piles, deck legs were assumed to be pinned as given in Figure 7.7.

7.4.2 The analysed model and the load cases.

Two load cases were investigated using ABAQUS Explicit module. The first case included the case with live load applied on deck levels together with equipment loads (Figure 7.6). The second case excluded the live load while equipment and self weight remained similar to the first case.

All components were modelled as 3-D deformable and quadrilateral shell elements (4SR). The sizes of structural components were meshed from the minimum 25 mm square to the maximum 100 mm square. The total number of elements created in the model was 296394.

The constitutive relation of Cowper – Symonds (Eq. 5.7) for strain rate was specified for all structural steel where the material constants adopted were $D = 40.4\ s^{-1}$ and $q = 5$.

7.5 The interaction of equipment - structural components

The analysed model was applied with blast loads according to the defined performance level mentioned in section 5.6. The defined performance level for safety of 1.5 bar is considered critical during which most major equipment is anticipated to be badly damaged and safe routes must be available for the rest of the personnel to escape before the next stage of blast escalation effects begin and spread.

Figure 7.9 shows the history plot of displacement in the middle of deck areas by plate girders PG 1000. Although a longer duration is required to include static load effects, displacements in the analysis at t = 210 ms are found to be comparable with a separate analysis using ABAQUS static implicit analysis with difference less than average 1.5 percent. The average maximum displacement of the plate girder PG 1000 at the upper level is 10.13 mm while on the lower level is 10. 86 mm (Figure 7.8). The difference is due to the fact that major equipment is located on the lower level and the omission of some live loads under the equipment.

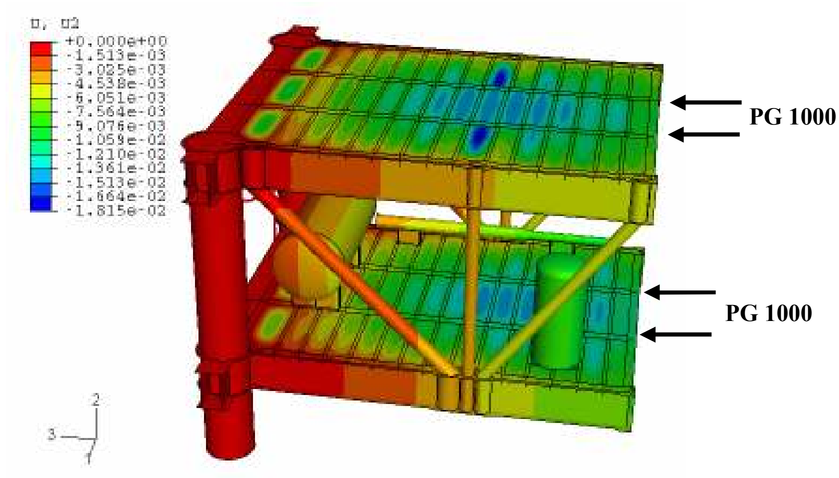

a. Displacement in vertical direction
Lower level = 10.86 mm, Upper level = 10.13 mm

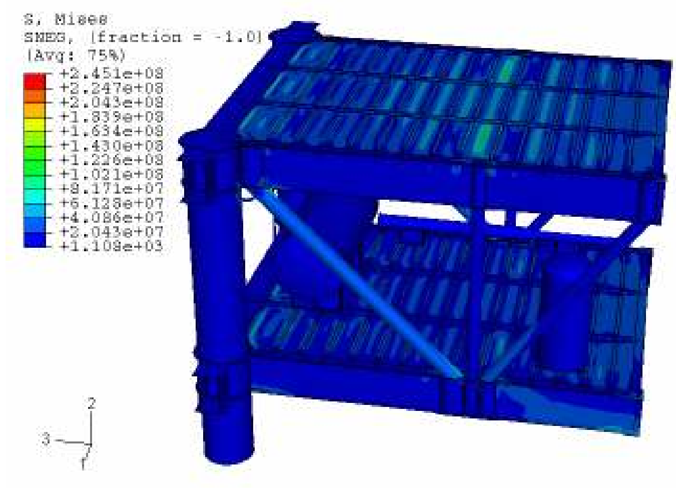

b. Von Mises stress
No structural components are experiencing stress greater than 248 MPa.

Figure 7.8

The displacement and stress at t = 210 ms with maximum live load of 10 kN/m^2.

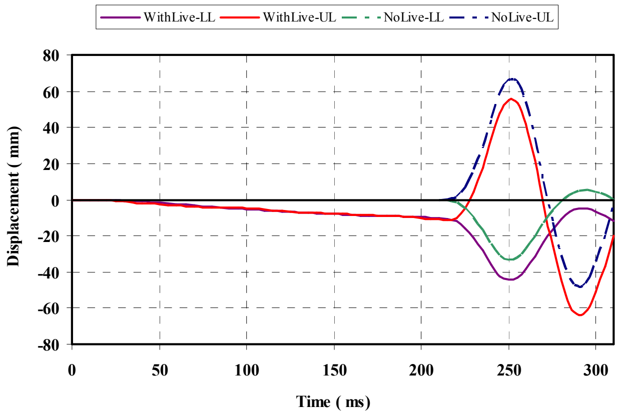

a. Pressure 0.5 bar
Structural members are elastic.

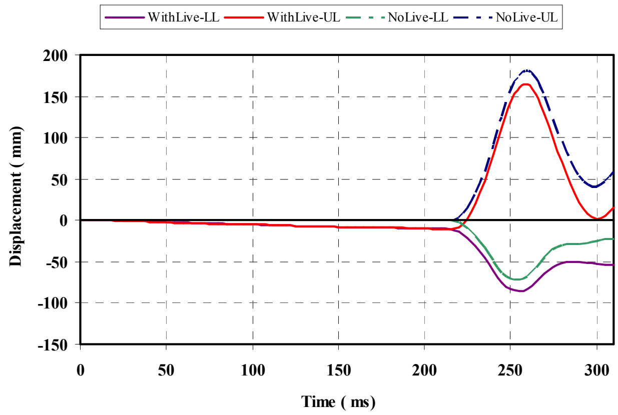

b. Pressure 1.0 bar
Stringer beams reach yield status.

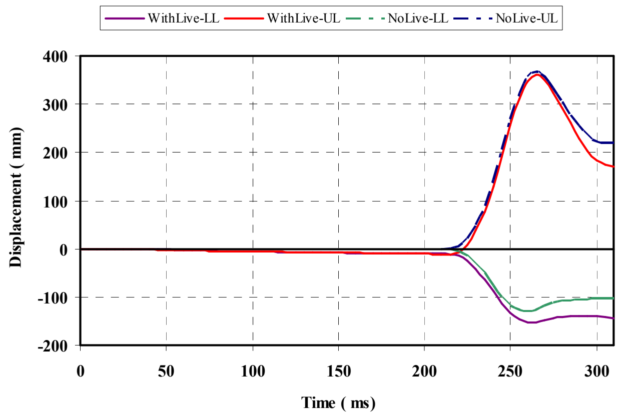

c. Pressure 1.5 bar
Plastic deformation in plate girders PG 1000.

Figure 7.9

History of average displacement at the middle of the deck area with live load and without live load

At 0.5 bar, because most structural members are elastic, responses on both deck levels are straightforward and predictable. First, a maximum displacement in the direction of the applied blast loads and then followed by a reverse displacement during rebound period. The magnitude of displacements is observed higher for the upper level compared to the lower which has been explained in section 5.9.1. However, it is also observed that displacement on the upper level has exceeded the lower during rebound period for the case with live loads. A similar response is also observed on the lower level but in the opposite direction, which can be explained by the effect of inertia load from live load and equipment which either reduces or increases the displacement depending upon the direction of rebound components.

At 1.0 bar, with reference to table 5.11 where the generalised damage level for PG 1000 is estimated to exceed severe damage of 6.0, a permanent deformation is observed for both the upper level and the lower level, as shown by Figure 7.10.

1. As shown most stresses concentrate on plate girders PG 1000 in the middle span and at the end span on the upper level and the lower level.

2. On average, the stress for deck plates is below 248 MPa but they are suppressed for clarity of main primary members.

3. Low stress for structural main truss and equipment.

4. Most IP 300 stringer beams have exceeded yield stress of 248 MPa.

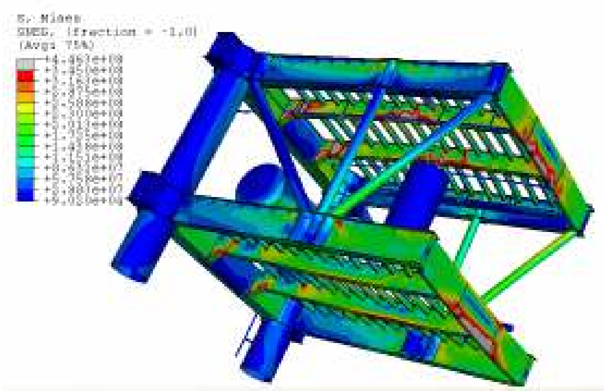

a. Looking towards east

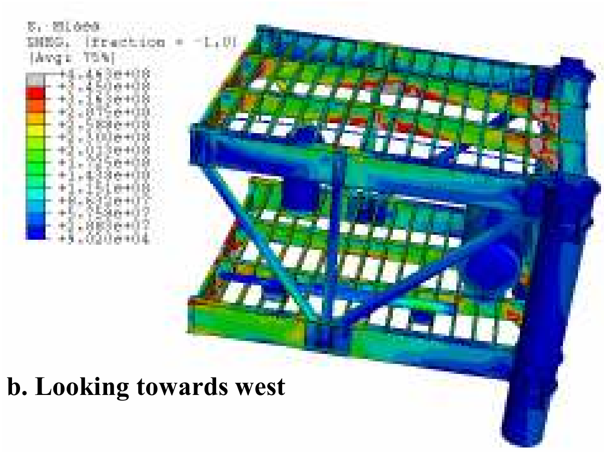

b. Looking towards west

Figure 7.10

Response at 1.0 bar, t = 235 ms

1. Similar to 1.0 bar, at 1.5 bar more damages are expected on plate girder PG 1000.

2. Supports for equipment are showing signs of yielding for the vertical and horizontal vessels. The firewater lines are still intact but supports of hangers attached to IP 300 stringer beams have yielded.

3. Local stress concentration and a sign of yielding at 508 mm ø supports both at the upper level and the lower level of plate girders PG 1600 -1.

4. The legs and boxed girders are still low in stress.

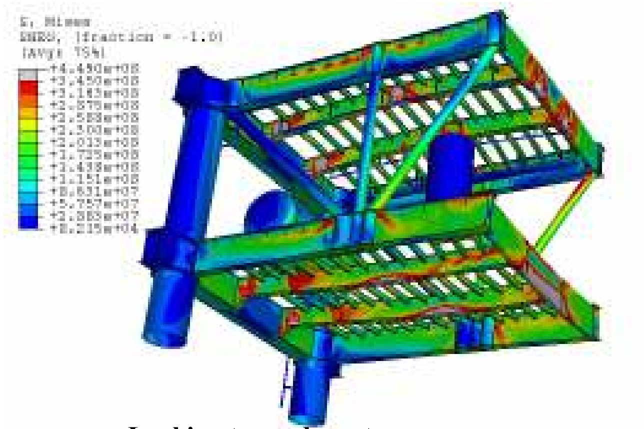

a. Looking towards east

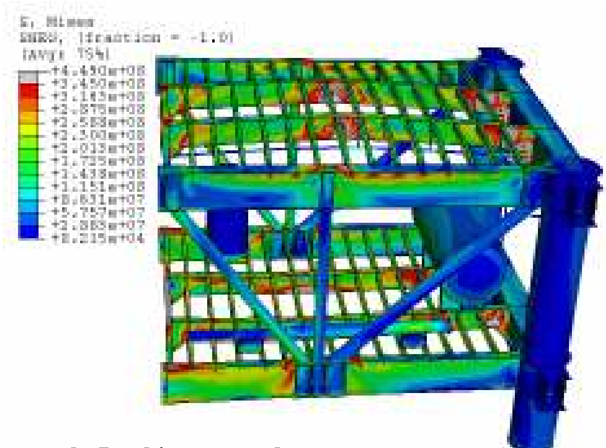

b. Looking towards west

Figure 7.11

Response at 1.5 bar, t = 235 ms

Like at 1.0 bar, at 1.5 bar more excessive permanent displacements are observed on both deck levels which is in agreement with the generalised damage level reaching about 20 (Table 5.11) The average displacement of 152 mm on the lower level has exceeded the serviceability limit for standard offshore practice at 67.0 mm (span length / 240 = 16000 mm / 240). At the congested connection between braces to plate girder PG 1600-1 on the lower level, more elements begin to yield while deck legs and boxed girders remain elastic.

The effect of equipment on structural supports can be explicitly described at 2.0 bar due to a significant influence of drag and inertial force during the rebound period.

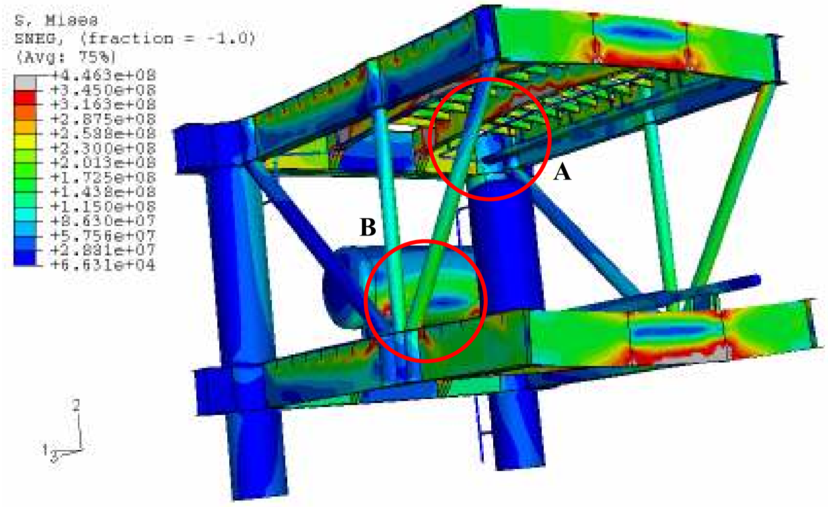

a. t = 235 ms, maximum pressure 2.0 bar

Note : [A] The pipelines and cable trays are still at the original position and very low in stress while [B] supports for modelled equipment have reached yield.

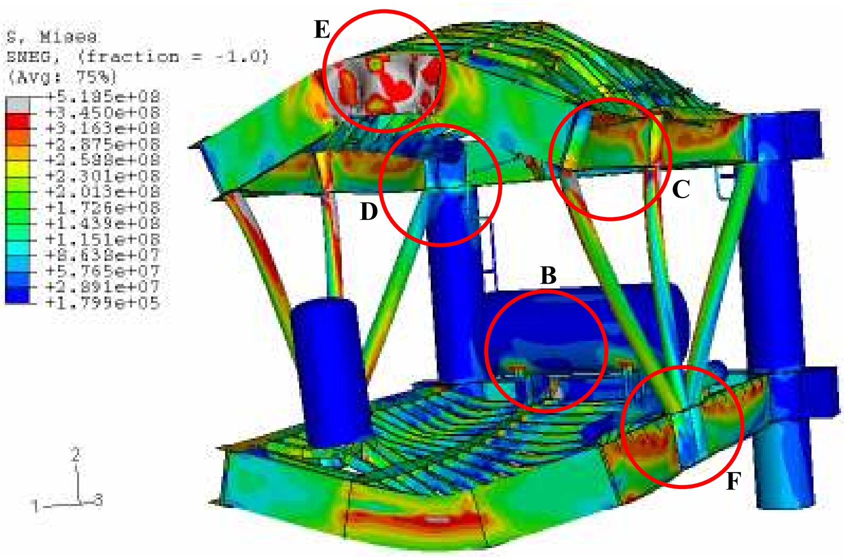

b. t = 295 ms, rebound period

Notes : [D] The cable trays and pipelines can been seen flying upwards due to the effect of inertia force and loss of support by hangers.
Similarly, [C and F] braces 508 mm ø are losing their connection to PG 1600-1 as well as support to PG 1600- 2 .
[E] Loss supports for plate girders PG 1000.

Figure 7.12

The behaviour and response at 2.0 bar

At 2.0 bar, as shown in Figure 7.12, structural members and equipment are highly stressed and have exceeded 345 MPa. Cable trays and piping lines are not much affected because they are flexible and the average stress is below yield level of 248 MPa. Hangers supports C 100 that are welded to IP 300 beams are being pulled upwards which causes the undamaged pipes and cable trays to fly away from their original positions as missiles. The piping lines welded to deck legs are still intact and show no deformation like the deck legs as given in Figure 7.13.

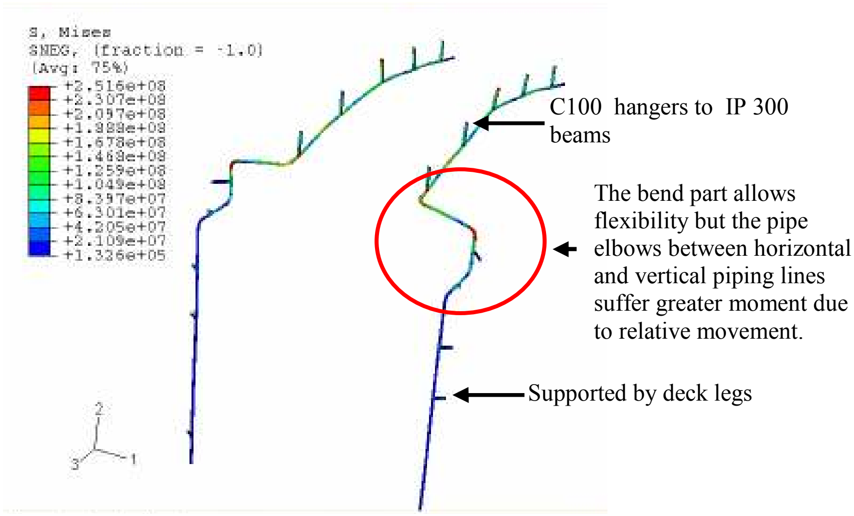

Figure 7.13

Behaviour of piping lines t = 255 ms at 2.0 bar

(Note: The bend is the weakest point on piping lines)

Despite having the flexibility to elongate which allows piping lines to follow the movement of their supports, pipe elbows are found to be the weakest spot. The top pipe elbow (supported by the deck beam) experiences out-plane moment contributed by in-plane moment of the horizontal 114 ø mm tubular and additional in plane moments from pipeline end reaction while the bottom pipe elbow (supported by the deck leg) experiences combined moments as a result of relative displacement between the two positions of elbows.

The response of cable trays is shown by Figure 7.14. At the end of the explosion period (t = 235 ms), despite having a low stress and like the piping lines, cable trays are dragged by hangers upwards which is following the behaviour of IP 300 stringer beams. The damage to cable trays is the result of its self impact onto the bottom flanges of IP 300 stringer beams.

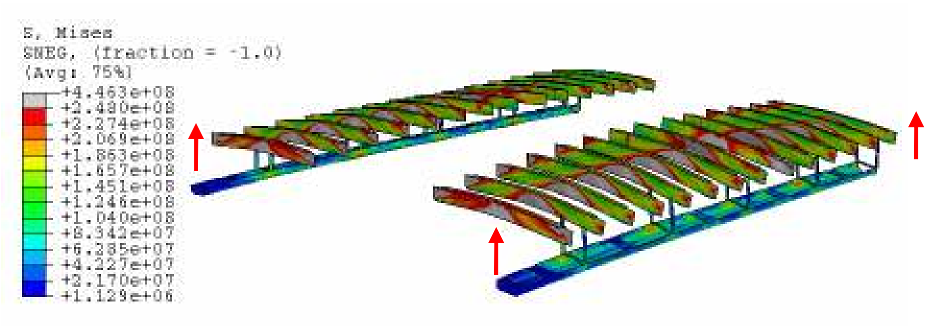

a. t = 235 ms

Note: The cable trays are dragged upwards

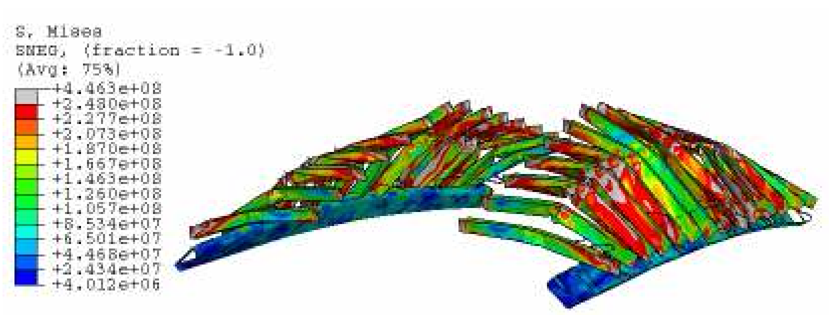

b. t = 265 ms

Note :When t = 235 ms is the end of the applied blast load but the drag force continues to force the trays to move upwards and at the same time damages the trays as a result of its impact to the stringer beams.

Figure 7.14

Behaviour of cable trays at 2.0 bar

For vertical vessels as given by Figure 7.15, the effect of blast load at maximum overpressure concentrates profoundly in the middle span of support beams. Failure at the connection between the vessel and beams causes the vessel to tilt to one side, thus the load on the vessel is changed from a uniformly distributed load to a concentrated load. This worsens the support beams. Under the influence of drag load, more deformation is expected even though the overpressure period has ceased. If a suitable protection frame is not provided, the displaced equipment can potentially pose further damage to nearby structural components.

a. t = 210 ms

The beginning of blast loads.

→ denotes the direction of the applied blast load

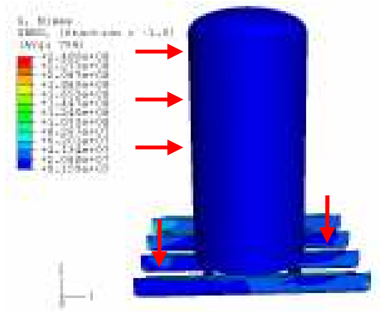

b. t = 235 ms

At peak overpressure, the middle spans of support beams are severely overstressed and damaged.

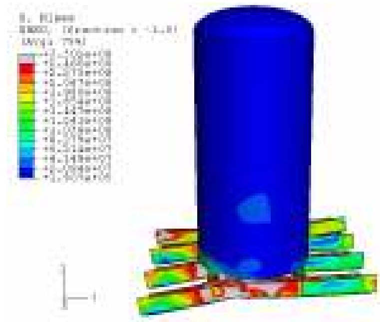

c. t = 305 ms

As the vessel sits directly on stringer beams and has a large footprint, the impact of inertia force of the tilted vessel pulls one part of support beams in tension while the other part in compression. The stringer beams fail due to web buckling as a result of single point reaction from self-weight and inertia.

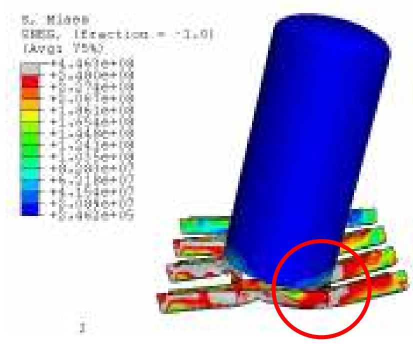

Change to point load

Figure 7.15

Behaviour of vertical vessel at 2.0 bar

For horizontal vessels, the condition below supports on plate girders PG 1000 is much more critical after the blast load period has ended. As the plate girders try to bounce back to their original position, the inertial reaction from the horizontal vessel resists the movement causing local web buckling below equipment foot prints and shear failure on the web to the boxed girder as given by Figure 7.16.

a. t = 210 ms

The beginning of the applied overpressure.

→ denotes the direction of the applied blast load

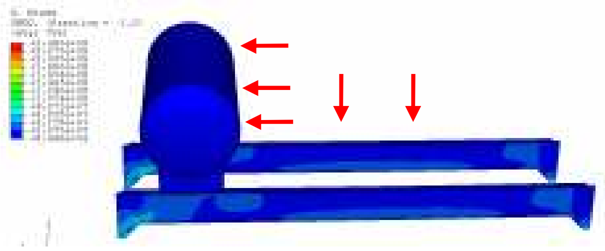

b. t = 235 ms

When the overpressure period is over, a small area in the web under the equipment is observed to experience shear failure.

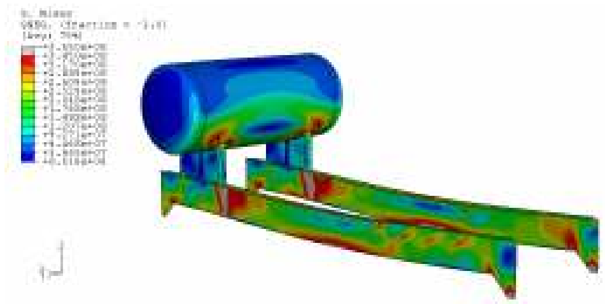

c. t = 300 ms

The rebound period with local web buckling and spreading of shear failure at supports close to boxed girder.

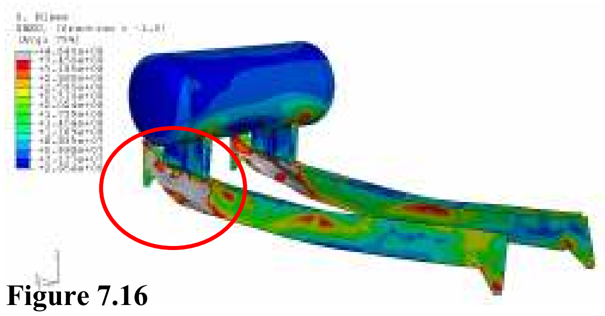

Figure 7.16

Behaviour of horizontal vessel at 2.0 bar

Compared to vertical vessels, the horizontal vessels provided with stools, the reaction on supports can be maintained as a uniform load that reduces damage on plate girders PG 1000.

The launcher / receiver pipe behaves proportionally to the size of exposed surface areas during the blast load period with more areas exceeding yield at stool support of 610 mm ø compared to 406 mm ø. However, because the stool of 406 mm ø is close to vertical pipes 508 mm ø (truss), likewise horizontal vessel at t = 300 ms, local web buckling below the support stools and shear failure at the end span of IP 300 stringer beams are observed as shown by Figure 7.17. This can be explained as a result of reverse movements between stringer beams and the truss system during rebound regime. The scenario is worsened with additional imposed load on stools from inertial reactions.

a. t = 210 ms

The beginning of the applied overpressure.

→ denotes the direction of the applied blast load

b. t = 235 ms

Slightly overstressed at 610 mm ø compared to 406 ø mm.

c. t = 300 ms

As highlighted, much more deformation is observed at the stool of 406 mm ø compared to 610 ø mm because the stool support is closer to braces 508 mm ø (the truss braces are omitted for clarity of the launcher / receiver).

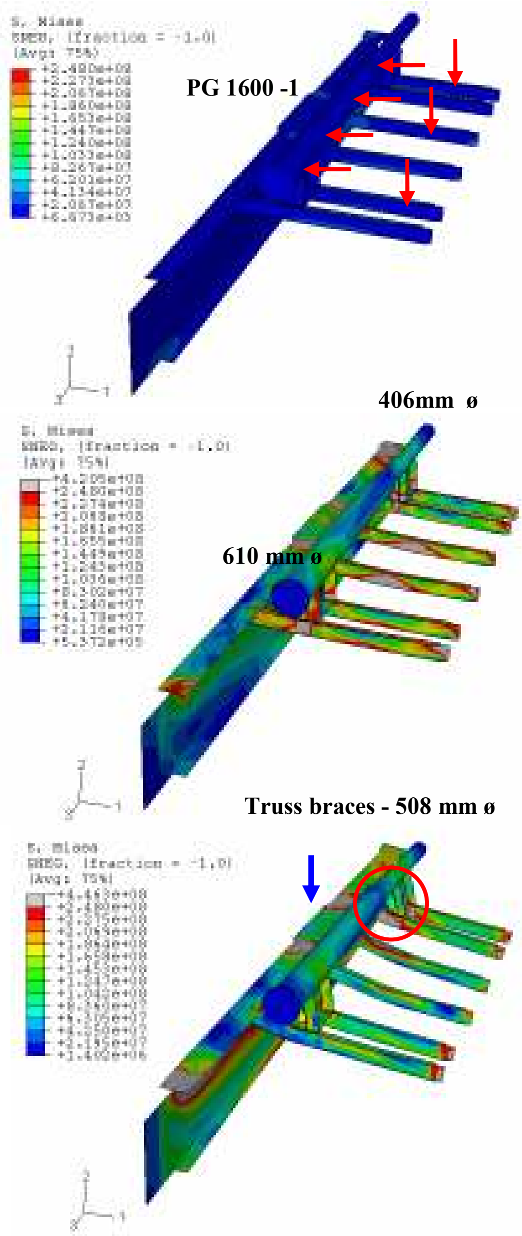

Figure 7.17

Behaviour of the launcher and receiver at 2.0 bar

Figure 7.18 shows the behaviour of the topside structure at 2.5 bar. Almost the entire deck areas for both the upper lever and lower level have reached the yield status. Severe and major deformation for the modelled primary structural components as predicated by the damage level introduced in chapter five while the boxed and deck legs remain with the least deformation. With average maximum displacements 862 mm and 437 mm for the upper deck and the lower deck respectively, no equipment is able to survive as the deck structural faming systems are at the point of total collapse.

a. t = 235 ms. Looking towards south west from top.

Yielding of deck plates over the entire deck areas of the upper level and the lower level.

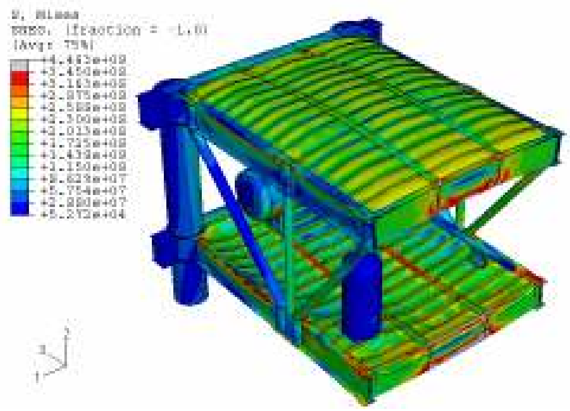

b. t = 235 ms. Looking towards south west from below.

Overstressed and highly strained at most connections of beams / plate girders

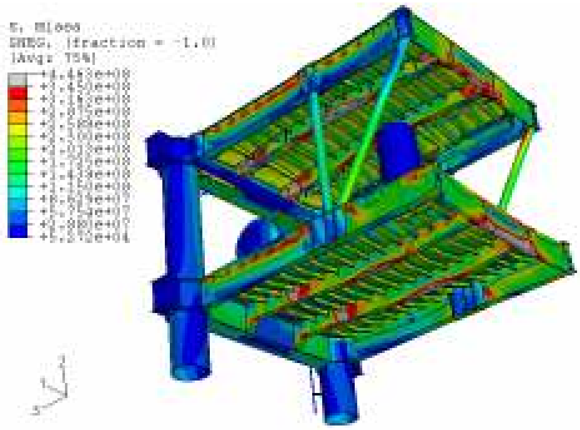

c. t = 265 ms. Looking towards south east.

After the end of explosion period during which the displaced equipment is seen damaging the structural member.

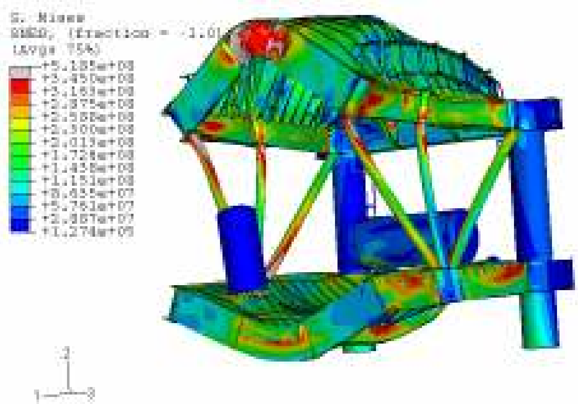

d. t = 265 ms. Looking towards north west.

Most structural components are experiencing plastic strain exceeding 0.15 percent except the deck legs and boxed girders.

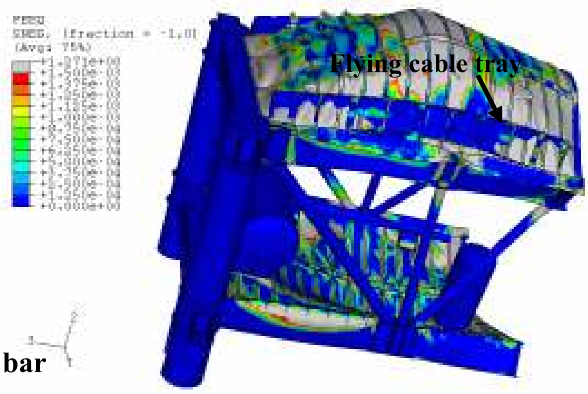

Figure 7.18

The behaviour and response at 2.5 bar

7.6 Proposed mitigation for equipment supports

With reference to behaviours shown by equipment, a summary of mitigation work on structural members is proposed as follows:

Equipment

Huge and heavy equipment such as vessels, tanks and generators are recommended to sit on support skid frame or individual support stools instead of sitting directly on structural supporting members. In addition, more stiffeners are required to prevent web local buckling. It has been demonstrated in the analysis that a failure at supports, such as the tilted vertical vessel, changes the load pattern from a uniform load to a point load. It is also observed that structural support members become highly overstressed during the rebound period instead of during the peak overpressure as a result of equipment movement in the opposite direction towards the displaced structural members. A skid frame enlarges the area for the load distribution and prevents damage from structural members spreading to equipment. The equipment is also recommended to be located at a minimum safe distance (reasonable stand off) that prevents the displaced equipment with large inertial force from pounding other structural members. Alternatively, a protection frame can be provided to contain the equipment.

Piping lines, cables and cable trays (less stiff and flexible)

Failures of piping lines and cable trays are originally caused by failures at hanger supports. Despite being low in stress, the piping lines and cable trays can easily been dragged away following the deformation of the structural members to which they welded. As the piping lines and cables are very flexible and able to elongate, they sometimes displace more than structural members and it is highly likely they will be damaged and become missiles as a result of collisions with structural members during the rebound period. Thus, having more supports on the deck level can prevent excessive displacement, while having extra loops or bends allows axial elongation that can reduce stress. On the deck leg, additional supports are not required because the effect of drag load is insignificant.

An elbow which joins two piping lines for a change in piping route direction is recommended to have a greater thickness since high stress is expected at the bend due to relative displacement and maximum bending moment.

Launchers / receivers and bigger pipes (stiff and rigid)

A frame to support the whole length of pipes for mitigation may be unpractical and too costly. However, the frame can be fabricated into many small stools. At least a pair of stools should be placed closer to each other when support beams are to be located in the vicinity of the truss system. It has been shown that the overstressed at the support of launcher and receiver pipe 406 ø mm occurs during the rebound period as a result of the combined effects between inertia force and the relative movement between supports.

7.7 Concluding Remarks

From the analysis of topside structure with equipment, most failures by structural members that support equipment are exhibited after the active period of the applied blast loads have completely ceased. The crucial stage is the rebound period during which the structure components are restoring to their original initial state while the inertia forces are dragging the equipment in the opposite direction. Depending on the direction of the blast load, the critical impact is when the equipment is located on the lower level. The equipment will drag in the opposite direction but towards the rebound direction of the plate girders or beams. This causes local buckling as the web is in compression. The upper level will be less critical as the web will be in tension since structural members are moving away from the equipment.

The effect of live load can not totally be ignored although the relative displacements are found to be of the same magnitude with the cases analysed without live load for overpressure from 0.0 bar to 1.0 bar. Above 1.0 bar, the average differences are about 19.8 percent for the lower level and 5.86 percent on the upper level. In reality, live loads represent temporary equipment hence the effects will be similar with permanent equipment, as was mentioned earlier.

With inventories being included in the topside structure model, this improves the understanding for mitigation work whereby the response of equipment to structural members can easily be observed and unnecessary strengthening can be eliminated.

Chapter Eight

CONCLUSION

This thesis investigates the application of a Performance Based design methodology for assessment and evaluation of topside structures of offshore installations. The approach, which is not a new concept, has been implemented elsewhere as mentioned in chapter 3 and can be applied in many fields. For the blast resistant design of offshore installations, ideally the approach begins with a quantitative risk assessment (QRA) study based upon available inventories on the topside structure. Embracing the risk assessment study provides a multi-level performance guide in terms of damage and fatalities for the topside structure. Integrating performance levels within reasonably acceptable non linear behaviour of structural components would finally optimise the design and provide stakeholders with an authoritative account of functionality, safety and protection levels for the assets on the topside structure.

As a result of implementing performance based design for topside structures subjected to blast loads, the thesis has successfully demonstrated some new outcomes as by products which can be used to improve the topside design. The outcomes are listed as follows;

a. A sniped bottom flange method, which is commonly employed in fabrication, degrades the performance level of the topside. The weakness is mitigated by having angles welded between sniped areas to support beams.

b. A design procedure with design flow chart (Figure 3.2) to assist engineers in design according to a performance based method is proposed. Deciding demand levels for a platform is not straightforward because it involves QRA. A proper QRA study can only be commenced when layout and equipment are firmed, thus a matrix of simplified performance levels (Figure 3.4) is proposed to facilitate and expedite the design process in the absence of data. The proposed performance level can be used for designing a new topside structure with typical equipment as well as for evaluating the existing topside structure.

c. Under the blast condition, it has been shown that secondary structural members play a paramount role in reducing damage to primary members because their surface areas are larger than other structural components which attract more overpressure load to pound their surfaces. Recognising this effect, a simplified deck plate analytical model according to performance based design is proposed. Adopting appropriate shape functions, the solution in terms of ordinary differential equations can be solved manually for the static case and numerically for the dynamic case. The study has also demonstrated that the optimum design for deck plate is when the plate slenderness (width / thickness) is in the range of 70 to 100.

d. Ductility ratio can be used to assess the performance and to benchmark the damage level of structural components. Based upon finite element simulation which includes the combined responses of structural components, a damage level of 6 shall be a ceiling to limit the upper bound value of ductility ratios for all supporting structural members. Any assessment made in design with less than 6, especially if design is based on a single member, probably will be on the conservative side. It has been demonstrated in the analyses that when ductility ratio crosses above this limit, the plastic strain increases dramatically. Hence, to avoid premature failure, all main structural components forming as a truss system should be limited to a lower value. A range from $2 \leq \mu < 3$ is recommended for design. On the contrary, having a low ductility ratio at higher overpressure as a result of membrane strain, a deck plate can be allowed to have a damage level above 6. However, the performance of the deck plate must be balanced with serviceability for normal operating conditions.

e. Likewise stringer beams with angles; placement of pairs of braces on the structural framing plan, substantially improves beam to beam connections which eventually enhance the global structural performance. Nevertheless, because the braces share the load between two structural components and shorten the load travel path to supports, stress concentration are observed at the transition on beam flanges and braces. This first shortcoming can be overcome by having angles welded between gusset and the flange to distribute the stress more uniformly (proven for IP 300 stringer beams) while the second shortcoming is not critical because they are not designed to carry any load under normal operating conditions and to be replaced with a new section immediately after explosions.

f. Comparing this with the conventional design method i.e. working stress design (WSD) which has uncertainties in term of safety levels, the approach of performance based design provides reasonable information that can easily be accepted by both technical and non technical communities. Instead of using stress check ratios governed by the design codes which only engineers can appreciate the meaning of, the ductility ratio used in performance based design gives the degradation status of structural members with reference to a yield limit. This value assists engineers in assessing the state of damage of individual components, while combining many more ductility ratios of other structural components from the same load level, enables engineers to appraise the whole system.

g. A few of typical fabrication techniques were modelled using ABAQUS in order to evaluate the effect on structural members.

   The modelled 20 mm cope hole (access hole) on the flange for full access of welding is found to have an insignificant effect at the connection while with the bottom flange extended, stress concentrations on the web of the support beam at high overpressures were found to occur.

   Having only end plates for improving beam to beam connection is not recommended for beams with equal depth. Despite their ability to increase the capacity at the end span on the load carrying beam, the method attracts more out of plane moments at the connection and weakens the support beam on the far side without the end plate.

   Strengthening is recommended for the support beam, which not only improves the end span of the load carrying beam but also assists to relocate yield away from the connection on the support beam.

   The optimum design for haunch is recommended between 1: 2 as the lower bound and 1: 3 as the upper bound. A short distance haunch enables gradual deformation along the non strengthened part, while a longer distance haunch can cause sudden catastrophic collapse at higher overpressure loads.

The approach of performance based design for topside structures is very demanding as it requires detailed structural analysis. This distinct drawback is unavoidable as the appraisal of structural components is based upon the behaviour and responses of structural members in the non-linear range. Although designers may have to invest in a better design infrastructure, the return results in terms of better design and well defined structural performance outnumber its drawbacks.

Modelling equipment on topside structures assists further understanding of equipment behaviour in relation to structural components. Large sized and heavy equipment is recommended to sit on its own equipment skid frame which will avert deformation from the structural components to be passed onto equipment and to dictate the response of the affected part. For small and flexible components, although they are not significantly affected, it is recommended to have additional loops (extra loose lengths) and extra supports. Additional loops assist in expanding and allowing elongation during maximum deformation with minimum strain on cables or pipelines while extra supports will guarantee failure parts remain supported and do not become missiles.

A water spray for explosion suppression is only effective at high flame speeds due to its ability to break water droplets into smaller sizes that increase surface areas which can extract more heat from the flame, thus reducing the overpressure as investigated by Johnson and Vassey (1996). Similarly, a feasibility study should be conducted prior to executing mitigation work on structural components. The study has illustrated that an effective mitigation work for structural members exposed to explosions primarily depends on sharing of loads. The load sharing concept utilises members or parts of members with low stress to experience higher stress but within acceptable limits. The new structural components may be designed to reasonably damage but they also must not pose further threats to other components.

Finally, modelling a topside structure in detail by utilising shell elements to represent all primary and secondary members, has the advantage of being able to demonstrate some local failures, many of which were overlooked in the design stage and sometimes being regarded as having relatively low influence and importance such as haunch details, stringer beams and deck plate. However, it has been demonstrated that they have a significant effect on the performance of other connected members.

Chapter Nine

PROPOSED FURTHER STUDY

The following lists potential study that is required for further investigation, which can be continued from the present research work.

a. To broaden the performance based design methodology for other design conditions. The potential design cases in which this methodology can be applied in structural design for offshore installations are as follows:

   1. The design against boat impact on a jacket structure and the protection of the riser lines.
      Although jacket legs are designed to be elastic at most times in all cases, other members such as braces, may reasonably be allowed to deform more without affecting the performance. However, as the majority of a jacket's structural components are submerged in sea water, the cost of repair and replacement must not be overlooked.

   2. The structural protection for equipment.
      On the topside structure, as a result of risk assessment, the equipment is to be protected against blast, fire and dropped objects. On many occasions, the proposed protection frames are designed because of safety requirements. However, the basis of the expected damage levels is usually not well defined. A guideline for safety and the establishing of a realistic damage level for design can be derived in the same manner to explosion cases.

3. Assessment of new loads for the existing structures.

   Many old platforms are loaded with new equipment to boost the production output. However, with the revised criteria in design, new environmental factors and new requirements in terms of safety from regulators, the existing platform is theoretically justified not fit to operate, although the structure has been installed and standing for many years. Because performance based design is dependent upon evaluation of local components and a global system, an authoritative account of performance can be established and it is highly likely that the platform will be allowed to operate to a certain load level.

b. Development of many more alternative structural framings and new mechanisms for connections that can absorb much more energy locally as well as able to transfer responses efficiently to supports as being demonstrated by haunches and placement of horizontal diagonal pipes.

c. A further enhanced technique for stringer beams connectivity, especially to main primary members. Although they are used for walkway supports under normal operating loads the beams are enormously scattered on the deck flooring. Simple and workable methods are preferred, for example angles below the sniped bottom flanges of IP 300 beams.

d. The incorporation of explosion suppression entities within the structural system for protection. The entities must be flexible and able to follow the structural deformation without jeopardising the efficacy of its function to mitigate.

e. Development of a simplified model for I beam using energy terms or equivalent methods for predicting responses and MAPLE's built-in mathematics commands for solving solutions similar to the deck plate analytical model.

f. The compilation of explosion recurrence data from other parts of the world for comparison with the proposed performance design level given by Figure 3.4.

References

[1]. **ABAQUS** Version 6.6 Manuals . Habbitt, Karlsson & Sorensen, Inc. www.abaqus.com.

[2]. **Alves M (2000),** *Material constitutive law for large strains and strain rates.* Journal of engineering mechanics, Feb., 215-218.

[3]. **Amdahl J (2005)**, *Static resistance of stiffened plates subjected to explosions.* FABIG Newsletter Issue 41, 4-7.

[4]. **Apostolakis G. E (2004),** *How useful is quantitative risk assessment?* Risk Analysis Vol. 24 No. 3, 515-520.

[5]. Army Technical Manual **TM 5-1300**: *Structures to resist the effects of accidental explosions*, Departments of Army, Navy and Air Force, 1990.

[6]. **Alimoradi A, Pezeshk S and Foley C.M State (2003),** *State-of-the-art in performance based design optimization- inference to consequence –based engineering optimization.* A report to the consequence–based Engineering Institute of the Mid-American Earthquake Centre, University of Illinois at Urbana-Champaign.

[7]. **Baker J. and Heyman J,** *Plastic Design of Frames.* Cambridge University Press, 1969.

[8]. **Baker W.E, Cox P.A, Westine P.S, Kulesz J.J and Strehlow R.A,** *Explosions hazards and evaluation.* Elsevier, 1983.

[9]. **Bakke J.R and Hansen O.R (2003)**, *Probabilistic analysis of gas explosions.* FABIG Newsletter Issue 34, 22-39.

[10]. **Biggs J.M**, *Introduction to structural dynamics.* Mac Graw-Hill, New York, 1964.

[11]. **Bjerketvedt D, Bakke J.R and Wingerden K.V,** *Gas Explosion Handbook.* www.gexcon.com/index.php?src=handbook/GEXHBChap8.htm.

[12]. **Blast and Fire Engineering Project for Topside Structures**, The Steel Construction Institute, 1991.

[13]. **Boh J.W, Louca L.A and Choo Y.S. (2004a),** *Numerical assessment of explosion resistant profiled barriers.* Marine Structures 17, 139-160.

[14]. **Boh J.W, Louca L.A and Choo Y.S (2004b)**, *Strain rate effects on the response of stainless steel corrugated firewalls subjected to hydrocarbon explosions.* Journal of Constructional Steel Research 60, 1-29.

[15]. **Boh J.W, Louca L.A and Choo Y.S (2005)**, *Energy absorbing passive impact barrier for profiled blastwalls.* International Journal of Impact Engineering 31, 976-995.

[16]. **Bruce R.L (1995),** *Blast Overpressure Prediction – Modelling the uncertainties.* Hazard, safety and engineering, ERA Report 94-0730, 3.2.1-3.2.11.

[17]. **Building Regulation 1992**, Department of Building and Housing, www.dbh.govt.nz/userFiles/Building/pdf/1992150.pdf.

[18]. **Carter D.A, Hirst I. L, Maddison T.E and Porter S.R (2003),** *Appropriate risk assessment methods for major accident establishments.* Trans IChemE, Vol. 81, Part B, 12-18.

[19]. **Chen W.F and Han D.J,** *Structural plasticity – Theory, problems and CAE software.* Springer-Verlag, 1991.

[20]. **Chen S.J, Tsao Y.C and Chao Y.C (2001)**, *Enhancement of ductility of existing seismic steel moment connections.* Journal of Structural Engineering, 538-545.

[21]. **Chen C.C, Lee J.M, and Lin M.C (2003),** *Behaviour of steel moment connections with a single flange rib.* Engineering Structures 25, 1419-1428.

[22]. **Choi J, Geol S.C and Stojadinovic B, (2003),** *Design of free flange moment connection.* Engineering Journal, American Institute of Steel Construction, 25, 25-41.

[23]. **Corr R.B, Tam VHY and Snell R.O (1999),** *Development of the limit state approach for design of offshore platforms.* ERA Conference Safety of Offshore Installation, 6.3.1-6.3.23.

[24]. **Crawley F.K and Grant M.M (1997),** *The concept risk assessment of offshore hydrocarbon production installations.* Trans IChemE, Vol. 75 Part B, 157-163.

[25]. **Crisfield M.A (1981),** *A fast increment/iterative solution procedure that handles snap-through.* Computers and Structures Vol 13, 55-62 .

[26]. **Da Silva L.S and Coelho A.G (2001),** *A ductility model for steel connection.* Journal of Constructional Steel Research, 45-70.

[27]. **Dubina D and Stratan A (2002)**, *Behaviour of welded connections of moment resisting frames beam-to-column joints*. Engineering Structures 24, 1431-1440.

[28]. **Eknes M.L and Moan T (1994),** *Escalation of gas explosion event offshore* . Offshore Structural Design, Hazard, Safety and Engineering, Conference Proceedings London, ERA Report No 94-0730, 3.1.1-3.1.16.

[29]. **Evans R.F (1994),** *Predicting the effects of vapour cloud explosions on offshore installations.* Second International Conference on Health, Safety and Environment in Oil and Gas Exploration and Production, Jakarta, Indonesia, SPE 27250, 1994, 393-398.

[30]. **Eurocode 3**: *Design of steel Structures- Part 1-1: General rules and rules for buidings*, BS EN 1993-1-1:2005

[31]. **Fire and Explosion Guidance Part 0**: *Fire and explosion ,management, Issue 2* UKOOA, 2003.

[32]. **Fire and Explosion Guidance Part 1** : *Avoidance and mitigation of explosions, Issue 1* UKOOA, 2003.

[33]. **Fire and Explosion Guidance Part 2** : *Avoidance and mitigation of explosions, Issue 2* UKOOA, 2006.

[34]. **Floren A and Mohammadi J (2001),** *Performance-based design approach in seismic analysis of bridges.* Journal of Bridge Engineering, Vol. 6 Issue 1, 37-45.

[35]. **Funderburk R.S (1998),** *Key concepts in welding engineering- Post weld heat treatment. Welding Innovation,* Vol. XV, No. 2.

[36]. **Gardner L and Nethercot D. A,** *Designers' guide to EN 1993-1-1, Eurocode 3: Design of steel structures general rules and rules for buildings*, Thomas Telford, London, 2005.

[37]. **Gruss E. (2006)**, *A correction for primary blast injury criteria.* The Journal of Trauma Injury, Infection, and Crictical Care, 60, 1284-1289.

[38]. **Guidance for safer design of offshore installations : An Overview**. Institute of Energy, London, 2005.

[39]. **Haldar A, Feng M.Q and Aktan A.E (2004***),* *Issue on performance-based engineering for buildings and bridges.* Structure Congress Building the Past : Securing the Future, Nashville, Tennessee, USA.

[40]. **Hamburger R.O and Whittaker A.S (2003),** *Considerations in performance – based blast design resistant design of steel structures.* Proceedings AISC-SINY Symposium on Resisting Blast and Progressive Collapse, American Institute of Steel Construction, New York.

[41]. **Hamburger R. O**, *The challenge of performance-based design*. http://peer.berkeley.edu.news/1999jan/challenge .html

[42]. **Heck A**, *Introduction to Maple*. Springer, Berlin, London, 2003.

[43]. History of the Building Code of Australia. www.abcd.gov.au.

[44]. **Hutcheon D. L and Waldram I. M (1994),** *Fire and blast protection for a small gas platform,* ERA Conference Proceeding, London.

[45]. **Inokuma A (2002***), Basic Study of Performance –Based in civil engineering.* Journal of Professional Issues in Engineering Education and Practice, ASCE Vol. 128 Issue 1, 30-35.

[46] **Izzuddin B.A and Smith D.L (1997)**, *Response of offshore structures to explosion loading.* International Society of Offshore and Polar Engineers, Vol. 7, No. 3, 212 -219.

[47]. **IGN** -*Interim guidance notes for the design and protection of topside structures against explosion and fire,* The Steel Construction Institute, 1992.

[48]. **Jones N**, *Structural impact*, Cambridge University Press, 1989.

[49]. **Jones N (1971),** *A Theoretical study of the dynamic plastic behaviour of beams and plates with finite deflections.* Int. Journal Solids Structures, Vol. 7, 1007-1029.

[50]. **Johnson D.M and Vassey M.W (1996),** *The prevention and mitigation of gas explosions.* International Conference on Health, Safety and Environmental, New Orleans, Louisiana, SPE 35810, 407-417.

[51]. **Krauthammer T (1999),** *Blast –resistant structural concrete and steel connections.* International Journal of Impact Engineering 22, 1999, 887-910.

[52]. **Langdon G.S, Yuen K.S.C and Nurick G.N (2005),** *Experimental and numerical studies on the response of quadrangular stiffened plates. Part II: Localised blast loading.* International Journal of Impact Engineering 31, 85-11.

[53]. **Langdon G.S and Schleyer G.K (2005),** *Inelastic deformation and failure of profiled stainless steel blast wall panels. Part I: Experimental investigations.* International Journal of Impact Engineering 31, 341-369.

[54]. **Langdon G.S and Schleyer G.K. (2005)**, *Inelastic deformation and failure of profiled stainless steel blast wall panels. Part II: Analytical modelling considerations.* International Journal of Impact Engineering 31, 371-399.

[55]. **Lees F.P,** *Lees's Loss Prevention in the Process Industries; Hazard Identification, Assessment and Control,* 2nd Edition – Volume 2 & 3, Butterworth/Heineman, 1996.

[56]. **Louca L.A and Wadee M.A (2002),** *Simplified non-linear analysis of plates subjected to hydrocarbon explosions.* Journal of Strain Analysis, Vol. 37 No. 4, 301-311.

[57]. **Louca L.A, Boh J.W and Choo Y.S (2004),** *Design and analysis of stainless steel profiled blast barriers.* Journal of Constructional Steel Research, 60, 1699 -1723.

[58]. **Louca L.A and Mohamed Ali R. M (2007)**, *Improving the ductile behaviour of offshore topside structures under extreme loads,* Engineering Structures (article in press).

[59]. **Mohamed Ali R.M and Louca L.A (2007a),** *Performance based design of blast resistant offshore topsides Part I – Philosophy* (submitted to JCSR for publication).

[60]. **Mohamed Ali R.M and Louca L.A (2007b),** *Performance based design of blast resistant offshore Topsides Part II – Modelling and design* (submitted to JCSR for publication).

[61]. Manual of steel construction allowable stress design ninth edition**, AISC (WSD)**, 1991.

[62]. Manual of steel construction, Volume II connections ASD ninth edition /LRFD first edition, AISC 1992.

[63]. **Medonos S and Rogers C. (1998)**, *Optimisation of fire and explosion protection on FPSO.* International Conference on Health, Safety and Environment in Oil and Gas Exploration and Production, Caracas, SPE 46819, 1-14.

[64]. **Moa C, Ricles J, Lu L.W and Fisher J (2001)**, *Effect of local details on ductility of welded moment connections.* Journal of Structural Engineering, 1036-1044.

[65]. **Nurick G.N and Martin J.B (1989),** *Deformation of thin plates subjected to impulsive loading – A review, part I theoretical considerations.* International Journal of Impact Engineering. Vol. 8 No. 2 , 159-170.

[66]. **Neal B.G**, *The plastic methods of structural analysis*. Chapman and Hall 3^{rd} SI Edition

[67]. **N-004** Norsok Standard – *Design of steel structures*, Rev. 1, December 1998

[68] **Ocel J, DesRoches R, Leon R.T, Hess W.G, Krumme R, Hayes J.R and Sweeney S (2004),** *Steel beam-column connection using shape memory alloys.* Journal of Structural Engineering, Vol. 130, Issue 5, 737-740.

[69]. Performance based seismic engineering of buildings, Volume I and II. Structural Engineers Association of California. April, 1995

[70]. Petroleum and natural gas industries- general requirements for offshore structures. **BS EN ISO 19900:2002.**

[71]. Recommended lateral force requirement and commentary. Seismology Committee Structural Engineers Association of California, 7th 1999.

[72]. Recommended practice for planning, designing and constructing fixed offshore platforms – load and resistance factor design 1st edition **API RP2A –LRFD**, 1993.

[73]. Recommended practice for planning, designing and constructing fixed offshore platforms – working stress design 21st edition **API RP2A –WSD**, 2000.

[74]. Recommended practice for the design of offshore facilities against fire and blast loading **API RP 2FB** First Edition 2006.

[75]. Recommendations for performance standards in building: contents and presentation, **BS 6019:1980 / ISO 6240:1980**, British Standard Institution.

[76]. Review of the performance of high strength steels – HSE Report 105.

[77]. **Ricles J.M, Fisher J.W, Lu L.W and Kaufmann (2002)**, *Development of improved welded moment connections for earthquake-resistance design.* Journal of Constructional Steel Research. 58, 565- 604.

[78]. **Riks E (1979)**, *An incremental Approach to the solution of snapping and buckling problems.* International Journal of Solids Structures Vol. 15, 529-551.

[79]. **Rudrapatna N.S, Vaziri R and Olson M.D (2000)**, *Deformation and failure of blast-loaded stiffened plates*. International Journal of Impact Engineering 24, 457-474.

[80]. **Sabuwala T, Linzell D and Krauthammer T (2005),** *Finite element analysis of steel beam to column connections subjected to blast loads.* International Journal of Impact Engineering 31, 2005, 861-876.

[81]. **Scheler,E.A, Salter, H.S, Valdivieso, J.B and Wood, B.J (1991),** *The Modelling of gas explosions and the response of topside structures.* SPE First International Conference on Health, Safety and Environment held in the Hague, The Netherlands, 10-4.

[82]. **Schleyer G.K and Campbell D (1996),** *Development of simplified analytical methods for predicting the response of offshore structures to blast and fire loading,* Marine structures 9, 949-970.

[83]. **Schleyer G.K, Hsu S.S and White M.D (1998)**, *Blast loading of stiffened plates: Experimental, analytical and numerical investigations*. Structures Under Extreme Loading Conditions PVP-Vol. 361, 237- 255.

[84]. **Schleyer G.K, Hsu S.S, White M.D and Birch R.S (2003)**, *Pulse pressure loading of clamped mild steel plates.* International journal of impact engineering 28, 223-247.

[85]. **Schleyer G.K. (2004),** *Simplified analysis of square plates under explosion loading.* Structures under shock and impact VIII, Jones N & Brebbia C.A (Editors), WIT Press, 83-94.

[86]. **Smith P. D and Hetherington J,** *Blast and ballistic loading of structures*, Butterworth-Heinemann, 1994.

[87]. **Smith P. D and Rose T.A (2002),** *Blast loading and building robustness.* Progress in Structural Engineering and Materials 4, 213-223.

[88]. **Structural Sections** in accordance with European Specifications, Corus Construction and Industrial, 2002.

[89]. **Soleiman Fallah A, Mohamed Ali R.M and Louca L.A (2007***)*. *Analytical – numerical study of interfacial stresses in plated beams subjected to pulse loading*, Engineering Structures (article in press).

[90]. **Szilard R**., *Theories and applications of plate analysis*: John Wiley & Sons. Inc, 2004.

[91]. **The building regulation 1991**. www.opsi.gov.uk/SI1991/uksi-19912768-en-1.htm#end

[92]. **Thompson B and Bank L (2006),** *The perception of risk in performance-based design of buildings.* Proceedings of the 2006 Architectural Engineering National Conference, Omaha, Nebraska, USA.

[93]. **Timoshenko S.P and Krieger S.W.,** *Theory of plates and shell*: MCGraw-Hill Int. Ed. Sing. Second Edition, 1959.

[94]. **Vinnem, J.E (2000)**, *Perspective on gas Explosions risk offshore; Low historic gas explosion frequencies revealed in north sea.* SPE International Conference on Health, Safety and Environmental in Oil and Gas Exploration and Production in Stavanger, Norway.

[95]. **Walker S, Bleach R, Carney S, Fairlie G and Louca L.A (2003),** *New guidance on the design of offshore structures to resist the explosion hazards.* Proceedings of OMAE03 22nd International Conference on Offshore Mechanics and Artic Engineering, Cancun, Mexico.

[96]. **Whittaker A, Hamburger R, Comartin C, Mahoney M, Bachman R. and Rojahn C. (2003),** *Performance based engineering of building and infrastructure for extreme loadings.* Proceeding of the 74th Annual Shock and Vibration Symposium, San Diego, California.

[97]. **Williams L.M (1986),** *Feasibility studies for offshore field development.* International Meeting on Petroleum Engineering, Beijing, SPE 14055, 1986, 25-32.

[98]. **Yasseri S (1997),** *Maximising the resistance of topside structure against blast loads.* FABIG newsletter Issue 19, 6-9.

[99]. **Yasseri S (2002)**, *Response of secondary systems to explosions*. FABIG Newsletter, Issue 33, 5-10.

[100]. **Yasseri S (2003a)**, *Probablistic cost-benefit analysis for blast resistant design.* FABIG Newsletter, Issue 34, 9-13.

[101]. **Yasseri S (2003b*),*** *Performance based blast resistant design*, FABIG Newsletter Issue 35, 18-23.

[102]. **Yasseri S and Menhennett P. A (2003)**, *Methodology for performance–based explosion resistant design.* Major Hazards Offshore Conference and Exhibition. Conference Proceedings, Report no: 2003-0548.

[103]. **Yasseri S (2004)**, *Practical blast reistant design of plates (including the effect of changes in geometry) –part 1: Theoretical Background.* FABIG Newsletter Issue 38, 4-11.

[104]. **Yasseri S (2005),** *Iso-damage diagrams for blast resistant design.* FABIG Newsletter Issue 42.

[105]. **Yuen S.C.K and Nurick G.N (2005),** *Experimental and numerical studies on the response of quadrangular stiffened plates.* Part I : Subjected to uniform blast load. International Journal of Impact Engineering 31, 55-83.

APPENDIX A

Adjusted Equipment Loads

This appendix provides calculations for the contents inside equipment which were modelled using ABAQUS program. The total weight inclusive the content is proportioned to the self steel weight (the modelled part) which gives a multiplier factor for density used in the analyses.

a. Horizontal Vessel (Diameter 3.0 m and Length 6.0 m)

Approximate volume $= \frac{\pi}{4} * (3.0)^2 * 6.0 = 42.41 m^3$

Assume 75 % full with crude oil, density $\rho = 900 kg / m^3$

Therefore, the weight of liquid $= 0.75 * 42.41 * 900 = 28626.8 kg$.

Self-weight of vessel = $\pi * t(D - t) * Length * \rho_{steel}$

$$= \pi * 0.04 * (3.0 - 0.04) * 6 * 7850 = 17,519.5 kg$$

The multiplier $= \frac{28626.8 + 17519.5}{17519.5} = 2.63$

Therefore, the adjusted density = $2.63 * 7850 = 20645.5 \frac{kg}{m^3}$

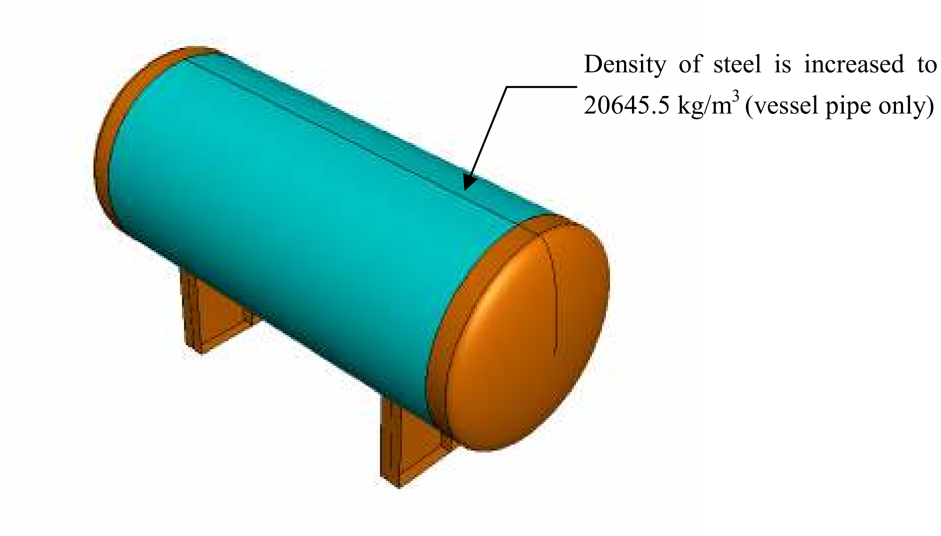

b. Vertical Vessel (Diameter 2.0 m and Length 3.0 m)

Approximate volume = $\frac{\pi}{4} * (2.0)^2 * 3.0 = 9.42m^3$

Assume 75% full with crude oil, density $\rho = 900kg/m^3$

Therefore, weight of liquid = $0.75 * 9.42 * 900 = 6358.5\,kg$

Self-weight of vessel = $\pi * t\,(D - t) * Length * \rho_{steel}$

= $\pi * 0.04 * (2.0 - 0.04) * 3 * 7850 = 5800.4kg$

Diaphragm at the bottom = $\frac{\pi}{4} * 2.0^2 * 0.04 * 7850 = 986.5kg$

The multiplier = $= \frac{6358.5 + 5800.4 + 986.5}{5800.4 + 986.5} = 1.94$

Therefore, the adjusted density = $1.94 * 7850 = 15229\ \frac{kg}{m^3}$

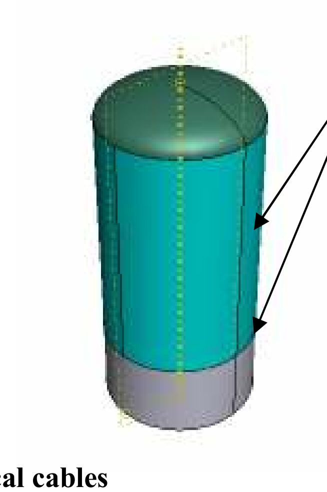

Density is increased to 15229 kg/m^3 (Vertical vessel and the bottom diaphragm only)

c. Electrical cables

The self-weight of cables = $5.0\ kg/m$

The cable tray $= 0.003 * 0.6 * 7850 = 14.13\ kg/m$

The multiplier $= \frac{5 + 14.13}{14.13} = 1.35$

Therefore, the adjusted density = $1.35 * 7850 = 10597.5\ \frac{kg}{m^3}$

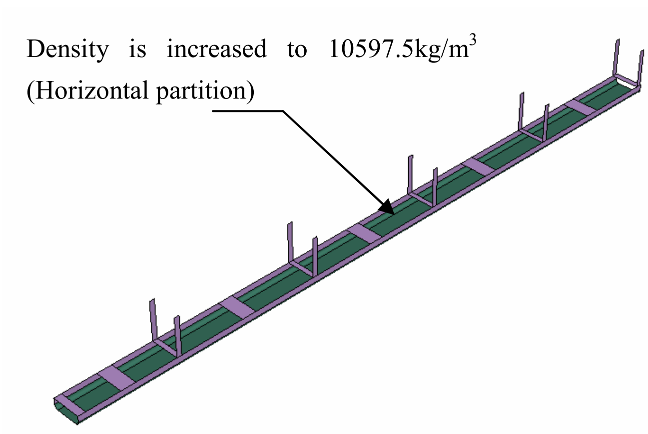

d. Launcher/Receiver

Volume for 610 dia. = $\dfrac{\pi}{4} * 0.610^2 * 6.60 = 1.93m^3$

Volume for 406 dia. = $\dfrac{\pi}{4} * 0.406^2 * 4.410 = 0.57\,m^3$

Total volume = 2.50 m^3

Liquid weight = $0.75 * 900 * 2.50 = 1687.5\ kg$

Self-weight for 610 dia. = $\pi * 0.013 * (0.610 - 0.013) * 6.60 * 7850 = 1263.2kg$

Self-weight for 406 dia. = $\pi * 0.013 * (0.406 - 0.013) * 4.41 * 7850 = 555.64kg$

The multiplier = $= \dfrac{1687.5 + 1263.23 + 555.64}{1263.23 + 555.64} = 1.93$

Therefore, the adjusted density = $1.93 * 7850 = 15150.5\ \dfrac{kg}{m^3}$

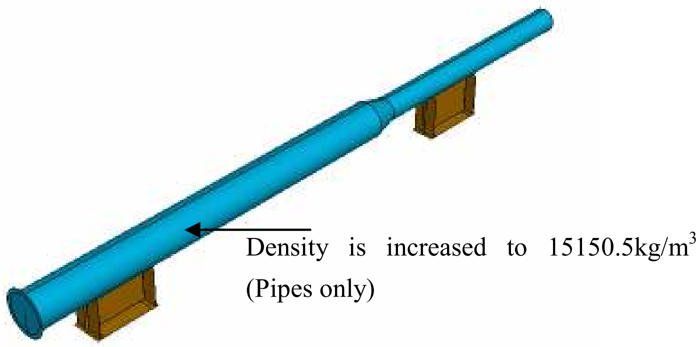

e. Firewater (114 mm dia. 5 mm)

Full area of 114 dia. pipe = $\frac{\pi}{4} * 0.114^2 = 0.0102 m^2$

Area of steel 114 dia. pipe = $= \pi * 0.005 * (0.114 - 0.005) = 0.0017 m^2$

The multiplier $= \frac{(0.0017 * 7850 + 0.0102 * 1025)}{(0.0017 * 7850)} = 1.78$

Therefore, the adjusted density = $= 1.78 * 7850 = 13,973 \frac{kg}{m^3}$

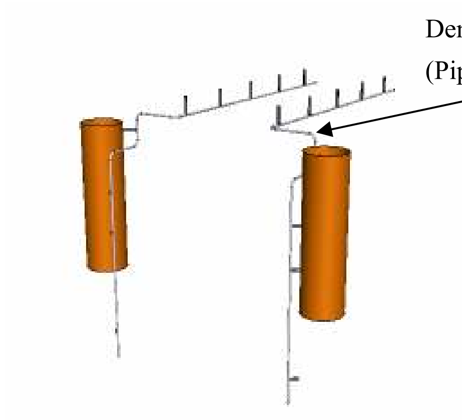

Density is increased to 13973 kg/m^3 (Pipes only)

APPENDIX B

MAPLE'S PROGRAMME CODES FOR DECK PLATE ANALYSIS

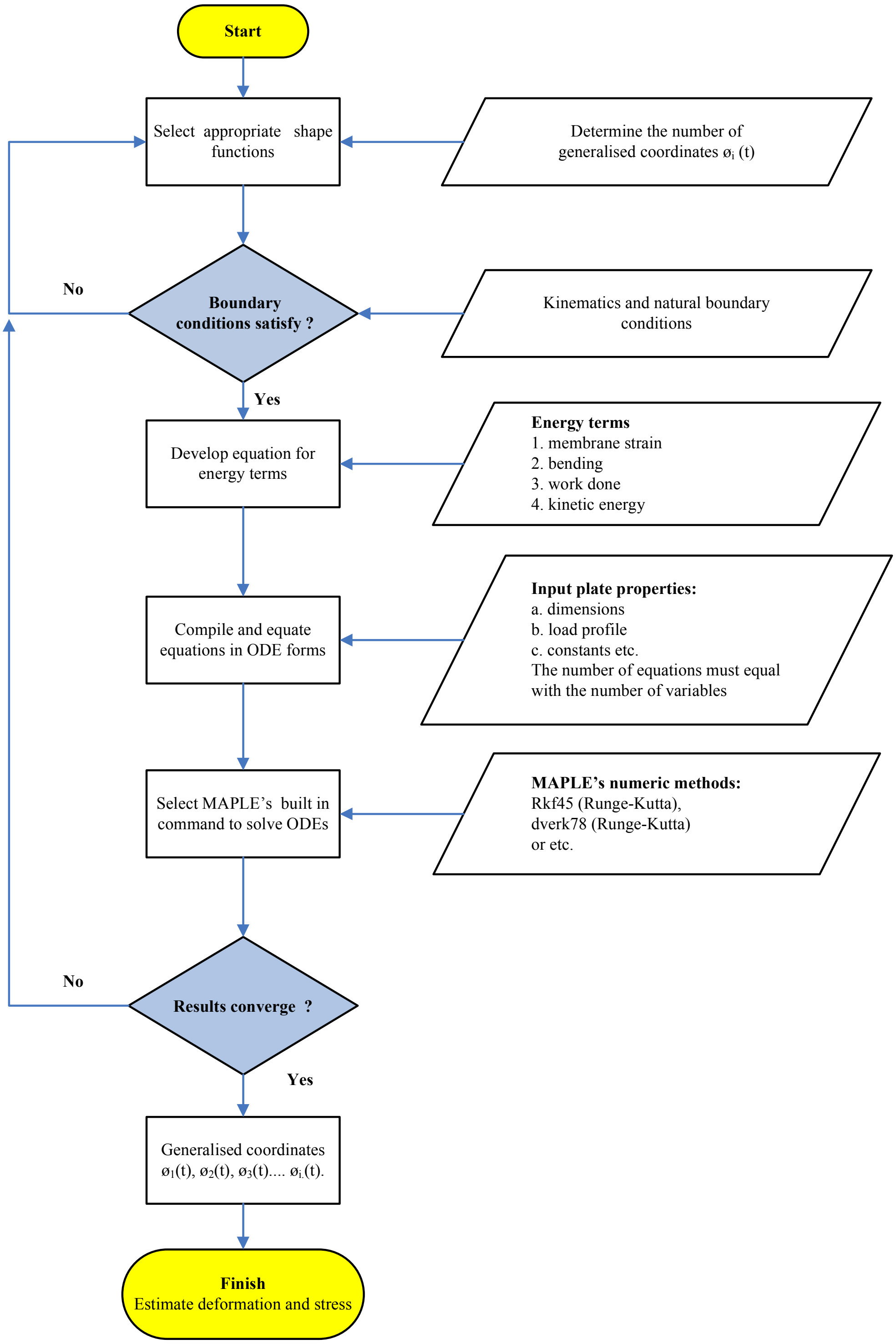

Flow Chart for Deck Plate Analysis Using MAPLE

This file is converted from original MAPLE Version 10.0 worksheet into Microsoft Office Words 2003 documents
The fonts in red are the MAPLE's commands or input data while the fonts in black are comments and some information. The blue fonts are the output.

```
> restart;
```

Title : Performance Based Design - The deck plate analytical model

Subject : **Comparing experiment result with Schleyer et al. (2003)**

This file is created with the following properties :

a. Analysed plate is 2mm thick.

b. The impulse profiles are as follows :

(1) 0 ms , P = 0 bar
(2) 13 ms, P = 0.528571 bar
(3) 35 ms, P = 1.0500bar

(4) 62ms, P = 0.0bar

(5) 100ms, P = 0.0bar

c. Live load :

Not considered

Constant values:

No - inputs are made in the formulations

```
> macro( a1  = phi[1](t),
       a2  = phi[2](t),
       a3  = phi[3](t));
  ES:=2.05e11;             # Young's Modulus
  c:=0.002;                # Plate thickness
  nu:=0.3;                 # Poisson's ratio
  DR:=ES*c^3/(12*(1-nu^2));  # Plate rigidity
  rho:=7850;               # Density
  C1:=ES*c*0.5/(1-nu^2);     # To simplify calculation
```

$$a1, a2, a3$$

$$ES := 2.05\ 10^{11}$$

$$c := 0.002$$

$$\nu := 0.3$$

$$DR := 150.1831502$$

$$\rho := 7850$$

$$C1 := 2.252747252\ 10^8$$

Reference points : centre of the plate

```
> w1:=(x,y,t)->a1*(a^2-x^2)^2*(b^2-y^2)^2;
  u1:=(x,y,t)->a2*x*(a^2-x^2)*(b^2-y^2)-x*0.001/a;
  v1:=(x,y,t)->a3*y*(a^2-x^2)*(b^2-y^2)-y*0.001/b;
```

$$w1 := (x, y, t) \to \phi_1(t)\ (a^2 - x^2)^2\ (b^2 - y^2)^2$$

$$u1 := (x, y, t) \to \phi_2(t)\ x\ (a^2 - x^2)\ (b^2 - y^2) - \frac{x\ 0.001}{a}$$

$$v1 := (x, y, t) \to \phi_3(t)\ y\ (a^2 - x^2)\ (b^2 - y^2) - \frac{y\ 0.001}{b}$$

Derivation of velocities

```
> w2:=diff(w1(x,y,t),t);
  u2:=diff(u1(x,y,t),t);
  v2:=diff(v1(x,y,t),t);
```

$$w2 := \left(\frac{d}{dt}\ \phi_1(t)\right)(a^2 - x^2)^2\ (b^2 - y^2)^2$$

$$u2 := \left(\frac{d}{dt}\ \phi_2(t)\right) x\ (a^2 - x^2)\ (b^2 - y^2)$$

$$v2 := \left(\frac{d}{dt}\ \phi_3(t)\right) y\ (a^2 - x^2)\ (b^2 - y^2)$$

Check boundary conditions
The deck plate is assumed as fixed

```
> BC1_x:=eval(diff(w1(x,y,t),x),x=a);
  BC1_y:=eval(diff(w1(x,y,t),y),y=b);
```

$$BC1\_x := 0$$

$$BC1\_y := 0$$

Potential energy -strain energy due to bending

```
> cd2w_xy2:= (x,y,t)->(diff(w1(x,y,t),x$2) + diff(w1(x,y,t),y$2))^2;
```

$$cd2w\_xy2 := (x, y, t) \rightarrow \left(\frac{\partial^2}{\partial x^2} w1(x, y, t) + \frac{\partial^2}{\partial y^2} w1(x, y, t) \right)^2$$

```
> PE:=(x,y,t)->(0.5*DR)*int(int(cd2w_xy2(x,y,t),x=-a..a),y=-b..b);
  PE1:=eval(simplify((0.5*DR)*int(int(cd2w_xy2(x,y,t),x=-a..a),y=-b..b)));
```

$$PE := (x, y, t) \rightarrow 0.5\, DR \int_{-b}^{b} \int_{-a}^{a} cd2w\_xy2(x, y, t)\, dx\, dy$$

$$PE1 := 1562.286188\, \phi_1(t)^2\, a^5\, b^9 + 892.7349712\, b^7\, \phi_1(t)^2\, a^7 + 1562.286185\, \phi_1(t)^2\, b^5\, a^9$$

Work done - distortation of plate

```
> WD:=(x,y,t)->int(int(q(t)*w1(x,y,t),x=-a..a),y=-b..b);
  WD1:=int(int((q(t)*w1(x,y,t)),x=-a..a),y=-b..b);
```

$$WD := (x, y, t) \rightarrow \int_{-b}^{b} \int_{-a}^{a} q(t)\, w1(x, y, t)\, dx\, dy$$

$$WD1 := \frac{256}{225}\, q(t)\, \phi_1(t)\, a^5\, b^5$$

Membrane strain Energy

```
> epsilon[x]:=(x,y,t)->diff(u1(x,y,t),x)+
                 1/2*(diff(w1(x,y,t),x))^2;
  epsilon[y]:=(x,y,t)->diff(v1(x,y,t),y)+
                 1/2*(diff(w1(x,y,t),y))^2;
  epsilon[xy]:=(x,y,t)->diff(u1(x,y,t),y)
                +diff(v1(x,y,t),x)
                +diff(w1(x,y,t),x)*diff(w1(x,y,t),y);
```

$$\varepsilon_x := (x, y, t) \to \frac{\partial}{\partial x} u1(x, y, t) + \frac{1}{2}\left(\frac{\partial}{\partial x} w1(x, y, t)\right)^2$$

$$\varepsilon_y := (x, y, t) \to \frac{\partial}{\partial y} v1(x, y, t) + \frac{1}{2}\left(\frac{\partial}{\partial y} w1(x, y, t)\right)^2$$

$$\varepsilon_{xy} := (x, y, t) \to \frac{\partial}{\partial y} u1(x, y, t) + \frac{\partial}{\partial x} v1(x, y, t) + \left(\frac{\partial}{\partial x} w1(x, y, t)\right)\left(\frac{\partial}{\partial y} w1(x, y, t)\right)$$

```
> STER1[m1]:=(x,y,t)->int(int(((epsilon[x](x,y,t))^2),y=-b..b),x=-a..a);
  STER[m1]:=simplify(expand(evalf(int(int(((epsilon[x](x,y,t))^2),y=-b..b),x=-a..a))));
```

$$STER1_{m1} := (x, y, t) \to \int_{-a}^{a}\int_{-b}^{b} \varepsilon_x(x, y, t)^2 \, dy \, dx$$

$$STER_{m1} := \frac{1}{a}\left(2.000000000\ 10^{-11}\, b \left(3.268490200\ 10^{10}\, \phi_1(t)^4\, b^{16}\, a^{14}\right.\right.$$

$$+ 500.\, a^{10}\, \phi_1(t)^2\, b^{10}\, \phi_2(t) - 9.9071807\ 10^7\, a^7\, b^8\, \phi_1(t)^2 + 8.533333330\ 10^{10}\, \phi_2(t)^2\, a^6\, b^4$$

$$\left.\left. + 2.00000\ 10^5\right)\right)$$

```
> STER2[m2]:=(x,y,t)->int(int(epsilon[y](x,y,t)^2,y=-b..b),x=-a..a);
  STER[m2]:=expand(evalf(int(int(epsilon[y](x,y,t)^2,y=-b..b),x=-a..a)));
```

$$STER2_{m2} := (x, y, t) \to \int_{-a}^{a}\int_{-b}^{b} \varepsilon_y(x, y, t)^2 \, dy \, dx$$

$$STER_{m2} := 0.65369760\ \phi_1(t)^4\, b^{13}\, a^{17}$$

$$+ 1.706666670\, a^5\, \phi_3(t)^2\, b^5 - 0.001981436130\, a^9\, \phi_1(t)^2\, b^6 - 1.\ 10^{-12}\, a^3\, \phi_3(t)\, b^2$$

$$+ \frac{0.000004000000000\, a}{b}$$

```
> STER3[m3]:=(x,y,t)->2*nu*int(int(epsilon[x](x,y,t)*epsilon[y](x,y,t),
                            y=-b..b),
                            x=-a..a);
  STER[m3]:=expand(evalf(2*nu*int(int(epsilon[x](x,y,t)*epsilon[y](x,y,t),
                            y=-b..b),
                            x=-a..a)));
```

$$STER3_{m3} := (x, y, t) \rightarrow 2\,\nu \int_{-a}^{a} \int_{-b}^{b} \varepsilon_x(x, y, t)\, \varepsilon_y(x, y, t)\, dy\, dx$$

$$STER_{m3} := -0.000594430844\, a^7\, b^8\, \phi_1(t)^2 + 0.079377484\, \phi_1(t)^4\, b^{15}\, a^{15}$$

$$+ 0.288208895\, \phi_2(t)\, a^{11}\, \phi_1(t)^2\, b^9$$

$$+ 0.2882088835\, a^9\, \phi_1(t)^2\, b^{11}\, \phi_3(t) - 0.000594430842\, a^8\, b^7\, \phi_1(t)^2$$

$$+ 0.1706666690\, a^5\, b^5\, \phi_2(t)\, \phi_3(t) - 1.\ 10^{-12}\, a^2\, b^3\, \phi_3(t) + 0.000002400000000$$

```
> STER4[m4]:=(x,y,t)->((1/2)*(1-nu))*int(int(epsilon[xy](x,y,t)^2,
                            y=-b..b),
                            x=-a..a);
  STER[m4]:=expand(evalf(((1/2)*(1-nu))*int(int(epsilon[xy](x,y,t)^2,
                            y=-b..b),
                            x=-a..a)));
```

$$STER4_{m4} := (x, y, t) \rightarrow \frac{1}{2}\,(1 - \nu) \int_{-a}^{a} \int_{-b}^{b} \varepsilon_{xy}(x, y, t)^2\, dy\, dx$$

$$STER_{m4} := 0.18521549\, \phi_1(t)^4\, b^{15}\, a^{15} - 0.168121864\, \phi_2(t)\, a^{11}\, \phi_1(t)^2\, b^9$$

$$- 0.168121846\, a^9\, \phi_1(t)^2\, b^{11}\, \phi_3(t) + 0.1422222227\, a^7\, b^3\, \phi_2(t)^2 + 0.1991111116\, a^5\, b^5\, \phi_2(t)\, \phi_3(t)$$

$$+ 0.1422222224\, a^3\, b^7\, \phi_3(t)^2$$

> CMST1:=eval(simplify((STER[m1]+STER[m2]+ STER[m3]+ STER[m4])*C1));

$$CMST1 := \frac{1}{a\,b}\Big(4.000000000\;10^{-13}\,\big(3.681541158\;10^{20}\,b^{18}\,\phi_1(t)^4\,a^{14}$$
$$+ 5.631868130\;10^{12}\,b^{12}\,a^{10}\,\phi_1(t)^2\,\phi_2(t) - 1.115918705\;10^{18}\,b^{10}\,a^7\,\phi_1(t)^2$$
$$+ 9.611721605\;10^{20}\,b^6\,\phi_2(t)^2\,a^6 + 2.252747252\;10^{15}\,b^2 + 3.681538680\;10^{20}\,\phi_1(t)^4\,b^{14}\,a^{18}$$
$$+ 9.611721628\;10^{20}\,a^6\,\phi_3(t)^2\,b^6 - 1.115918699\;10^{18}\,a^{10}\,\phi_1(t)^2\,b^7 - 5.63186813\;10^8\,a^4\,\phi_3(t)\,b^3$$
$$+ 2.252747252\;10^{15}\,a^2 - 3.347756125\;10^{17}\,a^8\,b^9\,\phi_1(t)^2 + 1.490152738\;10^{20}\,\phi_1(t)^4\,b^{16}\,a^{16}$$
$$+ 6.763143228\;10^{19}\,\phi_2(t)\,a^{12}\,\phi_1(t)^2\,b^{10}$$
$$+ 6.763143592\;10^{19}\,a^{10}\,\phi_1(t)^2\,b^{12}\,\phi_3(t) - 3.347756115\;10^{17}\,a^9\,b^8\,\phi_1(t)^2$$
$$+ 2.082539698\;10^{20}\,a^6\,b^6\,\phi_2(t)\,\phi_3(t) - 5.63186813\;10^8\,a^3\,b^4\,\phi_3(t) + 1.351648351\;10^{15}\,a\,b$$
$$+ 8.009768035\;10^{19}\,a^8\,b^4\,\phi_2(t)^2 + 8.009768018\;10^{19}\,a^4\,b^8\,\phi_3(t)^2\big)\Big)$$

>

Kinetic Energy of plate

> KE2:=(t)->(int(int(((1/2)*rho*c*(w2^2 + u2^2 +v2^2)), x=-a..a),y=-b..b));
> KE21:=eval(simplify(int(int(((1/2)*rho*c*(w2^2 + u2^2 +v2^2)), x=-a..a),y=-b..b)));

>

$$KE2 := t \rightarrow \int_{-b}^{b}\int_{-a}^{a} \frac{1}{2}\,\rho\,c\,(w2^2 + u2^2 + v2^2)\,dx\,dy$$

$$KE21 := 5.184757864\left(\frac{d}{dt}\phi_1(t)\right)^2 a^9\,b^9 + 1.275936508\,b^7\left(\frac{d}{dt}\phi_3(t)\right)^2 a^5$$
$$+ 1.275936505\,b^5\,a^7\left(\frac{d}{dt}\phi_2(t)\right)^2$$

Compling ODEs

```
> # Equation 1
  KE2(t):=simplify(subs({
     a1=a1_1,
     a2=a2_1,
     a3=a3_1,
     diff(a1,t)=a1p,
     diff(a2,t)=a2p,
     diff(a3,t)=a3p},KE2(t)));
  dK_dw1p:=(diff(KE2(t),a1p));
  dK_dw1p:=subs({
     a1_1=a1,
     a2_1=a2,
     a3_1=a3,
     a1p=diff(a1,t),
     a2p=diff(a2,t),
     a3p=diff(a3,t)},dK_dw1p);
  dK2_dw1p:=diff(dK_dw1p,t);
```

$$KE2(t) := 5.184757864\, a1p^2\, a^9\, b^9 + 1.275936508\, b^7\, a3p^2\, a^5 + 1.275936505\, b^5\, a^7\, a2p^2$$

$$dK\_dw1p := 10.36951573\, a1p\, a^9\, b^9$$

$$dK\_dw1p := 10.36951573 \left(\frac{d}{dt}\phi_1(t)\right) a^9\, b^9$$

$$dK2\_dw1p := 10.36951573 \left(\frac{d^2}{dt^2}\phi_1(t)\right) a^9\, b^9$$

```
> CMST1:=(subs({
     a1=a1_1,
     a2=a2_1,
     a3=a3_1,
     diff(a1,t)=a1p,
     diff(a2,t)=a2p,
     diff(a3,t)=a3p},CMST1));
  dCMST_dw1p:=(diff(CMST1,a1_1));
  dCMST_dw1p:=subs({
     a1_1=a1,
     a2_1=a2,
     a3_1=a3,
     a1p=diff(a1,t),
     a2p=diff(a2,t),
     a3p=diff(a3,t)},dCMST_dw1p);
```

$CMST1$

$$:= \frac{1}{a\,b}\,(4.000000000\;10^{-13}\;(3.681541158\;10^{20}\;b^{18}\;a1\_1^{4}\;a^{14}$$

$$+\,5.631868130\;10^{12}\;b^{12}\;a^{10}\;a1\_1^{2}\;a2\_1 - 1.115918705\;10^{18}\;b^{10}\;a^{7}\;a1\_1^{2}$$

$$+\,9.611721605\;10^{20}\;b^{6}\;a2\_1^{2}\;a^{6} + 2.252747252\;10^{15}\;b^{2} + 3.681538680\;10^{20}\;a1\_1^{4}\;b^{14}\;a^{18}$$

$$+\,9.611721628\;10^{20}\;a^{6}\;a3\_1^{2}\;b^{6} - 1.115918699\;10^{18}\;a^{10}\;a1\_1^{2}\;b^{7} - 5.63186813\;10^{8}\;a^{4}\;a3\_1\;b^{3}$$

$$+\,2.252747252\;10^{15}\;a^{2} - 3.347756125\;10^{17}\;a^{8}\;b^{9}\;a1\_1^{2} + 1.490152738\;10^{20}\;a1\_1^{4}\;b^{16}\;a^{16}$$

$$+\,6.763143228\;10^{19}\;a2\_1\;a^{12}\;a1\_1^{2}\;b^{10}$$

$$+\,6.763143592\;10^{19}\;a^{10}\;a1\_1^{2}\;b^{12}\;a3\_1 - 3.347756115\;10^{17}\;a^{9}\;b^{8}\;a1\_1^{2}$$

$$+\,2.082539698\;10^{20}\;a^{6}\;b^{6}\;a2\_1\;a3\_1 - 5.63186813\;10^{8}\;a^{3}\;b^{4}\;a3\_1 + 1.351648351\;10^{15}\;a\,b$$

$$+\,8.009768035\;10^{19}\;a^{8}\;b^{4}\;a2\_1^{2} + 8.009768018\;10^{19}\;a^{4}\;b^{8}\;a3\_1^{2}))$$

$dCMST\_dw1p$

$$:= \frac{1}{a\,b}\,(4.000000000\;10^{-13}\;(1.472616463\;10^{21}\;b^{18}\;a1\_1^{3}\;a^{14}$$

$$+\,1.126373626\;10^{13}\;b^{12}\;a^{10}\;a1\_1\;a2\_1 - 2.231837410\;10^{18}\;b^{10}\;a^{7}\;a1\_1$$

$$+\,1.472615472\;10^{21}\;a1\_1^{3}\;b^{14}\;a^{18} - 2.231837398\;10^{18}\;a^{10}\;a1\_1\;b^{7} - 6.695512250\;10^{17}\;a^{8}\;b^{9}\;a1\_1$$

$$+\,5.960610952\;10^{20}\;a1\_1^{3}\;b^{16}\;a^{16} + 1.352628646\;10^{20}\;a2\_1\;a^{12}\;a1\_1\;b^{10}$$

$$+\,1.352628718\;10^{20}\;a^{10}\;a1\_1\;b^{12}\;a3\_1 - 6.695512230\;10^{17}\;a^{9}\;b^{8}\;a1\_1))$$

$dCMST\_dw1p$

$$:= \frac{1}{a\,b}\left(4.000000000\;10^{-13}\left(1.472616463\;10^{21}\;b^{18}\;\phi_1(t)^{3}\;a^{14}\right.\right.$$

$$+\,1.126373626\;10^{13}\;b^{12}\;a^{10}\;\phi_1(t)\;\phi_2(t) - 2.231837410\;10^{18}\;b^{10}\;a^{7}\;\phi_1(t)$$

$$+\,1.472615472\;10^{21}\;\phi_1(t)^{3}\;b^{14}\;a^{18} - 2.231837398\;10^{18}\;a^{10}\;\phi_1(t)\;b^{7} - 6.695512250\;10^{17}\;a^{8}\;b^{9}\;\phi_1(t)$$

$$+\,5.960610952\;10^{20}\;\phi_1(t)^{3}\;b^{16}\;a^{16} + 1.352628646\;10^{20}\;\phi_2(t)\;a^{12}\;\phi_1(t)\;b^{10}$$

$$+ 1.352628718\ 10^{20}\ a^{10}\ \phi_1(t)\ b^{12}\ \phi_3(t) - 6.695512230\ 10^{17}\ a^9\ b^8\ \phi_1(t)\big)\big)$$

```
> PE1:=(subs({
     a1=a1_1,
     a2=a2_1,
     a3=a3_1,
     diff(a1,t)=a1p,
     diff(a2,t)=a2p,
     diff(a3,t)=a3p},PE1));
  dPE1_dw1p:=(diff(PE1,a1_1));
  dPE1_dw1p:=subs({
     a1_1=a1,
     a2_1=a2,
     a3_1=a3,
     a1p=diff(a1,t),
     a2p=diff(a2,t),
     a3p=diff(a3,t)},dPE1_dw1p);
```

$$PE1 := 1562.286188\ a1\_1^2\ a^5\ b^9 + 892.7349712\ b^7\ a1\_1^2\ a^7 + 1562.286185\ a1\_1^2\ b^5\ a^9$$

$$dPE1\_dw1p := 3124.572376\ a1\_1\ a^5\ b^9 + 1785.469942\ b^7\ a1\_1\ a^7 + 3124.572370\ a1\_1\ b^5\ a^9$$

$$dPE1\_dw1p := 3124.572376\ \phi_1(t)\ a^5\ b^9 + 1785.469942\ b^7\ \phi_1(t)\ a^7 + 3124.572370\ \phi_1(t)\ b^5\ a^9$$

```
> WD1:=(subs({
     a1=a1_1,
     a2=a2_1,
     a3=a3_1,
     diff(a1,t)=a1p,
     diff(a2,t)=a2p,
     diff(a3,t)=a3p},WD1));
  dWD1_dw1p:=(diff(WD1,a1_1));
  dWD1_dw1p:=subs({
     a1_1=a1,
     a2_1=a2,
     a3_1=a3,
     a1p=diff(a1,t),
     a2p=diff(a2,t),
     a3p=diff(a3,t)},dWD1_dw1p);
```

$$WD1 := \frac{256}{225}\ q(t)\ a1\_1\ a^5\ b^5$$

$$dWD1\_dw1p := \frac{256}{225}\ q(t)\ a^5\ b^5$$

$$dWD1\_dw1p := \frac{256}{225}\, q(t)\, a^5\, b^5$$

```
>
> # Equation 2
  KE2(t):=simplify(subs({
      a1=a1_1,
      a2=a2_1,
      a3=a3_1,
      diff(a1,t)=a1p,
      diff(a2,t)=a2p,
      diff(a3,t)=a3p},KE2(t)));
  dK_dw2p:=(diff(KE2(t),a2p));
  dK_dw2p:=subs({
      a1_1=a1,
      a2_1=a2,
      a3_1=a3,
      a1p=diff(a1,t),
      a2p=diff(a2,t),
      a3p=diff(a3,t)},dK_dw2p);
  dK2_dw2p:=diff(dK_dw2p,t);
```

$$KE2(t) := 5.184757864\, a1p^2\, a^9\, b^9 + 1.275936508\, b^7\, a3p^2\, a^5 + 1.275936505\, b^5\, a^7\, a2p^2$$

$$dK\_dw2p := 2.551873010\, b^5\, a^7\, a2p$$

$$dK\_dw2p := 2.551873010\, b^5\, a^7 \left(\frac{d}{dt}\, \phi_2(t)\right)$$

$$dK2\_dw2p := 2.551873010\, b^5\, a^7 \left(\frac{d^2}{dt^2}\, \phi_2(t)\right)$$

```
> CMST1:=(subs({
      a1=a1_1,
      a2=a2_1,
      a3=a3_1,
      diff(a1,t)=a1p,
      diff(a2,t)=a2p,
      diff(a3,t)=a3p},CMST1));
  dCMST_dw2p:=(diff(CMST1,a2_1));
  dCMST_dw2p:=subs({
      a1_1=a1,
      a2_1=a2,
      a3_1=a3,
      a1p=diff(a1,t),
      a2p=diff(a2,t),
      a3p=diff(a3,t)},dCMST_dw2p);
```

$CMST1$

$$:= \frac{1}{a\,b}\,(4.000000000\,10^{-13}\,(3.681541158\,10^{20}\,b^{18}\,a1\_1^4\,a^{14}$$

$$+ 5.631868130\,10^{12}\,b^{12}\,a^{10}\,a1\_1^2\,a2\_1 - 1.115918705\,10^{18}\,b^{10}\,a^7\,a1\_1^2$$

$$+ 9.611721605\,10^{20}\,b^6\,a2\_1^2\,a^6 + 2.252747252\,10^{15}\,b^2 + 3.681538680\,10^{20}\,a1\_1^4\,b^{14}\,a^{18}$$

$$+ 9.611721628\,10^{20}\,a^6\,a3\_1^2\,b^6 - 1.115918699\,10^{18}\,a^{10}\,a1\_1^2\,b^7 - 5.63186813\,10^8\,a^4\,a3\_1\,b^3$$

$$+ 2.252747252\,10^{15}\,a^2 - 3.347756125\,10^{17}\,a^8\,b^9\,a1\_1^2 + 1.490152738\,10^{20}\,a1\_1^4\,b^{16}\,a^{16}$$

$$+ 6.763143228\,10^{19}\,a2\_1\,a^{12}\,a1\_1^2\,b^{10}$$

$$+ 6.763143592\,10^{19}\,a^{10}\,a1\_1^2\,b^{12}\,a3\_1 - 3.347756115\,10^{17}\,a^9\,b^8\,a1\_1^2$$

$$+ 2.082539698\,10^{20}\,a^6\,b^6\,a2\_1\,a3\_1 - 5.63186813\,10^8\,a^3\,b^4\,a3\_1 + 1.351648351\,10^{15}\,a\,b$$

$$+ 8.009768035\,10^{19}\,a^8\,b^4\,a2\_1^2 + 8.009768018\,10^{19}\,a^4\,b^8\,a3\_1^2))$$

$dCMST\_dw2p$

$$:= \frac{1}{a\,b}\,(4.000000000\,10^{-13}\,(5.631868130\,10^{12}\,b^{12}\,a^{10}\,a1\_1^2 + 1.922344321\,10^{21}\,b^6\,a2\_1\,a^6$$

$$+ 6.763143228\,10^{19}\,a^{12}\,a1\_1^2\,b^{10} + 2.082539698\,10^{20}\,a^6\,b^6\,a3\_1 + 1.601953607\,10^{20}\,a^8\,b^4\,a2\_1))$$

$dCMST\_dw2p$

$$:= \frac{1}{a\,b}\left(4.000000000\,10^{-13}\left(5.631868130\,10^{12}\,b^{12}\,a^{10}\,\phi_1(t)^2 + 1.922344321\,10^{21}\,b^6\,\phi_2(t)\,a^6\right.\right.$$

$$\left.\left.+ 6.763143228\,10^{19}\,a^{12}\,\phi_1(t)^2\,b^{10} + 2.082539698\,10^{20}\,a^6\,b^6\,\phi_3(t) + 1.601953607\,10^{20}\,a^8\,b^4\,\phi_2(t)\right)\right)$$

```
> PE1:=(subs({
      a1=a1_1,
      a2=a2_1,
      a3=a3_1,
      diff(a1,t)=a1p,
      diff(a2,t)=a2p,
      diff(a3,t)=a3p},PE1));
  dPE1_dw2p:=(diff(PE1,a2_1));
  dPE1_dw2p:=subs({
```

```
     a1_1=a1,
     a2_1=a2,
     a3_1=a3,
     a1p=diff(a1,t),
     a2p=diff(a2,t),
     a3p=diff(a3,t)},dPE1_dw2p);
```

$$PE1 := 1562.286188\, a1\_1^2\, a^5\, b^9 + 892.7349712\, b^7\, a1\_1^2\, a^7 + 1562.286185\, a1\_1^2\, b^5\, a^9$$

$$dPE1\_dw2p := 0$$

$$dPE1\_dw2p := 0$$

```
> # Equation 3
  KE2(t):=simplify(subs({
     a1=a1_1,
     a2=a2_1,
     a3=a3_1,
     diff(a1,t)=a1p,
     diff(a2,t)=a2p,
     diff(a3,t)=a3p},KE2(t)));
  dK_dw3p:=(diff(KE2(t),a3p));
  dK_dw3p:=subs({
     a1_1=a1,
     a2_1=a2,
     a3_1=a3,
     a1p=diff(a1,t),
     a2p=diff(a2,t),
     a3p=diff(a3,t)},dK_dw3p);
  dK2_dw3p:=diff(dK_dw3p,t);
```

$$KE2(t) := 5.184757864\, a1p^2\, a^9\, b^9 + 1.275936508\, b^7\, a3p^2\, a^5 + 1.275936505\, b^5\, a^7\, a2p^2$$

$$dK\_dw3p := 2.551873016\, b^7\, a3p\, a^5$$

$$dK\_dw3p := 2.551873016\, b^7 \left(\frac{d}{dt}\,\phi_3(t)\right) a^5$$

$$dK2\_dw3p := 2.551873016\, b^7 \left(\frac{d^2}{dt^2}\,\phi_3(t)\right) a^5$$

```
> CMST1:=(subs({
     a1=a1_1,
     a2=a2_1,
     a3=a3_1,
     diff(a1,t)=a1p,
```

```
      diff(a2,t)=a2p,
      diff(a3,t)=a3p},CMST1));
  dCMST_dw3p:=(diff(CMST1,a3_1));
  dCMST_dw3p:=subs({
      a1_1=a1,
      a2_1=a2,
      a3_1=a3,
      a1p=diff(a1,t),
      a2p=diff(a2,t),
      a3p=diff(a3,t)},dCMST_dw3p);
```

$CMST1$

$$:= \frac{1}{a\,b} \left(4.000000000\ 10^{-13} \left(3.681541158\ 10^{20}\, b^{18}\, a1\_1^4\, a^{14} + 5.631868130\ 10^{12}\, b^{12}\, a^{10}\, a1\_1^2\, a2\_1 - 1.115918705\ 10^{18}\, b^{10}\, a^7\, a1\_1^2 + 9.611721605\ 10^{20}\, b^6\, a2\_1^2\, a^6 + 2.252747252\ 10^{15}\, b^2 + 3.681538680\ 10^{20}\, a1\_1^4\, b^{14}\, a^{18} + 9.611721628\ 10^{20}\, a^6\, a3\_1^2\, b^6 - 1.115918699\ 10^{18}\, a^{10}\, a1\_1^2\, b^7 - 5.63186813\ 10^8\, a^4\, a3\_1\, b^3 + 2.252747252\ 10^{15}\, a^2 - 3.347756125\ 10^{17}\, a^8\, b^9\, a1\_1^2 + 1.490152738\ 10^{20}\, a1\_1^4\, b^{16}\, a^{16} + 6.763143228\ 10^{19}\, a2\_1\, a^{12}\, a1\_1^2\, b^{10} + 6.763143592\ 10^{19}\, a^{10}\, a1\_1^2\, b^{12}\, a3\_1 - 3.347756115\ 10^{17}\, a^9\, b^8\, a1\_1^2 + 2.082539698\ 10^{20}\, a^6\, b^6\, a2\_1\, a3\_1 - 5.63186813\ 10^8\, a^3\, b^4\, a3\_1 + 1.351648351\ 10^{15}\, a\, b + 8.009768035\ 10^{19}\, a^8\, b^4\, a2\_1^2 + 8.009768018\ 10^{19}\, a^4\, b^8\, a3\_1^2\right)\right)$$

$dCMST\_dw3p$

$$:= \frac{1}{a\,b} \left(4.000000000\ 10^{-13} \left(1.922344326\ 10^{21}\, a^6\, b^6\, a3\_1 - 5.63186813\ 10^8\, a^4\, b^3 + 6.763143592\ 10^{19}\, b^{12}\, a^{10}\, a1\_1^2 + 2.082539698\ 10^{20}\, b^6\, a2\_1\, a^6 - 5.63186813\ 10^8\, a^3\, b^4 + 1.601953604\ 10^{20}\, a^4\, b^8\, a3\_1\right)\right)$$

$dCMST\_dw3p$

$$:= \frac{1}{a\,b}\left(4.000000000\ 10^{-13}\left(1.922344326\ 10^{21}\ a^6\ b^6\ \phi_3(t) - 5.63186813\ 10^8\ a^4\ b^3\right.\right.$$

$$+ 6.763143592\ 10^{19}\ b^{12}\ a^{10}\ \phi_1(t)^2 + 2.082539698\ 10^{20}\ b^6\ \phi_2(t)\ a^6 - 5.63186813\ 10^8\ a^3\ b^4$$

$$\left.\left.+ 1.601953604\ 10^{20}\ a^4\ b^8\ \phi_3(t)\right)\right)$$

```
> PE1:=(subs({
       a1=a1_1,
       a2=a2_1,
       a3=a3_1,
       diff(a1,t)=a1p,
       diff(a2,t)=a2p,
       diff(a3,t)=a3p},PE1));
  dPE1_dw3p:=(diff(PE1,a3_1));
  dPE1_dw3p:=subs({
       a1_1=a1,
       a2_1=a2,
       a3_1=a3,
       a1p=diff(a1,t),
       a2p=diff(a2,t),
       a3p=diff(a3,t)},dPE1_dw3p);
```

$$PE1 := 1562.286188\ a1\_1^2\ a^5\ b^9 + 892.7349712\ b^7\ a1\_1^2\ a^7 + 1562.286185\ a1\_1^2\ b^5\ a^9$$

$$dPE1\_dw3p := 0$$

$$dPE1\_dw3p := 0$$

```
> ode1:=collect(dK2_dw1p
          +dCMST_dw1p
          +dPE1_dw1p
          -dWD1_dw1p=0.0,
       {diff(phi[1](t),t$2),
        diff(phi[2](t),t$2),
        diff(phi[3](t),t$2),
        diff(phi[1](t),t),
        diff(phi[2](t),t),
        diff(phi[3](t),t)});
```

$$ode1 := 10.36951573\left(\frac{d^2}{dt^2}\phi_1(t)\right)a^9\ b^9 + 3124.572370\ \phi_1(t)\ b^5\ a^9$$

$$+ \frac{1}{a\,b}\left(4.000000000\ 10^{-13}\left(1.472616463\ 10^{21}\ b^{18}\ \phi_1(t)^3\ a^{14}\right.\right.$$

$$+ 1.126373626\ 10^{13}\ b^{12}\ a^{10}\ \phi_1(t)\ \phi_2(t) - 2.231837410\ 10^{18}\ b^{10}\ a^7\ \phi_1(t)$$

$$+ 1.472615472\ 10^{21}\ \phi_1(t)^3\ b^{14}\ a^{18} - 2.231837398\ 10^{18}\ a^{10}\ \phi_1(t)\ b^7 - 6.695512250\ 10^{17}\ a^8\ b^9\ \phi_1(t)$$

$$+ 5.960610952\ 10^{20}\ \phi_1(t)^3\ b^{16}\ a^{16} + 1.352628646\ 10^{20}\ \phi_2(t)\ a^{12}\ \phi_1(t)\ b^{10}$$

$$+ 1.352628718\ 10^{20}\ a^{10}\ \phi_1(t)\ b^{12}\ \phi_3(t) - 6.695512230\ 10^{17}\ a^9\ b^8\ \phi_1(t)\Big)\Big) + 3124.572376\ \phi_1(t)\ a^5\ b^9$$

$$+ 1785.469942\ b^7\ \phi_1(t)\ a^7 - 1.137777778\ q(t)\ a^5\ b^5 = 0.$$

```
> ode2:=collect(dK2_dw2p
            +dCMST_dw2p
            +dPE1_dw2p = 0.0,
   {diff(phi[1](t),t$2),
        diff(phi[2](t),t$2),
        diff(phi[3](t),t$2),
        diff(phi[1](t),t),
        diff(phi[2](t),t),
        diff(phi[3](t),t)});
```

$$ode2 := 2.551873010\ b^5\ a^7\left(\frac{d^2}{dt^2}\phi_2(t)\right)$$

$$+ \frac{1}{a\,b}\Big(4.000000000\ 10^{-13}\Big(5.631868130\ 10^{12}\ b^{12}\ a^{10}\ \phi_1(t)^2 + 1.922344321\ 10^{21}\ b^6\ \phi_2(t)\ a^6$$

$$+ 6.763143228\ 10^{19}\ a^{12}\ \phi_1(t)^2\ b^{10} + 2.082539698\ 10^{20}\ a^6\ b^6\ \phi_3(t) + 1.601953607\ 10^{20}\ a^8\ b^4\ \phi_2(t)\Big)\Big) =$$

$$0.$$

```
> ode3:=collect(dK2_dw3p
            +dCMST_dw3p
            +dPE1_dw3p = 0.0,
        {diff(phi[1](t),t$2),
        diff(phi[2](t),t$2),
        diff(phi[3](t),t$2),
        diff(phi[1](t),t),
        diff(phi[2](t),t),
        diff(phi[3](t),t)});
```

$$ode3 := 2.551873016\ b^7\left(\frac{d^2}{dt^2}\phi_3(t)\right)a^5$$

$$+\frac{1}{a\,b}\left(4.000000000\ 10^{-13}\left(1.922344326\ 10^{21}\,a^6\,b^6\,\phi_3(t) - 5.63186813\ 10^8\,a^4\,b^3\right.\right.$$

$$+ 6.763143592\ 10^{19}\,b^{12}\,a^{10}\,\phi_1(t)^2 + 2.082539698\ 10^{20}\,b^6\,\phi_2(t)\,a^6 - 5.63186813\ 10^8\,a^3\,b^4$$

$$\left.\left.+ 1.601953604\ 10^{20}\,a^4\,b^8\,\phi_3(t)\right)\right) = 0.$$

Specify the plate dimensions and plotting blast load profile

```
> a:=0.5;
  b:=0.5;
  t1:=0.013;
  t2:=0.0350;
  td:=0.0620;
  tlast:=0.35;
  p1:=52857;
  pmax:=105000;
  q:=t->piecewise(t>0  and t<=t1, (p1*t/t1),
           t>t1 and t<=t2, (p1+(t-t1)*(pmax-p1)/(t2-t1)),
           t>t2 and t<=td,pmax*(td-t)/(td-t2),
           t>td,0);
  plot(q(t),t=0.0..0.1,labels=["time (s)","Pressure (Pa)"]);
  initial_conditions:=phi[1](0)=0,
               phi[2](0)=0,
               phi[3](0)=0,
               D(phi[1])(0)=0,
               D(phi[2])(0)=0,
               D(phi[3])(0)=0;
  solution1:=dsolve({ode1,ode2,ode3,initial_conditions},
               {phi[1](t),phi[2](t),phi[3](t)},type=numeric, maxfun=0);
```

$$a := 0.5$$

$$b := 0.5$$

$$t1 := 0.013$$

$$t2 := 0.0350$$

$$td := 0.0620$$

$$tlast := 0.35$$

$$p1 := 52857$$

$$pmax := 105000$$

$$q := t \rightarrow piecewise\left(0 < t \text{ and } t \leq t1, \frac{p1\, t}{t1}, t1 < t \text{ and } t \leq t2, p1 + \frac{(t - t1)(pmax - p1)}{t2 - t1}, t2 < t \text{ and } t \leq td, \frac{pmax\,(td - t)}{td - t2}, td < t, 0\right)$$

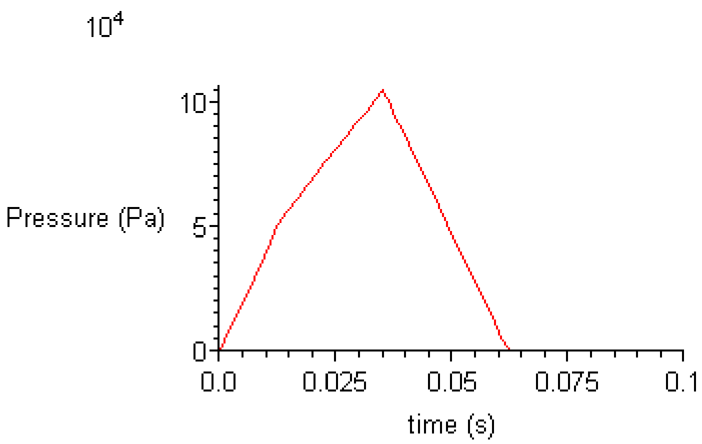

$$initial\_conditions := \phi_1(0) = 0, \phi_2(0) = 0, \phi_3(0) = 0, (D(\phi_1))(0) = 0, (D(\phi_2))(0) = 0, (D(\phi_3))(0) = 0$$

$$solution1 := \textbf{proc}(x\_rkf45) \;\ldots\textbf{end proc}$$

```
> x:=0:y:=0:
  Gr_w1:=seq([n/1000,rhs(solution1(n/1000)[2])*1000*((a^2-x^2)^2)*((b^2-y^2)^2)],n=0..100):
  Gr_u1:=seq([n/1000,rhs(solution1(n/1000)[4])],n=0..100):
  Gr_v1:=seq([n/1000,rhs(solution1(n/1000)[6])],n=0..100):
  curve1:=[Gr_w1]:
  curve2:=[Gr_u1]:
  curve3:=[Gr_v1]:
  plot(curve1,labels=["time (s)"," w"],title="Maximum Displacement-Z",
  titlefont=[times,bold,11]);
  max(seq(op(2,op(i,curve1)),i=1..100));
  min(seq(op(2,op(i,curve1)),i=1..100));
  Disp:=fopen(Platedisp,WRITE,TEXT):
  writedata(Disp,curve1):
  fclose(Disp):
  plot(curve2,labels=["time (s)"," u"],title="Maximum Displacement-X",
  titlefont=[times,bold,11]);
```

```
max(seq(op(2,op(i,curve2)),i=1..100));
min(seq(op(2,op(i,curve2)),i=1..100));
plot(curve3,labels=["time (s)"," v"],title="Maximum Displacement-Y",
titlefont=[times,bold,11]);
max(seq(op(2,op(i,curve3)),i=1..100));
min(seq(op(2,op(i,curve3)),i=1..100));
```

Maximum Displacement-Z

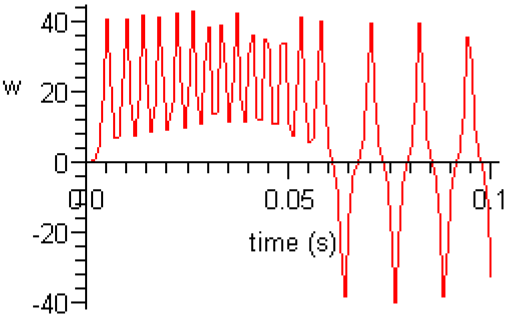

42.93800457

−40.47483137

0.

−0.00349345965272592408

Maximum Displacement-Y

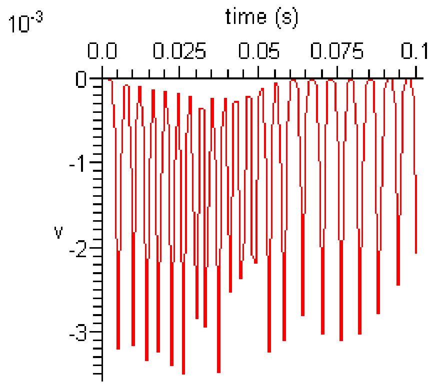

−0.00349345949072226012

Maximum Displacement-X

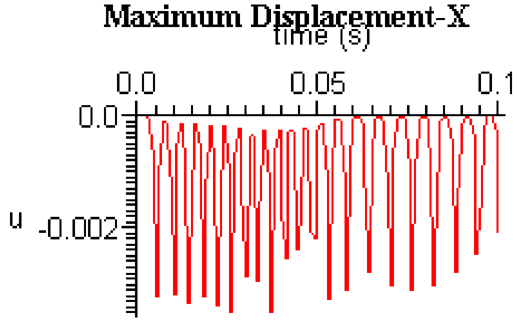

>

```
> restart;
```

Performance Based Design

Simplified deck plate analysis - Static case

Plate 4m x 1m

Design load 10 kN/m2 + selfweight = 10.885kN/m2

Constants values

This file for plate :

8mm thk <= = = =The selected thickness

10mm thk

12mm thk

Plate is mild steel.

```
> macro( a1  = phi[1],
        a2  = phi[2],
        a3  = phi[3]);
   ES:=2.05e11;              # Young's Modulus
   c:=0.0080;                # Plate thickness
   nu:=0.3;                  # Poisson's Ratio
   DR:=ES*c^3/(12*(1-nu^2));  # Plate rigidity
   rho:=7850;                # density
   C1:=ES*c*0.5/(1-nu^2);     # combined const for cacls.
```

$$a1, a2, a3$$

$$2.05\ 10^{11}$$

$$0.0080$$

$$0.3$$

$$9611.721612$$

$$7850$$

$$9.010989010\ 10^{8}$$

Reference points : centre of the plate

Generalised displacement functions

```
> w1:=(x,y)->a1*(a^2-x^2)^2*(b^2-y^2)^2;
  u1:=(x,y)->a2*x*(a^2-x^2)*(b^2-y^2);
  v1:=(x,y)->a3*y*(a^2-x^2)*(b^2-y^2);
```

$$(x, y) \to \phi_1\,(a^2 - x^2)^2\,(b^2 - y^2)^2$$

$$(x, y) \to \phi_2\,x\,(a^2 - x^2)\,(b^2 - y^2)$$

$$(x, y) \to \phi_3\,y\,(a^2 - x^2)\,(b^2 - y^2)$$

Check boundary conditions
Fixed end conditions- therefore the first derivaties against x and y =0

```
> BC1_x:=eval(diff(w1(x,y,t),x),x=a);
  BC1_y:=eval(diff(w1(x,y,t),y),y=b);
```

$$0$$

$$0$$

Potential energy -strain energy due to bending

```
> cd2w_xy2:= (x,y)->(diff(w1(x,y),x$2) + diff(w1(x,y),y$2))^2;
```

$$(x, y) \to \left(\frac{\partial^2}{\partial x^2}\,w1(x, y) + \frac{\partial^2}{\partial y^2}\,w1(x, y)\right)^2$$

```
> PE:=(x,y)->(0.5*DR)*int(int(cd2w_xy2(x,y),x=-a..a),y=-b..b);
```

PE1:=eval(simplify((0.5*DR)*int(int(cd2w_xy2(x,y),x=-a..a),y=-b..b)));

$$(x, y) \rightarrow 0.5\, DR \int_{-b}^{b} \int_{-a}^{a} cd2w\_xy2(x, y)\, dx\, dy$$

$$99986.31514\, \phi_1^2\, a^5\, b^9 + 57135.03692\, b^7\, \phi_1^2\, a^7 + 99986.31526\, \phi_1^2\, b^5\, a^9$$

Work done - distortation of plate

```
> WD:=(x,y)->int(int(q(t)*w1(x,y),x=-a..a),y=-b..b);
  WD1:=int(int((q*w1(x,y)),x=-a..a),y=-b..b);
```

$$(x, y) \rightarrow \int_{-b}^{b} \int_{-a}^{a} q(t)\, w1(x, y)\, dx\, dy$$

$$\frac{256}{225}\, q\, \phi_1\, a^5\, b^5$$

Membrane strain Energy

```
> epsilon[x]:=(x,y,t)->diff(u1(x,y),x)+
                1/2*(diff(w1(x,y),x))^2;
  epsilon[y]:=(x,y,t)->diff(v1(x,y),y)+
                1/2*(diff(w1(x,y),y))^2;
  epsilon[xy]:=(x,y,t)->diff(u1(x,y),y)
               +diff(v1(x,y),x)
               +diff(w1(x,y),x)*diff(w1(x,y),y);
```

$$(x, y, t) \rightarrow \frac{\partial}{\partial x} u1(x, y) + \frac{1}{2} \left(\frac{\partial}{\partial x} w1(x, y) \right)^2$$

$$(x, y, t) \rightarrow \frac{\partial}{\partial y} v1(x, y) + \frac{1}{2} \left(\frac{\partial}{\partial y} w1(x, y) \right)^2$$

$$(x, y, t) \rightarrow \frac{\partial}{\partial y} u1(x, y) + \frac{\partial}{\partial x} v1(x, y) + \left(\frac{\partial}{\partial x} w1(x, y) \right) \left(\frac{\partial}{\partial y} w1(x, y) \right)$$

```
> STER1[m1]:=(x,y)->int(int(((epsilon[x](x,y))^2),y=-b..b),x=-a..a);
  STER[m1]:=simplify(expand(evalf(int(int(((epsilon[x](x,y))^2),y=-b..b),x=-a..a))));
```

$$(x, y) \rightarrow \int_{-a}^{a} \int_{-b}^{b} \varepsilon_x(x, y)^2 \, dy \, dx$$

$$0.6536981100\, \phi_1^4\, b^{17}\, a^{13} + 1.000000000\; 10^{-8}\, a^9\, \phi_1^2\, b^{11}\, \phi_2 + 1.706666665\, \phi_2^2\, a^5\, b^5$$

```
> STER2[m2]:=(x,y)->int(int(epsilon[y](x,y)^2,y=-b..b),x=-a..a);
  STER[m2]:=expand(evalf(int(int(epsilon[y](x,y)^2,y=-b..b),x=-a..a)));
```

$$(x, y) \rightarrow \int_{-a}^{a} \int_{-b}^{b} \varepsilon_y(x, y)^2 \, dy \, dx$$

$$0.65369762\, \phi_1^4\, b^{13}\, a^{17} + 3.066666667\; 10^{-8}\, a^{11}\, \phi_3\, b^9\, \phi_1^2 + 1.706666664\, \phi_3^2\, a^5\, b^5$$

```
> STER3[m3]:=(x,y)->2*nu*int(int(epsilon[x](x,y)*epsilon[y](x,y),
                            y=-b..b),
                            x=-a..a);
  STER[m3]:=expand(evalf(2*nu*int(int(epsilon[x](x,y)*epsilon[y](x,y),
                            y=-b..b),
                            x=-a..a)));
```

$$(x, y) \rightarrow 2\,\nu \int_{-a}^{a} \int_{-b}^{b} \varepsilon_x(x, y)\, \varepsilon_y(x, y) \, dy \, dx$$

$$0.079377725\, \phi_1^4\, b^{15}\, a^{15} + 0.288208898\, \phi_2\, a^{11}\, \phi_1^2\, b^9 + 0.288208891\, a^9\, \phi_1^2\, b^{11}\, \phi_3 + 0.1706666680\, \phi_2\, a^5\, \phi_3\, b^5$$

```
> STER4[m4]:=(x,y)->((1/2)*(1-nu))*int(int(epsilon[xy](x,y)^2,
                            y=-b..b),
                            x=-a..a);
  STER[m4]:=expand(evalf(((1/2)*(1-nu))*int(int(epsilon[xy](x,y)^2,
                            y=-b..b),
                            x=-a..a)));
```

$$(x, y) \rightarrow \frac{1}{2}(1-\nu)\int_{-a}^{a}\int_{-b}^{b} \varepsilon_{xy}(x, y)^2 \, dy \, dx$$

$$0.18521549\ \phi_1^4 b^{15} a^{15} - 0.168121864\ \phi_2 a^{11} \phi_1^2 b^9 - 0.168121846\ a^9 \phi_1^2 b^{11} \phi_3 + 0.1422222227\ a^7 b^3 \phi_2^2 + 0.1991111116\ \phi_2 a^5 \phi_3 b^5 + 0.1422222224\ a^3 b^7 \phi_3^2$$

```
> CMST1:=eval(simplify((STER[m1]+STER[m2]+ STER[m3]+ STER[m4])*C1));
```

$$5.890466485\ 10^8\ \phi_1^4 b^{17} a^{13} + 9.010989010\ a^9 \phi_1^2 b^{11} \phi_2 + 1.537875456\ 10^9\ \phi_2^2 a^5 b^5 + 5.89046207\ 10^8\ \phi_1^4 b^{13} a^{17} + 27.63369963\ a^{11} \phi_3 b^9 \phi_1^2 + 1.537875455\ 10^9\ \phi_3^2 a^5 b^5 + 2.384246552\ 10^8\ \phi_1^4 b^{15} a^{15} + 1.082102944\ 10^8\ \phi_2 a^{11} \phi_1^2 b^9 + 1.082103043\ 10^8\ a^9 \phi_1^2 b^{11} \phi_3 + 3.332063508\ 10^8\ \phi_2 a^5 \phi_3 b^5 + 1.281562886\ 10^8\ a^7 b^3 \phi_2^2 + 1.281562883\ 10^8\ a^3 b^7 \phi_3^2$$

Equation 1 - Ordinary Differential Equation

```
> CMST1:=(subs({
    a1=a1_1,
    a2=a2_1,
    a3=a3_1},CMST1));
  dCMST_dw1p:=(diff(CMST1,a1_1));
  dCMST_dw1p:=subs({
    a1_1=a1,
    a2_1=a2,
    a3_1=a3},dCMST_dw1p);
```

$$5.890466485\ 10^8\ a1\_1^4 b^{17} a^{13} + 9.010989010\ a^9\ a1\_1^2 b^{11}\ a2\_1 + 1.537875456\ 10^9\ a2\_1^2 a^5 b^5 + 5.89046207\ 10^8\ a1\_1^4 b^{13} a^{17} + 27.63369963\ a^{11}\ a3\_1\ b^9\ a1\_1^2 + 1.537875455\ 10^9\ a3\_1^2 a^5 b^5 + 2.384246552\ 10^8\ a1\_1^4 b^{15} a^{15} + 1.082102944\ 10^8\ a2\_1\ a^{11}\ a1\_1^2 b^9 + 1.082103043\ 10^8\ a^9\ a1\_1^2 b^{11}\ a3\_1 + 3.332063508\ 10^8\ a2\_1\ a^5\ a3\_1\ b^5 + 1.281562886\ 10^8\ a^7 b^3\ a2\_1^2 + 1.281562883\ 10^8\ a^3 b^7\ a3\_1^2$$

$$2.356186594\ 10^9\ a1\_1^3 b^{17} a^{13} + 18.02197802\ a^9\ a1\_1\ b^{11}\ a2\_1 + 2.356184828\ 10^9\ a1\_1^3 b^{13} a^{17} + 55.26739926\ a^{11}\ a3\_1\ b^9\ a1\_1 + 9.536986208\ 10^8\ a1\_1^3 b^{15} a^{15} + 2.164205888\ 10^8\ a2\_1\ a^{11}\ a1\_1\ b^9 + 2.164206086\ 10^8\ a^9\ a1\_1\ b^{11}\ a3\_1$$

$$2.356186594\ 10^{9}\ \phi_1^3\ b^{17}\ a^{13} + 18.02197802\ a^{9}\ \phi_1\ b^{11}\ \phi_2 + 2.356184828\ 10^{9}\ \phi_1^3\ b^{13}\ a^{17} + 55.26739926\ a^{11}\ \phi_3\ b^{9}\ \phi_1 + 9.536986208\ 10^{8}\ \phi_1^3\ b^{15}\ a^{15} + 2.164205888\ 10^{8}\ \phi_2\ a^{11}\ \phi_1\ b^{9} + 2.164206086\ 10^{8}\ a^{9}\ \phi_1\ b^{11}\ \phi_3$$

```
> PE1:=(subs({
      a1=a1_1,
      a2=a2_1,
      a3=a3_1},PE1));
  dPE1_dw1p:=(diff(PE1,a1_1));
  dPE1_dw1p:=subs({
      a1_1=a1,
      a2_1=a2,
      a3_1=a3},dPE1_dw1p);
```

$$99986.31514\ a1\_1^{2}\ a^{5}\ b^{9} + 57135.03692\ b^{7}\ a1\_1^{2}\ a^{7} + 99986.31526\ a1\_1^{2}\ b^{5}\ a^{9}$$

$$1.999726303\ 10^{5}\ a1\_1\ a^{5}\ b^{9} + 1.142700738\ 10^{5}\ b^{7}\ a1\_1\ a^{7} + 1.999726305\ 10^{5}\ a1\_1\ b^{5}\ a^{9}$$

$$1.999726303\ 10^{5}\ \phi_1\ a^{5}\ b^{9} + 1.142700738\ 10^{5}\ b^{7}\ \phi_1\ a^{7} + 1.999726305\ 10^{5}\ \phi_1\ b^{5}\ a^{9}$$

```
> WD1:=(subs({
      a1=a1_1,
      a2=a2_1,
      a3=a3_1},WD1));
  dWD1_dw1p:=(diff(WD1,a1_1));
  dWD1_dw1p:=subs({
      a1_1=a1,
      a2_1=a2,
      a3_1=a3},dWD1_dw1p);
```

$$\frac{256}{225}\ q\ a1\_1\ a^{5}\ b^{5}$$

$$\frac{256}{225}\ q\ a^{5}\ b^{5}$$

$$\frac{256}{225}\ q\ a^{5}\ b^{5}$$

Equation 2 - Ordinary Differential Equation

```
> CMST1:=(subs({
     a1=a1_1,
     a2=a2_1,
     a3=a3_1},CMST1));
  dCMST_dw2p:=(diff(CMST1,a2_1));
  dCMST_dw2p:=subs({
     a1_1=a1,
     a2_1=a2,
     a3_1=a3},dCMST_dw2p);
```

$$5.890466485\ 10^8\, a1\_1^4\, b^{17}\, a^{13} + 9.010989010\, a^9\, a1\_1^2\, b^{11}\, a2\_1 + 1.537875456\ 10^9\, a2\_1^2\, a^5\, b^5 + 5.89046207\ 10^8\, a1\_1^4\, b^{13}\, a^{17} + 27.63369963\, a^{11}\, a3\_1\, b^9\, a1\_1^2 + 1.537875455\ 10^9\, a3\_1^2\, a^5\, b^5 + 2.384246552\ 10^8\, a1\_1^4\, b^{15}\, a^{15} + 1.082102944\ 10^8\, a2\_1\, a^{11}\, a1\_1^2\, b^9 + 1.082103043\ 10^8\, a^9\, a1\_1^2\, b^{11}\, a3\_1 + 3.332063508\ 10^8\, a2\_1\, a^5\, a3\_1\, b^5 + 1.281562886\ 10^8\, a^7\, b^3\, a2\_1^2 + 1.281562883\ 10^8\, a^3\, b^7\, a3\_1^2$$

$$9.010989010\, a^9\, a1\_1^2\, b^{11} + 3.075750912\ 10^9\, a2\_1\, a^5\, b^5 + 1.082102944\ 10^8\, a^{11}\, a1\_1^2\, b^9 + 3.332063508\ 10^8\, a^5\, a3\_1\, b^5 + 2.563125772\ 10^8\, a^7\, b^3\, a2\_1$$

$$9.010989010\, a^9\, \phi_1^2\, b^{11} + 3.075750912\ 10^9\, \phi_2\, a^5\, b^5 + 1.082102944\ 10^8\, a^{11}\, \phi_1^2\, b^9 + 3.332063508\ 10^8\, a^5\, \phi_3\, b^5 + 2.563125772\ 10^8\, a^7\, b^3\, \phi_2$$

```
> PE1:=(subs({
     a1=a1_1,
     a2=a2_1,
     a3=a3_1},PE1));
  dPE1_dw2p:=(diff(PE1,a2_1));
  dPE1_dw2p:=subs({
     a1_1=a1,
     a2_1=a2,
     a3_1=a3},dPE1_dw2p);
```

$$99986.31514\, a1\_1^2\, a^5\, b^9 + 57135.03692\, b^7\, a1\_1^2\, a^7 + 99986.31526\, a1\_1^2\, b^5\, a^9$$

$$0$$

$$0$$

Equation 3 - Ordinary Differential Equation

```
> CMST1:=(subs({
      a1=a1_1,
      a2=a2_1,
      a3=a3_1},CMST1));
  dCMST_dw3p:=(diff(CMST1,a3_1));
  dCMST_dw3p:=subs({
      a1_1=a1,
      a2_1=a2,
      a3_1=a3},dCMST_dw3p);
```

$$5.890466485\ 10^8\ a1\_1^4\ b^{17}\ a^{13} + 9.010989010\ a^9\ a1\_1^2\ b^{11}\ a2\_1 + 1.537875456\ 10^9\ a2\_1^2\ a^5\ b^5 + 5.89046207\ 10^8\ a1\_1^4\ b^{13}\ a^{17} + 27.63369963\ a^{11}\ a3\_1\ b^9\ a1\_1^2 + 1.537875455\ 10^9\ a3\_1^2\ a^5\ b^5 + 2.384246552\ 10^8\ a1\_1^4\ b^{15}\ a^{15} + 1.082102944\ 10^8\ a2\_1\ a^{11}\ a1\_1^2\ b^9 + 1.082103043\ 10^8\ a^9\ a1\_1^2\ b^{11}\ a3\_1 + 3.332063508\ 10^8\ a2\_1\ a^5\ a3\_1\ b^5 + 1.281562886\ 10^8\ a^7\ b^3\ a2\_1^2 + 1.281562883\ 10^8\ a^3\ b^7\ a3\_1^2$$

$$27.63369963\ a^{11}\ a1\_1^2\ b^9 + 3.075750910\ 10^9\ a^5\ a3\_1\ b^5 + 1.082103043\ 10^8\ a^9\ a1\_1^2\ b^{11} + 3.332063508\ 10^8\ a2\_1\ a^5\ b^5 + 2.563125766\ 10^8\ a^3\ b^7\ a3\_1$$

$$27.63369963\ a^{11}\ \phi_1^2\ b^9 + 3.075750910\ 10^9\ a^5\ \phi_3\ b^5 + 1.082103043\ 10^8\ a^9\ \phi_1^2\ b^{11} + 3.332063508\ 10^8\ \phi_2\ a^5\ b^5 + 2.563125766\ 10^8\ a^3\ b^7\ \phi_3$$

```
> PE1:=(subs({
      a1=a1_1,
      a2=a2_1,
      a3=a3_1,
      diff(a1,t)=a1p,
      diff(a2,t)=a2p,
      diff(a3,t)=a3p},PE1));
  dPE1_dw3p:=(diff(PE1,a3_1));
  dPE1_dw3p:=subs({
      a1_1=a1,
      a2_1=a2,
      a3_1=a3,
      a1p=diff(a1,t),
      a2p=diff(a2,t),
      a3p=diff(a3,t)},dPE1_dw3p);
```

$$99986.31514\ a1\_1^2\ a^5\ b^9 + 57135.03692\ b^7\ a1\_1^2\ a^7 + 99986.31526\ a1\_1^2\ b^5\ a^9$$

$$0$$

$$0$$

> a:=2.0; b:=0.5;q:=10.885e3;

$$2.0$$

$$0.5$$

$$10885.$$

> ode1:=dCMST_dw1p+dPE1_dw1p-dWD1_dw1p=0.0;

$$3.879991753\ 10^{10}\ \phi_1^3 + 8.656823597\ 10^{8}\ \phi_1\ \phi_2 + 5.410537322\ 10^{7}\ \phi_3\ \phi_1 + 3.326330451\ 10^{6}\ \phi_1 - 12384.71111 = 0.$$

> ode2:=dCMST_dw2p+dPE1_dw2p =0.0;

$$4.328411799\ 10^{8}\ \phi_1^2 + 7.176752147\ 10^{9}\ \phi_2 + 3.332063508\ 10^{8}\ \phi_3 = 0.$$

> ode3:=dCMST_dw3p+dPE1_dw3p = 0.0;

$$2.705268661\ 10^{7}\ \phi_1^2 + 3.091770446\ 10^{9}\ \phi_3 + 3.332063508\ 10^{8}\ \phi_2 = 0.$$

> S1:=solve({ode2,ode3},{phi[2],phi[3]});

$$\{\phi_3 = -0.002261316700\,\phi_1^2,\ \phi_2 = -0.06020657896\,\phi_1^2\}$$

```
> phi[3]:=-0.2261316699e-2*phi[1]^2;phi[2]:=-0.6020657892e-1*phi[1]^2;
  ode1:=dCMST_dw1p+dPE1_dw1p-dWD1_dw1p=0.0;
```

$$-0.002261316699\,\phi_1^2$$

$$-0.06020657892\,\phi_1^2$$

$$3.874767541\ 10^{10}\,\phi_1^3 + 3.326330451\ 10^6\,\phi_1 - 12384.71111 = 0.$$

```
> K1:=evalf(fsolve(ode1,phi[1]));
```

$$0.003303340680$$

```
> phi[1]:=K1;'phi[2]'=phi[2];'phi[3]'=phi[3];x:=0.0;y:=0;'q'=q;'thickness'=c;
  Static_Deflection:=a1*(a^2-x^2)^2*(b^2-y^2)^2;
  u1:=a2*x*(a^2-x^2)*(b^2-y^2);
  v1:=a3*y*(a^2-x^2)*(b^2-y^2);;
```

$$0.003303340680$$

$$\phi_2 = -6.569777805\ 10^{-7}$$

$$\phi_3 = -2.467562271\ 10^{-8}$$

$$0.$$

$$0$$

$$q = 10885.$$

$$thickness = 0.0080$$

$$0.003303340680$$

$$-0.$$

$$-0.$$

>

```
> restart;
```

Performance Based Design - Dynamic Analysis
This file is created for the following plates :

Pl 8mm thickness < = = = Selected Analysis

Pl 10mm thickness

Pl 12mm thickness

The impulse under investigation is as follows :

(a) Pmax = 0.5bar, td = 175ms, Return Period = 500yrs <= = = Selected for Analysis

(b) Pmax = 1.0bar, td = 157ms, Return Period = 1,000yrs

(c) Pmax = 1.5bar, td = 140ms, Return Period = 5,000yrs

(d) Pmax = 1.5bar, td = 140ms, Return Period = 100,000yrs

Live load :

Considered

Not considered = = => Yes

Constants values

```
> macro( a1  = phi[1](t),
       a2  = phi[2](t),
       a3  = phi[3](t));
  ES:=2.05e11;              # Young's Modulus
  c:=0.008;                 # Plate thickness
  nu:=0.3;                  # Poisson's ratio
  DR:=ES*c^3/(12*(1-nu^2));   # Plate rigidity
  rho:=7850;                # Density
  C1:=ES*c*0.5/(1-nu^2);      # Simplify
```

$$a1, a2, a3$$

$$ES := 2.05\ 10^{11}$$

$$c := 0.008$$

$$\nu := 0.3$$

$$DR := 9611.721612$$

$$\rho := 7850$$

$$C1 := 9.010989010\ 10^8$$

Reference points : centre of the plate

```
> w1:=(x,y,t)->a1*(a^2-x^2)^2*(b^2-y^2)^2;
  u1:=(x,y,t)->a2*x*(a^2-x^2)*(b^2-y^2);
  v1:=(x,y,t)->a3*y*(a^2-x^2)*(b^2-y^2);
```

$$w1 := (x, y, t) \to \phi_1(t)\left(a^2 - x^2\right)^2 \left(b^2 - y^2\right)^2$$

$$u1 := (x, y, t) \to \phi_2(t)\, x \left(a^2 - x^2\right) \left(b^2 - y^2\right)$$

$$v1 := (x, y, t) \to \phi_3(t)\, y \left(a^2 - x^2\right) \left(b^2 - y^2\right)$$

Velocity

```
> w2:=diff(w1(x,y,t),t);
  u2:=diff(u1(x,y,t),t);
  v2:=diff(v1(x,y,t),t);
```

$$w2 := \left(\frac{d}{dt}\phi_1(t)\right)\left(a^2 - x^2\right)^2 \left(b^2 - y^2\right)^2$$

$$u2 := \left(\frac{d}{dt}\phi_2(t)\right) x \left(a^2 - x^2\right) \left(b^2 - y^2\right)$$

$$v2 := \left(\frac{d}{dt}\phi_3(t)\right) y \left(a^2 - x^2\right) \left(b^2 - y^2\right)$$

Check boundary conditions
-assumed as fixed

```
> BC1_x:=eval(diff(w1(x,y,t),x),x=a);
  BC1_y:=eval(diff(w1(x,y,t),y),y=b);
```

$$BC1\_x := 0$$

$$BC1\_y := 0$$

Potential energy -strain energy due to bending

```
> cd2w_xy2:= (x,y,t)->(diff(w1(x,y,t),x$2) + diff(w1(x,y,t),y$2))^2;
```

$$cd2w\_xy2 := (x, y, t) \to \left(\frac{\partial^2}{\partial x^2} w1(x, y, t) + \frac{\partial^2}{\partial y^2} w1(x, y, t) \right)^2$$

```
> PE:=(x,y,t)->(0.5*DR)*int(int(cd2w_xy2(x,y,t),x=-a..a),y=-b..b);
  PE1:=eval(simplify((0.5*DR)*int(int(cd2w_xy2(x,y,t),x=-a..a),y=-b..b)));
```

$$PE := (x, y, t) \to 0.5\, DR \int_{-b}^{b} \int_{-a}^{a} cd2w\_xy2(x, y, t)\, dx\, dy$$

$$PE1 := 99986.31514\, \phi_1(t)^2 a^5 b^9 + 57135.03692\, b^7 \phi_1(t)^2 a^7 + 99986.31526\, \phi_1(t)^2 b^5 a^9$$

Work done - distortation of plate

```
> WD:=(x,y,t)->int(int(q(t)*w1(x,y,t),x=-a..a),y=-b..b);
  WD1:=int(int((q(t)*w1(x,y,t)),x=-a..a),y=-b..b);
```

$$WD := (x, y, t) \to \int_{-b}^{b} \int_{-a}^{a} q(t)\, w1(x, y, t)\, dx\, dy$$

$$WD1 := \frac{256}{225} q(t)\, \phi_1(t)\, a^5 b^5$$

Membrane strain Energy

```
> epsilon[x]:=(x,y,t)->diff(u1(x,y,t),x)+
                  1/2*(diff(w1(x,y,t),x))^2;
  epsilon[y]:=(x,y,t)->diff(v1(x,y,t),y)+
                  1/2*(diff(w1(x,y,t),y))^2;
  epsilon[xy]:=(x,y,t)->diff(u1(x,y,t),y)
                 +diff(v1(x,y,t),x)
                 +diff(w1(x,y,t),x)*diff(w1(x,y,t),y);
```

$$\epsilon_x := (x, y, t) \to \frac{\partial}{\partial x} u1(x, y, t) + \frac{1}{2}\left(\frac{\partial}{\partial x} w1(x, y, t)\right)^2$$

$$\epsilon_y := (x, y, t) \to \frac{\partial}{\partial y} v1(x, y, t) + \frac{1}{2}\left(\frac{\partial}{\partial y} w1(x, y, t)\right)^2$$

$$\epsilon_{xy} := (x, y, t) \to \frac{\partial}{\partial y} u1(x, y, t) + \frac{\partial}{\partial x} v1(x, y, t) + \left(\frac{\partial}{\partial x} w1(x, y, t)\right)\left(\frac{\partial}{\partial y} w1(x, y, t)\right)$$

```
> STER1[m1]:=(x,y,t)->int(int(((epsilon[x](x,y,t))^2),y=-b..b),x=-a..a);
  STER[m1]:=simplify(expand(evalf(int(int(((epsilon[x](x,y,t))^2),y=-b..b),x=-a..a))));
```

$$STER1_{m1} := (x, y, t) \to \int_{-a}^{a}\int_{-b}^{b} \epsilon_x(x, y, t)^2 \, dy \, dx$$

$$STER_{m1} := 0.65369811\, \phi_1(t)^4 b^{17} a^{13} + 1.\, 10^{-8} a^9 \phi_1(t)^2 b^{11} \phi_2(t) + 1.706666665\, \phi_2(t)^2 a^5 b^5$$

```
> STER2[m2]:=(x,y,t)->int(int(epsilon[y](x,y,t)^2,y=-b..b),x=-a..a);
  STER[m2]:=expand(evalf(int(int(epsilon[y](x,y,t)^2,y=-b..b),x=-a..a)));
```

$$STER2_{m2} := (x, y, t) \to \int_{-a}^{a}\int_{-b}^{b} \epsilon_y(x, y, t)^2 \, dy \, dx$$

$$STER_{m2} := 0.65369762\, \phi_1(t)^4 b^{13} a^{17} + 3.066666667\, 10^{-8} a^{11} \phi_3(t) b^9 \phi_1(t)^2 + 1.706666664\, \phi_3(t)^2 a^5 b^5$$

```
> STER3[m3]:=(x,y,t)->2*nu*int(int(epsilon[x](x,y,t)*epsilon[y](x,y,t),
                       y=-b..b),
                       x=-a..a);
  STER[m3]:=expand(evalf(2*nu*int(int(epsilon[x](x,y,t)*epsilon[y](x,y,t),
                       y=-b..b),
                       x=-a..a)));
```

$$STER3_{m3} := (x, y, t) \to 2\,\nu \int_{-a}^{a}\int_{-b}^{b} \epsilon_x(x, y, t)\, \epsilon_y(x, y, t) \, dy \, dx$$

$$STER_{m3} := 0.079377725\,\phi_1(t)^4\,b^{15}\,a^{15} + 0.288208898\,\phi_2(t)\,a^{11}\,\phi_1(t)^2\,b^9$$
$$+ 0.288208891\,a^9\,\phi_1(t)^2\,b^{11}\,\phi_3(t) + 0.1706666680\,\phi_2(t)\,a^5\,\phi_3(t)\,b^5$$

```
> STER4[m4]:=(x,y,t)->((1/2)*(1-nu))*int(int(epsilon[xy](x,y,t)^2,
                               y=-b..b),
                               x=-a..a);
  STER[m4]:=expand(evalf(((1/2)*(1-nu))*int(int(epsilon[xy](x,y,t)^2,
                               y=-b..b),
                               x=-a..a)));
```

$$STER4_{m4} := (x, y, t) \rightarrow \frac{1}{2}(1-\nu)\int_{-a}^{a}\int_{-b}^{b} \varepsilon_{xy}(x, y, t)^2\,dy\,dx$$

$$STER_{m4} := 0.18521549\,\phi_1(t)^4\,b^{15}\,a^{15} - 0.168121864\,\phi_2(t)\,a^{11}\,\phi_1(t)^2\,b^9$$
$$- 0.168121846\,a^9\,\phi_1(t)^2\,b^{11}\,\phi_3(t) + 0.1422222227\,a^7\,b^3\,\phi_2(t)^2 + 0.1991111116\,\phi_2(t)\,a^5\,\phi_3(t)\,b^5$$
$$+ 0.1422222224\,a^3\,b^7\,\phi_3(t)^2$$

```
> CMST1:=eval(simplify((STER[m1]+STER[m2]+ STER[m3]+ STER[m4])*C1));
```

$$CMST1 := 5.890466485\,10^8\,\phi_1(t)^4\,b^{17}\,a^{13} + 9.010989010\,a^9\,\phi_1(t)^2\,b^{11}\,\phi_2(t)$$
$$+ 1.537875456\,10^9\,\phi_2(t)^2\,a^5\,b^5 + 5.890462070\,10^8\,\phi_1(t)^4\,b^{13}\,a^{17} + 27.63369963\,a^{11}\,\phi_3(t)\,b^9\,\phi_1(t)^2$$
$$+ 1.537875455\,10^9\,\phi_3(t)^2\,a^5\,b^5 + 2.384246552\,10^8\,\phi_1(t)^4\,b^{15}\,a^{15}$$
$$+ 1.082102944\,10^8\,\phi_2(t)\,a^{11}\,\phi_1(t)^2\,b^9 + 1.082103043\,10^8\,a^9\,\phi_1(t)^2\,b^{11}\,\phi_3(t)$$
$$+ 3.332063508\,10^8\,\phi_2(t)\,a^5\,\phi_3(t)\,b^5 + 1.281562886\,10^8\,a^7\,b^3\,\phi_2(t)^2 + 1.281562883\,10^8\,a^3\,b^7\,\phi_3(t)^2$$

>

Kinetic Energy of plate

```
> KE2:=(t)->(int(int(((1/2)*rho*c*(w2^2 + u2^2 +v2^2)), x=-a..a),y=-b..b));
```

```
> KE21:=eval(simplify(int(int(((1/2)*rho*c*(w2^2 + u2^2 +v2^2)), x=-a..a),y=-b..b)));
>
```

$$KE2 := t \rightarrow \int_{-b}^{b} \int_{-a}^{a} \frac{1}{2} \rho c \left(w2^2 + u2^2 + v2^2 \right) dx\, dy$$

$$KE21 := 20.73903157 \left(\frac{d}{dt} \phi_1(t) \right)^2 a^9 b^9 + 5.103746032 b^7 \left(\frac{d}{dt} \phi_3(t) \right)^2 a^5$$
$$+ 5.103746020 b^5 a^7 \left(\frac{d}{dt} \phi_2(t) \right)^2$$

```
> # Equation 1
  KE2(t):=simplify(subs({
     a1=a1_1,
     a2=a2_1,
     a3=a3_1,
     diff(a1,t)=a1p,
     diff(a2,t)=a2p,
     diff(a3,t)=a3p},KE2(t)));
  dK_dw1p:=(diff(KE2(t),a1p));
  dK_dw1p:=subs({
     a1_1=a1,
     a2_1=a2,
     a3_1=a3,
     a1p=diff(a1,t),
     a2p=diff(a2,t),
     a3p=diff(a3,t)},dK_dw1p);
  dK2_dw1p:=diff(dK_dw1p,t);
```

$$KE2(t) := 20.73903157\, a1p^2 a^9 b^9 + 5.103746032 b^7\, a3p^2 a^5 + 5.103746020 b^5 a^7\, a2p^2$$

$$dK\_dw1p := 41.47806314\, a1p\, a^9 b^9$$

$$dK\_dw1p := 41.47806314 \left(\frac{d}{dt} \phi_1(t) \right) a^9 b^9$$

$$dK2\_dw1p := 41.47806314 \left(\frac{d^2}{dt^2} \phi_1(t) \right) a^9 b^9$$

```
> CMST1:=(subs({
     a1=a1_1,
     a2=a2_1,
     a3=a3_1,
     diff(a1,t)=a1p,
     diff(a2,t)=a2p,
     diff(a3,t)=a3p},CMST1));
  dCMST_dw1p:=(diff(CMST1,a1_1));
  dCMST_dw1p:=subs({
     a1_1=a1,
     a2_1=a2,
     a3_1=a3,
     a1p=diff(a1,t),
     a2p=diff(a2,t),
     a3p=diff(a3,t)},dCMST_dw1p);
```

$$CMST1 := 5.890466485\ 10^{8}\ a1\_1^{4}\ b^{17}\ a^{13} + 9.010989010\ a^{9}\ a1\_1^{2}\ b^{11}\ a2\_1 + 1.537875456\ 10^{9}\ a2\_1^{2}\ a^{5}\ b^{5} + 5.890462070\ 10^{8}\ a1\_1^{4}\ b^{13}\ a^{17} + 27.63369963\ a^{11}\ a3\_1\ b^{9}\ a1\_1^{2} + 1.537875455\ 10^{9}\ a3\_1^{2}\ a^{5}\ b^{5} + 2.384246552\ 10^{8}\ a1\_1^{4}\ b^{15}\ a^{15} + 1.082102944\ 10^{8}\ a2\_1\ a^{11}\ a1\_1^{2}\ b^{9} + 1.082103043\ 10^{8}\ a^{9}\ a1\_1^{2}\ b^{11}\ a3\_1 + 3.332063508\ 10^{8}\ a2\_1\ a^{5}\ a3\_1\ b^{5} + 1.281562886\ 10^{8}\ a^{7}\ b^{3}\ a2\_1^{2} + 1.281562883\ 10^{8}\ a^{3}\ b^{7}\ a3\_1^{2}$$

$$dCMST\_dw1p := 2.356186594\ 10^{9}\ a1\_1^{3}\ b^{17}\ a^{13} + 18.02197802\ a^{9}\ a1\_1\ b^{11}\ a2\_1 + 2.356184828\ 10^{9}\ a1\_1^{3}\ b^{13}\ a^{17} + 55.26739926\ a^{11}\ a3\_1\ b^{9}\ a1\_1 + 9.536986208\ 10^{8}\ a1\_1^{3}\ b^{15}\ a^{15} + 2.164205888\ 10^{8}\ a2\_1\ a^{11}\ a1\_1\ b^{9} + 2.164206086\ 10^{8}\ a^{9}\ a1\_1\ b^{11}\ a3\_1$$

$$dCMST\_dw1p := 2.356186594\ 10^{9}\ \phi_1(t)^{3}\ b^{17}\ a^{13} + 18.02197802\ a^{9}\ \phi_1(t)\ b^{11}\ \phi_2(t) + 2.356184828\ 10^{9}\ \phi_1(t)^{3}\ b^{13}\ a^{17} + 55.26739926\ a^{11}\ \phi_3(t)\ b^{9}\ \phi_1(t) + 9.536986208\ 10^{8}\ \phi_1(t)^{3}\ b^{15}\ a^{15} + 2.164205888\ 10^{8}\ \phi_2(t)\ a^{11}\ \phi_1(t)\ b^{9} + 2.164206086\ 10^{8}\ a^{9}\ \phi_1(t)\ b^{11}\ \phi_3(t)$$

```
> PE1:=(subs({
     a1=a1_1,
     a2=a2_1,
     a3=a3_1,
     diff(a1,t)=a1p,
```

```
        diff(a2,t)=a2p,
        diff(a3,t)=a3p},PE1));
  dPE1_dw1p:=(diff(PE1,a1_1));
  dPE1_dw1p:=subs({
        a1_1=a1,
        a2_1=a2,
        a3_1=a3,
        a1p=diff(a1,t),
        a2p=diff(a2,t),
        a3p=diff(a3,t)},dPE1_dw1p);
```

$$PE1 := 99986.31514\, a1\_1^2\, a^5\, b^9 + 57135.03692\, b^7\, a1\_1^2\, a^7 + 99986.31526\, a1\_1^2\, b^5\, a^9$$

$$dPE1\_dw1p := 1.999726303\ 10^5\, a1\_1\, a^5\, b^9 + 1.142700738\ 10^5\, b^7\, a1\_1\, a^7 + 1.999726305\ 10^5\, a1\_1\, b^5\, a^9$$

$$dPE1\_dw1p := 1.999726303\ 10^5\, \phi_1(t)\, a^5\, b^9 + 1.142700738\ 10^5\, b^7\, \phi_1(t)\, a^7 + 1.999726305\ 10^5\, \phi_1(t)\, b^5\, a^9$$

```
> WD1:=(subs({
        a1=a1_1,
        a2=a2_1,
        a3=a3_1,
        diff(a1,t)=a1p,
        diff(a2,t)=a2p,
        diff(a3,t)=a3p},WD1));
  dWD1_dw1p:=(diff(WD1,a1_1));
  dWD1_dw1p:=subs({
        a1_1=a1,
        a2_1=a2,
        a3_1=a3,
        a1p=diff(a1,t),
        a2p=diff(a2,t),
        a3p=diff(a3,t)},dWD1_dw1p);
```

$$WD1 := \frac{256}{225}\, q(t)\, a1\_1\, a^5\, b^5$$

$$dWD1\_dw1p := \frac{256}{225}\, q(t)\, a^5\, b^5$$

$$dWD1\_dw1p := \frac{256}{225}\, q(t)\, a^5\, b^5$$

```
>
```

```
> # Equation 2
  KE2(t):=simplify(subs({
      a1=a1_1,
      a2=a2_1,
      a3=a3_1,
      diff(a1,t)=a1p,
      diff(a2,t)=a2p,
      diff(a3,t)=a3p},KE2(t)));
  dK_dw2p:=(diff(KE2(t),a2p));
  dK_dw2p:=subs({
      a1_1=a1,
      a2_1=a2,
      a3_1=a3,
      a1p=diff(a1,t),
      a2p=diff(a2,t),
      a3p=diff(a3,t)},dK_dw2p);
  dK2_dw2p:=diff(dK_dw2p,t);
```

$$KE2(t) := 20.73903157\, a1p^2\, a^9\, b^9 + 5.103746032\, b^7\, a3p^2\, a^5 + 5.103746020\, b^5\, a^7\, a2p^2$$

$$dK\_dw2p := 10.20749204\, b^5\, a^7\, a2p$$

$$dK\_dw2p := 10.20749204\, b^5\, a^7 \left(\frac{d}{dt}\phi_2(t)\right)$$

$$dK2\_dw2p := 10.20749204\, b^5\, a^7 \left(\frac{d^2}{dt^2}\phi_2(t)\right)$$

```
> CMST1:=(subs({
      a1=a1_1,
      a2=a2_1,
      a3=a3_1,
      diff(a1,t)=a1p,
      diff(a2,t)=a2p,
      diff(a3,t)=a3p},CMST1));
  dCMST_dw2p:=(diff(CMST1,a2_1));
  dCMST_dw2p:=subs({
      a1_1=a1,
      a2_1=a2,
      a3_1=a3,
      a1p=diff(a1,t),
      a2p=diff(a2,t),
      a3p=diff(a3,t)},dCMST_dw2p);
```

$$CMST1 := 5.890466485\, 10^8\, a1\_1^4\, b^{17}\, a^{13} + 9.010989010\, a^9\, a1\_1^2\, b^{11}\, a2\_1 + 1.537875456\, 10^9\, a2\_1^2\, a^5\, b^5$$
$$+ 5.890462070\, 10^8\, a1\_1^4\, b^{13}\, a^{17} + 27.63369963\, a^{11}\, a3\_1\, b^9\, a1\_1^2 + 1.537875455\, 10^9\, a3\_1^2\, a^5\, b^5$$

$$+ 2.384246552\ 10^8\ a1\_1^4\ b^{15}\ a^{15} + 1.082102944\ 10^8\ a2\_1\ a^{11}\ a1\_1^2\ b^9$$

$$+ 1.082103043\ 10^8\ a^9\ a1\_1^2\ b^{11}\ a3\_1 + 3.332063508\ 10^8\ a2\_1\ a^5\ a3\_1\ b^5$$

$$+ 1.281562886\ 10^8\ a^7\ b^3\ a2\_1^2 + 1.281562883\ 10^8\ a^3\ b^7\ a3\_1^2$$

$$dCMST\_dw2p := 9.010989010\ a^9\ a1\_1^2\ b^{11} + 3.075750912\ 10^9\ a2\_1\ a^5\ b^5 + 1.082102944\ 10^8\ a^{11}\ a1\_1^2\ b^9$$

$$+ 3.332063508\ 10^8\ a^5\ a3\_1\ b^5 + 2.563125772\ 10^8\ a^7\ b^3\ a2\_1$$

$$dCMST\_dw2p := 9.010989010\ a^9\ \phi_1(t)^2\ b^{11} + 3.075750912\ 10^9\ \phi_2(t)\ a^5\ b^5 + 1.082102944\ 10^8\ a^{11}\ \phi_1(t)^2\ b^9$$

$$+ 3.332063508\ 10^8\ a^5\ \phi_3(t)\ b^5 + 2.563125772\ 10^8\ a^7\ b^3\ \phi_2(t)$$

```
> PE1:=(subs({
     a1=a1_1,
     a2=a2_1,
     a3=a3_1,
     diff(a1,t)=a1p,
     diff(a2,t)=a2p,
     diff(a3,t)=a3p},PE1));
  dPE1_dw2p:=(diff(PE1,a2_1));
  dPE1_dw2p:=subs({
     a1_1=a1,
     a2_1=a2,
     a3_1=a3,
     a1p=diff(a1,t),
     a2p=diff(a2,t),
     a3p=diff(a3,t)},dPE1_dw2p);
```

$$PE1 := 99986.31514\ a1\_1^2\ a^5\ b^9 + 57135.03692\ b^7\ a1\_1^2\ a^7 + 99986.31526\ a1\_1^2\ b^5\ a^9$$

$$dPE1\_dw2p := 0$$

$$dPE1\_dw2p := 0$$

```
> # Equation 3
  KE2(t):=simplify(subs({
     a1=a1_1,
     a2=a2_1,
     a3=a3_1,
     diff(a1,t)=a1p,
     diff(a2,t)=a2p,
```

```
    diff(a3,t)=a3p},KE2(t)));
  dK_dw3p:=(diff(KE2(t),a3p));
  dK_dw3p:=subs({
    a1_1=a1,
    a2_1=a2,
    a3_1=a3,
    a1p=diff(a1,t),
    a2p=diff(a2,t),
    a3p=diff(a3,t)},dK_dw3p);
  dK2_dw3p:=diff(dK_dw3p,t);
```

$$KE2(t) := 20.73903157\, a1p^2\, a^9\, b^9 + 5.103746032\, b^7\, a3p^2\, a^5 + 5.103746020\, b^5\, a^7\, a2p^2$$

$$dK\_dw3p := 10.20749206\, b^7\, a3p\, a^5$$

$$dK\_dw3p := 10.20749206\, b^7 \left(\frac{d}{dt}\,\phi_3(t)\right) a^5$$

$$dK2\_dw3p := 10.20749206\, b^7 \left(\frac{d^2}{dt^2}\,\phi_3(t)\right) a^5$$

```
> CMST1:=(subs({
    a1=a1_1,
    a2=a2_1,
    a3=a3_1,
    diff(a1,t)=a1p,
    diff(a2,t)=a2p,
    diff(a3,t)=a3p},CMST1));
  dCMST_dw3p:=(diff(CMST1,a3_1));
  dCMST_dw3p:=subs({
    a1_1=a1,
    a2_1=a2,
    a3_1=a3,
    a1p=diff(a1,t),
    a2p=diff(a2,t),
    a3p=diff(a3,t)},dCMST_dw3p);
```

$$CMST1 := 5.890466485\; 10^8\, a1\_1^4\, b^{17}\, a^{13} + 9.010989010\, a^9\, a1\_1^2\, b^{11}\, a2\_1 + 1.537875456\; 10^9\, a2\_1^2\, a^5\, b^5$$

$$+ 5.890462070\; 10^8\, a1\_1^4\, b^{13}\, a^{17} + 27.63369963\, a^{11}\, a3\_1\, b^9\, a1\_1^2 + 1.537875455\; 10^9\, a3\_1^2\, a^5\, b^5$$

$$+ 2.384246552\; 10^8\, a1\_1^4\, b^{15}\, a^{15} + 1.082102944\; 10^8\, a2\_1\, a^{11}\, a1\_1^2\, b^9$$

$$+ 1.082103043\; 10^8\, a^9\, a1\_1^2\, b^{11}\, a3\_1 + 3.332063508\; 10^8\, a2\_1\, a^5\, a3\_1\, b^5$$

$$+ 1.281562886\ 10^8\ a^7\ b^3\ a2\_1^2 + 1.281562883\ 10^8\ a^3\ b^7\ a3\_1^2$$

$$dCMST\_dw3p := 27.63369963\ a^{11}\ a1\_1^2\ b^9 + 3.075750910\ 10^9\ a^5\ a3\_1\ b^5 + 1.082103043\ 10^8\ a^9\ a1\_1^2\ b^{11}$$
$$+ 3.332063508\ 10^8\ a2\_1\ a^5\ b^5 + 2.563125766\ 10^8\ a^3\ b^7\ a3\_1$$

$$dCMST\_dw3p := 27.63369963\ a^{11}\ \phi_1(t)^2\ b^9 + 3.075750910\ 10^9\ a^5\ \phi_3(t)\ b^5 + 1.082103043\ 10^8\ a^9\ \phi_1(t)^2\ b^{11}$$
$$+ 3.332063508\ 10^8\ \phi_2(t)\ a^5\ b^5 + 2.563125766\ 10^8\ a^3\ b^7\ \phi_3(t)$$

```
> PE1:=(subs({
      a1=a1_1,
      a2=a2_1,
      a3=a3_1,
      diff(a1,t)=a1p,
      diff(a2,t)=a2p,
      diff(a3,t)=a3p},PE1));
  dPE1_dw3p:=(diff(PE1,a3_1));
  dPE1_dw3p:=subs({
      a1_1=a1,
      a2_1=a2,
      a3_1=a3,
      a1p=diff(a1,t),
      a2p=diff(a2,t),
      a3p=diff(a3,t)},dPE1_dw3p);
```

$$PE1 := 99986.31514\ a1\_1^2\ a^5\ b^9 + 57135.03692\ b^7\ a1\_1^2\ a^7 + 99986.31526\ a1\_1^2\ b^5\ a^9$$

$$dPE1\_dw3p := 0$$

$$dPE1\_dw3p := 0$$

```
> ode1:=collect(dK2_dw1p
          +dCMST_dw1p
          +dPE1_dw1p
          -dWD1_dw1p=0.0,
        {diff(phi[1](t),t$2),
         diff(phi[2](t),t$2),
         diff(phi[3](t),t$2),
         diff(phi[1](t),t),
         diff(phi[2](t),t),
         diff(phi[3](t),t)});
```

$$ode1 := 41.47806314\left(\frac{d^2}{dt^2}\phi_1(t)\right)a^9\,b^9 + 55.26739926\,a^{11}\,\phi_3(t)\,b^9\,\phi_1(t)$$
$$+ 2.356186594\,10^9\,\phi_1(t)^3\,b^{17}\,a^{13} + 18.02197802\,a^9\,\phi_1(t)\,b^{11}\,\phi_2(t) + 2.356184828\,10^9\,\phi_1(t)^3\,b^{13}\,a^{17}$$
$$+ 1.999726303\,10^5\,\phi_1(t)\,a^5\,b^9 + 9.536986208\,10^8\,\phi_1(t)^3\,b^{15}\,a^{15} + 2.164205888\,10^8\,\phi_2(t)\,a^{11}\,\phi_1(t)\,b^9$$
$$+ 2.164206086\,10^8\,a^9\,\phi_1(t)\,b^{11}\,\phi_3(t) + 1.142700738\,10^5\,b^7\,\phi_1(t)\,a^7$$
$$+ 1.999726305\,10^5\,\phi_1(t)\,b^5\,a^9 - 1.137777778\,q(t)\,a^5\,b^5 = 0.$$

```
> ode2:=collect(dK2_dw2p
            +dCMST_dw2p
            +dPE1_dw2p = 0.0,
  {diff(phi[1](t),t$2),
        diff(phi[2](t),t$2),
        diff(phi[3](t),t$2),
        diff(phi[1](t),t),
        diff(phi[2](t),t),
        diff(phi[3](t),t)});
```

$$ode2 := 10.20749204\,b^5\,a^7\left(\frac{d^2}{dt^2}\phi_2(t)\right) + 9.010989010\,a^9\,\phi_1(t)^2\,b^{11} + 3.075750912\,10^9\,\phi_2(t)\,a^5\,b^5$$
$$+ 1.082102944\,10^8\,a^{11}\,\phi_1(t)^2\,b^9 + 3.332063508\,10^8\,a^5\,\phi_3(t)\,b^5 + 2.563125772\,10^8\,a^7\,b^3\,\phi_2(t) = 0.$$

```
> ode3:=collect(dK2_dw3p
            +dCMST_dw3p
            +dPE1_dw3p = 0.0,
      {diff(phi[1](t),t$2),
        diff(phi[2](t),t$2),
        diff(phi[3](t),t$2),
        diff(phi[1](t),t),
        diff(phi[2](t),t),
        diff(phi[3](t),t)});
```

$$ode3 := 10.20749206\,b^7\left(\frac{d^2}{dt^2}\phi_3(t)\right)a^5 + 27.63369963\,a^{11}\,\phi_1(t)^2\,b^9 + 3.075750910\,10^9\,a^5\,\phi_3(t)\,b^5$$
$$+ 1.082103043\,10^8\,a^9\,\phi_1(t)^2\,b^{11} + 3.332063508\,10^8\,\phi_2(t)\,a^5\,b^5 + 2.563125766\,10^8\,a^3\,b^7\,\phi_3(t) = 0.$$

```
> a:=2.0;
```

```
b:=0.5;
tpmax:=0.0875;
td:=0.175;
tlast:=0.35;
pmax:=50000;
q:=t->piecewise(t>0 and t<=tpmax,(pmax*t/tpmax),
        t>tpmax and t<=td,pmax*(td-t)/(td-tpmax),
        t>td,0);
plot(q(t),t=0.0..0.4,labels=["time (s)","Pressure (Pa)"]);
initial_conditions:=phi[1](0)=0,
            phi[2](0)=0,
            phi[3](0)=0,
            D(phi[1])(0)=0,
            D(phi[2])(0)=0,
            D(phi[3])(0)=0;
solution1:=dsolve({ode1,ode2,ode3,initial_conditions},
            {phi[1](t),phi[2](t),phi[3](t)},type=numeric, maxfun=0);
solution1(0.025);
solution1(0.01);
```

$$a := 2.0$$

$$b := 0.5$$

$$tpmax := 0.0875$$

$$td := 0.175$$

$$tlast := 0.35$$

$$pmax := 50000$$

$$q := t \rightarrow piecewise\left(0 < t \textbf{ and } t \le tpmax, \frac{pmax\, t}{tpmax}, tpmax < t \textbf{ and } t \le td, \frac{pmax\,(td - t)}{td - tpmax}, td < t, 0\right)$$

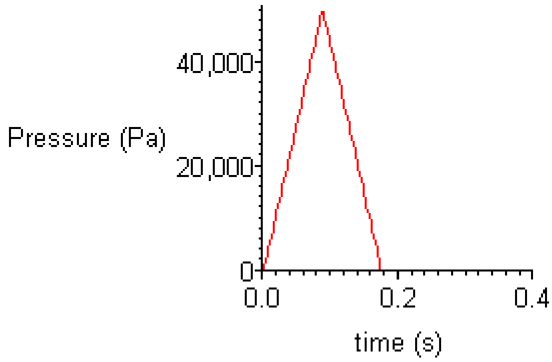

$$initial\_conditions := \phi_1(0) = 0, \phi_2(0) = 0, \phi_3(0) = 0, \left(D\left(\phi_1\right)\right)(0) = 0, \left(D\left(\phi_2\right)\right)(0) = 0, \left(D\left(\phi_3\right)\right)(0) = 0$$

$$solution1 := \mathbf{proc}(x\_rkf45) \ \ldots \mathbf{end\ proc}$$

$$\left[t = 0.025, \phi_1(t) = 0.00345983918004641282, \frac{d}{dt}\phi_1(t) = 0.120162534667288212, \phi_2(t) = -7.20517852670067316\ 10^{-7}, \frac{d}{dt}\phi_2(t) = -0.0000500438182263106824, \phi_3(t) = -2.73659864821405509\ 10^{-8}, \frac{d}{dt}\phi_3(t) = -0.00000221968491075185716\right]$$

$$\left[t = 0.01, \phi_1(t) = 0.00173805229015889683, \frac{d}{dt}\phi_1(t) = 0.375954802969690194, \phi_2(t) = -1.81757532839092995\ 10^{-7}, \frac{d}{dt}\phi_2(t) = -0.0000786494168510499198, \phi_3(t) = -6.81319007196589174\ 10^{-9}, \frac{d}{dt}\phi_3(t) = -1.53373476329919320\ 10^{-7}\right]$$

```
> x:=0;y:=0;
  Gr_w1:=seq([n/1000,rhs(solution1(n/1000)[2])*1000*((a^2-x^2)^2)*((b^2-y^2)^2)],n=0..400):
  Gr_u1:=seq([n/1000,rhs(solution1(n/1000)[4])],n=0..400):
  Gr_v1:=seq([n/1000,rhs(solution1(n/1000)[6])],n=0..400):
  curve1:=[Gr_w1]:
  curve2:=[Gr_u1]:
  curve3:=[Gr_v1]:
  plot(curve1,labels=["time (s)"," w"],title="Maximum Displacement-Z",
  titlefont=[times,bold,18]);
  max(seq(op(2,op(i,curve1)),i=1..400));
  min(seq(op(2,op(i,curve1)),i=1..400));
  plot(curve2,labels=["time (s)"," u"],title="Maximum Displacement-X",
  titlefont=[times,bold,18]);
  max(seq(op(2,op(i,curve2)),i=1..400));
  min(seq(op(2,op(i,curve2)),i=1..400));
  plot(curve3,labels=["time (s)"," v"],title="Maximum Displacement-Y",
  titlefont=[times,bold,18]);
  max(seq(op(2,op(i,curve3)),i=1..400));
  min(seq(op(2,op(i,curve3)),i=1..400));
```

$$x := 0$$

$$y := 0$$

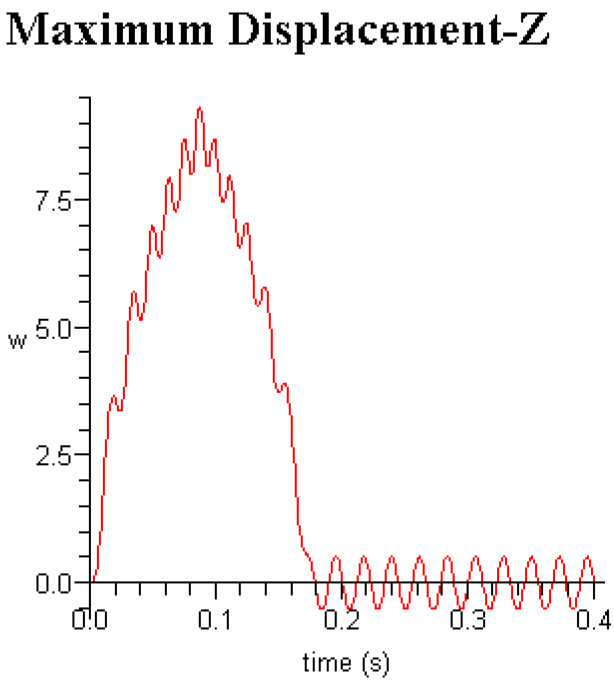

$$9.357844925$$

$$-.5229210310$$

Maximum Displacement-X

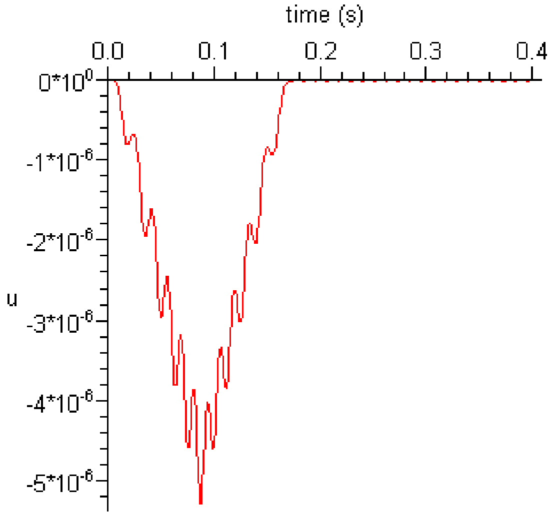

$2.19698587712806790\ 10^{-11}$

$-0.00000527322333669898570$

Maximum Displacement-Y

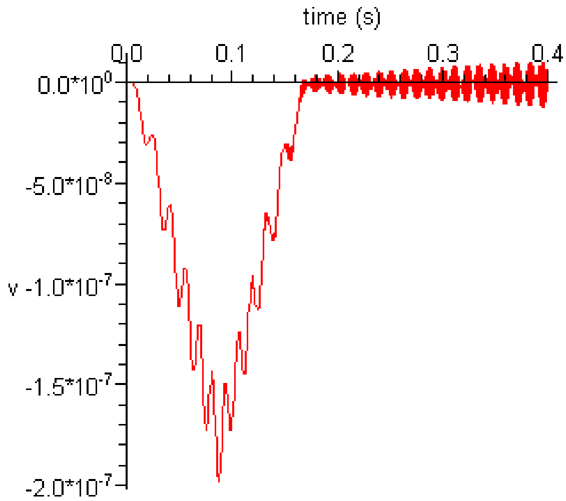

$1.09387519506021964\ 10^{-8}$

$-1.97814345607592834\ 10^{-7}$